Laser-Based Measurements Of Two-Phase Flashing Propane Jets

John Thomas Allen

Thesis submitted in partial fulfilment of the requirements for the award of the degree of Doctor of Philosophy by The University of Sheffield.

The work was undertaken at The Health and Safety Laboratory, of The Health and Safety Executive, at Buxton, Derbyshire, under the auspices of The Department of Mechanical and Process Engineering, Chemical Engineering and Fuel Technology, 1992-1998.

December 1998

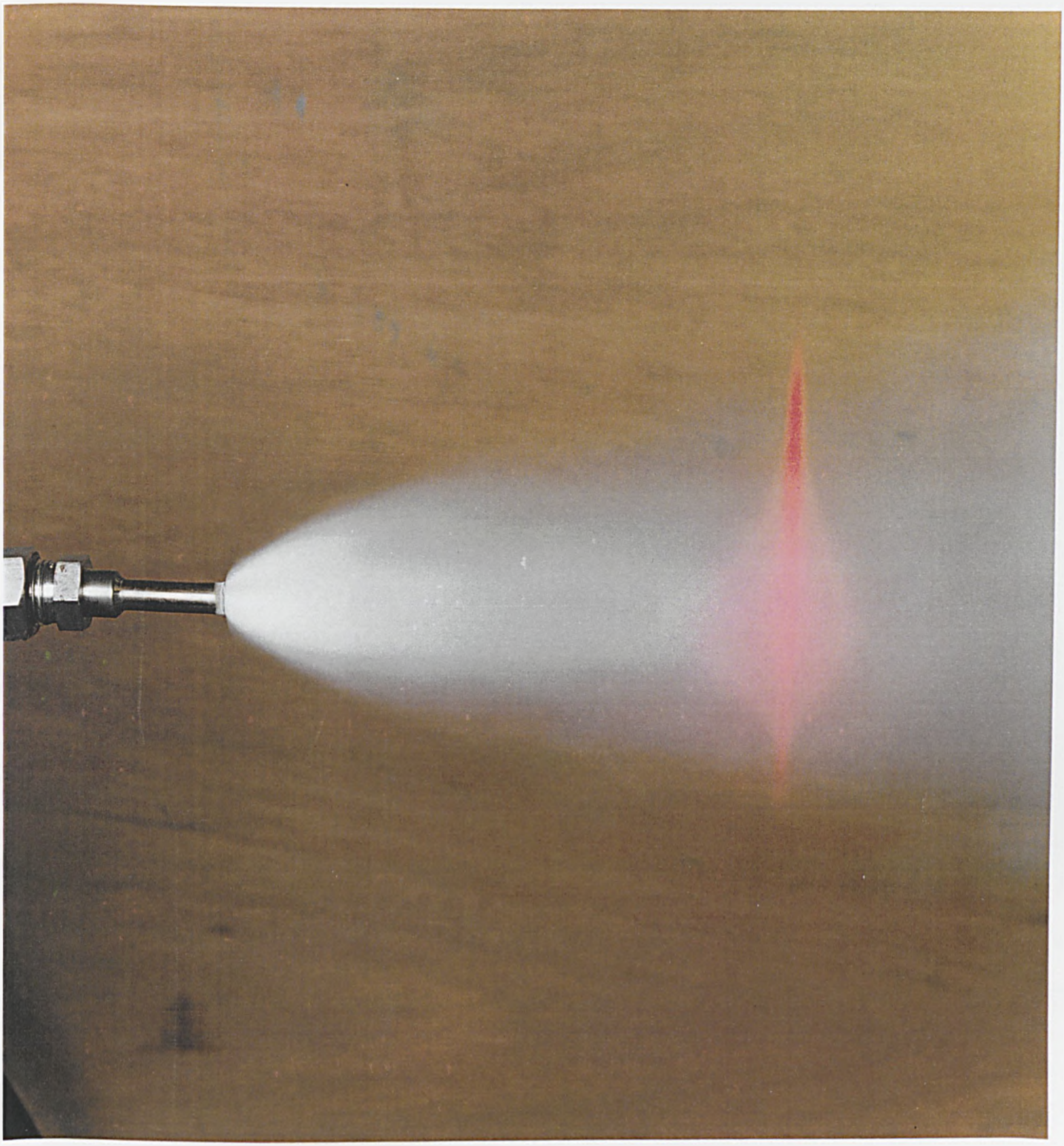

FRONTISPIECE

Two-Phase Flashing Propane Jet

SUMMARY

Two-phase flows hold an interest in many areas of science and engineering. In the safety field, one such topic is the accidental release of flammable and toxic pressure-liquefied gases (PLGs) such as propane and chlorine, which may result in great loss of life and material losses.

Of specific interest in this area are the mathematical models and predictive computer codes which may be applied to such releases in order to inform risk assessment on transport, storage and accidental release scenarios in land use planning. Currently such models can only accurately predict the behaviour of the later stages of accidental releases of pressure liquefied gases and there is a little experimental data against which to validate near-field models.

A facility has been designed and constructed to allow the safe study, by non-intrusive techniques, of two-phase flashing propane jets; propane (and LPG) being involved in the majority of major industrial two-phase accidental releases resulting in loss of life. Each jet release has been characterised by the measurement of its mass release rate, and temperature and pressure parameters at storage and exit positions.

Liquid phase velocity and size distributions have been measured in the near-field regions using Laser Doppler Anemometry (LDA) and a diffraction-based sizer respectively. Various data manipulation techniques have been applied to the raw data in order to obtain the best quality results from the measurements. Centreline and lateral profiles of the velocity and droplet size parameters are presented, along with conventionally measured liquid temperature centreline and lateral profiles.

The data generated can be used to evaluate and develop predictive mathematical models, and comparison with certain models is presented.

A technique has also been developed for the non-intrusive measurement of liquid propane temperature in a two-phase flashing jet scenario, and its suitability confirmed and calibrated.

Overall, a body of data has been produced, and made available, for a two-phase flashing propane jet, improving upon the little that previously existed.

Acknowledgements

I would like to acknowledge the support and encouragement of my supervisors, Prof J Swithenbank and Dr B C R Ewan. I would also like to thank Dr R J Bettis for his support, advice, and assistance throughout the course of this research project.

Acknowledgement is also due to Prof. F Pragst, University of Humboldt, Berlin, for information and supply of small quantities of NpaNmaap and associated compounds in relation to the fluorescence temperature work.

Thanks are also due to the Health and Safety Laboratory (formerly Research Laboratory Services Division) of the Health and Safety Executive for their financial support and sponsoring during both this project and previous study. Especial thanks are due to Dr A F Roberts and Mr J A Barton for their efforts in initiating the H.S.E. support of my studies.

I would also like to thank the technical staff of Fire Safety (formerly Fire and Thermofluids) Section for their practical assistance, and fellow colleagues for their (often!) constructive criticism and advice.

... and last, but by no means least, my parents and family.

Stipendium

Vitae

Mors Est

CONTENTS

CHAPTER SIX - LDA MEASUREMENTS

CHAPTER SEVEN - DROPLET SIZE MEASUREMENTS

REFERENCES

APPENDICES

CHAPTER ONE

OVERVIEW AND AIMS OF RESEARCH

1.1 INTRODUCTION

Two-phase flows hold an interest in many areas of science and engineering. In the safety field, one such topic is the accidental release of flammable and toxic pressure-liquefied gases (PLGs) such as propane and chlorine. Of specific interest in this area are the mathematical models and predictive computer codes which may be applied to such releases. It is hoped that these models will embody an adequate understanding of the processes involved and may be used in design and assessment to improve transport and storage design, site location and layout, and other safety features. Currently, such models have only been shown to predict the later stages of these releases; the jet behaviour after any effects of the early two-phase stages and subsequent passive dispersion in the atmosphere.

For the accurate prediction of the likely consequences of any given two-phase release from known initial storage condition, all the significant parts of that release must be modelled. In the initial, flashing stage of the jet, where the system is furthest from an equilibrium state and measurement is most difficult, little experimental work has been published. This area is, therefore, the least understood and there is a need for accurate and reliable data in order to generate and/or refine useful mathematical models and computer codes.

Due to the non-equilibrium nature of the near-field regions accurate data measurement is not possible with intrusive techniques such as thermocouples. Non-intrusive methods, such as laser-based techniques, may present the only possibility of obtaining accurate data measurement.

1.2 AIMS OF THE RESEARCH

The aim of this research programme is to explore the possibility of utilising laser-based measurement techniques in order to characterise a two-phase flashing propane jet. Where possible it is intended to apply such techniques in order to obtain

quality data from a two-phase flashing propane jet, such that this data may be used (by others) to generate, validate, and improve mathematical predictive codes for such releases. As stated, there is currently a dearth of such information available for modelling purposes.

As part of the process to explore the possibility of applying laser-based techniques, it is also necessary to design, and construct, a facility which will permit these measurements to be safely undertaken. This will also include the writing of safe operation and maintenance procedures.

Conventional, intrusive, techniques may be applied to this work in order to improve the body of data generated, and novel laser-based techniques may be developed where none currently exist.

Some work has been previously undertaken applying laser-based techniques to two-phase flashing jets of CFC substitutes [1, 2, 3, 4, 5], due to their lack of flammable and toxic properties and therefore relative ease of use and study.

For this work propane/LPG has been chosen as the material of interest, it being one of the actual PLGs involved in accidental releases resulting in loss of life and material losses (e.g. Mexico City [6]). Propane/LPG is also one of the major hazards due to its large volume of usage, production, storage etc.

CHAPTER TWO

INTRODUCTION

2.1 TWO-PHASE RELEASES

In its most simplistic form, a two-phase release is a release of material in which the material is present in two physical states, or phases. An example of this would be a jet of boiling water, where there is both liquid water and gaseous water (steam) present. Alternatively, a multi-component release composed of two phases is also, strictly, a two-phase release, e.g. particulate metal in a water jet, or an aerosol system (solid particles in a gaseous jet). A two-phase system moving within a constrained environment, e.g. water containing air bubbles travelling along a pipework system, is more accurately referred to as two-phase flow, although precise differentiation can sometimes be difficult.

A common source of accidental two-phase releases in the field of industrial safety is the release of a pressure-liquefied gas, giving rise to a gas/liquid two-phase jet or cloud. It is with this type of two-phase event, a single component unconstrained release of a volatile material, that this research project is concerned.

There is a strong interest in this type of release event in the safety field, due to the nature of several widely produced, stored, transported and utilised materials. The importance of understanding, and being able to predict the consequences of such two-phase accidental releases in the safety field are illustrated by the small selection of incidents presented in Tables 2.1 and 2.2. From the tables it can be seen that major incidents resulting in loss of life and severe material loss have continued to occur despite 'improved' safety practices and awareness. Indeed the most disastrous events have occurred within the last fourteen years.

DATE	PLACE	MATERIAL INVOLVED	FATALITIES
1959	Meldrin, USA	LPG	26
1962	Berlin, USA	Propane	10
1966	Feyzin, France	Propane	18
1966	West Germany	Light Hydrocarbons	45
1969	Laurel, USA	LPG	2
1974	Decatur, USA	Isobutane	7
1975	Eagle Pass, USA	LPG	16
1978	Dharan, Saudi Arabia	LPG	4
1978	San Carlos, Spain	Propylene	211
1978	Waverly, USA	Propane	12
1983	Nile River, Egypt	LPG	317
1984	Mexico City, Mexico	LPG	700
1984	Chicago, USA	Propane	17
1984	Romeoville, USA	Propane	15
1985	Glenwood Springs, USA	Propane	12
1987	Pampa, USA	Butane	3
1988	Shanghai, China	LPG	25
1989	Asha-Ufa, CIS	LPG	>500
1989	Almetyevsk, CIS	Propane	4
1990	North Blenheim, USA	Propane	2
1990	Bangkok, Thailand	LPG	63
1991	San Luis Potosi, Mexico	Butane	30
1992	Ankara, Turkey	LPG	22
1993	Lahore, Pakistan	LPG	14
1993	Chongju, South Korea	LPG	27
1995	Port harcourt, Nigeria	LPG	4
1996	Lusaka, Zambia	LPG	5

TABLE 2.1

A Selection Of Major Incidents Involving Propane and Similar Materials [1, 2]

One of the main problem materials is propane (including LPG), along with its chemical analogue butane, as can be seen from the small selection of incidents presented in Table 2.1. This is, in part, due to the large quantities of propane and LPG used for primary heat sources (e.g. heating, cooking) and hence the large

volumes produced, stored, and transported. This large scale production is illustrated in Table 2.3.

DATE	PLACE	MATERIAL INVOLVED	FATALITIES
1976	Houston, USA	Ammonia	6
1981	Montanas, Mexico	Chlorine	28
1983	Toledo, Philippines	Ammonia	5
1984	Los Pajaritos, Mexico	Ammonia	4
1985	San Antonio, USA	Ammonia	4
1989	Billingham, UK	Ammonia	2
1990	Matanzas, Ruba	Ammonia	3
1990	Mexico	Hydrofluoric Acid	2
1990	Borneo	Ammonia	17
1991	Mexico	Chlorine	5
1991	Corpus Christi, USA	Hydrofluoric Acid	2
1991	Dhaka, Bangladesh	Ammonia	7
1992	Dakar, Senegal	Ammonia	41
1992	Haryana, India	Ammonia	>11
1994	Middletown, USA	Ammonia	4

TABLE 2.2

Major Incidents Involving Toxic PLGs [1, 2]

Propane presents a major industrial safety hazard for several reasons. It forms a flammable/explosive mixture with air over a relatively wide range (2.2%-9.5% v/v in air), and due to the fact that its ambient pressure boiling point is -42°C, its liquefying pressure is relatively high (8 to 11 bara). Its pressure-liquefied volume is considerably less than its atmospheric gaseous volume, and hence any accidental loss of the high pressurising force will result in a rapid release, usually in the form of a high velocity two-phase jet, leading to a large volume, flammable gaseous cloud.

Due to its high density at this point with respect to air, having cooled through the rapid boiling process, the propane will tend to remain close to, and spread out at, ground level.

MATERIAL	LPG USAGE (tonnes p.a.)			DELIVERY FORMAT	
				Packed (cylinder)	Bulk (tanker)
	1990	1991	1992		
Butane	275,000	314,000	251,000	60%	40%
Propane	764,000	905,000	860,000	23%	76%
Total	1,039,000	1,219,000	1,111,000		

TABLE 2.3

Propane and Butane Usage and Delivery Format [3]

Figure 2.1 - Consequences of Ignition of a Two-Phase Propane Release

Any portion of this cloud attaining a flammable/explosive concentration, and coming into contact with an ignition source, will result in at least a severe flash fire, or sustained jet fire, if not the more damaging VCE (Vapour Cloud Explosion). Figure 2.1 illustrates the results of ignition of an accidental release of propane.

An accidental two-phase release of the type described above may occur in a number of forms:

Jet

A two-phase flashing jet is a long duration high velocity release, usually highly directional. A common source of such jets is a broken transfer pipe, or any situation where the escape orifice is small in comparison to the volume/pressure contained in the vessel/pipeline. The majority of accidental two-phase releases occur initially as jets, an example of which is shown in Figure 2.2.

The physical parameters and behaviour of a jet release are related to the initial storage, and ambient, conditions, otherwise known as the source terms.

Catastrophic Failure

This is a two-phase release of short duration, lower velocity, and possessed of lesser directionality than the jet. It occurs when the escape orifice is comparable to the volume/pressure contained. This is usually the case, as the name suggests, when a containment vessel instantaneously loses its integrity, e.g. an end-cap weld completely fails on a 'bullet' storage tank. As with jet releases, the behaviour of a catastrophic release is related to its source terms.

Cloud

Clouds tend to form as a result of both jet and catastrophic failure releases of volatile materials, if ignition of the initial release does not occur. They are not so much a type of release as a secondary hazard generated by the initial release. The behaviour of the cloud is effectively independent of the source terms, and is controlled by atmospheric dispersion.

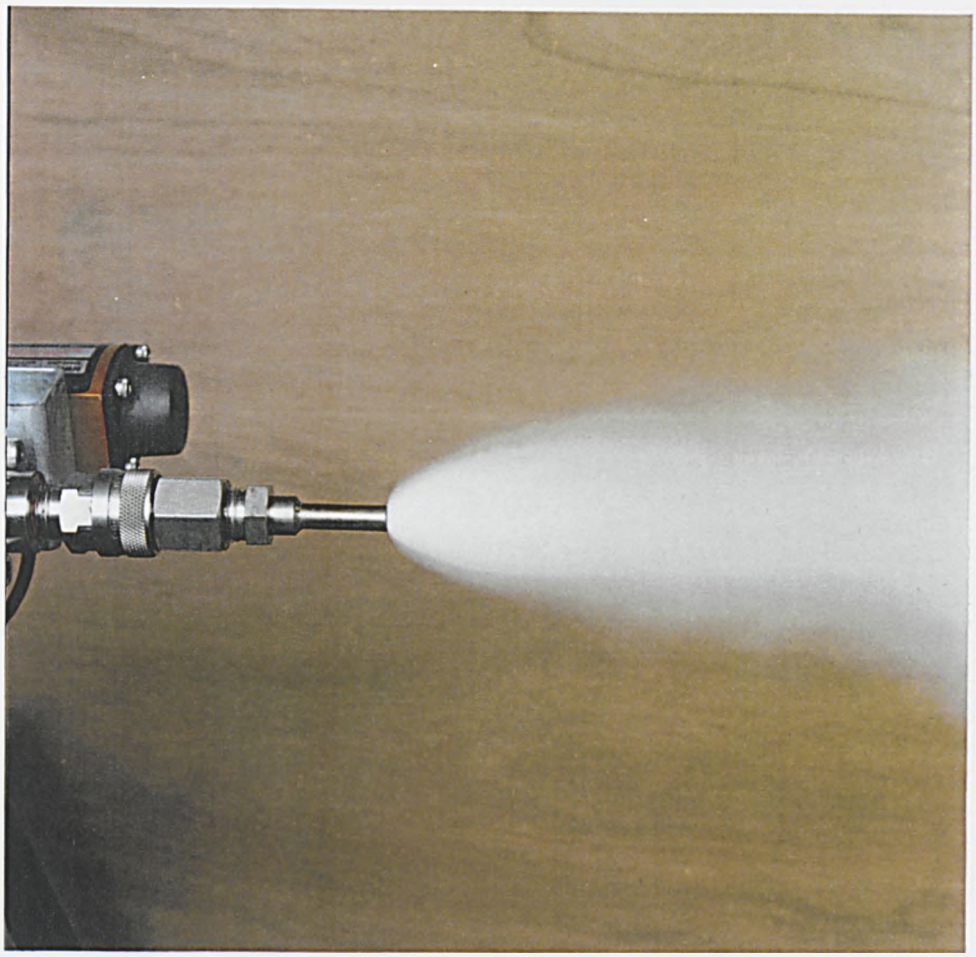

Figure 2.2 - Experimental Two-Phase Flashing Propane Jet

2.2 PROBLEMS ASSOCIATED WITH MEASUREMENTS ON TWO-PHASE RELEASES

To understand the problems associated with studying accidental two-phase releases, it is necessary to take a closer look at the actual release mechanism.

As stated earlier, in its storage condition the propane will be contained as a liquid at ambient temperature by the application of high pressure, usually its own saturated vapour pressure (no cooling system is employed). When the containment system fails, e.g. through pipe breakage or vessel failure, the liquefying pressure is lost. This pressure loss occurs at sonic velocities, but any change in the liquid temperature is governed by mass transport across the phase interface (i.e. boiling/evaporation)

which is a far slower process. The liquid temperature state hence temporarily lags behind its pressure state - a superheated liquid state is generated.

Put simply, a loss of containment results in a liquid which is unable to boil at a fast enough rate to maintain its temperature/pressure equilibrium, the material remaining in its liquid state at temperatures far in excess of its boiling point.

The fact that the liquid/vapour system, in its initial stages, is far from an equilibrium condition is of great importance in terms of obtaining measurements of its physical parameters. Being far from equilibrium makes the system ultra-sensitive to its surroundings.

Thus any measurement technique which intrudes into the system will vastly influence it, and measurements thus obtained will not truly reflect the system. An example of this is temperature measurement by the use of thermocouples. In a two-phase jet situation, as described above, liquid droplets may adhere to the thermocouple and bias its readings. This is especially a problem if vapour phase temperatures are required. In any event the presence of the thermocouple will perturb the flow, disturb the physical processes which are occurring (e.g. boiling), and distort downstream parameters such as the droplet size distribution and velocity.

Unfortunately, many of the traditional techniques employed to obtain measurements of the physical parameters of a system fall into this category. This includes thermocouples, hot wire anemometers, any sample capture technique (for void fraction, or chemical composition analysis), pitot tubes etc.

This is therefore an area of research where laser-based measurement techniques are of use. These techniques are non-intrusive, i.e. they have a negligible effect on systems, due to the fact that they rely on electromagnetic radiation (light) to provide both their system interrogation source and information signal. The next chapter of this thesis will present a review of the various laser-based techniques which are of relevance to two-phase measurements.

2.3 TWO-PHASE RELEASE MODELLING

As detailed, the main area of interest for this study in two-phase events lies in accidental releases of hazardous pressure liquefied gases, primarily propane/LPG (flammable) and chlorine (toxic), i.e. two-phase flashing jets. Of specific interest, to the wider safety-science community are the mathematical models and predictive computer codes which may be applied to such releases.

At present, if we consider a simplified two-phase jet release structure as shown in Figure 2.3, only the later region of a jet (Region 4), where atmospheric dispersion is dominant, is adequately modelled.

The flashing region (Region 2) is currently ignored in all models (of which the author is aware) - ie the distance between the nozzle exit (Region 1) and the non-flashing momentum driven part of the jet (Region 3) is taken to be zero. Modelling starts at the end of Region 2, where it is assumed that most, if not all, of the liquid phase has boiled off and the minimum jet temperature has been achieved. Thus current models only begin calculation at the start of Region 3, where air is being entrained into the jet and it can be considered as single phase, and on to Region 4, where atmospheric dispersion is the dominant factor.

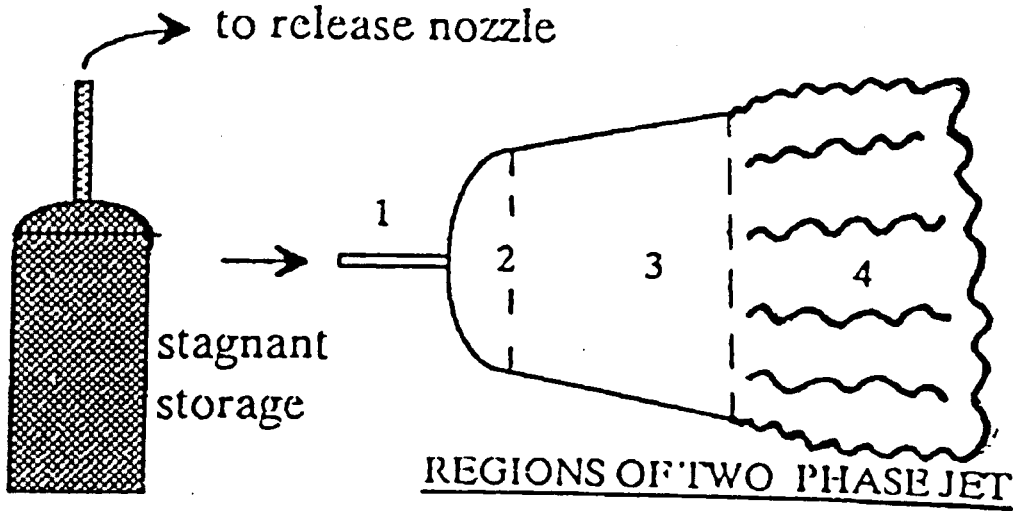

Figure 2.3 - Schematic of Two-Phase Jet Release

For a comprehensive review of 'simple' and Computer Fluid Dynamic (CFD) models and sub-models of two-phase flashing jets, which is outside the scope of this work, the reader is directed to [6].

For accurate prediction of the likely consequences of any release, it is desirable that all regions may be modelled from known initial storage conditions, i.e. the source terms. In the momentum-driven regions of the propane jet (Regions 2 and 3), especially where the system is furthest from its equilibrium state (Region 2) and measurement is most difficult, little or no experimental work has been published (see Section 2.4).

There is therefore a need for accurate and reliable data from these regions in order to generate and/or refine useful predictive computer codes. It is hoped that these may ultimately be employed to mitigate the consequences of accidental releases through a better understanding of the processes, resulting in improved transport and storage design, storage site placement, and other safety features.

Important physical properties required as source terms for the predictive computer codes of two-phase jets include:

a) droplet exit velocity
b) droplet temperature
c) droplet size distribution
d) droplet number density
e) vapour exit velocity
f) vapour temperature
g) vapour concentration
h) degree and rate of air entrainment
i) rate of droplet evaporation
j) mass release rate
k) degree or rate of droplet fall-out

The source terms also include information regarding the type of release event including the size of release orifice (ie slit, 'hole', catastrophic failure, pipework failure, nozzle/slit dimensions etc).

It is also necessary to know other properties in order to estimate some of the source terms mentioned above. These include:

l) exit void fraction
m) stagnation conditions
n) exit pressure conditions
o) exit temperature conditions

This series of experiments will attempt to undertake measurements of a), b), c), j), m), n), and o). Some comment may also be possible on d), h), i), and k), although no direct measurements will be attempted.

As discussed, the measurement of some of these properties is, however, problematical, and laser-based techniques may present the best, or in some cases only, method of obtaining them.

2.4 AVAILABLE DATA FOR TWO-PHASE FLASHING PROPANE JET RELEASES

A review of the available literature on two-phase flashing propane jets was undertaken at the start of this work, and no references were found.

During the course of this research a paper was published [4] detailing velocity and droplet size measurements in a two-phase propane jet. This paper, however, reported the intrusive use of a phase-Doppler particle analyser (PDPA) with quoted accuracies of 20% and 40% for velocity and size respectively. Additional details of this work are presented under the relevant velocity (Chapter Six) and droplet size (Chapter Seven) chapters of this thesis.

Data has also been made available to the author, obtained during a CEC project of which the work presented in this thesis formed a part, by Battelle GmbH [5]. Velocity and droplet size data measurements were undertaken, by the use of a Phase Doppler Analyser (PDA), on a 32mm i.d. nozzle release of propane. These measurements were undertaken 'in the field' and, as a consequence, the data is somewhat variable in quality and reproducibility. Further details are presented in the relevant chapters.

A recent modelling paper [7], utilising the data of Hervieu and Veneau [4], comments on the lack of data available for propane releases. Indeed, efforts are made to compare two-phase water/steam data against their modelling predictions for propane by consideration of the difference in physical parameters between the two materials.

No additional data has been reported, apart from that generated by the work contained in this thesis (details of which are presented in the Published Work Chapter of this document).

CHAPTER THREE

LITERATURE SURVEY OF LASER-BASED MEASUREMENT TECHNIQUES

3.1 INTRODUCTION

Laser-based optical measurement techniques have seen widespread use in many areas of investigation during the past decade, including medicine, combustion, fluid dynamics, aeronautics and safety. This increase in usage is illustrated by the large numbers of articles involving laser-based techniques, regular dedicated conferences and reviews devoted to the subject [141, 142, 144, 145, 146, 147, 151, 152 amongst others] . In many fields of interest these techniques are becoming the standard ones employed, and in certain environments they are the only ones capable of obtaining information.

The wide applicability and usefulness of such techniques is primarily due to the properties of the laser itself. These are summarised below, being treated in more detail in standard reference texts for example [122, 123, 124].

3.2. LASER PROPERTIES

A laser (light amplification by the stimulated emission of radiation) generates light from various physico-chemical processes. This light is useful as it can possess high temporal and spatial resolution, coupled with high power and monochromaticity. Put simply, the light from a laser can deliver a large amount of energy at a specific wavelength in a small volume over large distances. This energy can also be supplied in controllable duration pulses, down below picoseconds, or as a continuous source.

For many of the applications discussed, its most important property is its non-intrusiveness, ie its ability to be used to gain information from a system without having any effect upon that system. This property is of paramount importance in 'delicate' systems such as two-phase flow and combustion. The fact that optical

information can flow in opposite directions simultaneously also provides advantages where access to a particular system is difficult.

Figure 3.1 shows an Argon Ion laser and simple sheet optics system.

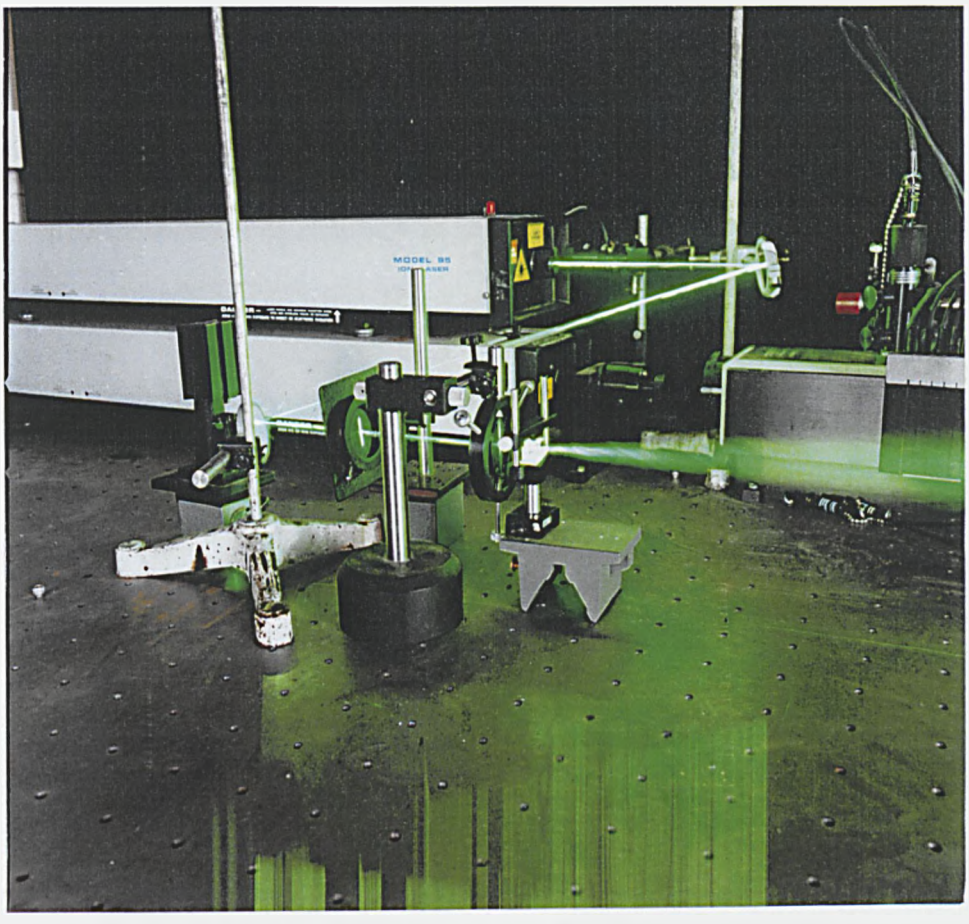

Figure 3.1 - Argon Ion Laser and Sheet Optics System

3.3 CATEGORISATION OF TECHNIQUES

The field of optical techniques, according to a review by Durst [24], can be divided into three categories:

image formation based

interference pattern formation based

intensity measurement based

and the field of laser-based measuring techniques, according to Kurosaki and Kashiwagi [95], categorised according to the principle employed:

geometrical optics
wave optics
scattering and spectroscopy

The categories and sub-classes suggested by Durst are shown in Figure 3.2 and their relationship is explained in detail in the review [24]. The measuring techniques and their features classified by Kurosaki and Kashiwagi are given in Table 3.1.

In this review no attempt has been made to categorise techniques in either of these ways. Alternatively, the various techniques have been considered to consist of two separate areas - the phenomenon that the technique utilises, and the practical stages involved in deriving information from that phenomenon. The various phenomena will be discussed initially, followed by the practical aspects involved in information generation.

It is hoped that this methodology will demonstrate the features of the various techniques and will highlight the interchangability of several of the practical aspects.

3.3.1 Theoretical Aspects

All of the laser-based techniques fundamentally revolve around the fact that molecules and particles 'scatter' light. In this context, the term scattering is used to imply that light incident on a molecule/particle is re-emitted by it at the same, or a different, wavelength and may be spatially redistributed.

Some techniques study the properties of the scattered light, some its intensity only, and some are only interested in the intensity of light which remains unscattered.

The scattering of light can be divided into two distinct types, elastic and inelastic.

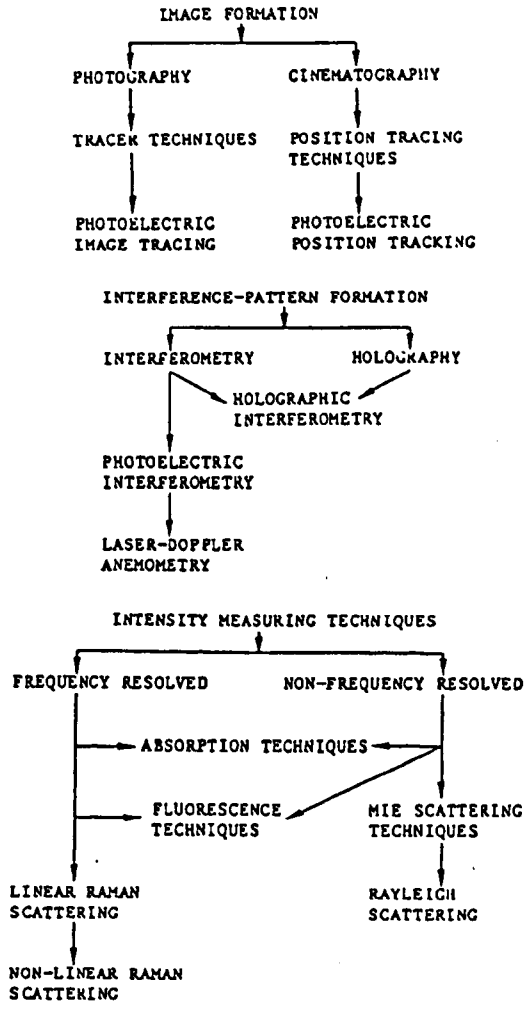

Figure 3.2 - Categorisation of Optical Techniques [24]

3.3.1.1 Elastic Scattering

Elastic scattering is used to describe processes in which the incident light is re-emitted at the same wavelength (energy value) after interaction with a molecule/particle. That is to say, there is no energy exchange between the light and the molecule/particle. There are two main elastic processes, Rayleigh and Mie scattering, which are principally differentiated by the scale on which the interactions occur.

Rayleigh scattering is defined as taking place when the size of the molecule/particle is considerably smaller than the wavelength of light being used, ie:-

$$\text{diameter/wavelength} << 1$$

The emitted light can be used to derive temperature measurements by virtue of Doppler linewidth broadening, but only in situations where the pressure is such that pressure broadening doesn't dominate the total broadening observed. It can be used for total density measurements, but is not species specific and therefore cannot be used for concentration determinations. Rayleigh signal strength is relatively high, but suffers from contamination from Mie scattering, and is only really useful in well-conceived, artificial experimental scenarios.

Principle		Methodology		Light Source (Laser)	Measuring Subjects	Features
GEOMETRICAL OPTICS		Shadowgraph		He-Ne	temp./pressure profiles	Easy to handle. Suitable for visualization of the profiles of density change.
		Schlieren method		He-Ne	temp./pressure profiles	Effective for the fields with large density gradient.(e.g. shock-wave, boundary layer)
WAVE OPTICS	Two path int.	Mach-Zehnder interferometry		He-Ne	temp./pressure profiles	Suitable for the quantitative measurements of temp./pressure distributions in gaseous media. Finite fringe method is applicable.
	Laser holographic interferometry	transmitted light type		He-Ne	temp./pressure profiles	Suitable for the quantitative measurements of temp./pressure distributions with density contour fringes in liquids. High precision optical setup is unnecessary.
		multi-color		He-Ne + Ar^+	temp. + concentration profiles	Temperature and concentration profiles are simultaneously measurable. Optical setup is complicated.
		fun-beam		Ruby, Ar^+	velocity profiles	2-D velocity distributions are measurable. A double-pulse laser is required for high velocity fields.
	Speckle method	Speckle photography		Ar^+, Ruby	velocity profiles	Easy to handle. 2-D velocity distributions are measurable. Image processing techniques are required.
		Speckle correlation		He-Ne, Ar^+	local velocity	Easy to handle. High time resolution.
SCATTERING AND SPECTROSCOPY	Absorption	Laser tomography		He-Ne, Dye, Ar^+	temp. and concentration profiles	3-D temperature and concentration profiles are simultaneously measurable. High-speed image processing techniques are required for measurements.
	Elastic Scattering	Laser doppler method	Laser doppler anemometer	He-Ne, Ar^+	local velocity	High resolution. Suitable for velocity measurements of turbulent/multi-phase flow.
			Laser doppler image system	Ar^+	velocity profiles	2-D velocity distributions are measurable. Easy to visualize velocity contour.
		Rayleigh scattering method		Ar^+	temp./pressure	Intensity of the scattered light is weak. Mie scattering affects the measurement.
	Inelastic Scattering	Raman scattering method		Ar^+, YAG	temp./ concentration	High resolution. Concentrations of gas mixture are measurable due to monochromatic light source. Intensity of the scattered light is weak.
		Fluorescence method		Dye	temp./ concentration	High resolution. Suitable for measurements of low concentration components.
	Nonlinear Effects	CARS		YAG + Dye	temp./ concentration	High resolution. Intensity of the scattered light is strong compared to Rayleigh/Raman scattering, and the high S/N ratio is obtainable.

Table 3.1

Classification of Laser-Based Techniques [95]

Mie scattering is the phenomenon utilised in particle sizing, LDV and similar techniques. It is similar to Rayleigh scattering in principal, but occurs when the condition for the former, that diameter/wavelength << 1, is not met. Mie scattering is essentially from particulate matter and thus is not species dependent, and cannot be used to obtain specific temperature or molecular density information. Due to its source, particulate matter, it is a very strong signal/process.

3.3.1.2 Inelastic Scattering

Inelastic processes are ones in which an exchange of energy takes place. Here the interrogating light beam interacts with the molecules and the resulting scattered light either loses energy through this process, or gains energy from it. Put simply, the scattered light occurs at a different frequency to the incident light.

Raman scattering is an almost instantaneous (10^{-12} secs) inelastic process. It may be classed as vibrational, electronic, or rotational depending upon what type of energy exchange is taking place between the light and the molecule. Raman is essentially Rayleigh scattering that has lost, or gained, some amount of energy. The molecule gains vibrational, rotational or electronic energy from the light and inhabits a higher energy level. Depending on its initial energy state, the molecule can then emit radiation with more, or less, energy than the original incident light. The radiation with more energy is termed anti-Stokes radiation, and is far less likely to be emitted than Stokes radiation, with less energy. Raman processes are species specific, and depend linearly on species number density - their main drawback being that they generate very weak signals and hence have poor signal-to-noise ratios.

Fluorescence is effectively an inelastic scattering phenomenon, with re-emission times ranging from 10^{-5} to 10^{-10} secs. In this case the molecule is promoted to an excited electronic state by photon absorption. The molecule may then immediately revert to its initial energy state by emission of radiation of the same energy (wavelength) as the absorbed photon (termed resonance fluorescence). It is far more likely however that the molecule will lose energy, through collisions, intersystem crossing etc, before emitting radiation of a lower energy value. In practice virtually

all fluorescence processes involve energy loss prior to emission. Fluorescence is a strong scattering process, is highly species specific and thus is a sensitive tool for concentration and temperature measurements.

SCATTERING PROCESS	SCATTERING CROSS SECTION
Sphere (100μm diameter)	10^{-8} m^2/sr
Micron particles (Mie scattering)	10^{-12} m^2/sr
Free electrons (Thompson scattering)	10^{-30} m^2/sr
Molecules (Rayleigh scattering)	10^{-33} m^2/sr
Atomic fluorescence	10^{-19} to 10^{-24} m^2/sr
Molecular fluorescence	10^{-25} to 10^{-30} m^2/sr
Raman scattering:	
Rotational CARS	10^{-27} to 10^{-30} m^2/sr
Vibrational CARS	10^{-28} to 10^{-31} m^2/sr
Rotational LRS	10^{-35} to 10^{-36} m^2/sr
Vibrational LRS	10^{-37} m^2/sr

Table 3.2

Scattering Cross Sections for Various Scattering Processes [24]

The strength of the various scattering processes is shown in Table 3.2. The greater the cross-sectional area, the greater the scattered signal intensity. A mathematical treatment of scattering is presented in [125] and a mathematical review of optical phenomenon is given in [117]. A more qualitative approach is given in various standard text books including [123], reference [77] describing the phenomena with particular reference to combustion.

3.3.2 Practical Aspects

To avoid confusion, the various components of the practical aspect have been defined as follows:

source - the laser, or its beam
medium - the species which interacts with the source
primary signal - the scattered light generated by the interaction of the medium with the source

For any of the phenomena discussed, the practical aspect of the technique can be divided into three main parts; the medium and geometric form of the primary signal, the means of storage (detection) of the primary signal, and the means by which the desired information is obtained from the stored signal.

3.3.2.1 Medium And Geometric Form Of Signal

The primary signal may arise from the interaction of the interrogating light with the material under study, as in particle sizing or certain fluorescence techniques, or with an added material.

In the latter case a 'mimic' is placed into the system of interest, which must mimic the bahaviour of the material under study, to provide the scattering medium. This situation will occur when the materials involved do not themselves interact sufficiently with the light source, examples being certain fluorescence and scattering scenarios. In this case it is important that the mimic does in fact copy the host material as required, eg acquire the same temperature, velocity or follow the same flow pattern.

The interrogating light source itself may also be either (effectively) a point source yielding single-point localised information (eg LDA), a line source (Malvern particle sizer, LIFS), or a planar source. The planar source, termed a light sheet can be used to generate full-field 2D, or pseudo-3D information.

3.3.2.2 Method Of Primary Signal Capture And Storage

The primary signal, eg fluorescence, scattered light etc, may be captured and stored in a variety of ways. The oldest method, photography, can be employed both as storage and information. In the former case the information stored, such as intensity or velocity, may be obtained by digital image processing or manual interpretation. In the latter case the photograph is the information, being purely qualitative flow visualisation. In fundamental photographic storage, including still shadowgraphy and Schlieren techniques, only two-dimensional representation is possible.

The technique of cinematography may be used in exactly the same way as photography, although it will also yield temporal information, such as velocity.
Holography currently provides, by use of double-exposure techniques and image analysis, three dimensional temporally resolved information. The temporal information is, however, discontinuous. For a detailed review of optical data capture and storage media see reference [92].

The primary signal may be changed into an electrical signal via a photomultiplier, or similar device, and stored in a data collection system. The information in this case is then available for interpretation and manipulation by computer.

3.3.2.3 Method Of Information Generation

Once stored, the desired information may be obtained via visual interpretation, as in the case of qualitative imaging, or calculation from the stored signal. Information initially stored visually (photography, cinematography) must be transferred to another format so that quantitative analysis (digital image analysis) may be performed. Holography is a special case of this in that the stored information must be regenerated and then re-recorded before being quantified.

In most situations the final information generation involves the use of computers. This is mainly due to the complexity of the information extraction procedure (image analysis) and the combination of speed and accuracy afforded by these machines.

The extraction procedure may simply involve direct calculations to determine desired parameters from measured quantities, or may involve detailed data manipulation.

There are slight variations to the above three part system, primarily when information generation occurs in real time. In this case there is effectively no stored signal information, the primary signal being interpreted, usually by computer, directly from the medium source.

3.4 LASER-BASED TECHNIQUES

The following references are not intended to be an exhaustive survey of all work carried out using laser-based techniques, but are intended to illustrate the applications of potential interest.

3.4.1 Photography, Cinematography and Related Techniques

These techniques are, in the main, more accurately defined as storage media for laser generated information (as described in section 3.3.2.2), and will not be dealt with in depth.

Photography is used mainly for qualitative purposes, but double and long exposure techniques may be utilised for particle velocity and particle tracking determination respectively [154]. The extension of these techniques to quantitative measurements is more fully described in section 3.4.2. The information provided by a photograph is usually temporally unresolved, double and long exposure images providing some (limited) degree of temporal resolution.

Cinematography provides temporally resolved 2D images, which may be digitally analysed to yield quantitative information. A major expanding area in optical measurement techniques currently is the development of improved image analysis processes to yield 'real-time' capabilities.

Shadowgraphy, and its variant Schlieren photography, have also been used [15] to obtain density information though principally qualitative. A multiple spark camera (chronoloupe) has been used with such techniques to study two-phase flows [45].

For extensive discussion on these techniques, see [92].

3.4.2 Particle Image and Particle Tracking Velocimetry

Particle tracking velocimetry (PTV) is a 2D imaging technique used, as its name suggests, to determine particle velocities by tracking their movement over a known time period. It accomplishes this through the use of a pulsed laser light sheet, which is used to generate a scattered light signal from (usually seeded) particles in the flow being studied. This scattered light is then captured on a photographic medium. The film negative is later interrogated to identify individual particle tracks and determine the velocities from them. A problem with PTV is that, for individual particle tracks to be easily (unambiguously) identified, the number density of the seeding particles must be low. This requirement thus results in low and random velocity data acquisition, giving the technique poor spatial resolution. The technique has however been employed, examples including [130-133].

Particle image velocity (PIV) is similar to PTV, but does not suffer from such low seeding number requirements. Various names exist for this technique; particle image displacement velocimetry (PIDV), pulsed laser velocimetry (PLV), digital pulsed laser velocimetry (DPLV), and laser speckle velocimetry (LSV) are all essentially the same technique. The latter name, LSV, is usually applied to the technique when the particle seeding number density is sufficiently high for particle image overlap to occur and form a true laser speckle image [109, 129].

As with PTV, a pulsed laser light sheet is used to generate a 2D illumination source, which is scattered by particles in the system being studied. This scattered light is recorded, at 90° to the sheet, on a photographic film. The film negative is later illuminated, an area at a time, by a light beam, the image thus generated being magnified and focussed onto a ccd camera. The small area captured is then analysed

by computer methods, eg fast Fourier transforms etc, to generate velocity information. It is possible to bypass the film stage and directly digitise the scattered light by use of, say, a vidicon camera, thus removing the time-costly re-imaging process [108]. This is the process employed for DPLV.

This technique has been used to determine velocities in propane/air laminar flows with TiO_2 as the seeding particle [96], and to study velocity fields around prosthetic heart valves [97], amongst others [Lisb, Lond].

The above techniques are based simply on the intensity of scattered light by particles (principally Mie scattering) which is well understood. Most of the current research in this field is aimed at improving the image capture and analysis techniques employed. A detailed theoretical evaluation of the techniques and the data analysis procedures is presented in [22], additional information on early examples being presented in [107]. Temperature measurement by scattering techniques is dealt with extensively in [161, 155].

Rayleigh scattering has also been employed to obtained real-time concentration measurements in a propane/air co-flowing jet [50].

3.4.3 Holography

Holography is a photographic technique which is capable of generating 3D images. It accomplishes this by storing both amplitude and phase information from a coherent wave disturbance. Basically coherent light impinges upon, and is reflected (scattered) by an object of interest. This reflected light, of unknown properties (ie phase,amplitude) is then interacted with a coherent light source of known properties to form an interference pattern. This interference pattern, the hologram, is then recorded on a suitable media (photographic film, plate). By illumination of the hologram with a reference beam, a 3d image of the system recorded may be generated. This may then be analysed, usually by computer, to provide quantitative flow information. An holographic recording system is shown in Fig 3.3. A detailed study of holography is presented in [92, 157], with a good early review in [104].

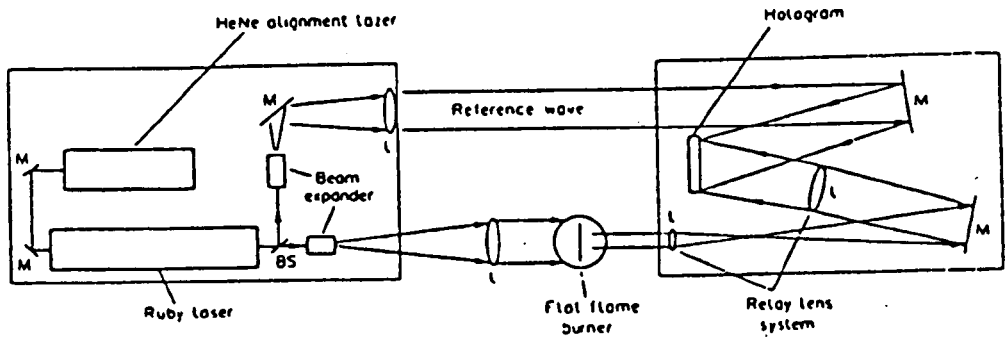

Figure 3.3 - Typical Holographic Arrangement [115]

Holography can be used purely to obtain 3D qualitative images of flow structure [16,93], or to obtain quantitative information such as particle velocities,temperature [95], particle size and particle number densities [13,25]. The information available depends on the specific holographic technique employed. Pulsed laser and double exposure holography provide velocity information [16,93,94,104], with pulsed 'laser-knife' techniques being employed for high particle concentration uses [18]. The holograph does provide a means of measuring several parameters simultaneously in 3D.

The use of holography in real time, for fast events, is not feasible. Cameras by their nature are unable to store 3D information, and even reconstructed holographic images must be saved as multiple planar 2D images and analysed thus. To run a real time holographic system the hologram would have to be scanned and its information removed in time scales far less than that of the event it was measuring.

3.4.4 Laser Doppler Anemometry

Throughout this section the term LDA is used to imply both LDA and laser Doppler velocimetry (LDV), the two techniques being identical.

Laser Doppler anemometry, first introduced as a measuring technique in fluids as early as 1964 [128], has become the most widely used commercial laser-based technique, it being available in 'off the shelf' forms from several companies. LDA utilises light scattering by particles from an interference pattern to provide particle velocity information.

A simple description of the technique will be presented, a more involved discussion being presented in, amongst others, [24, 103, 148].

Two coherent light beams, usually derived from one laser light source, are made to cross at a point in the flow system of interest. In the crossing volume a stationary fringe interference pattern is formed, and particles passing through this volume scatter light with varying intensities depending on their position within the fringe system. The frequency of the received light signal, as detected by, say, a photodetector, will be proportional to the velocity component of the particle moving perpendicular to the fringe pattern.

The fringe spacing of the system is proportional to the laser beam wavelength and the half-angle between the two beams. Hence knowing the wavelength and half-angle allows easy calculation of the velocity, without need for calibration or any temperature, density or viscosity alignment procedures.

If one of the laser beams is shifted slightly in frequency, then a moving fringe pattern is formed. The interaction of the particle with a moving pattern allows the resolution of negative and positive velocities to be determined.

A typical LDA layout is schematically shown in Fig 3.4, along with the fringe principle.

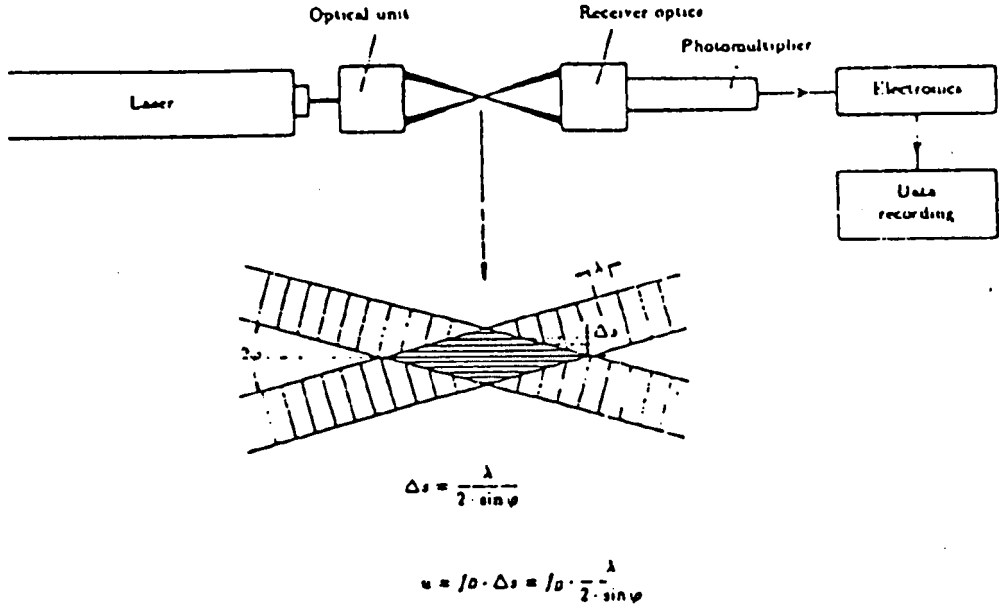

Figure 3.4 - Schematic of LDA Arrangement and Fringes [127]

Being a firmly established technique, it has been used in a wide variety of fields, including engine combustion, fluid flow, geographical modelling [20, 21, 49,111,113,114,116,118,121] and the available literature on the subject is considerable. For the latest applications, the reader is directed to the annual American Society of Mechanical Engineers' (ASME) publication [112], dedicated conference proceedings [145, 152] and other general laser conferences [147, 146, 151].

A limitation of LDA is its effectively single point measurement - thus many measurements are required to get a full-field velocity profile. Thus it is of limited use in turbulent situations where instantaneous full-field measurements are required. Another requirement is that the seeding particles, if used, must accurately follow the flow. Optimisation of seeding is discussed in [163]..

A simplified velocity measurement technique, the laser-two-focus method [58], has been suggested. This simply involves scattering from two independent, non-crossed laser beams which cut through the flow at a known distance apart. The velocity is

calculated by time-of-flight methodology. This technique is said to have advantages over LDA due to its higher data rate, and its ability to deal with changes in particle size and velocities without the need for changing the optical configuration.

3.4.5 Degenerate Four Wave Mixing (DFWM)

This technique studies the non-linear response of molecules to two opposing laser beams by simultaneous interrogation with a third. Explained simplistically, the two opposing beams effectively 'write' an interference pattern onto the molecules and the third beam is reflected from this interference grating. This beam, the conjugate of the probe beam, is then detected by a ccd camera, or similar 2D detector. The intensity of the beam is proportional to species concentration^2, and by comparing the intensities of signals, which must contain information on at least two transitions from different rotational energy levels, temperature may be determined.

The information that has been obtained from this technique, in the field of combustion, includes 2D mapping of temperature fields [135] and flame temperature measurements [126] along with spatially resolved species distributions [137]. A more detailed treatment is given in [44].

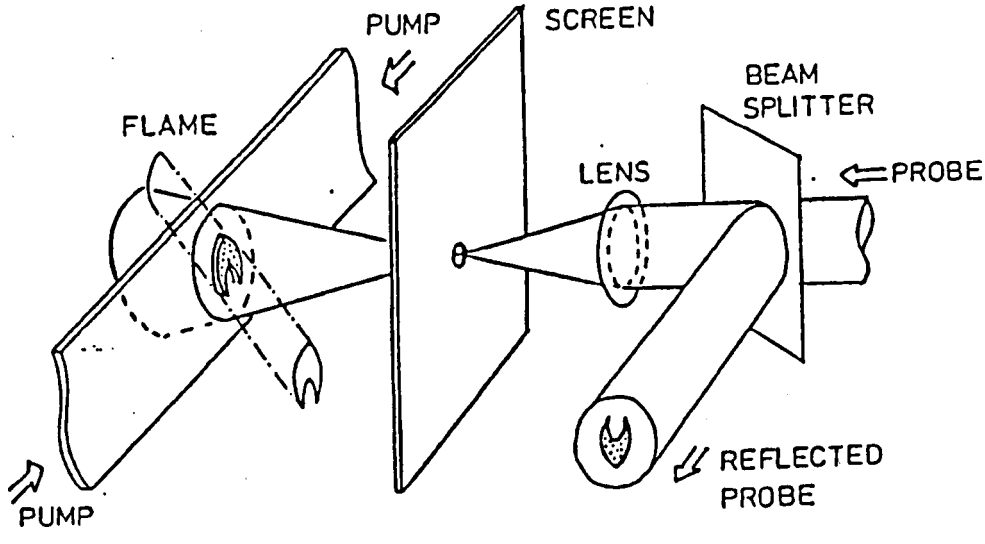

Figure 3.5 - The Pinhole Noise Filtering Effect [44]

Being a non-linear technique means that the primary signal is very weak, and high power beams are required. An advantage of this system is that the primary signal, by virtue of being the conjugate of the probe beam, exactly retraces the path of the probe beam. Hence if the probe beam is focussed through a pinhole then the primary signal beam will also pass back through the pinhole. This allows unwanted 'noise' such as fluorescence signals to be eliminated resulting in good signal to noise ratios. The pinhole noise filtering effect is shown diagramatically in Figure 3.5. At this time the main area of application of DWFM is in combustion studies where its noise reduction capabilities make it a complimentary tool for CARS and LIFS.

3.4.6 Raman Scattering

The processes involved in Raman scattering (strictly termed spontaneous Raman scattering) have already been discussed (see section 3.3.1.2). Its main area of application is combustion diagnostics, [161] but even here its use is limited due to poor signal strength. The temperature of a Raman active species is determined by the shape of its spectrum, the correlation obtained by least squares methods. The concentration of a species is proportional to the scattered light intensity. Concentration measurements have been made in a turbulent non-reacting concentric methane/air jet [14] where the primary signal was captured directly by camera, and evaporation rates and chemical characterisation [168] have also been determined.

Coherent Anti-Stokes Raman Spectroscopy (CARS) is a non-linear extension of Raman scattering, being also similar to DFWM. It provides the same information as spontaneous Raman scattering, temperature and concentration measurements, but is several orders of magnitude more intense due to its coherent nature. As with Raman scattering, its main area of applicability is combustion study and details of CARS will not be presented here, but information may be found in [77] and [44] including experimental results, a review being presented in [166].

3.4.7 Fraunhofer Diffraction Particle Sizing

This technique works on the principle of Fraunhofer diffraction whereby incident light is scattered, or diffracted, by particles through an angle which is proportional to

the particle size. A review of this and other particle size techniques can be found in [153].

The technique was developed as a particle size measurement tool by Swithenbank et al [78], the basics of which are shown in Fig 3.6.

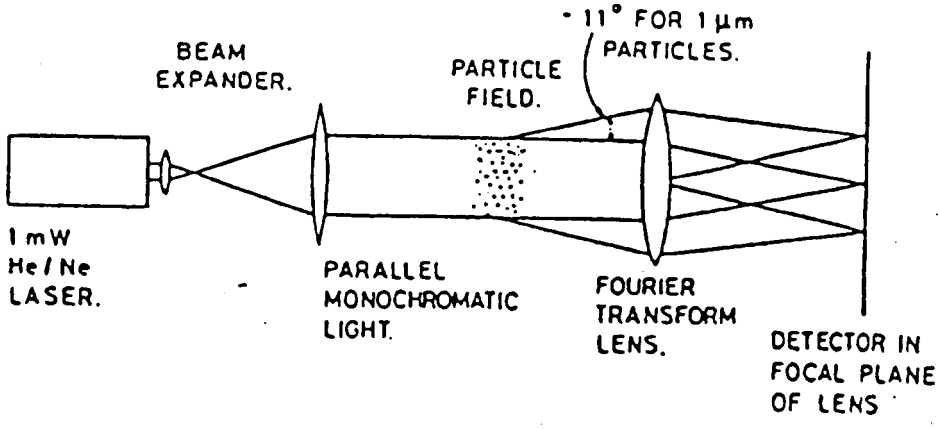

Figure 3.6 - Diffraction Particle Sizing Technique [78]

The monochromatic light from the laser source is expanded, and then formed into a parallel beam. This beam passes through the particle field (eg fuel jet, two-phase flow) wherein it is diffracted by the particles. The light is then focussed by a Fourier transform lens (FTL) onto a light detector array, the signals from which are interpreted by computer to yield size distributions.

The important element in the system is the FTL. Light parallel to the axis of an FTL is always focussed by it onto a point on the axis of the beam, and the diffracted light is 'focussed' around it. The position at which the diffracted light is 'focussed' is dependent solely upon the angle at which it enters the lens, and is independent of the position of the particle in the laser beam. Hence the motion of any particles also has no influence upon the focussed diffraction pattern, and so the technique can be applied to moving particles, ie flow scenarios.

There are problems associated with this technique. Firstly multiple diffraction of the laser light, due to high particle number densities, requires correction to avoid

inaccurate results. Light scattered by one particle is assumed to undergo no further interaction with the particle field before reaching the FTL [78]. In a dense spray, however, this is not the case, and the scattered light is then subsequently scattered by other particles. This results in the calculated distribution being artificially displaced towards larger angles of scattering, ie smaller particles. Overall, unless taken into account in the calculation process, a broader distribution with a smaller mean size value than is actually present is determined. This problem has been extensively investigated and both empirical and theoretical solutions proposed [79,80,81,82,85,86,89]. The modelling algorithms derived have extended the obscuration limit of applicability from 50% up to 98% [80], although different algorithms have been applied to the Rosin-Rammler, Log-Normal distributions (up to 97.5%) [79] and to the model-independent distributions (2% oversize estimation at 95.9% obscuration, 10% oversize at 99.4% obscuration) [80].

A further problem [89] is related to the inversion of light scattering data to drop size distributions. This is basically the potential error which may arise through the theoretical assumptions and approximations made in the energy to size distribution conversion modelling process (ie. inaccuracies in the conversion models).

In the case of rapidly evaporating droplets, such as would be the case for a superheated fluid, there is also the possibility of incorrect measurement due to diffraction from the 'ring' of dense vapour surrounding the liquid droplet. This would give rise to smaller particle size values, and would also give rise to 'dense' spray type problems.

Fraunhofer diffraction has been proven as a measurement tool, and is available commercially as the Malvern Instruments particle sizer. This technique, principally in the Malvern guise, has been used in various particle measuremeent arenas, including two-phase flow, and as a yardstick for other techniques. References include [83,84,87,88,90,93,99,105, 162]

Identical scattering techniques have recently been developed employing different numerical analyses [91] which appear to provide a greater degree of accuracy and a wider range of particle size applicability.

Disadvantages are that this technique only supplies 1D information, and because of the wavelength of light employed its size range is also limited to particles >1μm.

A further disadvantage of the Fraunhofer/Malvern style of instrument is that it measures only the particle size distribution and concentration. Current trends have been towards using the phase Doppler based systems due to their simultaneous velocity/size/position distribution determination capabilities.

3.4.8 Fluorescence Techniques

A basic theory of fluorescence has already been presented (section 3.3.1.2), more detailed information may be found in [35,70,71, 149], and Chapter Eight of this thesis and references therein. In this section a systematic experimental arrangement for fluorescence measurements will be presented.

The practical use of fluorescence in fluid flow can be split into two distinct parts:

It can be used purely as a flow tracer. In this case the fluorescence aids visualisation only, its image providing a way of observing the fluid motion. This may be used, indirectly, to obtain quantitative velocity information by manual, or digital, distance/time correlations. These techniques usually employ photography, or cinematography as their information storage medium, and digital image analysis. Examples include [10,27,30,31,32].

Photochromic dye techniques have also been employed in a similar manner to true fluorescence techniques in order to visualise flow patterns, and obtain velocity measurements [46,47].

Quantitative information may be obtained directly from the fluorescence radiation. The fluorescence spectrum (peak wavelength, intensity, width etc) has been found to be dependent on various physical parameters. These dependencies can be used to obtain temperature, concentration and other useful measurements. This technique is strictly termed laser-induced fluorescent spectroscopy, LIFS.

In both the above cases the fluorescent properties of the actual material being studied can be utilised, but in many situations it is better to use other, more strongly fluorescent, materials instead (termed fluorophores). This is generally the case where the system contains no suitably fluorescent species, or a stronger signal is required.

Fluorescence techniques, principally LIFS, possess the usual advantages of laser-based techniques; they are non-intrusive, and capable of high spatial and temporal resolution (if required). They may also be employed in-situ, in real time. Employing laser light sheets also permits 2D and pseudo-3D measurements to be made. References include [54, 55, 75, 76].

Fluorescence, as detailed previously, has the advantage over other 'scattering' processes, eg Raman and Rayleigh, that its scattering cross section is greater. This essentially means that stronger signals are generated from this technique, resulting in better signal to noise ratios and easier detection. Detection of the information signal is further simplified by the fact that the emitted signal wavelength is different to the excitation wavelength, thus removing, by the use of suitable filters, problems caused by reflected laser light. The emitted fluorescence wavelength is also usually in the visible range which is a practical experimental advantage.

A potential disadvantage of the technique is that in many cases it is a 'mimic' technique, ie the host temperature is effectively inferred from the measured temperature of the fluorophore. Care must therefore be taken to ensure that the fluorescing material accurately mimics the host. The fact that O_2 quenches fluorescence from many materials is also a problem for some in-situ measurements. However, Laser-Induced Predissociation Fluorescence, LIPF, can be used to

overcome quenching problems. In this variation of standard LIFS, quenching of the excited state is avoided by exciting the molecule into a predissociative electronically excited state. Such a state has a very short light emission lifetime, sufficiently short so that collisional effects can be neglected, even for elevated pressures [59]. This technique has been employed to obtain quantitative density and temperature measurements in combustion studies of a methane/air flame[59].

In a typical LIFS arrangement, a laser is used to provide the excitation source required to excite the specific fluorophore contained in the system. Most often this source will be in the ulta-violet region of the spectrum, and the resulting fluorescence will be in the visible. The fluorescence is then captured, and stored for later information retrieval. The means by which the fluorescence is detected and stored is via monochromators and photodetectors for most precise quantitative analyses, or photographic film processes for less involved quantitative or qualitative analyses. The system shown in Figure 3.7 is one used to obtain fluorescence signals from two-phase flow for temperature measurement purposes.

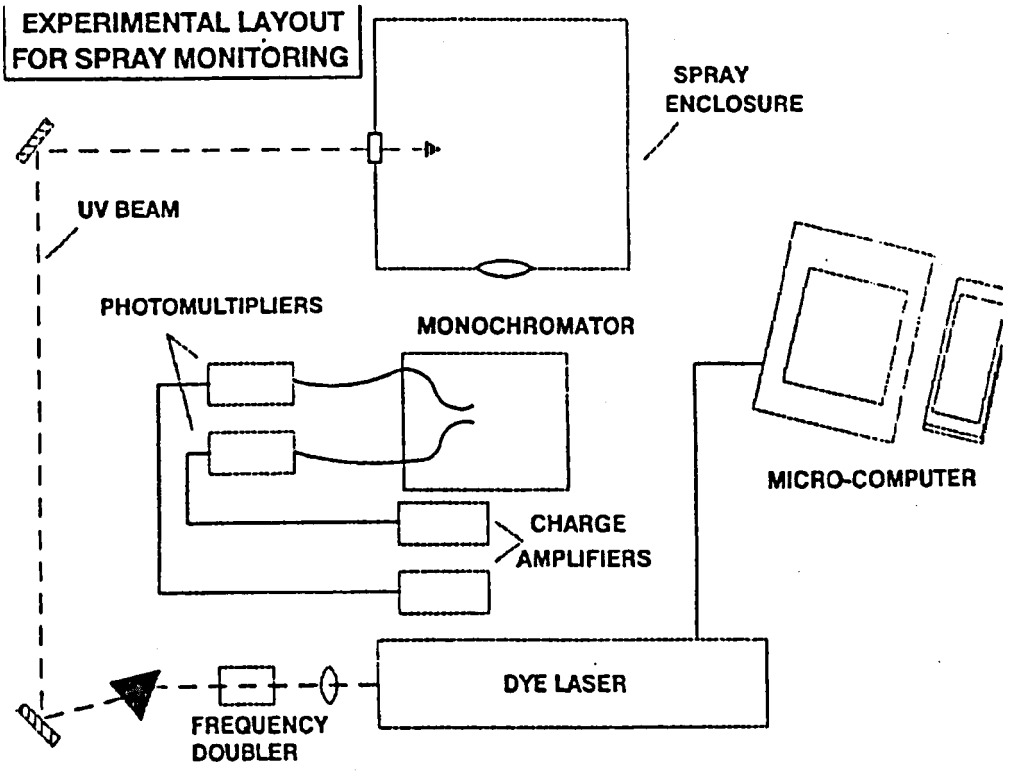

Figure 3.7 - Typical Arrangement for LIFS Measurements [38]

By virtue of its employment of fluorophores to mimic the behaviour of the host material, the system has a relatively large degree of flexibility. By judicious choice of fluorescing system, the fluorescence can be made phase specific, and there is some degree of control over the emission and absorption characteristics [65-71,36,38,40].

Fluorescence can be used directly to measure several desired parameters. The exact property of fluorescence used to quantify the parameters varies.

Simple measurement of the fluorescence intensity has been found to yield quantitative information on temperature [2,49,156] and concentration [8,72], with intensity ratio-ing being used to remove sources of error in several two-phase tempereature measurement arenas [3,6,33,34]. The fluorescence lifetime can also be used to determine temperature [1,4,7].

Variation of spectra (peak height, peak position) with temperature [33, 34, 38,39,40] have been utilised, either by using the variation of the ratio of fluorescence intensities of different exciplex/monomer combinations, or one wavlength intensity variation, with temperature.

More involved measurements have involved looking at the Doppler effects on fluorescence spectra. Velocity has been found to be determinable from the Doppler shift [3,17,56], and Doppler line broadening is dependent upon the pressure field [3].

The laser source for the technique can be varied, as discussed in section 2.2.1. 1D line measurements can be taken, 2D information may be obtained using laser light sheets (PLIFS-planar laser-induced fluorescent spectroscopy), or pseudo-3D studies are possible using multiple PLIFS [158, 159, 169]. Fibre optic probes may also be used to generate evanescent local fluorescence measurements [73] from dye-labelled proteins and solutions.

Fluorescence techniques have the ability to be applied over wide temperature ranges: surface thermometry for cryogenic work (4 - 125K) [7,52,53] and higher

temperatures (300-1700K) employing rare-earth-doped inorganic compounds such as Dy:YAG, La_2O_2S:Eu, and Y_2O_3:Eu [1,5,6] illustrate this.

Similar materials have also been employed in other extremes such as high pressure measurements [5] and in-situ temperature determination of lime kiln samples (900-1100°C) [4].

Certain compounds/moieties fluoresce sufficiently well to be of use without recourse to doping. One such moiety is the OH radical. The fluorescence signal can be used in combustion scenarios to determine local and full-field pressure, temperature, and velocity measurements [3]. Even O_2 has been used as a source of fluorescence [2,59] to measure heated air temperature (500-1100K) in a PLIFS experiment, and density in a methane/air flame.

LIFS can be applied to gaseous species, temperature and velocity measurements have been made in an Argon jet [17] with Iodine as the fluorophore. Vapour phase exciplex emission on its own has been extensively demonstrated, for example [8,60-63,68,69].

In direct relation to two-phase studies, Melton first used the technique of fluorescence as a differentiating simultaneous visualisation technique [30] for the liquid and vapour phases of a diesel spray. Using laser sheets, he collected the independent liquid and vapour fluorescence in 'frozen flow' photographs, which were then digitally analysed (not in real time). Possible problems were discussed, such as large droplets biasing the temperature obtained for an area if they are optically thin, and reabsorption of fluorescence (this doesn't occur with exciplexes) in [31,32].

The dependency on temperature was noted, and exciplex systems were used to obtain liquid temp measurements [33] at relatively high temperatures. The technique was extended, by the choice of suitable fluorophores, to lower temperature boiling point materials (0-100°C) [34], including butane. An accuracy of ±1°C in hydrocarbons up to 400°C using intramolecular exciplexes was obtained [64].

The work of Melton has been extended by Ewan to materials of direct relevance to this study of two-phase flows [36-43]. These are studies of two-phase jets of freons and the applicability of laser-based techniques to such studies [37,41,42,43].

LIFS has been used successfully in Freon 11 jets to obtain liquid temperature measurements [36,38,40] and LIFS gas phase measurements developed [39,40].

A limited literature review of EFT (exciplex fluorescence thermometry) is presented in [139], and REMPI (resonance-enhanced multiphoton ionisation), a complementary intrusive laser technique to LIFS for use with weakly fluorescing species, is described by Melton in [140]. A detailed review of the application of fluorescence for droplet and vapour temperature measurement is presented in [170].

3.4.9 Beam Attenuation Techniques

Whereas most of the techniques are based upon observing changes (frequency, spatial distribution) in the interrogating light as a result of interaction with the flow, some use has been made of the unaltered (unscattered) light. In these techniques the ratio of initial beam intensity to received beam intensity is used to determine desired parameters. Their complexity varies from simple measurement of single beam attenuation, used to derive particle velocities [11], to a two-colour laser-transmissometer (TCLT) system [101]. In the latter case measurement of the ratio of the extinction coefficient at two different wavelengths in a system has been used to determine particle sizes and number densities.

A slightly more involved process has been utilised to obtain temporally resolved concentration profiles around an impeller in a liquid/liquid mixer [12]. In this case great care was taken to ensure that, by refractive index matching, transmission through the two liquids at any concentration mixture was 100%. A dye was then added to the dispersed phase to attenuate the beam slightly, thus giving a direct correlation between beam attenuation and dispersed phase concentration. This experiment also showed a transmission/temperature dependence to be present, a 1°C change resulting in a 25% error of concentration.

A beam attenuation technique has also been utilised to determine two-phase void fraction, details of this are presented in the next section.

3.4.10 Optical Void Fraction Measurement Techniques

Several optical methods for local void fraction measurement have been tried [19,51,98] and reviewed [134]. These techniques however placed a restriction on the phase refractive index value that could be studied. An alternative technique employing infra-red laser light and a multimode fibre probe has been tried on air/water two-phase flows [100] which does not suffer from this problem. It is however, like its predecessors, not a non-intrusive technique. It determines highly localised void fractions based on the reflection of an infra-red beam at gas/liquid interfaces. When the probe tip is in either the liquid or gas phase then refraction takes place, and no signal is reflected back into the probe. At a gas/liquid interface however reflection occurs and a signal is sent back down the probe to a data collection system. The void fraction at this localised point may thus be determined from these readings.

A further optical measurement technique for void fraction measurement is presented in detail in [110A, 110B, 110C]. Here beam attenuation of a gas laser is used to determine void fraction in bubbly two-phase air/water flow. The technique employed here is non-intrusive, but gives 1-d (line) void fractions (unlike the previous techniques which give local values). The experimental set-up of this technique also allows simultaneous local liquid velocity determinations.

3.4.11 Laser Photoacoustic Spectroscopy

This technique is used to determine the number density of gaseous species, but needs to be calibrated for each species. It has been used in laboratory conditions for gas analysis utilising infra-red laser sources [143]. The basis of this technique is as follows:

Laser light, tuned to the resonance frequency of a known rotational/vibrational transition of the species under study, is passed through a sample of the species. The

species is excited by the laser light, and undergoes thermal de-excitation, ie the laser energy is lost by partial, and local, conversion into thermal energy. This de-excitation process has associated with it a pressure rise, which results in an acoustic signal. The strength of this signal is proportional to the number density of the species being studied.

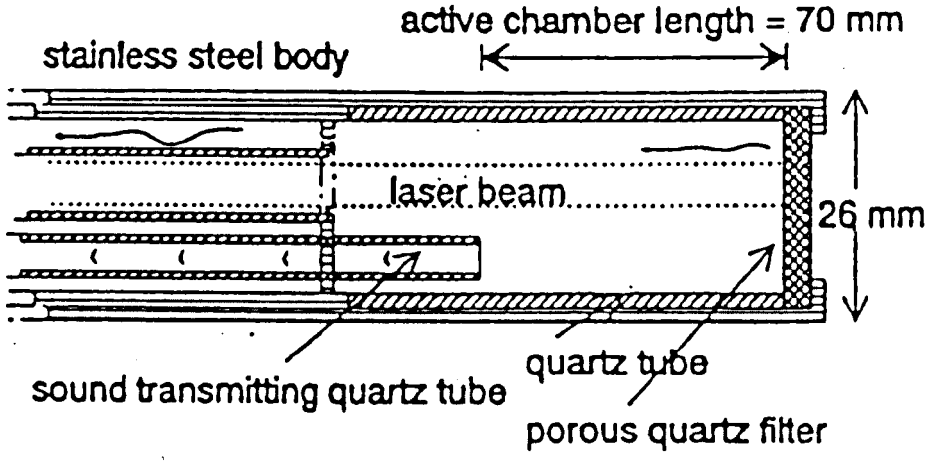

Figure 3.8 - Laser Photoacoustic Test Cell [138]

An experimental probe, utilised for making in-situ gas analyses in a fluidised bed reactor [138], has been developed and is shown in Figure 3.8. Here the gas to be analysed is sucked into a test cell (in situ), and laser light is supplied to this cell via a probe. The resultant acoustic signal is detected by a microphone, and its resultant electrical signal passed to a data acquisition system.

3.5 CONCLUSIONS DRAWN FROM THE REVIEW

3.5.1 Previous Work

Laser-based measurement techniques have been widely applied in the field of fluid mechanics, combustion, two-phase flow, and related areas. Several measurement techniques are available for the attempted determination of desirable two-phase source terms, the exact system utilised depending upon experimental and financial constraints.

Despite the widespread use of such techniques and the variety of situations in which they have been employed, with the exception of combustion studies, the range of materials studied is relatively limited. In most of the two-phase studies combinations of water, steam, air and inert gases (eg nitrogen) have dominated, due primarily to the link with nuclear accidents and ease of study. This literature survey has uncovered no relevant laser-based two-phase research with propane, and (excluding combustion studies) very little with other hydrocarbons of interest.

The vast majority of two-phase work has been undertaken to attempt to apply techniques to difficult experimental conditions, eg nuclear cooling bundles, or to merely assess their capabilities in measuring desired parameters, eg bubble size, void fraction. This has almost always been done with 'uncomplicated' media so as to simplify the data interpretation. Even in these cases the work has been centred around solid/liquid flows, non-volatile liquid sprays, and liquid/vapour flows (where gas dissolved in liquid is the principal study).

The small amount of work that has been undertaken on gas/liquid two-phase jet, or flashing jet, releases has centred on non-hazardous simulant fluids, such as Freons, water, or diesel jets [167].

3.5.2 Chosen Techniques

As detailed in Chapter Two, a range of physical parameters are required to fully specify the behaviour of a two-phase release. In this work the liquid phase parameters will be studied, such as the droplet velocities, distribution, and temperature. Other desired parameters will also be determined from the liquid phase measurements. No vapour phase measurements will be attempted.

The following laser-based techniques were chosen for this phase of the experiment:

Droplet Size Distribution - Malvern particle sizer

(Fraunhofer diffraction technique)

Droplet Velocity - Laser Doppler Anemometry system

Droplet/Liquid Phase Temperature - Laser-Induced Fluorescence Technique

The storage conditions, and approximate exit temperature and pressure are to be measured by use of traditional techniques, such as thermocouples and pressure transducers. The mass loss, and hence mass release rate, will be determined by the use of load cells.

An explanation of the choice of laser-based techniques is presented in the following sub-sections. It should be noted, however, that the choice of techniques being employed on this research project was also, to some extent, determined by their availability to the author.

:

3.5.2.1 Malvern Particle Sizer

The Malvern Particle Sizer was chosen for droplet size determinations on the ground that it covers a size range which is appropriate to the droplet sizes expected, and the fact that it is a well tried and documented technique.

As shown in the review of techniques, problems occur with this technique in high obscuration scenarios where multiple diffraction of the probe beam invalidates the measurements. A multiple diffraction computer code, allowing accurate measurements up to approximately 96% obscuration will be utilised, as it is expected that measurements taken towards the release nozzle will be subject to this problem (regions 2 and 3). It is also expected that obscurations greater than 96% will be encountered close to the exit nozzle (Region 2) such that accurate measurements will not be possible. There is no physical solution to this problem, and no other technique offers the same level of obscuration penetration coupled with well-established performance and simplicity.

3.5.2.2 Laser Doppler Anemometry

This technique has similar advantages to the Malvern system in that it is a very well-established, widely used and documented measurement technique. In a recent paper on laser techniques applied to combustion [137], it was deemed the best technique for velocity measurements ahead of PIV (particle image velocimetry).

Compared with PIV it generates only, effectively, single point velocity data as opposed to 2D information, but under the present experimental set-up this is not a problem. Both techniques are affected by high particle/droplet density due to probe and signal beam attenuation. Distortion of the measurement fringe pattern with LDA through high droplet density is also a potential problem, but as with the Malvern system, measurements will be taken until its reliability to generate accurate data is lost.

The co-flowing air may also be studied with the use of LDA, and suitable seeding particles, to enable information to be obtained on air entrainment by the jet.

Holography was not considered as a possible alternative (3D velocity) due to the complex and labour-intensive data analysis routines required.

A further reason for the use of LDA was that an LDA system is already in the possession of Fire and Thermofluids Section, where this work is to be undertaken.

3.5.2.3 Laser-Induced Fluorescence Spectroscopy

The obvious advantage of using this relatively novel technique for temperature measurements is its non-intrusiveness and high signal intensity when compared with Raman techniques (eg CARS) and DFWM (Degenerate Four Wave Mixing). A further advantage of this technique is that it has already been successfully applied to temperature measurements in two-phase Freon jets [36-43]. This was achieved as an extra-mural part of this research project, and hence a relatively high degree of competence and knowledge in this area is available to this experiment.

One problem with this technique is identifying a suitable fluorophore for use with propane. Work by Melton [34] has identified some fluorescing systems for use with lower order alkanes, and Ewan [36-43] has successfully applied this technique to Freons. With this technique the choice of propane as the subject material is an advantage on the grounds that fluorescence quantum yields increase with decreasing solvent polarity and decreasing temperature. In both cases propane will provide a fluorescence enhancing environment, being both non-polar and having a low boiling point.

Fluorescence quenching by oxygen is also a problem in LIFS experiments, although by only studying the liquid phase the effect should be negligible.

Compared to combustion experiments, signal qualities should also be high due to a lack of background fluorescence usually present with a combustion process taking place.

LIFS may also be employed, in the longer term, to generate temperature and concentration data from the vapour phase.

3.5.2.4 Other Techniques

Other non-intrusive techniques may be applied to this experimental system as, and when, they are deemed necessary, or become available. It is envisaged that simplistic quantitative flow visualisation techniques, such as photography and cinematography, will be utilised as a matter of course. Other techniques employed in subsequent work on this experiment will depend, in part, on the success of the first phase, and the available time and resources.

3.6 OVERALL CONCLUSIONS

The initial phases of accidental two-phase releases, especially of propane/LPG, have received very little experimetal attention. Little or no accurate data exists for the early stages of a release, making computer model validation impractical. This is

principally due to the difficulty of obtaining valid data where conditions depart widely from those of thermal equilibrium, such as exist in the early stages of a two-phase jet.

Laser-based measurement techniques have been identified as suitable methods of obtaining valid data, due to their non-intrusive nature. Several techniques exist which may be successfully employed in two-phase release studies, the majority of which were originally developed for combustion studies.

A number of these techniques have been chosen for use in an initial experimental programme which should permit the generation of accurate and valid data points for regions approaching the release point of a two-phase jet. It is unlikely that the data will be obtained for the densest parts of the release (ie the release point itself, and parts of Region 2 very close to it), but any data obtained in Regions 2 and 3 will be a significant improvement on what is currently available. Data obtained from this experiment will be of great use in improving and extending the presently limited two-phase release models.

CHAPTER FOUR
EXPERIMENTAL FACILITY DESIGN AND CONSTRUCTION

4.1 INTRODUCTION

One of the first requirements of this work was to design and construct a facility which would permit non-intrusive techniques to be safely used to study a two-phase flashing propane jet release in a laboratory environment.

This work was undertaken, and the facility was constructed, at the Health and Safety Laboratory (HSL) of the Health and Safety Executive (HSE: the UK regulatory body on industrial safety). Due to the potential hazards of the experiment, the facility design and construction required detailed consideration. The facility, its components, and associated procedures for operation, maintenance and emergency events, was fully documented in an Equipment Documentation File (EDF). Thus a comprehensive guide to the facility, including design plans, design progression pathways, material test documentation, material compliance data etc, can be found elsewhere [1, 2].

This chapter presents the philosophy behind the facility, a detailed description of its components, and the associated paper controls (safety assessment, operating procedure, emergency procedures etc). The operating, emergency and maintenance procedures are presented in Appendices 4A and 4B. A list of the technical components, and their relevant specifications, are presented in Appendix 4C.

4.2 FACILITY DESCRIPTION

4.2.1 Facility Philosophy

The experimental facility being utilised for this work is a completely new purpose-built system. It basically consists of an instrumented storage vessel, an instrumented nozzle release system, an experimental chamber, and an extract system. The experimental facility will allow variable, and controlled, conditions of propane releases to be studied at stagnant liquid temperatures up to 44°C, and pressures up to

15 barg. Using nitrogen padding, releases may also be undertaken with propane at non-equilibrium stagnant pressure/temperature conditions. The propane mass flow rate can also be varied between known limits.

Small scale laboratory releases were chosen for the following reasons:
The small scale was advantageous in that it reduced the costs both of the facility and consumables. There is also a larger scale outdoor release facility already present at HSL, Buxton so the small scale facility allows comparative experiments to be undertaken, and scaling effects to be investigated.

Some of the laser-based techniques, eg LIFS, may not as yet be applied outside a laboratory environment, and some are not suitable in their current form to large scale measurements.

The main reason, however, for a small scale laboratory based facility was safety. The laboratory environment is a much more controllable environment in terms of both ambient conditions and 'human factors'. Thus a comprehensive safety system could be developed for the facility and the associated laser-based techniques. Safe controlled dispersion of the propane (which is always unignited) was also more easily accomplished in such an environment.

The release facility was purpose built so that each aspect of it could be specifically designed to take into account the experimental requirements and the safety essentials. Safety was considered an integral part of the design of the facility, it being designed from the start around certain safety philosophies.

The facility was also designed with maximum lifetime, long-term usage in mind. This is shown for example in the use of construction materials which allow a wide range of fluids and gases to be used in the facility with little or no modifications required.

The actual design has been carefully thought out to maximise the potential applications to which the facility may be put, including constructing one side of the

experimental chamber from three hinged independent large clear perspex sheets. This allows both good visibility into the chamber and the ability to place relatively large objects inside it, for the purpose of jet impingement studies or flow field studies around obstacles.

The extract system combined with the experimental chamber can also be used as a low velocity (~1.0 m/s wind tunnel). The fact that the experimental chamber has been designed for laser-based studies, and therefore has a high degree of optical access, further increases the potential usefulness of the facility.

The facility was located in the current Laser Laboratory of the HSL at Buxton, Derbyshire, due to the fact that it was already equipped with a door-laser interlock system, into which the various laser-based techniques could be, or already were, connected.

4.2.2 Brief Description Of Experimental Layout And Procedure

A schematic diagram of the experimental facility is shown in Figure 4.1.

The storage vessel is instrumented to give mass (Tedea-Huntleigh 104H load cell system), temperature (k-type thermocouple) and pressure (Druck 0-20Barg transducer) data.

Pressure-liquefied propane is uniformly heated to the desired temperature (in the range ambient to 45 °C) by the use of an external trace heating tape, a temperature control system, and a pneumatically driven pump. The storage pressure can also be set independently to the temperature of the liquid propane by the application of nitrogen into the propane vapour space. Both the liquid propane storage temperature and pressure are measured for data collection purposes. The heating control system monitors the liquid temperature, via an independent thermocouple link, to keep it at the desired value.

The entire vessel is contained within a one-hour rated flameproof safety store as shown in Figure 4.2. All electrical appliances inside the store are zone 0 or zone 1 flameproof, appropriate equipment being fitted with Zener barriers. All control panels are situated inside the main laboratory building.

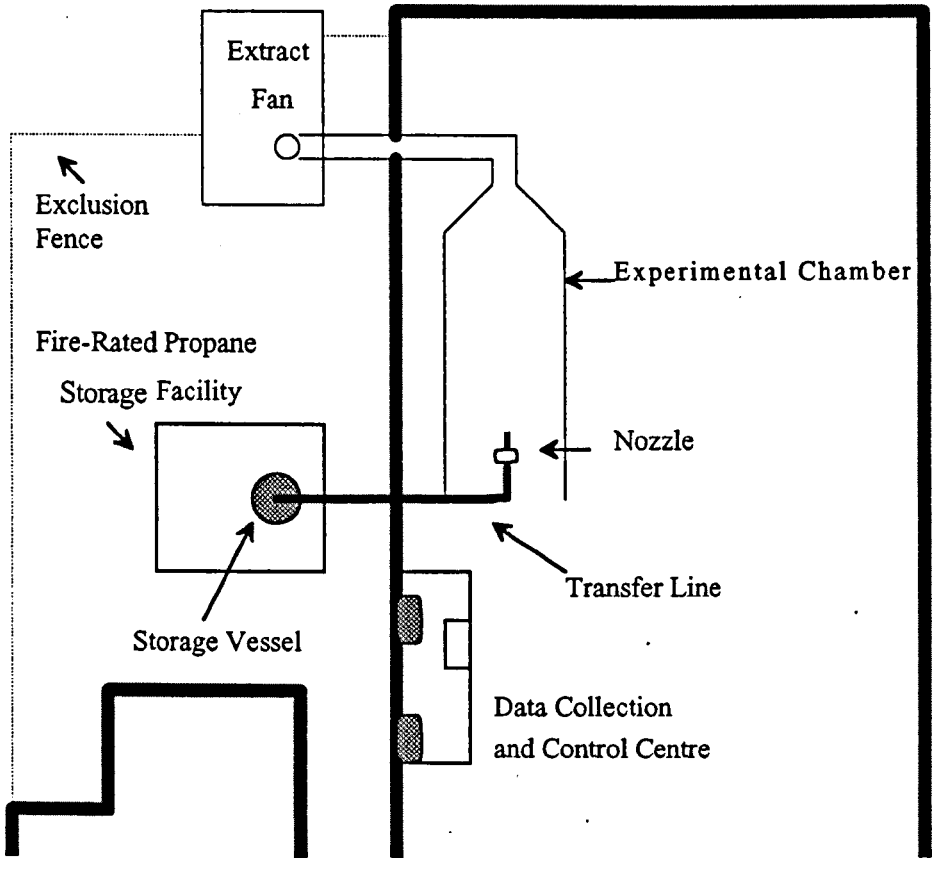

Figure 4.1 - Schematic of Experimental Facility

Once the desired storage conditions have been obtained, the liquid propane is released by the opening of remotely controlled pneumatic valves, one situated on the vessel outlet pipe and the other between the header tank and the nozzle system. The liquid propane then travels down the transfer line, into the header tank (where further temperature and pressure measurements are obtained with the same type of instrumentation as that employed on the storage vessel), and out through the nozzle system.

A range of nozzles was designed for use with this facility: 4mm i.d. x 40mm length, 4mm i.d. x 80mm, 6mm i.d. x 60mm, and 6mm i.d. x 120mm. The majority of this work, however, employed only the 4mm i.d. x 40mm length nozzle due to time constraints.

Figure 4.2 - Storage Vessel and Flameproof Store

The propane jet is released into the experimental chamber, where various physical parameters are measured non-intrusively by the use of laser-based techniques. A co-flowing air stream mixes with the propane jet, by entrainment, as it travels down the chamber.

The propane is thus exhausted to atmosphere by the extract system, being diluted in the process to a maximum concentration of 50% of the Lower Flammable Limit (LFL).

After the desired results have been obtained, the propane release is stopped by closing the remote valve. The data is then saved, transferred, analysed, equipment adjusted (as suitable) and the process is repeated.

4.2.3 Description of Individual Components

This facility can be considered as being comprised of four distinct sections:

a) propane storage and delivery system
b) experimental chamber
c) jet traversing system
d) extract system
along with the data acquisition system

4.2.3.1 Propane Storage and Delivery System

The vessel and its associated components are shown in Figure 4.3.

The vessel is cylindrical, of stainless steel construction, and has an internal volume of 50 litres. It is designed to operate at pressures up to 15 barg, and 44°C. The vessel is seated on a platform, supported by three load cell devices (Tedea-Huntleigh 104H).

It has one liquid inlet port, and one vapour inlet port. Both of these ports are closed by the use of independent manually operated valves. The vapour inlet port may also be used to allow escape of vapour.

A one inch nominal bore liquid take-off pipe extends from approximately the bottom of the vessel up to a remotely controlled pneumatic valve.On the top face of the vessel are ports for pressure transducer (Druck 0-20Barg) and thermocouple (k-type) attachment. There is also a port in which is placed a bursting disk relief valve, as shown in Figure 4.4.

A remotely operated pneumatically driven pump is attached to the vessel at one side. This pump is used to mix the liquid during the heating process to ensure a uniformly

heated fluid. The liquid is removed from the vessel by the pump at the bottom of the vessel and pumped back in at a higher location.

Figure 4.3 - Liquid Propane Storage Vessel

Heating of the liquid is achieved by a trace heating tape externally attached to the sides of the vessel. This heating system is remotely controlled by an intelligent system. There is an insulated covering around the vessel, covering the trace heating tape. The tape is capable of heating the vessel up to the required maximum temperature, 44°C.

The transfer line is of one inch nominal bore stainless steel construction. It is attached to the vessel pneumatic valve via a quick disconnect system, which is in turn attached to a manual valve. The delivery line is of a flexible nature between the vessel and the wall of the storage facility. From the storage facility to the inside wall of the laboratory it is of rigid construction, before becoming flexible once again.

The flexible sections are to provide ease of connection and movement of the storage vessel inside the storage facility, and to allow the delivery system to be easily traversed inside the experimental chamber. Inside the experimental chamber the delivery line is connected to the header tank via another quick disconnection fitting. The header tank is of 0.75 litres volume, and is also equipped with a pressure transducer (Druck 0-20Barg) and a thermocouple (k-type) port. At its outlet there is a remotely controlled pneumatic valve, leading to the nozzle via a quick release coupling. These elements can be seen in detail in Figure 4.5.

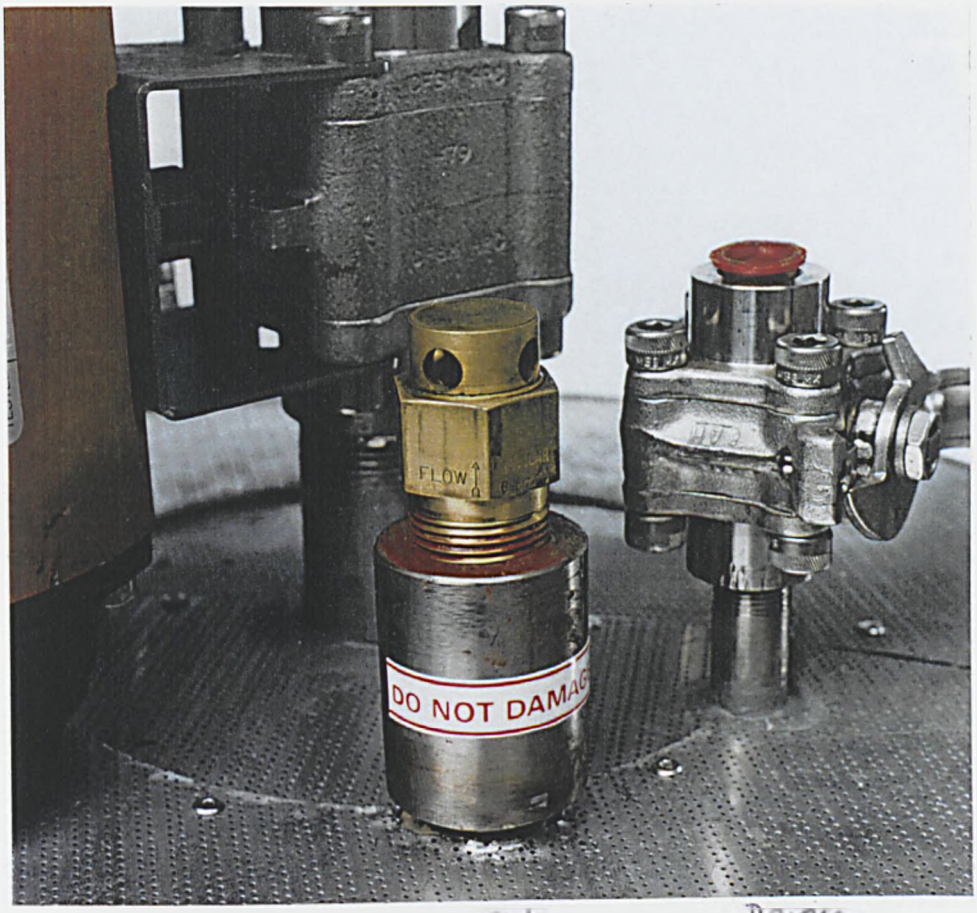

Figure 4.4 - Bursting Disc Pressure Relief Valve

4.2.3.2 Experimental Chamber

The dimensions of the experimental chamber are approximately 1m x 1 m (H x W) x 4.5 m (L). It is of wooden construction on its top and bottom faces, and one side. The other side is comprised of three independently hinged perspex panels. Both the wooden and perspex panels are held within a steel rectangular framework, mounted

at a reasonable working height from the floor by a metal support structure. The entire chamber is secured to the floor of the laboratory, as can be seen in Figure 4.6.

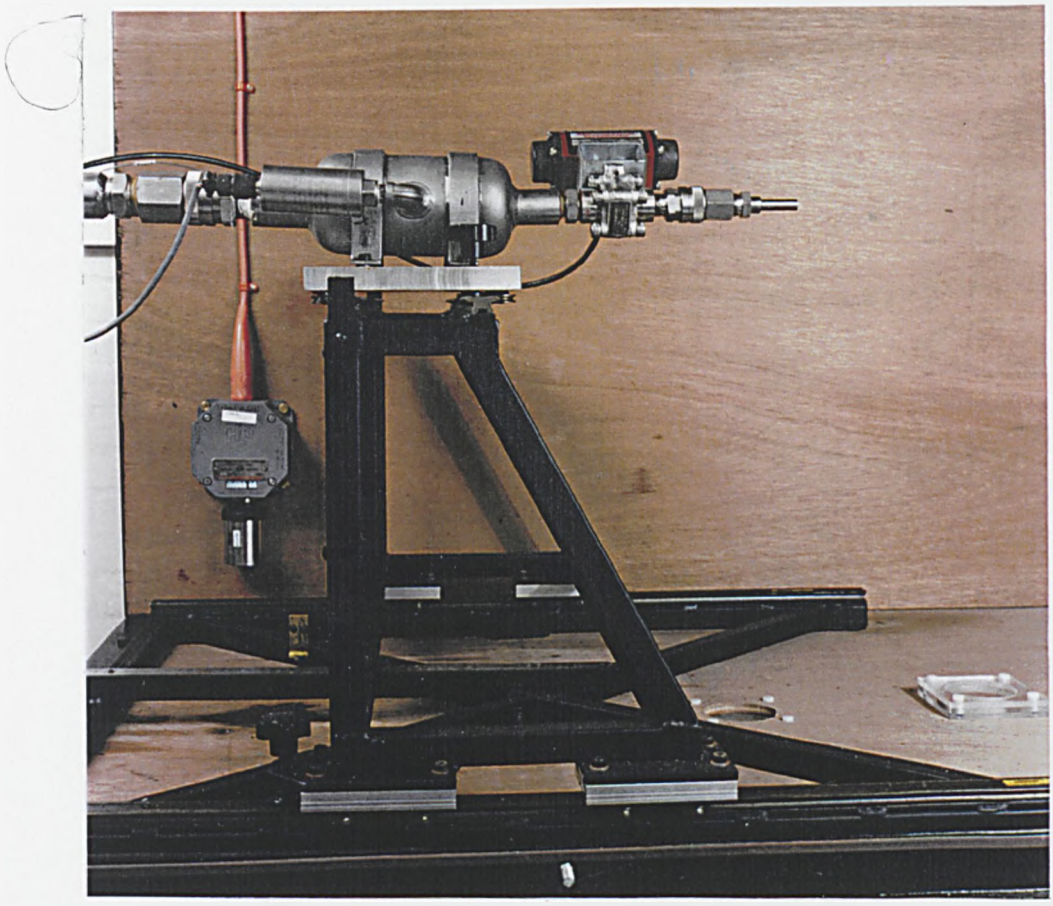

Figure 4.5 - Header Tank and Nozzle System

Optical access ports are placed at separations of 25 cm (centre to centre) axially on the top and bottom face wooden panels, and on the perspex sheeted side. Specific window attachments (lens holders) are able to be easily fastened around the ports, the type of attachment depending upon the optical technique being employed. Perspex 'blank' attachments are used to seal the window ports not in use.

The experimental chamber is fitted with a propane detector head at the (open) header tank end. This is connected to the detection system which in turn feeds into the safety control system.

Figure 4.6 - External View of Experimental Chamber

A flowswitch is fitted to the inside top face of the chamber. It is designed to 'fail' if the minimum required flow is not achieved or maintained and will, via interaction with the safety control system, result in release system shut-down. The chamber is connected directly, through an anti-vibration coupling, to the extract system.

4.2.3.3 Jet Traversing System

The traversing system is shown, with header and nozzle unit attached, in Figure 4.7. It is of metal construction, and is manually operated. the header unit is attached directly to the top of the traversing system.

It is capable of traversing 50 cm axially down the length of the experimental chamber, and 30 cm laterally in either direction from the chamber centre-line.

Quantitative positioning of the system is achieved by the use of the attached metallic rules, one on each axis of movement. The positional accuracy is to within 1 mm.

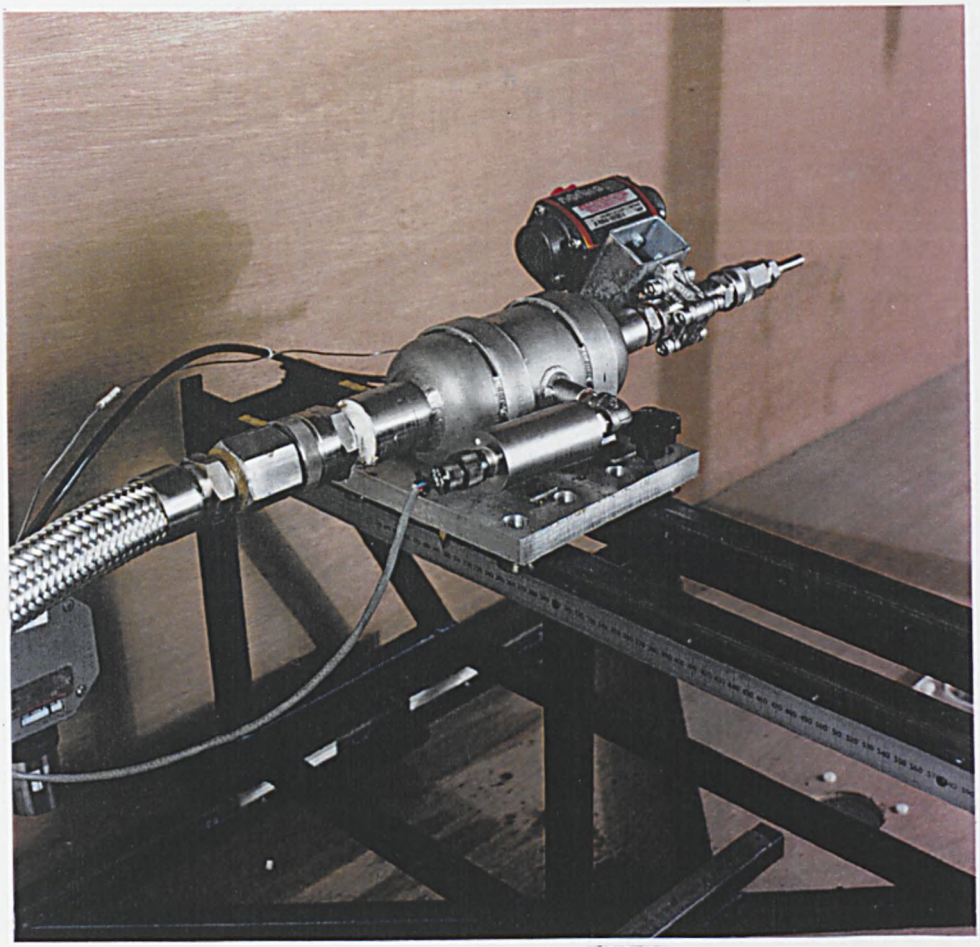

Figure 4.7 - Header Tank Mounted on Traversing System

4.2.3.4 Extract System

The extract system is of stainless steel construction. The extraction is provided by an axial fan, driven by a flameproof motor, at a rate of 12 m^3/sec. 1 m^3/sec of this is drawn through the experimental chamber to provide a co-flow to the propane release, and the remainder is derived from an external air source. Figure 4.8 shows the extract fan unit, and its position in relation to the safety storage facility. It should be noted that these photographs were taken before the exclusion fence was erected.

The extract system was designed to reduce the maximum expected propane release rate (250g/sec as determined by MPIPE) to less than 50% of LFL.

The system is equipped with a 'failsafe' flow switch which operates in the same manner as that in the experimental chamber.

Figure 4.8 - Extract System Fan Unit

4.2.3.5 Data Acquisition System and Control Area

As shown in Figure 4.1, the control area was located at the nozzle end of the facility. Within this area were situated the various facility control and safety panels such as the trace heating control unit, the air supply controls, propane detection monitor and alarm systems, valve control panel, the data acquisition system and instrument amplifiers, as can be seen in Figure 4.9. Other data collection devices, such as a Biodata Microlink system, were also set up in this area when required.

The primary component of the data acquisition system was a personal computer fitted with a CyberDas 402 data capture card. It was used to collect data, at a rate of

5Hz, from the vessel and header tank thermocouples, vessel and header tank pressure transducers, platinum resistance thermocouple (PRT) and load cells.

An owner-modified CyberDas software program was used for controlling the data collection and storage. Data from the Cyberdas system was processed through Jandel Scientific Sigmaplot software.

Bit accuracy for the CyberDas collection system was:

Temperature 1 bit = 0.26°C

Pressure 1 bit = 0.009 barg

Load Cells 1 bit = 0.049kg

Figure 4.9 - Control Area

4.3 SAFETY SYSTEMS DESIGN

As already detailed, the facility was designed from the outset with safety in mind. The actual operation of the facility, and hence the design, was conceived within the framework of certain safety concepts. These were concerned primarily with the hazards associated with propane, fire and explosion, or leakage resulting in fire and explosion. The main concepts were:

1) Safety Control System: any problem with the facility either as a result of a release, or likely to cause one, activates a safety system which closes down the release facility automatically.

2) Containment Concept: the vessel should be protected from external hazards, and that any accidental release should, contrary to general thinking, be contained and protected from ignition sources.

3) Dilution Control: propane released from the facility should be safely released into the atmosphere

4) Negative Pressure Concept: the experimental chamber was to be operated at an effective negative pressure. Any flow around the (open) header unit end of the chamber was always drawn into it and taken through the extract system.

4.3.1 Safety Control System

This was achieved by the design of a safety system, and control panel, which performed the following functions:

It controlled the opening of the two pneumatic solenoid valves, both independently and synchronously. Both valves were of the 'fail-safe' type, so loss of air supply resulted in their closure.

It provided visual warning signals inside the laboratory that the two flowswitch alarms, one in the experimental chamber and the other in the extract fan housing,

were operational. It cut off power to the solenoid valves when an electrical 'unsafe condition' signal was received from either of the flowswitches, or either of the two propane detector heads (one in the safety store, one in the experimental chamber).

Loss of electrical power to the control unit, or any of its satellites (flowswitches, propane detectors) would also result in safety shutdown.

The system is equipped with a manual emergency stop function button. All of the shutdown mechanisms are latching and therefore require re-setting after being triggered, even if the 'emergency' situation has passed and the system satellites have returned to normal operation.

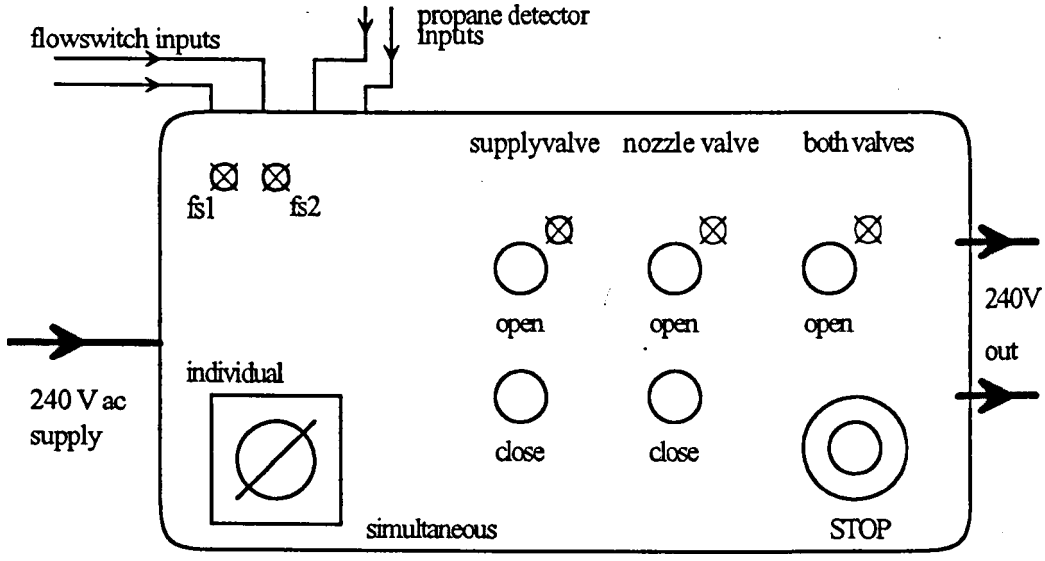

Figure 4.10 - Schematic of Control Panel

The propane detection system, whilst linked into the safety system, is an autonomous unit. It possesses its own audible and visual alarm system, both inside the laboratory and outside the storage facility, and back-up power supply. The system was purchased for the facility from Crowcon Ltd.

Control Panel Components:

1) individual 'open' and 'closed' switches for the two solenoid valve systems

2) a joint (simultaneous) 'open' switch

3) a select switch to allow choice of operation between 1) and 2)

4) an emergency stop switch to operate under any condition

5) individual indication lamps to illuminate if safe condition exists for flowswitches

6) individual indication lamps to illuminate if the 'open' switch is operational on valve systems (both when individually operated and simultaneously)

The layout of the Control Panel is shown in Figure 4.10.

Functional Requirements:

The safety system and valve control unit were designed to operate as follows:

Under 'normal' operation, use of the control panel switches supplies 240 V ac to the solenoid valve systems.

Under 'emergency' conditions, 240 V ac supply to valves is cut off, irrespective of switch positions. The supply cannot be re-set until emergency condition no longer exists.

'Emergency' condition implies EITHER:

i) detection of propane by detector system

AND/OR

ii) insufficient flow to 'make-safe' either flowswitch

'Emergency' response from any single propane detector or flowswitch (or multiple) MUST activate the safety system and close down the system.

All flowswitches/detectors are wired up such that an open circuit is unsafe. This is to ensure that loss of power to any detector/switch (eg by power failure, accidental disconnection) results in 'emergency' condition (shutdown) at the control panel. The

system must not be able to be operated unless a definite 'safe' signal is received from all safety elements.

4.3.2 Containment Concept

This was achieved by the use of a storage facility. The storage facility is one-hour fire resistant, designed specifically for use with flammable liquids and their vapours.

It is equipped with eight flame arrester vents, and secured by the use of a high quality security lock. This prevents any external ignition source, including those of a 'human factor' nature, igniting propane inside the store whilst allowing it to slowly diffuse away, or at worst slowly flare off. In the unlikely event of a fire inside the storage facility, it will be contained for a minimum of one hour, assuming no missile damage, allowing adequate time for emergency procedures to be undertaken.

All items inside the store are pneumatically operated unless an electricity supply was unavoidable. All electrical items are, or have been made by the use of barriers, intrinsically safe.

The transfer line and the vessel are protected from static discharge problems by the application of an earthing strap.

4.3.3 Dilution Control

This concept is concerned with the removal and disposal of the propane during an experiment. It was decided that an extract/dilution system was the best method for accomplishing both the removal of propane from the experimental chamber and its safe disposal. Flaring off was considered as an alternative to dilution, but posed too many problems in both expenditure, design, and safety considerations.

A figure of 50% LEL at the maximum calculated mass flowrate was chosen as the maximum post-dilution propane concentration (v/v in air). The fan system used to accomplish this was an axial fan, with non-metallic blades, driven by a flameproof

motor as it posed considerably fewer problems and was extremely safe, especially when coupled with the safety system.

Problems arising through static discharge inside the extract system have also been addressed by the application of an earthing strap system.

4.3.4 Negative Pressure Concept

The premise of this concept is that the pressure on the inside of the experimental chamber is negative with respect to that of the laboratory. This is achieved by the extract system always pulling air from the laboratory, through the chamber, and out into the atmosphere. This ensures that any flow of fluid is always into the chamber and out through the extract system, thus preventing propane escaping into the laboratory subsequent to its release.

The experimental chamber flowswitch constantly monitors this flow. If the flow into the chamber drops below the specified value, ~1.0 m/sec, then the safety system is tripped and the propane release system is shut-down.

Additional chamber safety measures include a propane detector, located at the (open) header tank end of the chamber. This acts both as propane detector in case of emergency releases and also as secondary flow monitor. If propane flows back out towards the open end of chamber, then it will activate the detector and the system will shutdown.

All steps have been taken to minimise the likelihood of static build-up and discharge, resulting in ignition of propane, inside the chamber. Coupled with the application of earthing straps to the chamber itself (along with the delivery system and extract system) the presence of any metallic objects inside the chamber has been reduced. Any remaining metal objects, especially those terminating in a small surface area, have been coated in silicone rubber compound.

4.4 FACILITY SAFETY ASSESSMENT

This section firstly considers, in a qualitative manner, the potential hazards present in the facility and details the aspects of the safety system designed to prevent or mitigate them.

A quantitative appraisal of the likely hazards is then presented, including a failure frequency study and human involvement probabilities calculated from the failure values.

4.4.1 Material Hazards

Propane: Molecular formula C_3H_8, colourless gas

Boiling point: - 42.1° C

Lower explosive limit: 2.3% v/v in air

Upper explosive limit: 9.5% v/v in air

Flash point: - 156 ° F (-104.4°C)

Density: 0.5852 at - 44.5° C

Auto-ignition temperature: 842° F (467.8° C)

Vapour density: 1.56

Soluble in water, ether, and alcohol

Synonyms: dimethylmethane, propyl hydride

Fire hazard: highly dangerous when exposed to heat, flame, or oxidisers

Spontaneous heating: no

Explosion hazard: severe when exposed to flame or ClO_2

Disaster hazard: dangerous; can react vigorously with oxidising materials

To fight fire: stop flow of gas or liquid if possible; use fire extinguishers (dry powder) if safe to do so

Specific hazards relating to the various components of the facility will be dealt with under individual headings.

4.4.2 Individual Facility Hazards

4.4.2.1 Storage Vessel:

MATERIAL HAZARD PRESENT	NATURE OF HAZARD
Liquid propane at pressure (maximum 50 litres at 15 barg)	Flammable release of propane resulting in fire/explosion
Compressed air (site supply to run pneumatic valve and pump)	Release/spillage of liquid propane resulting in 'cold' burns
Compressed nitrogen (cylinder required for vessel padding/'purifying')	Release of pressurised gas at high velocity

POTENTIAL SOURCE OF RELEASE	PREVENTATIVE/MITAGATIVE MEASURES
Vessel failure	The vessel has been designed and constructed so as to allow a suitable safety margin between the maximum operating pressure, and any pressure that would result in failure. The vessel, and its constituent parts, have been fully checked and inspected for compliance with the relevant safety standards and codes. This information is contained in Appendix A4.1. In the event of an accidental release arising, the vessel is contained within a safety store (see Appendix A22) external to the laboratory. The store is designed for pressure-liquefied materials such as propane, and is protected against ingress of heat or fire (one hour fire resistant construction and eight flame arrester vents). The store also contains no integral electrical systems, or other ignition sources.

Overheating of propane leading to vessel failure, or venting through bursting disk	Heating is controlled by 'intelligent' system which monitors temp. If temp exceeds specified value then heating system is closed down. Should this fail to work, bursting disk vents contents into safety store to avoid destruction of vessel. Propane sensor inside safety store gives visual external warning if leak occurs, and automatically shuts down system via pneumatic release valves.
Failure of mechanical equipment, eg pump, pipework	Built to relevant BS standards. Failure inside the safety store is contained as per bursting disk venting. Failure inside experimental chamber is dealt with by extract system. Failure between these two points is not easily dealt with, but is highly unlikely. Emergency procedures for such an event are presented in the relevant section.
Human error during filling process	Filling of storage vessel - burns/leakages etc avoided by following filling procedure, wearing protective clothing (gloves etc)

POTENTIAL SOURCES OF IGNITION	COMMENTS
Naked flame	No open flame sources will be present in the vicinity of the vessel (ie inside the safety store). As detailed above, the store in which the vessel is placed is capable of withstanding fire attack for up to one hour. This fire integrity does however rely on the store entrance being closed, which will form part of the operating procedures. Area covered by warning signs.
Electrical	Where possible non-electrically driven devices have been utilised, such as the pneumatic pump and valve. Where electrical devices were unavoidable these have been specified as zone 0 items. This includes the load cells and pressure transducers.
Friction/static charges	No static or frictional ignition sources will be present (have been identified?) inside the safety store. transfer line earthed.

4.4.2.2 Experimental Chamber:

MATERIAL HAZARD PRESENT	NATURE OF HAZARD
Liquid and vapour propane in air, some at flammable concentrations (maximum 250 g/sec for durations of approx 10 secs)	Ignition of flammable propane/air mixture inside chamber Escape of propane into laboratory (leading to fire/explosion)

POTENTIAL SOURCE OF PROPANE RELEASE INTO LABORATORY	COMMENTS
Failure of pipework/extract line	Safety features covered in previous part
Failure of experimental chamber integrity	Shouldn't happen (design/built to standard?) even so, extract should still ensure that mixture travels down extract path and not into lab (rig designed to operate at negative pressure)
Loss of co-flowing air supply (ie failure of extract system)	If air flow through rig drops below specified value (1.0 m/sec) then propane delivery system is closed off. Same situation occurs if fan flow rate not to specified limit. Should be sufficient momentum in fan to keep it extracting for a period after power has been lost.

POTENTIAL SOURCES OF IGNITION	COMMENTS
Naked flame	None present (see above)
Electricity	None present
Friction/static	Checked with Dr Tolson, Ignition Control, RLSD (HSL) - not a problem. Earth straps fitted as added safety precaution to frame of chamber and transfer line.

4.4.2.3 Extract System:

MATERIAL HAZARD PRESENT	POTENTIAL HAZARD
Propane vapour, some at flammable concentrations (maximum 250 g/sec, ~0.133 m^3/sec)	Ignition of mixture
	Noise from operating fan
	Blockage of external air supply to fan, resulting in excessive air intake from laboratory (possible structural damage, asphyxia)

POTENTIAL SOURCES OF IGNITION	COMMENT
Naked flame	No naked flames allowed. Area covered by warning signs.
Electrical	Motor is certified flameproof
Friction/static	Should not be a problem (extract earthed for additional safety)

OTHER HAZARDS	MITIGATION
Noise generation by extract system	Check noise level. Use ear defenders if necessary.
Blockage of external air inlet	Regular check of fan inlet. Air flow meter linked into safety shut-down system.
Compressed air line failure to pneumatic valves	Both valves are of the fail-safe spring return type, and lack of control air supply results in valves closing.

4.4.2.4 Traversing system:

The traversing system has no major hazards associated with it. Possible injury through trapped fingers, and similar minor (first aid) injuries.

Note: In addition to the above safety systems, dry powder fire extinguishers, suitable for use with propane fires, are situated at each exit to the laboratory (two in total) and outside the safety store (one).

4.4.2.5 Additional Hazards Associated With Experiment

Laser equipment - see individual laser equipment files (eg hazards to eyes/skin)

Electrocution - three phase electricity used on extract fan, standard 240V used on ancillary equipment (240 V is rcd protected)

Manual lifting - filling of storage vessel by decanting from propane cylinder. Problem addressed in filling procedure. See Appendix B4

Indirect 'cold' burns - pipes etc cooled by boiling propane. Problem addressed in operating procedure.

4.4.3 Quantitative Assessment of Risks

HAZARD	SEVERITY OF HARM	LIKELIHOOD	RISK
COLD BURNS	4	3	12
FIRE/EXPLOSION	10	2	20
LIFTING INJURIES	4	3	12
ELECTROCUTION	10	1	10
PRESSURE LINE & BOTTLE INJURIES	1	2	2

4.4.4 Failure Frequency Study

All data presented here is culled from industrial sources, and as such any failure is likely to occur more frequently in an industrial environment due to the greater degree of use of the critical components (valves, pipework etc).

This data is provided as a very rough guide to the possible expected failure frequencies of the jet rig facility. As detailed above, the data presented here will tend, if anything, towards the pessimistic in terms of safety of the system.

Bursting disk failure rate (disk rupture at normal pressure)

0.2/year [A]

Frequency of spontaneous failure of pressure vessels (LPG, HF, Ammonia)

10^{-5}-10^{-4}/year [B1]

Frequency of failure of pipework (LPG)

$5x10^{-3}$/year [B2]

Frequency of large vapour release at LPG filling point

$5x10^{-3}$/year [B3]

Frequency of missile generation

10^{-5}-10^{-4}/year [*]

[A] Lawley, H G Operability studies and hazard analysis. Loss Prevention, vol. 8, p. 105, 1974

[Bx] The data is taken from the Canvey Island study (HSE, 1978). The data is, in most cases, heavily qualified and the original report should be consulted for the description of the background and application to which it may be put.

[*] The frequency of missile generation is assumed to be equal to that of spontaneous vessel failure. This assumes that missiles are not generated by any other type of failure, and that the vessel failure/missile generation ratio is 1:1.

4.4.4.1 Probability of People Being Present in the Event of a Failure

Probability of person present on site is equal to:

fraction of hours worked per day x fraction of days worked per year

$$=7.5/24 \times 226/365$$

$$= 0.1935$$

Note: Hours worked per day is exclusive of lunch hour.

Frequency of events occurring in the presence of a person (ie with risk of injury) is:

Bursting disk failure: $0.2 \times 0.1935 = 0.0387$/year*

Frequency of spontaneous failure of vessel: 10^{-5}-$10^{-4} \times 0.1935$

$$= 1.935 \times 10^{-6} - 1.935 \times 10^{-5}\text{/year*}$$

Frequency of failure of pipework: $5 \times 10^{-3} \times 0.1935 = 9.675 \times 10^{-4}$/year*

Frequency of large vapour release at filling point: $5 \times 10^{-3} \times 0.1935$

$$= 9.675 \times 10^{-4}\text{/year*}$$

* This figure assumes that the entirety of the working day is spent around the facility, which is almost always not the case. The probability of personnel being at work on the vessel (ie in close proximity to it) on average is:

$$2/24 \times 226/365 = 0.0516$$

In the case of vessel failure resulting in missile generation, this translates to a probability of:

$$5.16 \times 10^{-7}\text{-}10^{-6}$$

No account is taken of the likelihood of an ignition of the release occurring - this would further reduce the frequency values towards a safer value. No account is taken of the special precautions (zoned areas and ignition-free environments) and environments associated with this facility compared to those encountered in industrial sites, to which the frequency data relates.

4.4.4.2 Maximum Volume Propane Release

The maximum volume release possible would be less than fifty litres of liquid (the volume of the vessel is fifty litres, and the maximum permissible fill level is less than 100%). This is equivalent to 13.397m^3 of propane vapour at 20°C.

Propane forms flammable mixtures in the range 2.3 - 9.5% v/v in air. This results in flammable mixture volumes of between 582.48m^3 and 141.02m^3. The potential danger area following a full release however could be larger.

Inside the safety storage facility a release, if it was from a pipe or vessel leak (as opposed to a catastrophic failure) would be effectively contained, and would diffuse out through the eight arrester elements. The release would also have triggered the propane detector device, thus activating the audible and visual warning systems, and the safety system. This would reduce the likelihood of harm to personnel, as the alarms would be activated before a flammable mixture had been formed and the probability of personnel being in the 'hazard area' when/if an ignition took place would be expected to be considerably lower.

4.4.4.3 Missiles

The probability of missile generation is thought to be low. It is highly unlikely ($<10^{-6}$) that vessel failure due to heat generated pressure failure will occur due to the combination of the bursting disk (which will quickly dump the entire contents of the vessel once its bursting pressure has been reached), and the heater control mechanism (which cuts off the heater unit). Missile generation from both hot and cold vessel failures is reduced by the lack of ignition sources inside the storage facility.

In the event of missile generation inside the storage facility, it is expected that the storage facility itself will, whilst probably not containing the missiles, have a marked effect upon the momentum with which they escape (ie reduce it).

Damage to people is most likely to occur if they are situated in direct sight of the storage facility, unprotected by any building walls. This effectively means the car park area, the road, and the area around the vessel and storage facility itself.

An estimate for the time spent in the car park/road area (by pedestrians) is 25 minutes per day, including lunch hour when several people walk past the facility. As a probability this gives the probability of someone (other than personnel working on the facility) being in the line of fire as:

$$25/1440 \times 226/365 = 0.01075$$

An estimate of the average number of daily vehicle passes of the facility is 30 (inward + outward). This excludes security personnel. Assuming that a vehicle is in the line of sight of the storage facility for 1 minute, this gives a probability for vehicle presence of:

$$30/1440 \times 226/365 = 0.01290$$

Taking the probability of a release occurring with missile generation into the areas described above as being 10^{-5} - 10^{-4}, the probability of vehicle/pedestrian interaction is:

$$1.075 \times 10^{-7} - 10^{-6} + 1.29 \times 10^{-7} - 10^{-6} = 1.387 \times 10^{-7} - 10^{-6}$$

Note: the above figure assumes an involvement/injury relationship of 1:1, which is most likely to not be the case. A likely probability of injury in the above case is <0.01

This would give values of: $1.387 \times 10^{-9} - 10^{-8}$

For personnel working on the vessel a likely probability of injury would be 1. this therefore gives:

$$5.16 \times 10^{-7} - 10^{-6}$$

Assuming non-interdependency, this gives a total probability for missile injury of:

$$\sim 5.17 \times 10^{-7} - 10^{-6}$$

Probability of injury to personnel not working on the facility can thus be seen to be relatively negligible.

4.4.4.4 Conclusions From The Failure Frequency Study

From the failure frequency study, it can be clearly seen that the most likely event giving rise to a release of propane is the bursting disk, with a failure frequency of 0.2/year. This value was considerably higher than any other event and it was decided to investigate this problem further.

The question of reliability was raised with the manufacturers of the specific system currently utilised on the facility, an A9/D Disc from BS&B Safety Sytems Ltd. It was suggested that a visual check of the device should be undertaken every twelve months (which is already part of the facility maintenance procedure) with a view to replacement every 18 to 24 months.

It was stated however that this 'lifetime' was greatly dependent upon the operating conditions (process material, ambient atmosphere, temperature etc.) and that in many cases discs were not replaced for periods of 5-10 years.

An initial replacement time of 2-3 years was suggested for the current system, subject to satisfactory annual visual checks, before the final suggestion of 18-24 months was made.

Under the circumstances, ie the original disc having been returned to the manufacturers for replacement of the disc due to (minor) leaking (despite having seen little or no 'active service'), it is deemed wise to opt for an annual visual inspection coupled with replacement at 18-24 month intervals. In theory, whilst the failure frequency for a new disc will still be 0.2/year, this should effectively reduce the likelihood of a release due to bursting disc failure.

CHAPTER FIVE

CONVENTIONAL TEMPERATURE MEASUREMENTS

5.1 INTRODUCTION

It is understood, from the review of the literature, that no temperature profile in the early regions of a flashing two-phase propane jet has been produced, and that such data is a requirement for validation and generation of relevant mathematical codes and models. These experiments will therefore provide the first measurements in this environment. Jet temperature profiles have been obtained, again as part of an earlier project, [1] for other less hazardous materials, such as Freon 11, and the propane temperature profile is expected be similar in shape.

Despite the fact that, as already discussed, intrusive measurements do not necessarily yield accurate data in this environment it was determined that a conventional temperature profile would prove useful on several counts:

a) it would provide the first temperature profile, by any method, of the near-field regions of a two-phase flashing propane jet.

b) it would allow comparison with measurements undertaken in other two-phase media

c) it would generate a baseline temperature profile and information to inform the application of other, non-intrusive, techniques in this work.

Other considerations in deciding to undertake intrusive measurements included the lack of a suitable non-intrusive technique at the outset of the project. Succesful development of such a technique, at a later stage of this work, would also require a reference intrusive profile for comparison - ultimately permitting previous intrusive measurements in other media to be re-assessed.

It should also be noted that the configuration of the thermocouple array was designed such that measurements were made in a plane across the width of the jet,

thus minimising the effect of the array's intrusion on any measurement obtained. No simultaneous measurements were made downstream of the array.

5.2 EXPERIMENTAL EQUIPMENT

The small scale two-phase jet release facility, described in Chapter Four, was utilised for this work and was operated with a 4mm i.d. x 40mm length nozzle. This was the first operational use of the facility.

The temperature was determined by the use of a thermocouple array, containing five k-type thermocouples. The thermocouples were calibrated after the experimental series, as detailed below. All other measurement equipment contained within the small scale two-phase jet release facility was calibrated to a suitable standard, both as part of the comissioning procedure and subsequently.

Capture of the temperature and pressure data from the facility was done by the Cyberdas data card and personal computer, as detailed in Chapter Four. The thermocouple array data was read into a Biodata Microlink data capture unit and passed to the personal computer.

Subsequent thermocouple array data processing was undertaken using Jandel Scientific's Sigmaplot software.

5.2.1 Calibration of Thermocouple Array

The thermocouples were calibrated after the experimental series, using the same data collection system as that used in the series. The thermocouples (including the data collection system) were individually calibrated at seven points, using a water bath to vary the temperature, against a NAMAS calibrated thermocouple and readout unit.

The calibration data points obtained were used to generate regressional-fit equations, which in turn were used to calculate accurate temperature values from the collected

data. The calibration plots, with regression lines shown, are presented in Appendix 5A.

The calibration equations determined for the five thermocouples are given below:

Thermo 400 (FaTS #T0410):

$$T = \frac{x - 3.5232}{0.99}$$

Thermo 401(FaTS #T0403):

$$T = \frac{x - 3.5775}{0.9929}$$

Thermo 402 (FaTS #T0409):

$$T = \frac{x - 3.3391}{0.9948}$$

Thermo 403 (FaTS #T0404):

$$T = \frac{x - 2.2273}{0.9927}$$

Thermo 404 (FaTS #T0401):

$$T = \frac{x - 0.5726}{0.9939}$$

where x is the measured temperature, and T is the corrected standard temperature (in °C).

The corrected data has been used in plotting all Figures presented in this thesis. Tabulated data, if required by the reader, can be found in the relevant Health and Safety Laboratory report [2].

5.3 EXPERIMENTAL PROCEDURE

The vessel heater system was set to a desired temperature and the system left to attain an equilibrium between heater element and propane liquid. In certain

circumstances it was necessary to further manually adjust the heater setting to maintain the liquid propane temperature within the chosen temperature range.
When a suitable liquid propane temperature had been attained, the CyberDas and Microlink data acquisition systems were set in operation. The two remote pneumatic valves, one on the vessel and one between the header tank and the nozzle, were then opened simultaneously by use of the manual valve control panel. The duration of each release was determined by the operator.

In the initial stages of this work, due to a lack of familiarity with the system, the jets were of insufficient duration to reach a steady minimum temperature. This arose through the fact that some backing up of propane/condensed water vapour occurred. To err on the side of caution the jet release was terminated prematurely in some of these instances. This problem is discussed later.

The thermocouple array consisted of five unshielded K-type thermocouples mounted on a stand. This can be seen in Figure 5.1. The thermocouple tips protruded upstream from the stand by approximately 75mm, thus minimising any effect of the presence of the stand.

The five thermocouples were in a line across the width of the chamber, at a height level with the release nozzle. The central thermocouple was placed approximately on the axis line of the jet. Subsequent detailed measurements indicated that the central thermocouple was in fact ~1cm from the axial line.

For the majority of the temperature measurements all the thermocouples were logged, recorded, and processed, with a minimum of three measured releases at each position. For the detailed width profile, the nozzle position was moved by use of the traversing system, all five thermocouples were logged, and recorded, but only the central one was processed.

Measurements were taken initially with the nozzle in its central position (in relation to the chamber width). The differing axial distances (measured from the nozzle tip to

the tip of the central thermocouple) were obtained by either relocating the thermocouple array inside the chamber, or by use of the header/nozzle traversing system. More detailed cross jet measurements were taken at one axial distance (approximately where the centre-line temperature measurements were at a minimum) with the width position being varied by use of the header/nozzle traversing system.

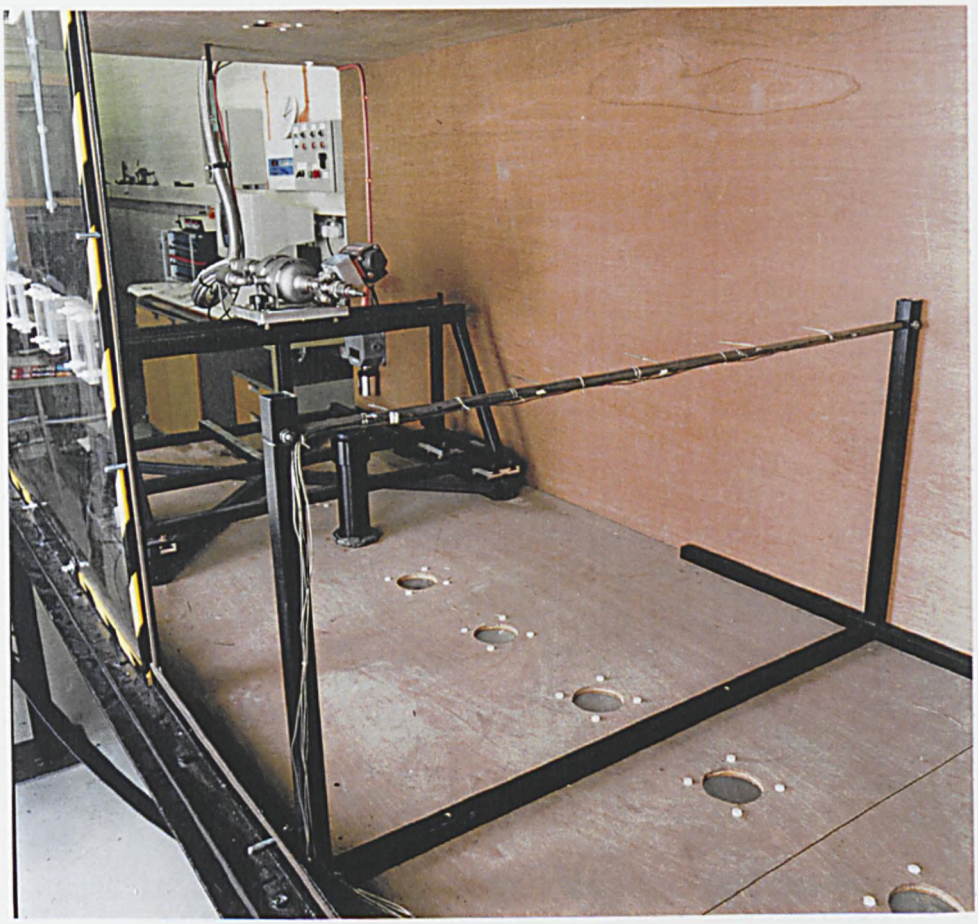

Figure 5.1 Thermocouple Array

5.4 RESULTS AND DISCUSSION

The complete corrected data set is presented in Figure 5.5. Full tabulated data sets can be found elsewhere [2]. Some temperature data values obtained may be erroneous, due to operation of the jet release facility. These values are discussed later. Where values are absent, this is due to 'useful' data not being available. This is also discussed later.

The releases were undertaken with an initial vessel liquid temperature in the range 15.8-17.7°C.

5.4.1 Temperature

The temperature profile fits in with the expected profile. There is a rapid decrease in the first region of the jet where the internal superheat energy is driving the liquid boiling process (although this is implied by the shape of the plot-very little data was obtained in this region). There is then a sharp decline in temperature to a minimum value-this being the forced evaporation region. The temperature then increases in an exponential manner, the increase being due to entrainment of ambient temperature air. The final temperature being slightly below that of the initial ambient due to the cooling effect of the jet. This is shown in Figure 5.2, the centre-line minimum temperature profile. More detailed discussion of this profile is presented in Section 5.4.2

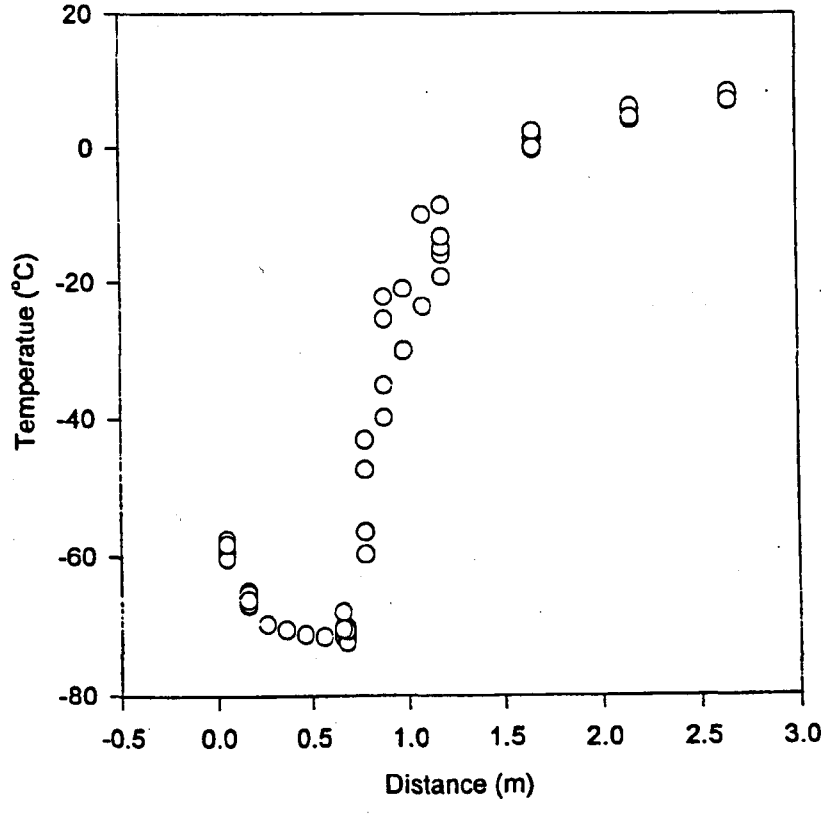

Figure 5.2 - Jet Centre-line Minimum Temperature Profile

It should be noted that Figure 5.2 contains all the data points obtained, including those where the steady minimum temperature state was probably not achieved. In most cases these points are obvious, and are never the sole representative point. All minimum temperature data points presented, both in plots and tabular form, are the average temperature value for the minimum temperature trough of each release.
Figure 5.3 shows a detailed temperature profile across a half width of the jet, at the minimum temperature axial distance (0.66m). This indicates the pattern that was expected from the previous work with other PLGs (Pressure Liquefied Gases) [1].

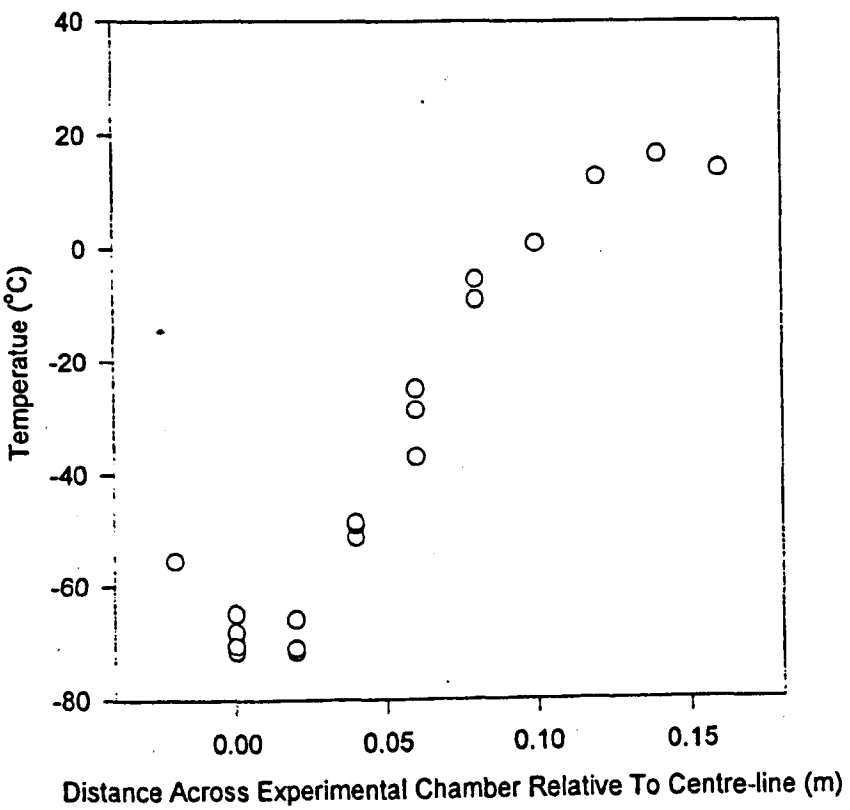

Figure 5.3 - Minimum Temperature Profile Across Jet Axis

A single centreline temperature profile during one release is shown in Figure 5.4. A constant temperature (chamber air temperature) is seen to rapidly drop to the minimum temperature at that location. The minimum temperature is maintained for the remaining duration of the jet, followed by an exponential increase after the jet has been terminated.

This increase is due solely to the thermocouple warming up after having been cooled by the jet. In some early releases the jet duration was insufficient for the minimum temperature trough to be achieved. This gave rise to incorrect higher value "minimum" temperatures, discussed above in relation to Figure 5.2.

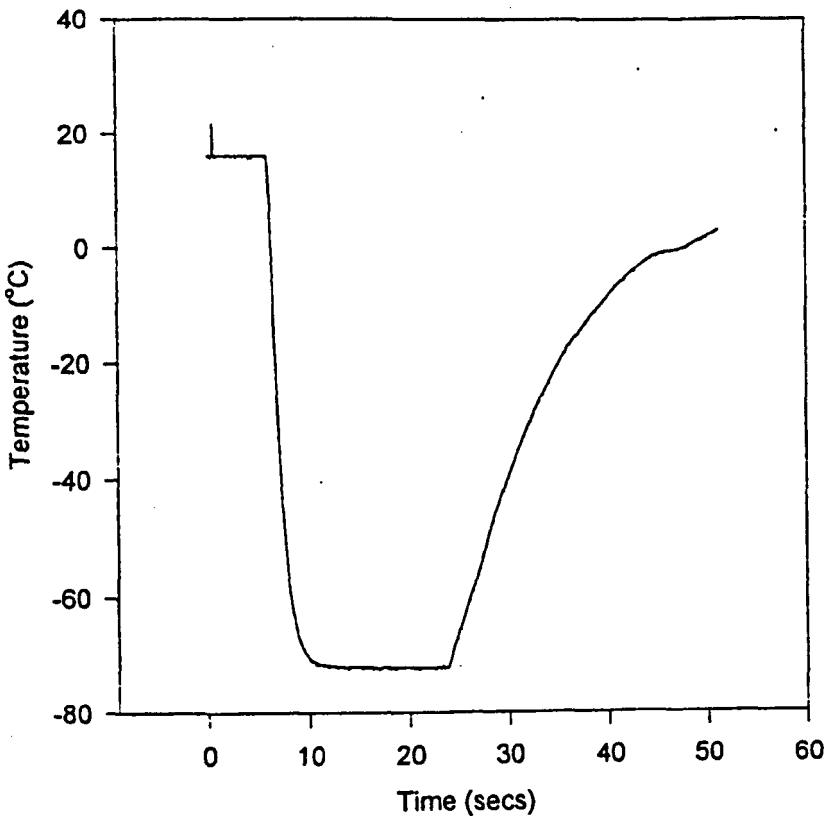

Figure 5.4 - Single Release (Ret25) Jet Centre-line Temperature

The complete temperature data set is presented graphically in Figure 5.5. The 3D mesh plot and 2D contour plot were calculated from the corrected results. The 3D mesh plot also shows the actual data points from which the mesh was determined.

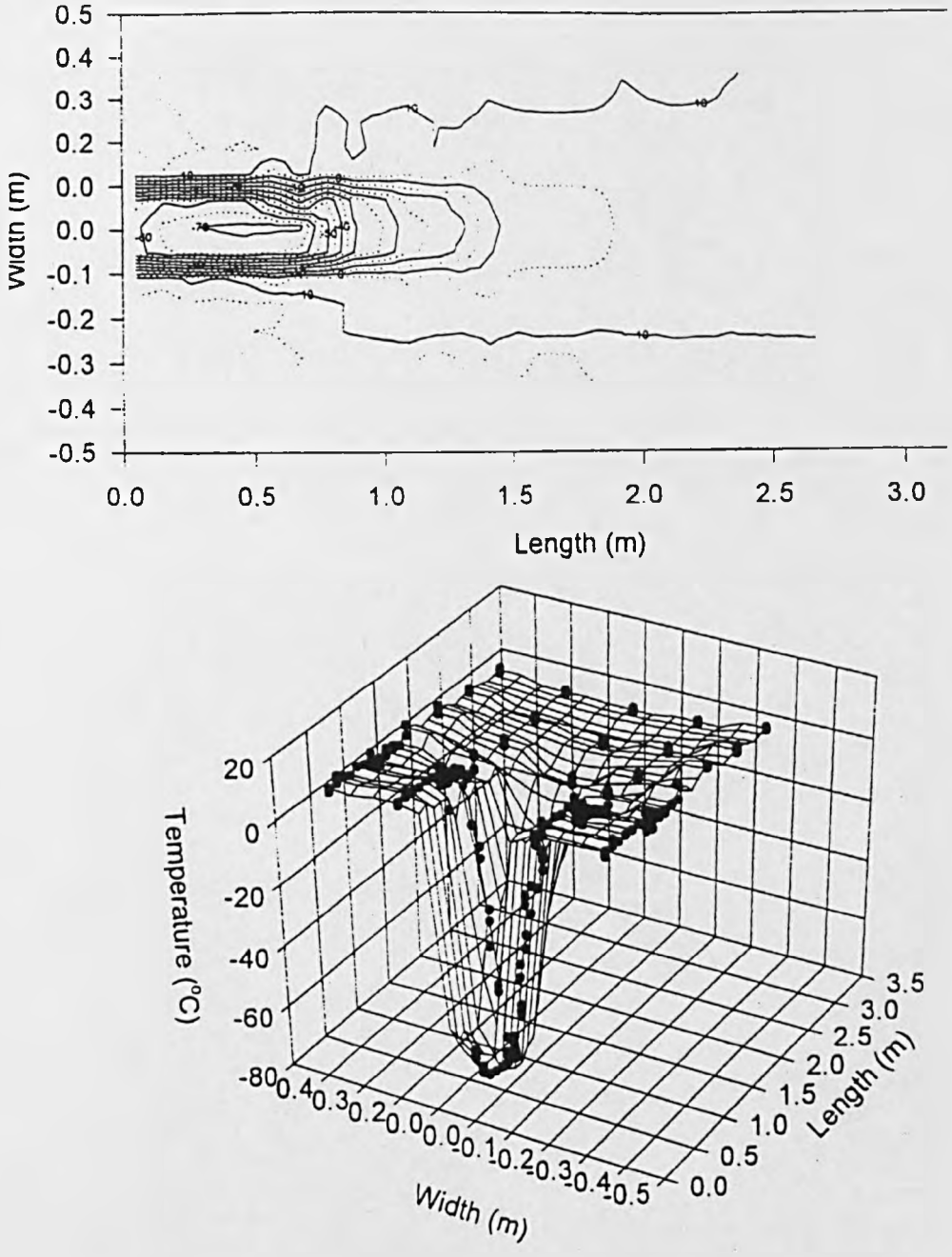

Figure 5.5 - 2D Contour and 3D Representation Of Jet Temperature Profile

5.4.2 Comparison with TRAUMA Model

AEA ran their TRAUMA modelling program for several release of liquid propane scenarios [3]. The runs were conducted prior to the experimental series, and the various parameters of the model, such as ambient conditions, initial storage temperature were arbitrarily chosen. Runs were carried out for both a 'liquid phase only at nozzle exit' condition, and a 'two-phase mixture at nozzle exit' condition (both of which result in a flashing two-phase jet). These are presented in Figure 5.6, with a comparative experimental data plot shown in Figure 5.7.

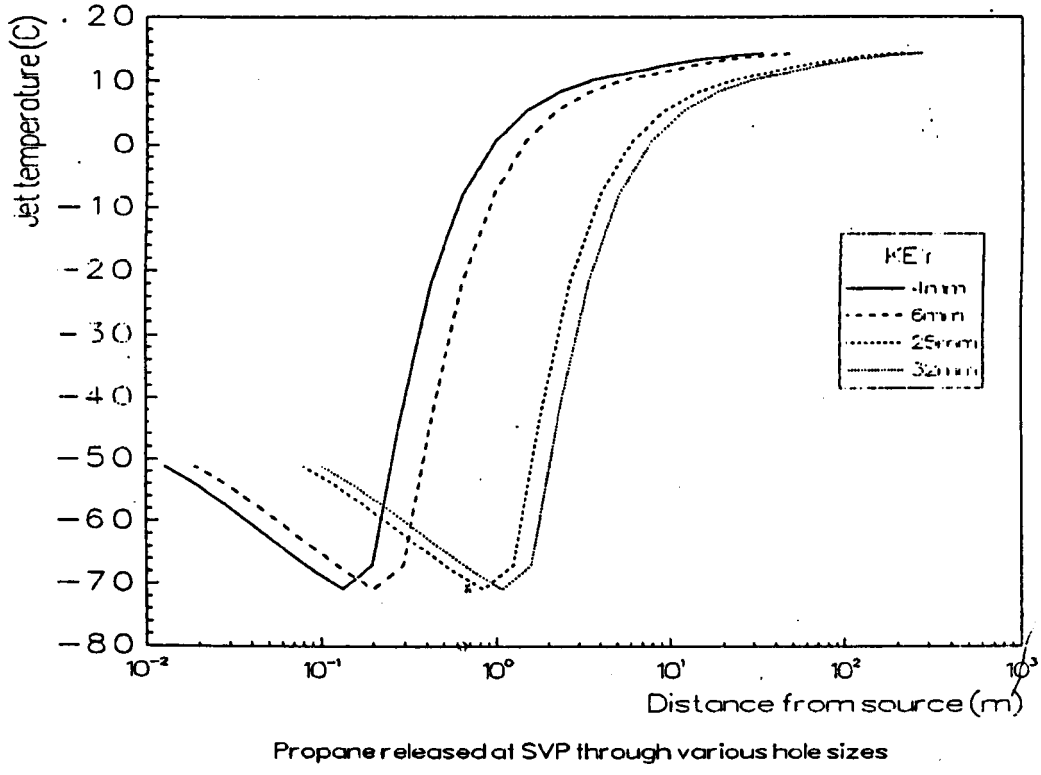

Figure 5.6 - Jet Centreline Minimum Temperatures as Calculated by TRAUMA [3]

As can be seen, the 'liquid only at nozzle exit is the best fit to the data. Use of this assumption gives a good prediction of the minimum temperature distance for the 4mm i/d nozzle, and a reasonable minimum temperature.

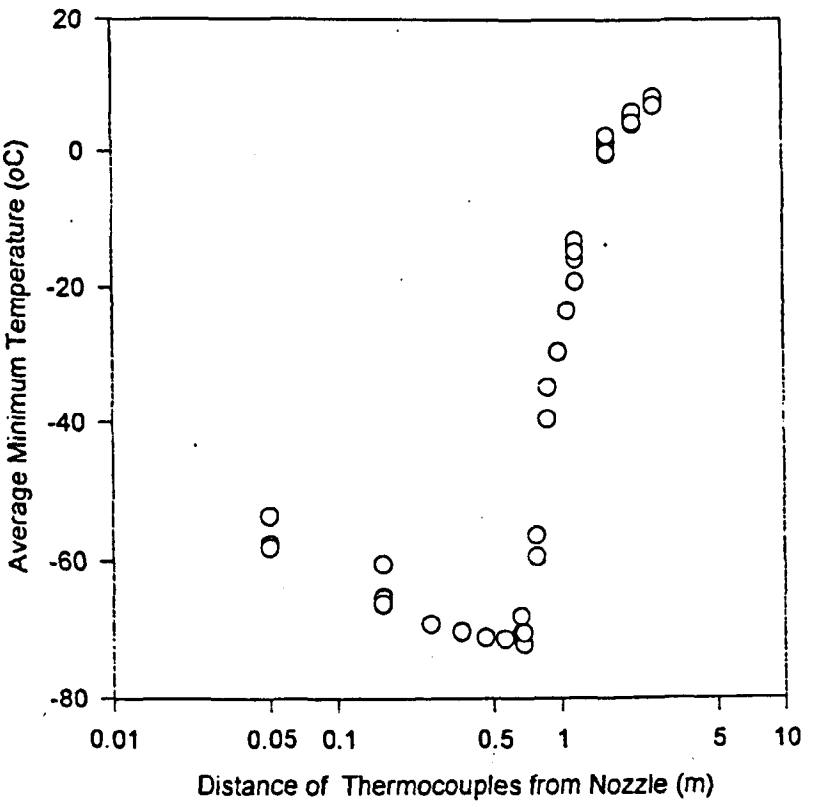

Figure 5.7 - Experimental Centre-line Data In TRAUMA Format

The model also predicts the sharp increase in temperature after this point, although its shape in the entrainment region is not that close to the data. Model assumptions included incorrect ambient air temperature and storage release temperature. There is generally good agreement between the model and the data.

It should be noted that the TRAUMA model assumes equilibrium temperature conditions between the liquid and vapour phases, ie that they have the same value, at all points in the jet. This may also lead to discrepancies between the calculated and measured temperatures.

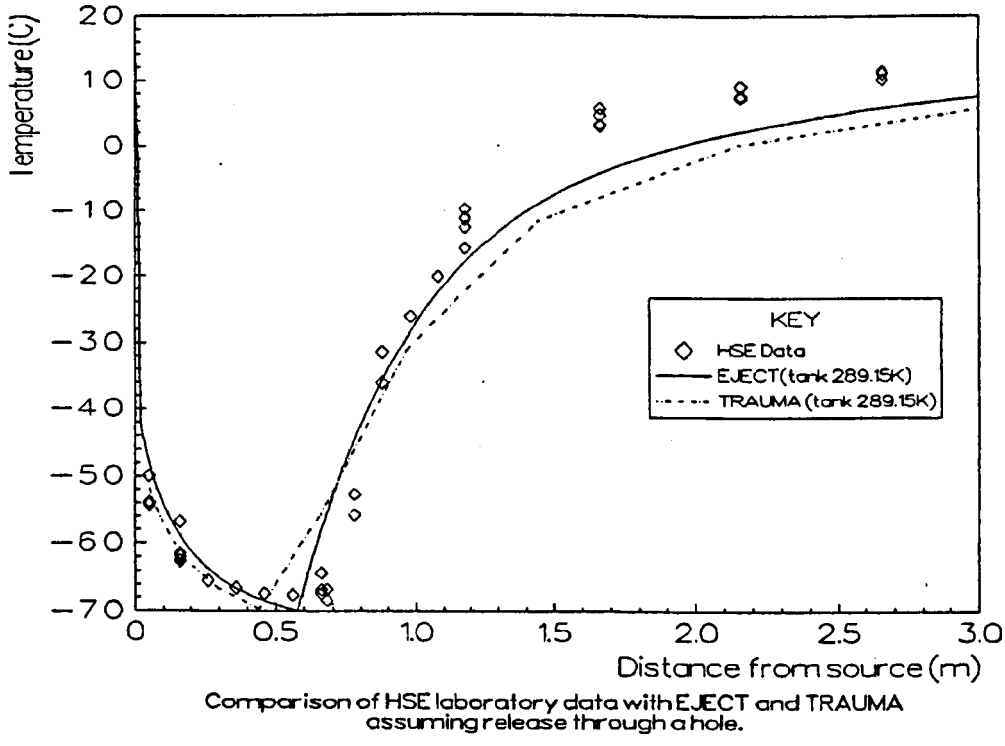

Figure 5.8 - Improved EJECT and TRAUMA Comparisons With Data [4]

From assumptions made by the model it seems likely that at, or shortly after, the minimum temperature distance all of the liquid propane has evaporated. This hypothesis was tested when laser-based droplet size measurements were taken later in the project.

Preliminary sensitivity tests are being undertaken by AEA to assess the effect of the arbitrary parameters on the predictions, using those of the data set where possible. Attempts to compare the data with EJECT, the next generation TRAUMA model, are shown in Figure 5.8.

Figure 5.9 illustrates the lateral temperature profiles collapsed in a non-dimensional manner, assuming a linear jet spread. As can be seen the data collapses well, thus implying that the jet conforms to a Gaussian linear spread (single phase) jet model. Further comments on this fit are given in Chapter Six, section 6.7.1.

More extensive comparisons of two-phase flashing models against the temperature data presented in this thesis, by AEATechnology and the University of Madrid, can be found elsewhere [4,5].

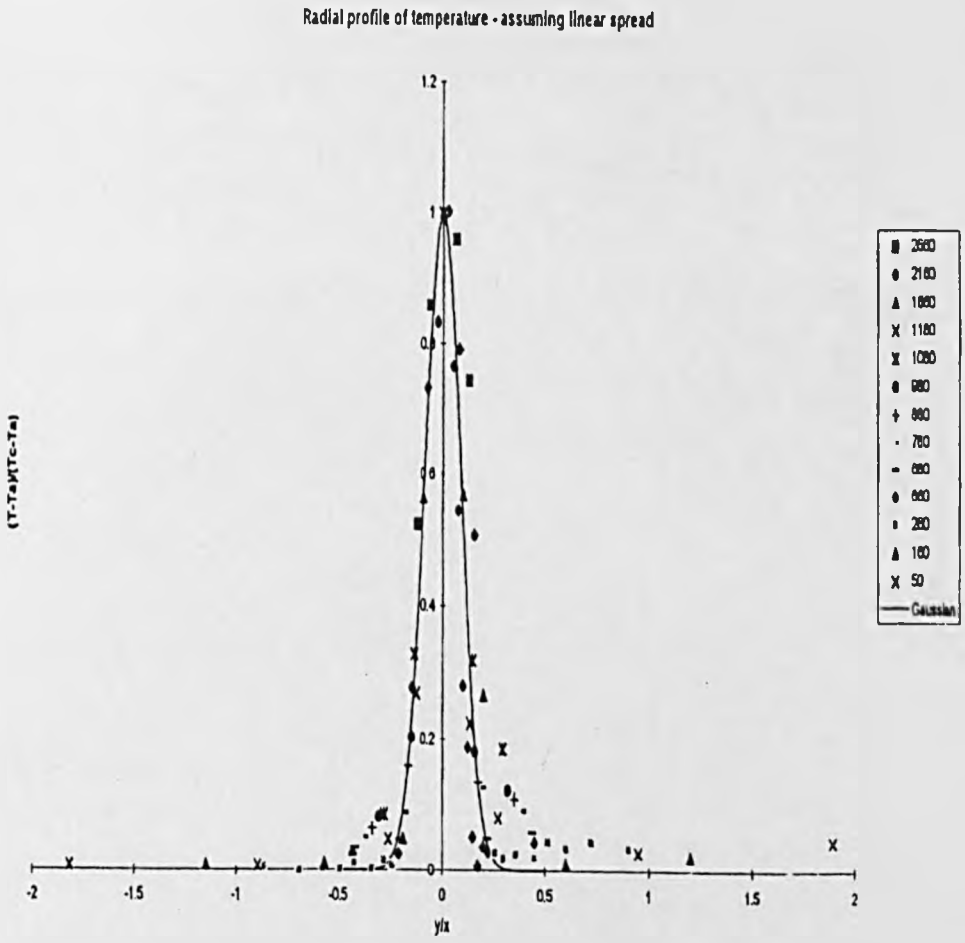

Figure 5.9 - Normalised Temperature Profile [3]

5.4.3 Minimum Temperature Distance

The minimum temperature distance (MTD) was determined as a function of the nozzle diameter, and was found to be ~ 150 diameters away from the nozzle exit. Additional data [6] was obtained using larger nozzles, 32mm and 6mm, in a large-scale external facility at HSL, Buxton, and the MTD in these cases was also found to be approximately 150 diameters from the nozzle exit point. There was some variation in the MTD for the larger scale releases, but these were undertaken in ambient conditions and factors such as wind speed and direction may have been the

cause of such deviation. It is believed that the MTD for any release will fall in the range 150-170 diameters from the nozzle exit point.

Temperature data obtained by Battelle [7] generated MTD values of ~3.5m for a 32mm nozzle (~109diameters) and 6m for a 50mm nozzle (120 diameters) for a two-phase flashing propane jet. It should be borne in mind, however, that these experiments were undertaken in the field and are thus subject to distortion of the jet by atmospheric conditions.

Overall, due to a lack of variation (and similarity) in the experimental parameters (nozzle length, orifice diameter, similar release conditions) no definite conclusions can be drawn from this measurement. It seems promising, however, that the 32mm and 4mm data sets undertaken by HSL show a consistent relationship (of the order of 150 diameters) between the nozzle i.d. and the MTD.

No temperature data was reported by Hervieu and Veneau.

5.4.4 Mass Release Rates

The mass release rates (MRR) presented in Figure 5.10 are average values for the duration of the jet. This however gives a relatively distorted view of the true release rate. In the initial phase of the jet, due to the moments imposed on the load cells by the mass transfer along the transfer line, the indicated mass increases and then drops sharply to the correct mass. This generates a false high value mass release rate for this (short) duration. In most of the releases a constant release rate was not achieved for the complete duration of the jet. A better reflection of the MRR would probably be 50-80g/sec.

As can be seen from Figure 5.10, short duration releases tend towards a higher MRR, biased for the reason outlined above. Long duration jets, especially those undertaken towards the end of a series, result in a lower MRR. This is considered to be due to a reduced mass level in the vessel, resulting in a lowered driving pressure, and occasionally boiling in the vessel.

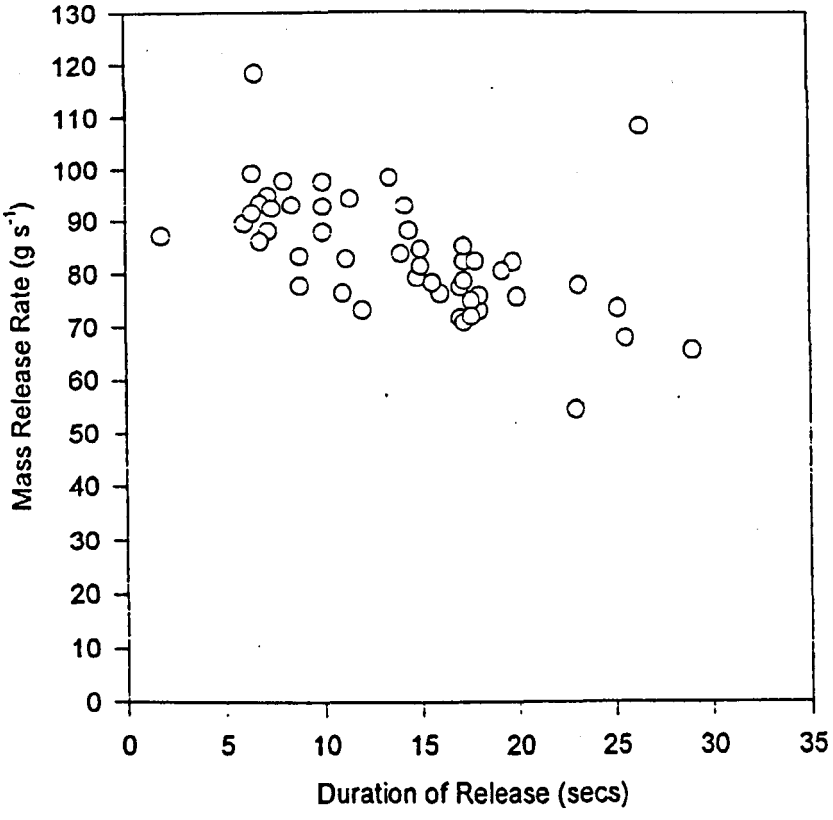

Figure 5.10 - Average Mass Release rates (as a function of release duration)

The accuracy of the MRR is better for long duration releases. Due to the load cell system (including data capture) the load cell data value error is 50g (total), which is transferred directly to the release rate accuracy. Thus the MRR error is therefore equal to 50g divided by the release duration. Figure 5.11 shows the mass profile for a single release.

5.4.5 Vessel Temperature and Pressure

These were seen to decrease during the course of a release in many instances. Large decreases in vessel liquid temperature data observed at the end of a series of tests is attributable to the low liquid mass level. Energy for vapourisation, to maintain an equilibrium pressure in the vessel, under these circumstances, is taken directly from the liquid phase, and hence a large drop in temperature is seen. Similarly a drop in pressure is seen, possibly due to the rapid mass loss. These effects tend to generate a

pulsing in the jet, possibly as a result in increased flashing in the transfer line, and a stable situation is often not obtainable for long periods.

This could be remedied by the application of a reactive Nitrogen pad pressure, but due to a desire to conduct both the large and small scale experiments under similar conditions this was not done (it is impractical, due to its construction, to pad the large scale releases). It is believed however that this non-constant release scenario, given a sufficiently long duration release, had no effect upon the minimum temperature values observed.

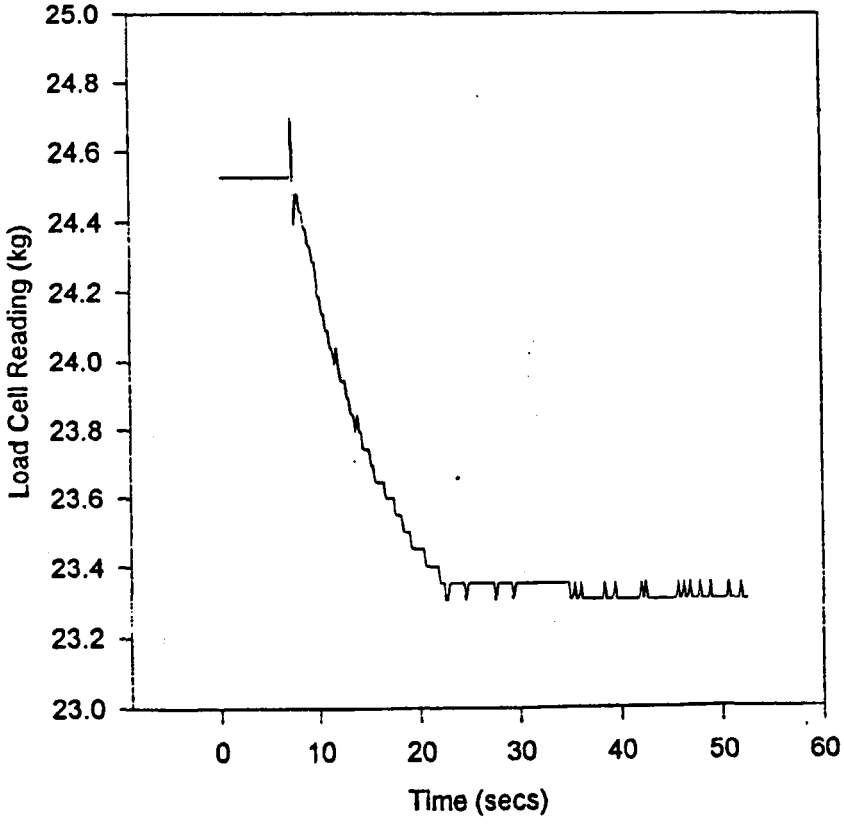

Figure 5.11 - Mass Release Profile For Single Release

Figure 5.12 - Small-Scale Facility In Operation

5.5 FACILITY PERFORMANCE

The small scale facility produced repeatable two-phase flashing jets, as can be seen in Figure 5.12. There were however a few problems. The jet was not completely stable due, perhaps, to changing vessel pressure/temperature equilibrium throughout the duration of a release.

A further disadvantage, in terms of data analysis, was the lack of any definitive indication of the start and finish of a release on the data record. This was not too difficult to determine from the behaviour of the many parameters, but the inclusion of an easily identifiable artificial signal would probably have made data analysis and calculations much simpler and less time consuming.

5.6 EXPERIMENTAL CONCLUSIONS

These experiments have provided the first useful temperature data set for the early stages of a flashing two-phase propane jet. They will permit scaling comparisons to be undertaken with the larger scale releases, and will be useful as comparative data for the laser-based temperature measurements.

The temperature data and the predictions of TRAUMA appear to be in general agreement, although further work is required before a full assessment can be made. Deviations between the data and TRAUMA may be due to incorrect source term input, or a more fundamental problem in the program. It is most probably the former.

The small scale two-phase release facility operated repeatedly and reliably, and generated (within certain limitations) good two-phase flashing jet releases.
Minor modifications to the facility should improve the data analysis procedure, increasing the accuracy of certain calculated parameters and decreasing the time required to perform such calculations.

In order to alleviate the problems in jet duration determination, it is intended to attach a pressure triggered signal device to the air supply of the pneumatic valve control system. This will then impose a small spike signal on the data channels when the valves are opened and closed, giving a permanent record of the events.

On the modelling side, sensitivity studies of TRAUMA will be required to determine how accurately it predicts the temperature profile in its current state. Refinement to the program may, or may not, be necessary in the light of this sensitivity study*.

* since being written a more detailed study of the modelling of this data has been completed by AEA Technology, and the reader is directed to [4] for information.

CHAPTER SIX
LDA MEASUREMENTS

6.1 INTRODUCTION

The HSL small scale facility was purpose built to permit laser-based techniques to be employed on flashing two-phase propane jets. This chapter details the measurement of propane droplet velocity in the small scale jet by the use of a laser Doppler anemometry system (LDA).

It was understood, from a review of the literature undertaken at the outset of this work, that no such velocity data existed for the early regions of a flashing two-phase propane jet. This project therefore intended to provide the first such measurements in this environment. A paper was, during the course of this work, published [1] detailing the measurement of velocity and droplet size distribution in a two-phase flashing propane jet. These measurements were, however, obtained by the intrusive use of a phase Doppler particle analyser technique due to the harsh optical environment present in the jet. This intrusion may have resulted in distortion of the jet behaviour, especially the droplet size distribution and velocity profiles, both at and downstream of the measurement point. Errors in the obtained velocity were reported by the authors as ca. 40%.

This present series of experiments resulted in velocity data being obtained in the near-field regions of the jet without the need for intrusion into it, although complex data assessment and manipulation was necessary to generate valid data.
Velocity profiles have been obtained, as part of the an earlier project [2], for other less hazardous materials, such as Freon 11. The propane velocity profile is expected to be similar in shape.

6.2 EXPERIMENTAL FACILITY

The experimental facility used in this series of experiments was that detailed in Chapter Four. The system was modified, relative to that utilised in the conventional

temperature measurement experiments, by the addition of a pressure switch to the release mechanism.

The pressure switch was added to the original system in an attempt to overcome difficulties encountered, during the conventional temperature studies, in determining the exact 'start' and 'stop' times of the release in relation to the other measured parameters. The switch was simply a high/low electrical output switch which was triggered to change state by the operation of the pneumatic valve release sysem. This was recorded by the CyberDas data collection card at a rate of 5Hz, along with the other storage and release parameters.

A selection of release nozzles was available for use with the system. In this series the bulk of the experiments were undertaken with the 4mm i/d x 40mm length nozzle, as with the conventional temperature data, however a few tests were undertaken using the 6mm i/d x 60mm nozzle for comparative purposes.

6.3 LASER DOPPLER ANEMOMETRY (LDA)

6.3.1 Technique

Laser Doppler anemometry (LDA) has been applied to measurement of velocities in fluids since 1964 [3]. It is the most widely used commercial laser-based experimental technque and is readily available in 'off the shelf' forms from several companies. LDA utilises light scattering by particles passing through an interference pattern to provide particle velocity information. It is also possible to obtain particle size information from the scattered signal, although in most commercial systems this is not undertaken.

A simple description of the technique will be presented, a more involved discusion being presented in, amongst others, [4, 5, 6].

Two coherent light beams, usually derived from a single laser light source, are made to cross at a point in the flow system of interest. In the crossing volume a stationary

fringe interference pattern is formed, and particles passing through this volume scatter light with varying intensities depending upon their positions within the fringe system. The frequency of the amplitude change of the received scattered light signal, as detected by a photodetector, will be proportional to the velocity component of the particle moving perpendicular to the fringe pattern.

The fringe spacing of the system is proportional to the laser beam wavelength and the half-angle between the two beams. Hence knowing the wavelength and half-angle allows easy calculation of the velocity without need for calibration or any temperature, density or viscosity alignment procedures.

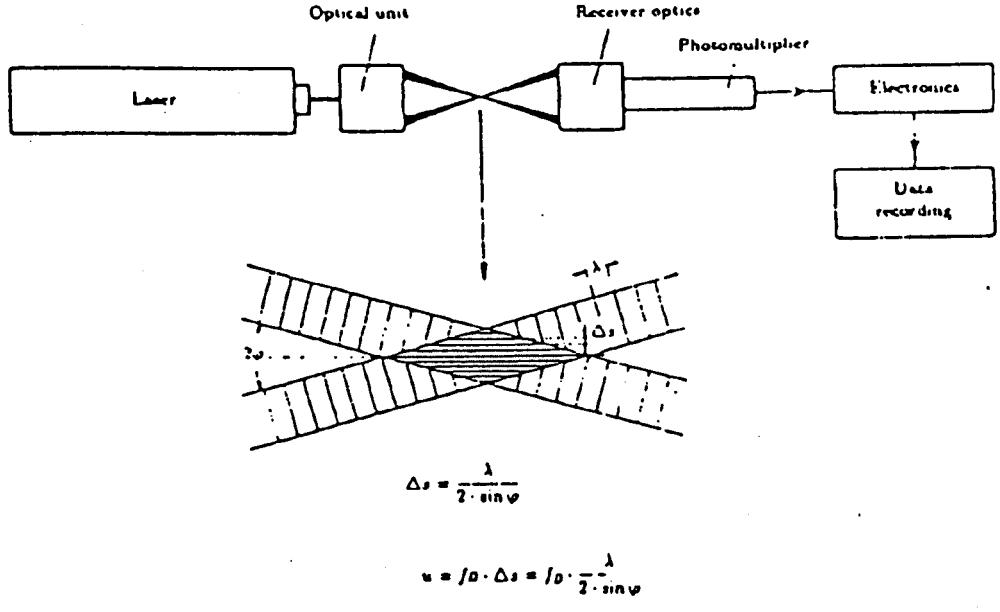

Figure 6.1 - Schematic of LDA System and Fringe Principle [7]

If one of the laser beams is shifted slightly in frequency, then a moving fringe pattern is created. The interaction of the particle with a moving fringe pattern allows the true velocity of one velocity component, ie magnitude and direction, to be determined. A typical LDA layout is shown schematically in Figure 6.1 , along with the fringe principle.

6.3.2 Experimental LDA System

The LDA system employed on this work is manufactured by TSI, USA, and is powered by a 4 Watt continuous wave Argon Ion laser. It is comprised of the 'Colorburst' unit (which generates the frequency shifted beams), the combined fibre-optic light delivery and signal detector probe, the 'Colorlink' unit (which receives the incoming optical signal and converts it to an electrical sgnal, and is the control unit for the frequency shift unit), and the IFA750 processor unit. The complete system is shown in Figure 6.2.

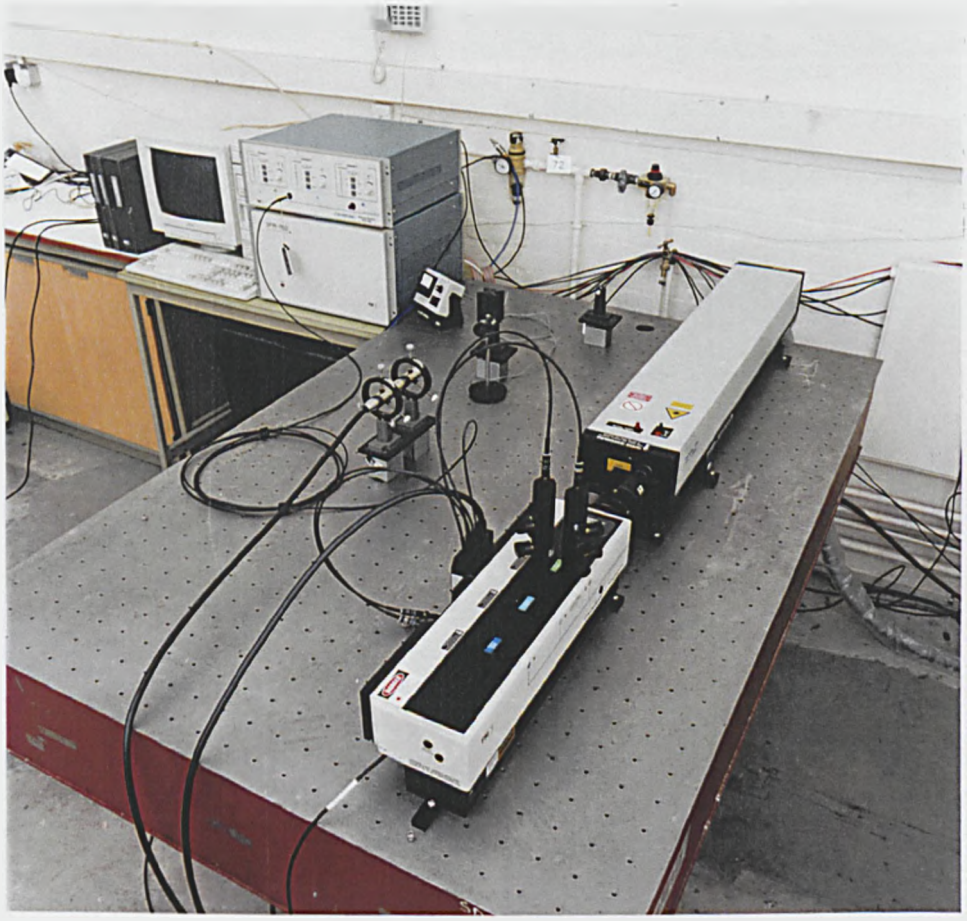

Figure 6.2 - LDA System

It should be noted that this system generates velocity data, but is not intended to provide particle size information, in keeping with all commercial LDA sytems.

The system delivers two pairs of laser beams, and is thus able to simultaneously measure two velocity components, perpendicular to each other. The processor unit,

recently upgraded to permit two component measurements to be undertaken, contains the most recent IFA755 components.

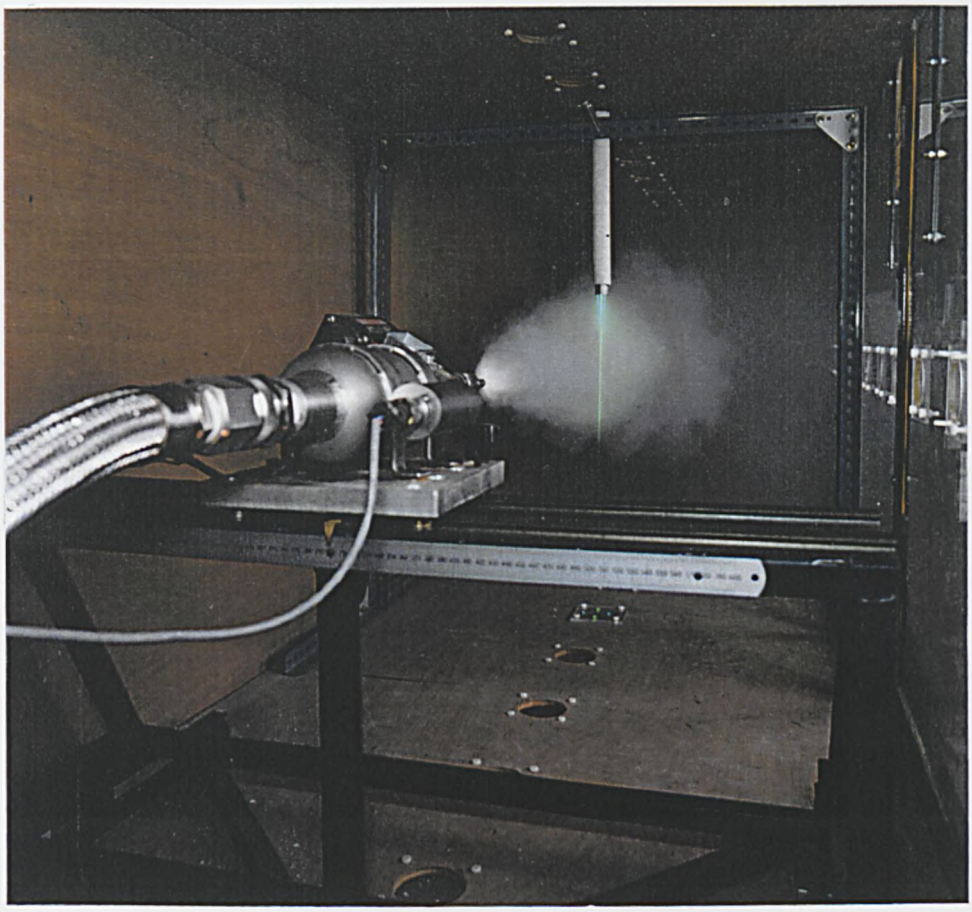

Figure 6.3 - LDA In Operation Inside Facility

The measurement volume of the system is 135mm from the end of the probe, which meant that the probe was required to protrude some distance into the experimental chamber to allow centreline measurements to be made. This intrusion however did not negate the non-intrusive capability of the LDA, which can be seen operating within a two-phase propane jet in Figures 6.3 and 6.4. Further information on the system may be found elsewhere [8].

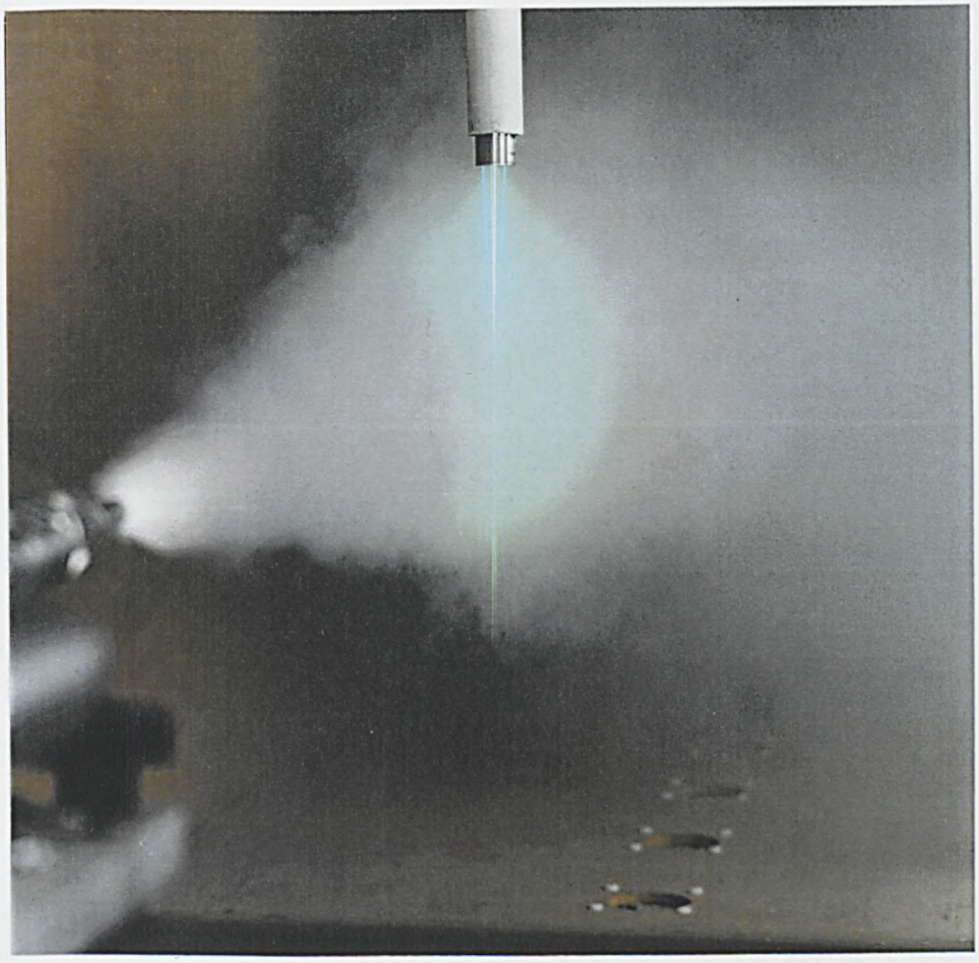

Figure 6.4 - LDA Beams Inside Two-Phase Flashing Propane Jet

6.4 EXPERIMENTAL PROCEDURE

The vessel heater system was set to a desired temperature and the system left to attain an equilibrium between heater element and propane liquid. In certain circumstances it was necessary to further manually adjust the heater setting to maintain the liquid propane temperature within the chosen temperature range.

During the heating period, the LDA probe was situated in the required window location for the measurements being undertaken, and then powered up.

When a suitable liquid temperature, within the acceptable range, had been attained, under single operator conditions, the CyberDas and LDA systems were set in operation. The two remote pneumatic valves, one on the vessel and one between the

header tank and the nozzle, were then opened simultaneously by use of the manual valve control panel. The duration of each release was dictated either by the LDA data collection duration, or the operator, and was typically of the order of 20 to 30 seconds.

In a few circumstances, where a second person was available, the LDA collection system was set in operation once the jet had 'established' itself. This effectively removed the need to eliminate the first section of data from the data file, which did not represent a stable two-phase flashing jet.

The various measurement positions were obtained by use of the nozzle traversing system, within a limited range for axial and lateral movement, and by the relocation of the laser probe for gross axial positional changes.

6.5 VELOCITY DATA ANALYSIS

Initial analysis of the velocity data revealed the presence of two independent velocity peaks for the axial velocity component. As this result was unexpected, a thorough evaluation of the data was undertaken, coupled with an experimental investigation of the system's performance under various conditions. Details of the experimental investigation are given in section 6.5.2.

6.5.1 Twin Peaks

As detailed above, the axial component of the velocity data frequently exhibited an unexpected bi-modal distribution. In some cases the two peaks were clearly separated, and in others they effectively formed one 'lumpy' merged peak. Examples of these are presented in Figures 6.5 and 6.6.

Once it had been clearly established that there were two peaks present, the velocity data for each release was analysed to give an average velocity value for each of the two distributions. This was achieved either by the use of a mathematical transform, user-written within the framework of Jandel Scientific's Sigmaplot software, on the

data set, or by visual interpretation of a graphical presentation of the data. In some cases only one axial peak was present, in which case the average velocity value was determined from its distribution.

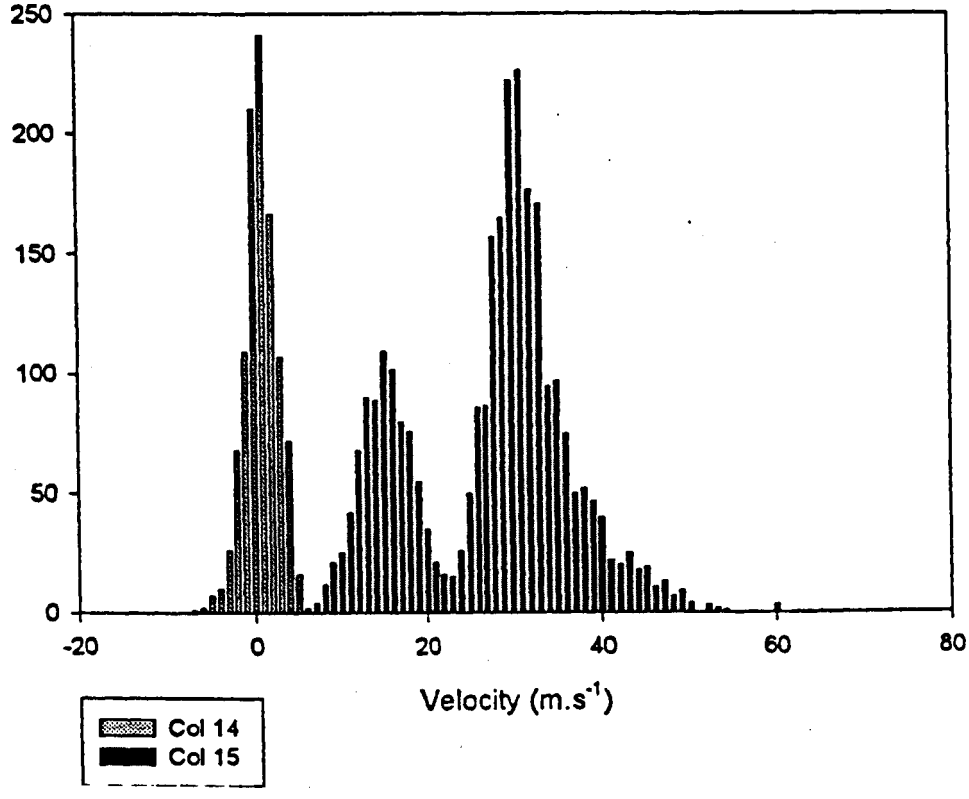

Figure 6.5 - Twin Peaks Data (I) Separated Peaks

The lateral velocity component did not exhibit the 'twin peak' behaviour.

Due to the fact that the presence of two independent axial distributions was so unexpected it was decided to try to eliminate the possibility of system error.

6.5.2 Error Investigation

A series of experiments was undertaken, using relatively simple water and air jets to establish to what degree the peak was a real function of the two-phase propane jet. Using previous LDA set-up conditions (processor settings mainly), and utilising a water jet of a similar density to that of the propane jet, it was possible to get a twin

peak distribution. This implied that the fault possibly lay with the LDA system rather than being a physical reality.

The processor from another LDA system was borrowed from Workplace Air Quality Section, HSL. This system is also manufactured by TSI, USA, but is the more basic IFA550 processor. It does not allow such a large degree of flexibility or range in its settings, and is much more of a 'black box'. Several measurements were made with the IFA750 set to mimic the performance of the IFA550 as much as was possible. Both processors were linked in parallel to the same output signal from the 'Colorlink' unit. With the IF550, no twin peak behaviour was observed from a basic water jet, but it was imposssible to obtain a sufficiently high data rate in the propane jet. The only other observation made was that the IFA550 processor failed to detect small velocity particles with the same frequency as the IFA750.

It was later found possible to induce the false peak by the triggering of the frequency shift function. Another false peak was also discovered which fell outside the range of the cut-off filter. This was obviously system generated, but being outside of the filter range was less of a problem.

Throughout these investigations, there was constant communication with both the supplier of the system, BIRAL, UK, and the manufacturer, TSI, USA. From the experiments undertaken, and the communication, it was determined that the false signals were due to ringing being set up in the frequency filter, and by noise from the photomultiplier tube (PMT). We were advised that these effects were known, and that they were normally not a problem, and could be removed by reducing the 'level of performance' of the processor. However, under the extreme conditions in which we were operating it was impossible to remove the false data whilst still obtaining a sufficiently high valid data acquisition rate. In our case, to be able to get a high data rate, the processor had to be configured to operate towards its upper limit. Under these conditions, a significant amount of noise data, generated from the PMT, was processed as a valid Doppler signal. Unfortunately, the valid data rate was such that the false and valid rates were comparable for many regions of the jet. The ringing

problem could also not be removed, due to the fact that the jet event was of such a transient nature that the full data set had been obtained before the ringing had totally ceased.

6.5.3 Conclusions

From the error investigation, it was concluded that the IFA750 system was operating within the real performance expectations of the manufacturer. These expectations however did not tally with those originally presented by the supplier. The system is perfectly capable of operating satisfactorily in up to relatively difficult environments, although the extreme conditions of the early regions of a two-phase propane jet mean that it is only possible to get a sufficiently high valid data rate at the expense of a large false data rate. Measurements taken in these type of environments, and the resultant data, need to be analysed carefully and not taken 'on trust'. It was possible, in many cases to separate the valid data from the false data. This will be presented in the following section.

6.5.4 Final Data Analysis

Having determined that one peak of the axial component was valid data, and that the other was not, it was decided to try to separate the two wherever possible. In data sets where the two peaks were independent of each other, or were relatively easily identifiable, the 'twin peaks' user-generated mathematical transform was employed on the data set. Basically the transform split the data at a specified velocity value, and then calculated the mean velocity on both sides of the split. This then gave rise to a high peak average velocity and a low peak average velocity. The valid data averages, which were the low peak values, are the ones presented in the results tables detailed in Section 6.6. It should be borne in mind that in certain cases the split method employed may have resulted in slight over or underestimation of the average velocity.

In cases where the 'twin peaks' transform would clearly not give an accurate average velocity, the value was determined by eye. This simply involved obtaining a visual

determination of the average velocity value for a supposed distribution from a graphical representation of the data set.

A number of releases resulted in the presence of a single axial component peak. In these circumstances the average value of that peak has been presented in the data table, although in some cases the peak was determined to be due to false data, and has been omitted from the centreline axial velocity profile shown in Figure 6.7.

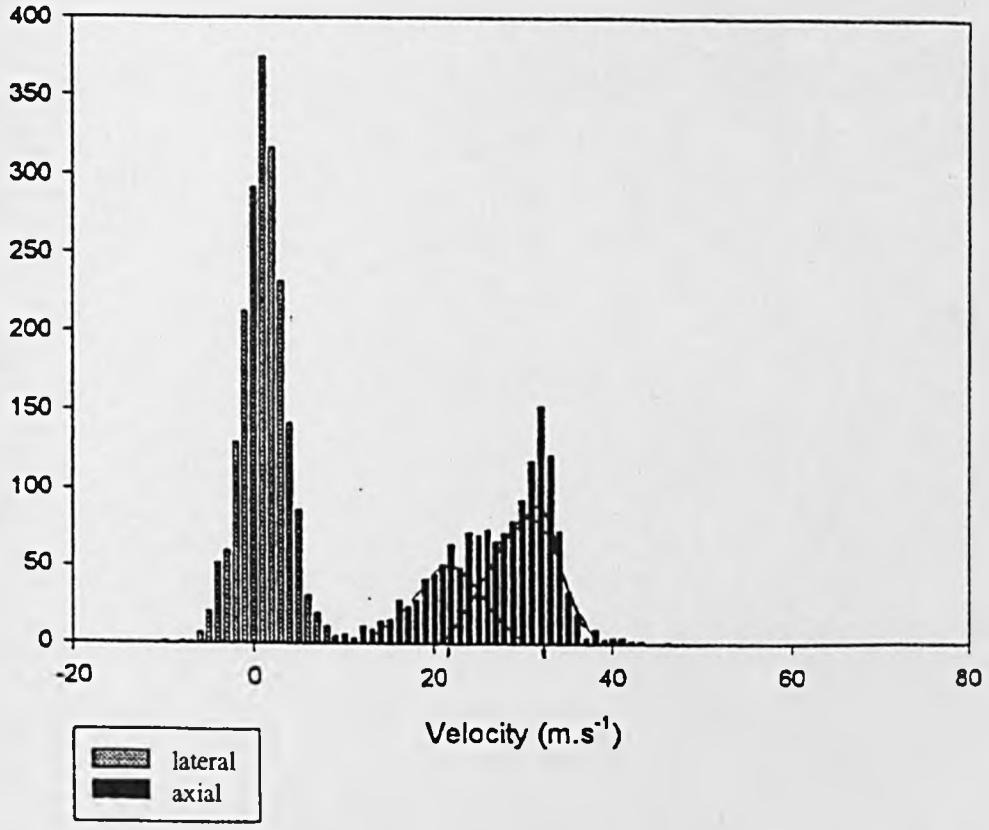

Figure 6.6 - Twin Peaks Data (II) Merged Peaks

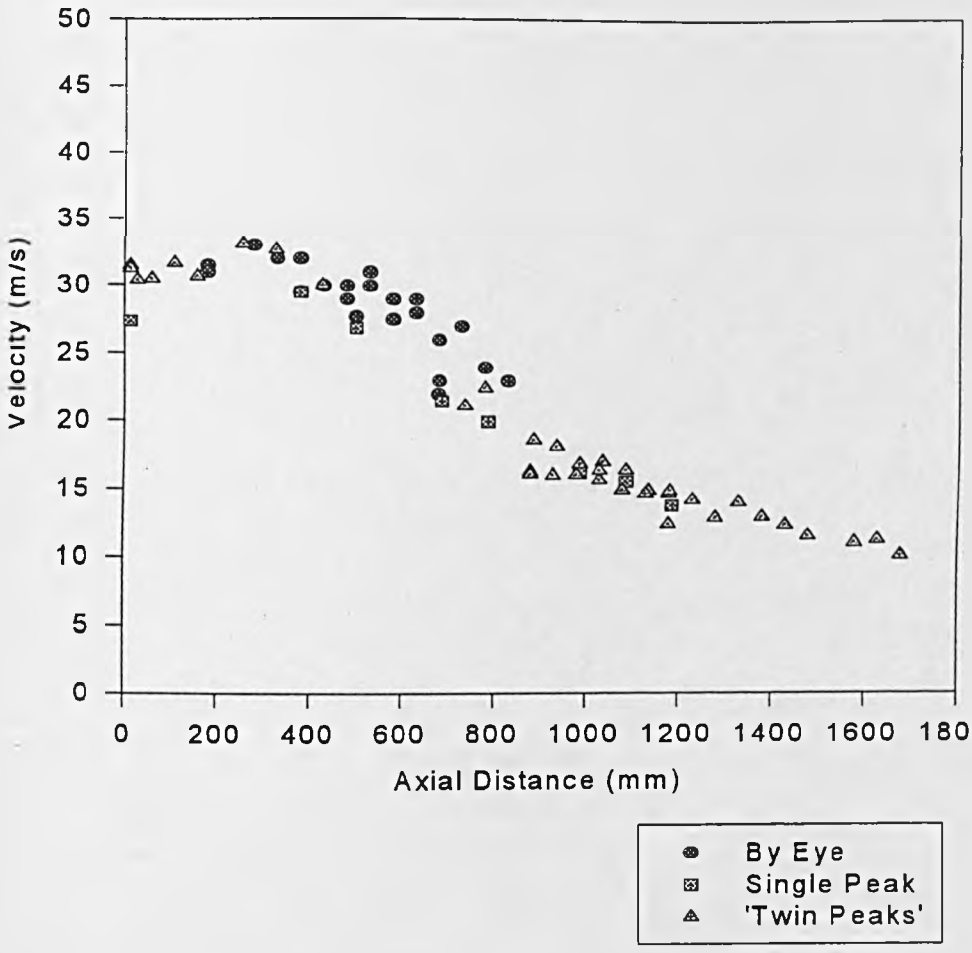

Figure 6.7 - Centreline Axial Velocity Profile

6.6 RESULTS

6.6.1 Velocity Data

The experimental results are presented graphically in Figures 6.7 to 6.17. Tabulated data may be found elsewhere [9]. A small number of data points obtained are not included in the corresponding Figure. The reasoning for this has been presented in Section 6.5.4.

Figure 6.7 presents the centreline axial velocity profile, with Figures 6.8-6.11 giving lateral axial velocity profiles.

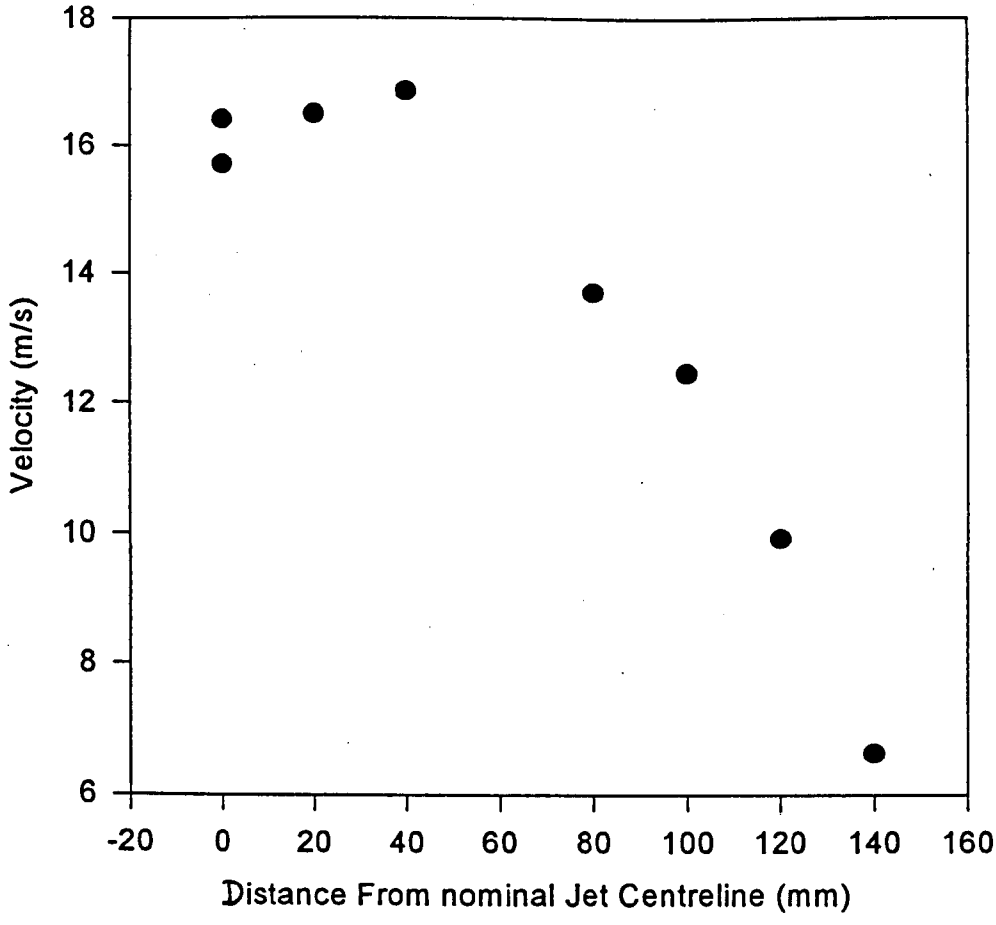

Figure 6.8 - Lateral Axial Velocity Profile at 1028mm

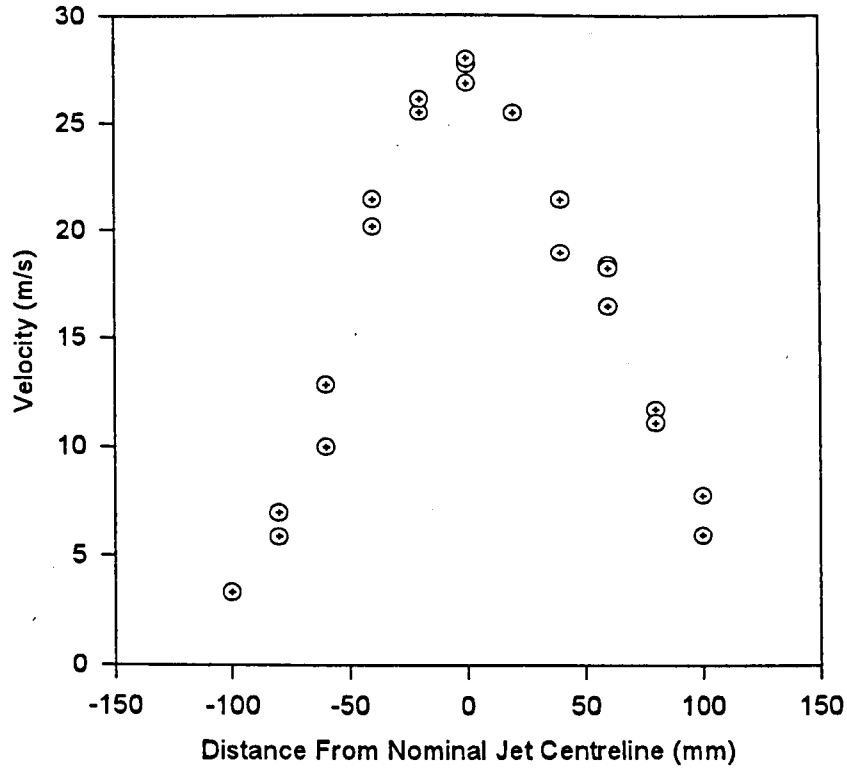

Figure 6.9 - Lateral Axial Velocity Profile at 500mm

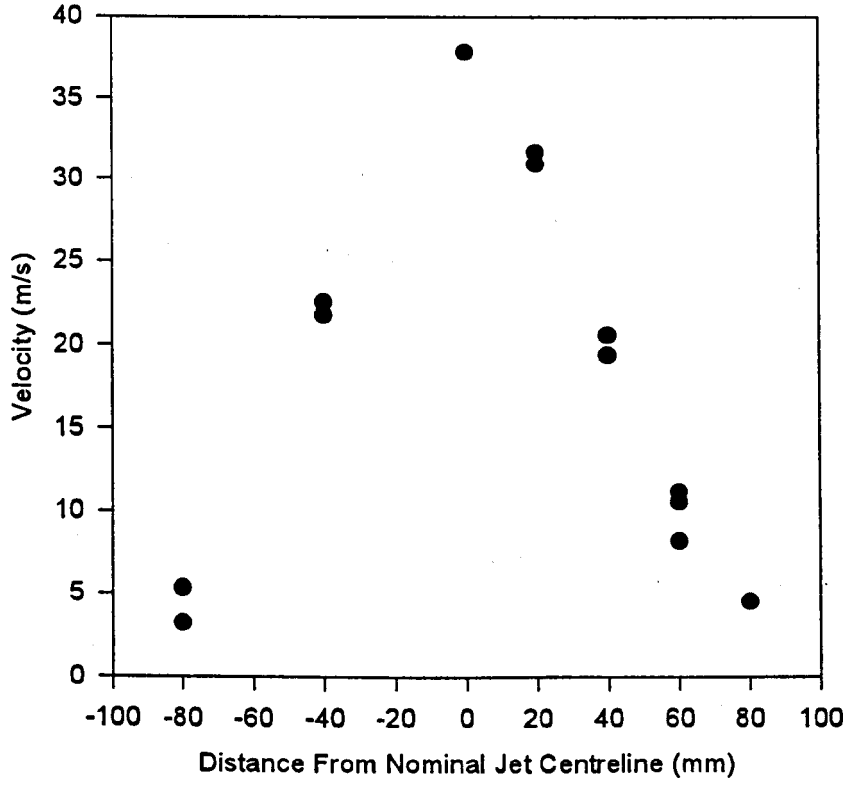

Figure 6.10 - Lateral Axial Velocity Profile at 300mm

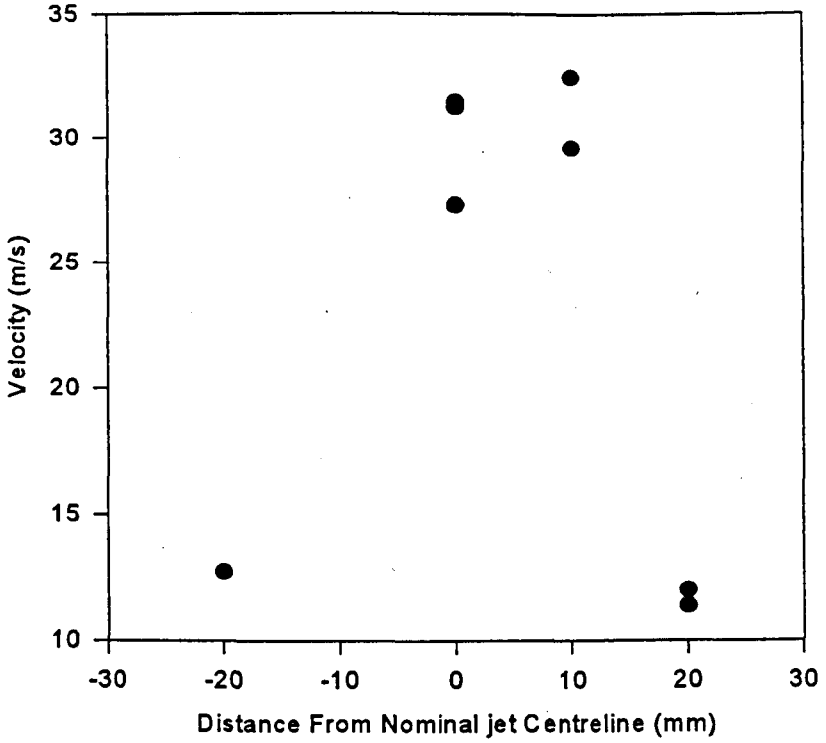

Figure 6.11 - Lateral Axial Velocity Profile at 12mm

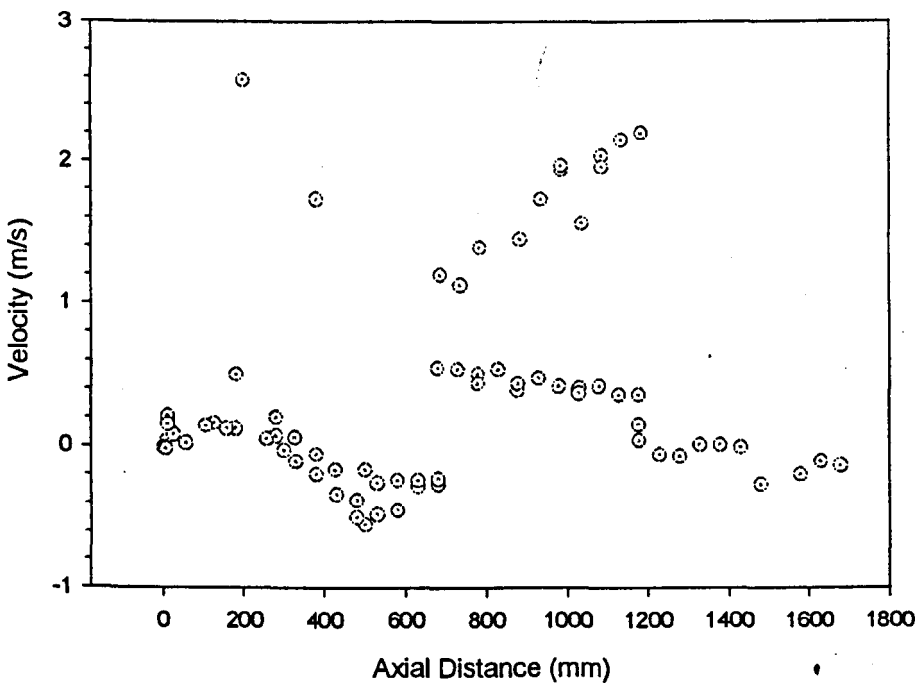

Figure 6.12 - Centreline Lateral Velocity Profile

A centreline lateral velocity profile is presented in Figure 6.12, with width profiles of lateral velocity shown in Figures 6.13 -6.16.

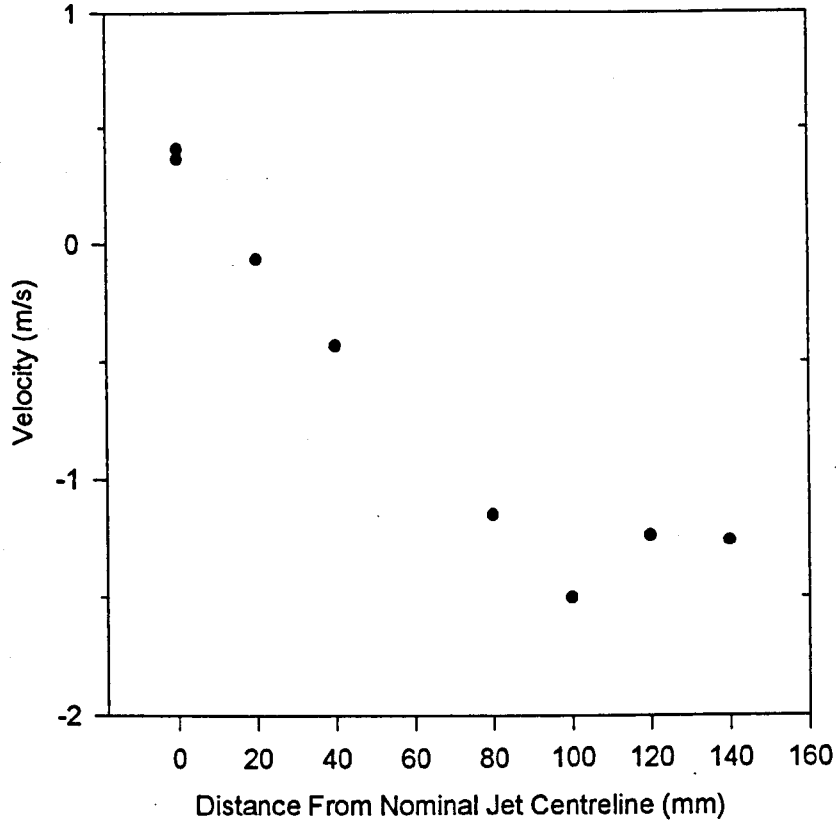

Figure 6.13 - Width Profile of Lateral Velocity at 1028mm

A comparison of centreline axial velocities obtained with 4 x 40mm and 6 x 60mm nozzles is presented in Figure 6.17.

A non-dimensional plot [10] of the lateral axial velocity profiles is presented in Figure 6.18. The basis for this is presented in Section 6.7.1.

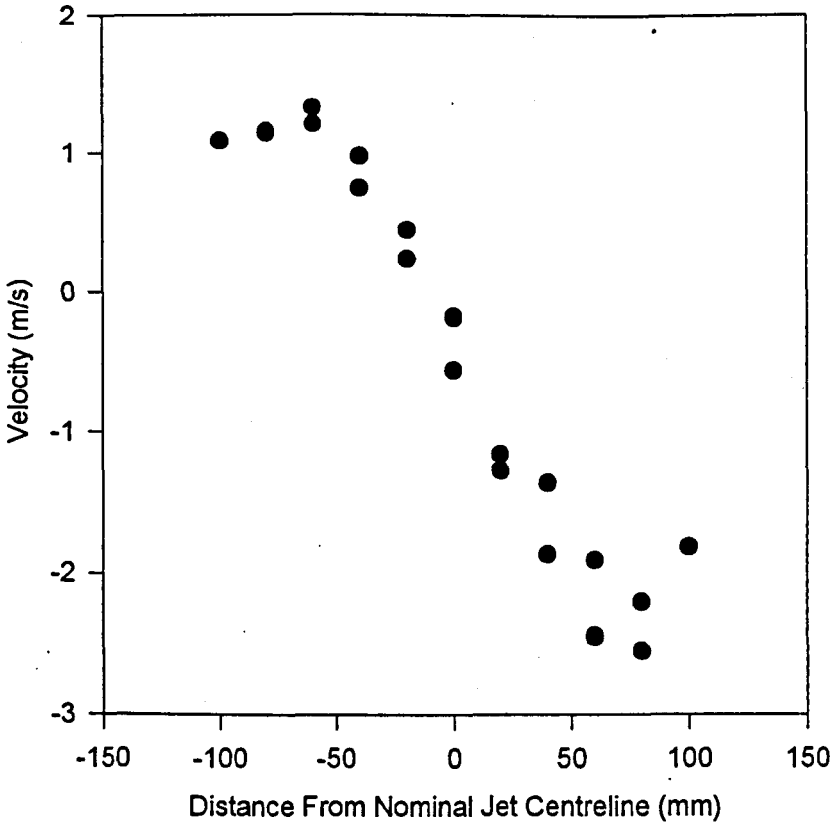

Figure 6.14 - Width Profile of Lateral Velocity at 500mm

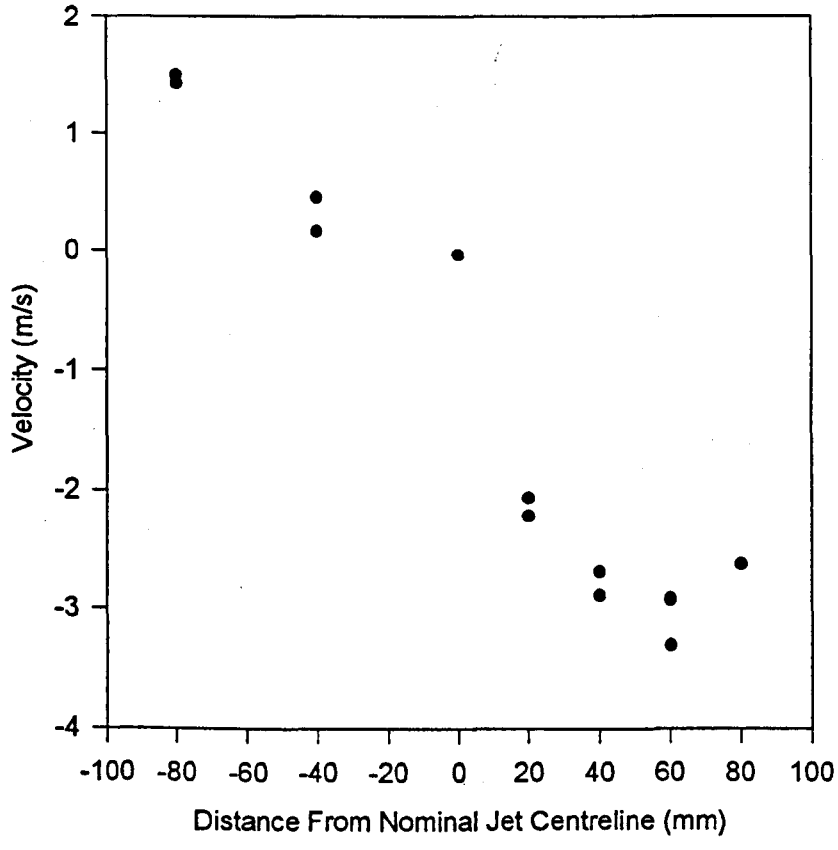

Figure 6.15 - Width Profile of Lateral Velocity at 300mm

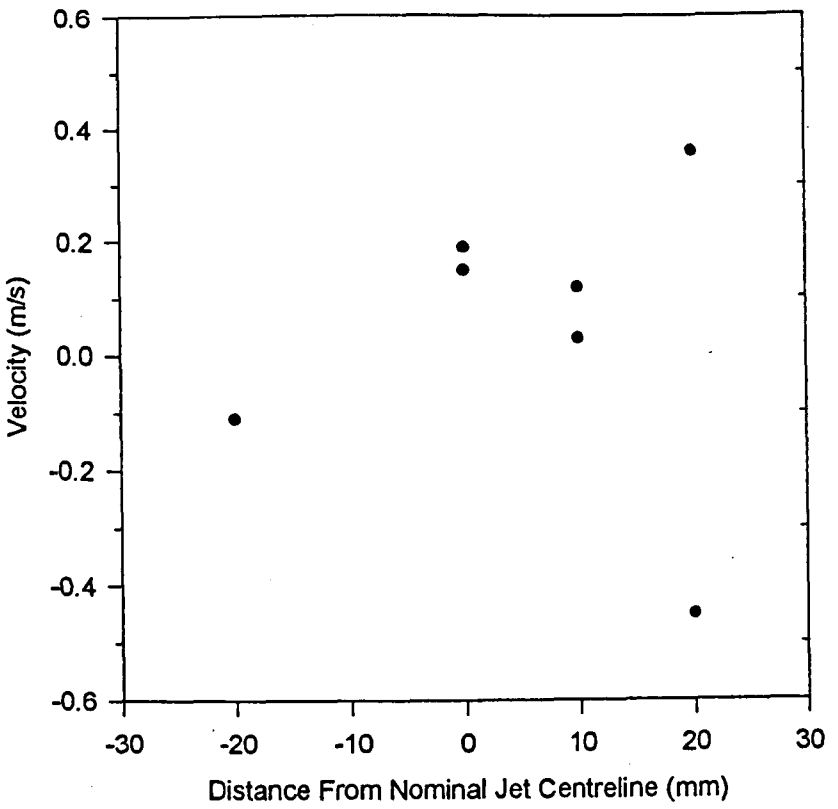

Figure 6.16 - Width Profile of Lateral Velocity at 12mm

6.6.2 Mass Release Rate Data

The average mass release rates for each set of experiments undertaken using the 4 x 40mm nozzle are presented in Table 1 (at the end of this chapter), along with an average value for the complete series. Standard deviation values are also presented. Certain mass release rates from each set of experiments are not included in the Table, or the average value calculations. The reason for this is given in section 6.7.

For the 6 x 60mm nozzle, individual experimental mass release rates are presented in Table 2 (at the end of this chapter), again with overall average mass release rate and standard deviation information.

The average mass release rates were obtained by the following formula:

$$(B_{sv}-A_{sv}) / T_r$$

where,

B_{av} is the average of x mass data points before the pressure switch is activated

A_{av} is the average of x mass data points after the pressure switch is deactivated

T_r is the duration for which the pressure switch is activated (=jet release duration)

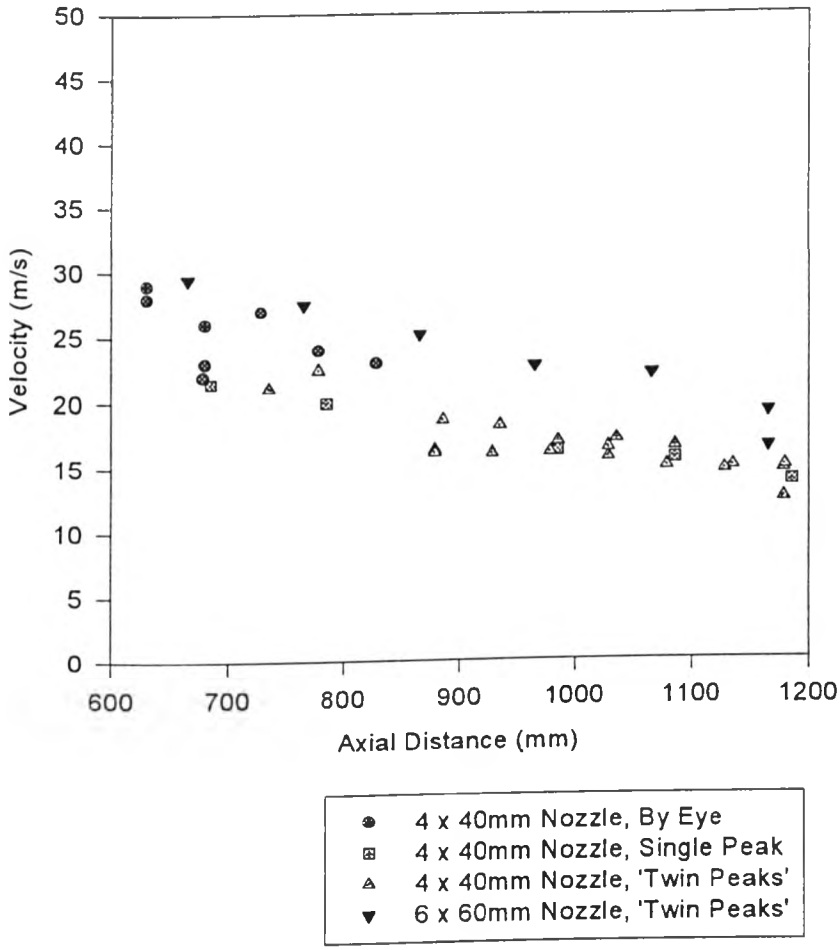

Figure 6.17 - Comparison of Centreline Axial Velocities For 4mm and 6mm i.d. Nozzles

6.6.3 Temperature Release Data

The average release temperature for each experiment is shown in Figure 6.19. It is the average temperature of all temperature data points taken between the activation and deactivation of the pressure switch. This was determined in a similar manner to the average mass release rate, as part of the same software program.

The average release temperature of the experimental series was 15.8 °C with a standard deviation of 0.89°C.

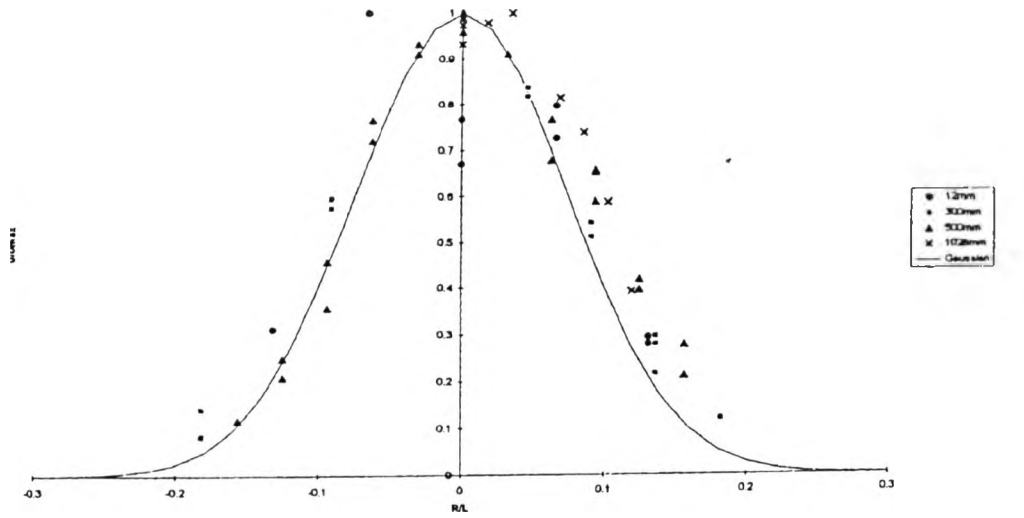

Figure 6.18 - Non-Dimensionalised Lateral Axial Velocity Profile [10]

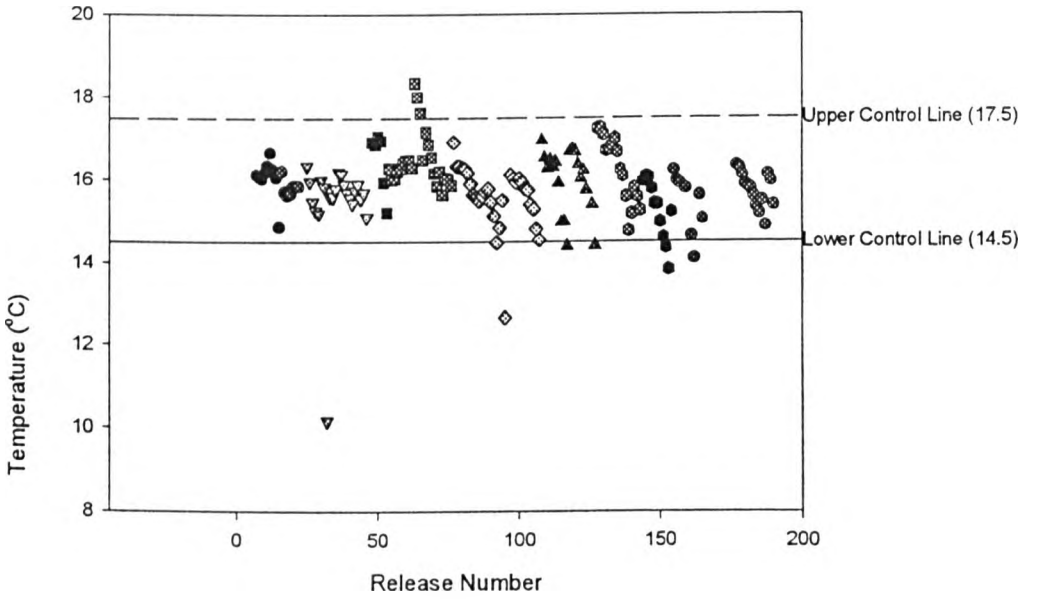

Figure 6.19 - Average Storage Vessel Temperatures For Individual Releases

6.7 DISCUSSION AND INTERPRETATION

6.7.1 Velocity Data

The axial centreline velocities exhibited approximately the expected trend. In the first part of the jet the velocity increases slightly as distance increases from the nozzle, or could be said to be approximately constant. This is then followed by the expected decrease in axial velocity with increasing distance downstream.

All lateral axial velocity plots generally show the same Gaussian shape. This is best illustrated in Figure 6.18, where the full set of data points has been plotted in a non-dimensional form [10]. As can be seen, all of the data (except that for 12mm) collapses down to lie on, or close to, one Gaussian curve. The data taken at 12mm from the nozzle shows the greatest deviation from this distribution on the centreline, which is most likely due to the difficulty in making valid measurements at this point, or possibility due to the fact that the flow may still be developing at this point.

The non-dimensional plot was produced in the following manner:

The lateral position (R) was non-dimensionalised by the axial distance (L), allowing for an offset for non-zero radius giving (R/L) as the non-dimensional distance parameter. The non-dimensional velocities (U/U_{max}) were determined by dividing the axial velocity data (U) by the maximum observed velocity.

The fact that the data collapses well in this format suggests that the jet spreads at a constant rate, in the same way that occurs with ambient density jets. This is further supported by the fact that the previously obtained conventional temperature measurements have also been found to collapse in a similar manner if a linear spread is assumed (the collapsed temperature profile can be found in Chapter Five, Figure 5.9).

The centreline lateral velocities would all be expected to be around zero. Although they are very small, this is evidently not the case, with both positive and negative non-zero values being measured. It is felt that the reason for this is that the

measurements were not taken exactly on the centreline. A slight deviation from the centreline would result in the observation of quite high lateral velocities. The direction of such velocities (ie positive or negative in data terms) would depend upon which side of the centreline the measurement was taken. It is believed that the marginally off-centre measurement positions suggested by these results would not greatly affect the centreline axial velocity values.

The width profile of lateral velocity at 500mm is as expected. The shape of the curve generated by the data gives the expected profile, with points at opposite sides of the jet centreline being of equal magnitude and opposite sign. This indicates an equal degree of lateral expansion either side of the centreline. Unfortunately, as detailed previously, the actual jet centreline (as determined by the shape of the profile) and that position deemed to be the centreline for plotting purposes are not the same. This is also evident on the other width profiles. Although it is more difficult to determine the shape of the other profiles, the pattern is similar to that for 500mm. It should be noted that the 1028mm profile covers only one half of the width. The 12mm profile differs from the others in its shape, which is difficult to determine due to the small number of data points.

6.7.2 Mass Release Rates

The mass release rates presented in Tables 1 and 2 show relatively small standard deviation. Certain values from each set of experiments have been omitted. This is due to two reasons:

i) In the majority of cases, the first release of each set of experiments gave an apparently high mass release rate. This was due to the fact that the first release started with an empty transfer line, and was terminated with a full one.Thus the mass of liquid propane lost from the vessel did not represent the mass of liquid released in the jet.

ii) In many cases, the final one, or occassionally two, mass release rate values were low. This was a physical effect, due to a reduction in the volume of propane

remaining in the vessel, and hence the reduced pressure/temperature of that liquid. This mainly effected the mass release rate due to the automated method of averaging employed.

Overall, the repeatability of the mass release rate for a given set of stagnation conditions is good. The variability that exists is most likely due to varying (small) degrees of phase change by the liquid prior to its arrival at the nozzle, caused by differing heat transfer rates between the liquid and the transfer line/header tank.

6.7.3 Temperature Release Data

As can be seen in Figure 6.19, there is a steady decrease in the vessel temperature for the majority of releases. The vessel temperature however stays within the intended range in most cases. The standard deviation for the data is good, especially if it is taken into consideration that one series of experiments was commenced at a temperature outside the intended range. The rapid decrease in temperature at the end of some experimental series is due to the fact that the loss of energy (through mass loss) far exceeded the ability of the heating system and the remaining small volume of liquid propane to input or redistribute energy. This meant that the temperature of the remaining volume of liquid was not maintained within the intended range. Where the data has been obviously affected by this process, it has been omitted.

6.8 COMPARISON WITH TRAUMA

The data obtained has been compared with the AEA/HSE code TRAUMA. Uncertainty in the precise exit conditions means that different results are obtainable from TRAUMA by making slightly differing, yet equally plausible, assumptions about the exit flow conditions. It should be noted that no model parameters are adjusted to fit the observed data, rather slightly different assumptions are made about the exit flow conditions.

The choice of exit conditions which give the best fit to the conventional centreline temperature data do not generate a best fit to the velocity data, and vice versa. A

good fit to the centreline velocity data is possible, but only at the expense of the good temperaturte agreement. It therefore appears that it is not possible to simultaneously fit both temperature and velocity without modifying the model. This is currently being investigated within the EJECT model by AEA Technology. A more comprehensive account of the modelling of this data can be found elsewhere [11, 12].

6.9 CONCLUSIONS

Despite the problems involved in obtaining valid data from the optically difficult environment of the early stages of a two-phase flashing propane jet, a good centreline axial velocity profile has been produced. This is the first such profile obtained.

Good lateral velocity profiles have also been obtained at several positions, although in many cases these demonstrated that some difficulty existed in being able to accurately determine the exact centreline of the jet prior to undertaking measurements. A more accurate positioning system for the LDA would facilitate the comparison of lateral measurements made at differing axial positions.

The LDA system is capable of obtaining velocity information from such difficult environments, but the data obtained must be carefully analysed. The LDA cannot be used as a 'black box' device in such environments, as this may result in inaccurate data and erroneous conclusions. It is not possible to use more automated LDA systems in such environments, as the low data rate obtained would render them ineffective.

TABLE 1

Average Mass Release Rates For 4mm i.d. Nozzle

RELEASE NUMBER	MEAN (kg/s)	STANDARD DEVIATION	MINIMUM (kg/s)	MAXIMUM (kg/s)
7-15	0.12	7.170e-3	0.12	0.14
16-22	0.11	8.597e-3	0.1	0.13
25-32	0.12	0.01	0.1	0.14
33-46	0.12	0.02	0.09	0.14
48-53	0.12	0.01	0.11	0.13
54-76	0.13	0.03	0.1	0.24
77-95	0.11	0.01	0.09	0.13
97-107	0.09	8.311e-3	0.08	0.11
108-117	0.11	0.01	0.08	0.12
118-127	0.11	0.01	0.1	0.12
128-143	0.12	0.01	0.1	0.14
144-154	0.12	0.02	0.1	0.14
155-165	0.1	0.01	0.08	0.11
176-190	0.1	0.01	0.08	0.13
Full Data Set	0.11	0.02	0.08	0.24

TABLE 2

Mass Release Rate data For 6mm i.d. Nozzle

RELEASE NUMBER	MASS RELEASE RATE (kg/s)		Mean (kg/s)	Standard Deviation
192	0.25	Full Data Set	0.22	0.02
193	0.23			
194	0.24			
195	0.21			
196	0.2			
197	0.21			

CHAPTER SEVEN

DROPLET SIZE DISTRIBUTION MEASUREMENTS

7.1 INTRODUCTION

Droplet size distribution is another one of the parameters required to enable predictive two-phase flashing jet mathematical models and codes to be validated and refined. Prior to the commencement of this work no published droplet size distribution data for the near-field regions of two-phase flashing propane jets had been produced. During the course of this work, as already detailed in Chapter Six, a paper was published [1] which presented some laser-based measurements of velocity and droplet size distribution in this region.

Their work, however, generated data by the intrusive use of a phase Doppler particle analyser (PDPA), protective cylinders being introduced into the jet to reduce jet density around the measurement point so as to enable data to be acquired. Due to the physical intrusion into the jet, distortion of the jet's behaviour may have taken place, especially in relation to the droplet velocity and size distribution characteristics. The experimental set-up described in this chapter resulted in data acquisition in the near-field regions of the jet without the need for physical intrusion into it. Any experimental measurement error of the droplet size distribution due to this effect, reported by the previous authors [1] as ca 20% is, therefore greatly reduced.

However, the normal physical characteristics of the jet resulted in an optically harsh environment, especially in the near-field regions, that necessitated considerable data analysis and manipulation in order to obtain useful information.

7.2 EXPERIMENTAL SYSTEM

The small scale two-phase release facility, as described in Chapter Four, was utilised for this series of measurements. No additional modifications, relative to the ones described in Chapter Six, were made to the facility for this aspect of the work.

As previously, the storage and approximate release point temperature and pressure measurements were acquired using the CyberDas data collection card and a personal computer, at a collection rate of 5Hz.

Details of the particle size measurement system and its application are detailed in subsequent sections.

7.3 MALVERN PARTICLE SIZER

7.3.1 Technique

The Malvern particle sizer works on the principle of Fraunhofer diffraction, whereby incident light is scattered, or diffracted, by particles through an angle which is inversely proportional to the particle size.

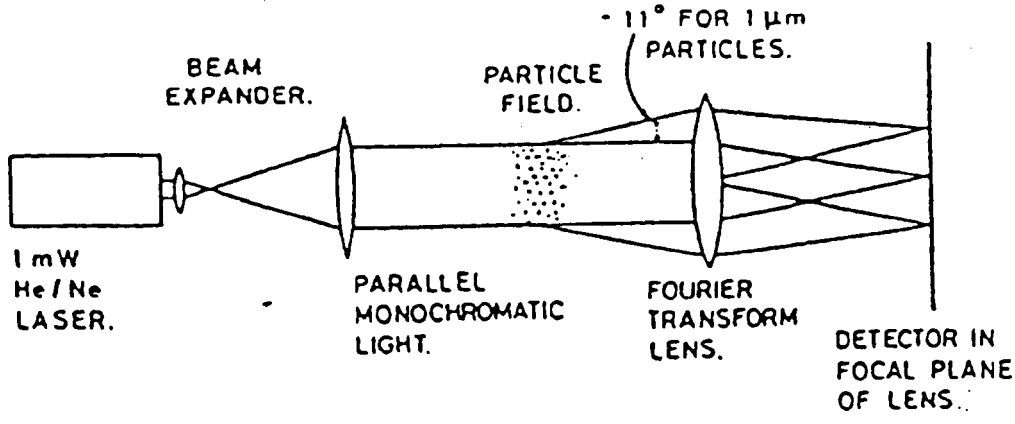

Figure 7.1 - Schematic of Particle Size Technique [2]

The technique was developed as a particle size measurement tool by Swithenbank et al [2], the basics of which are shown schematically in Figure 7.1, and was first exploited commercially by Malvern Instruments.

The monochromatic light from the laser source is expanded, and then formed into a parallel beam. This beam passes through the particle field (e.g. droplets in the two-phase jet) wherein it is diffracted by the particles. The light is then focussed by a

Fourier Transform Lens (FTL) onto a light detector array, the signals from which are interpreted by computer to yield size distributions.

The important element in the system is the FTL. Light parallel to the axis of an FTL is always focussed by it onto a point on the axis of the beam, and the diffracted light is 'focussed' around it. The position at which the diffracted light is focussed is dependent solely upon the angle at which it impinges upon the lens, and is independent of the position of the particle in the laser beam. Hence the motion of any particle has no influence upon the focussed diffraction pattern, and so the technique can be applied to moving particles, i.e. flow scenarios.

There are problems associated with this technique. Firstly multiple diffraction of the laser light, due to high particle number densities, gives rise to inaccurate results. Light scattered by one particle is assumed, in the standard commercial data analysis software, to undergo no further interaction with the particle field before reaching the FTL [2]. In a dense spray, however, such as a two-phase jet, this may not be the case, and the scattered light is then subsequently scattered itself by other particles.

This results in the calculated distribution being displaced, relative to the true distribution, towards larger angles of scattering, i.e. smaller particles. Overall, unless taken into account in the calculation process, a broader distribution with a smaller mean size value than is actually present will be determined. This problem has been extensively investigated and both empirical and theoretical solutions proposed [3, 4, 5, 6, 7, 8, 9]. The modelling algorithms derived have extended the obscuration limit of applicability from 50% up to 98% [4] for certain of the modelling codes (Rosin-Rammler and Log-Normal distribution), although no commercial algorithm exists for the Model Independent code which was used in these experiments.

A further problem [9] is related to the inversion of the light scattering data to droplet size distributions. This is the potential error which may arise through the theoretical assumptions and approximations made in the energy to size distribution conversion modelling process. Some inversion algorithms, e.g. Rosin-Rammler, assume that the

size distribution will be of a specific form, and generate a 'best fit' to that form. If the true size distribution does not follow the prescribed form then errors are introduced during the inversion process.

In the case of rapidly evaporating droplets, such as would be the case for a superheated fluid, there is also the possibility of measurement error due to diffraction of the laser light by the 'shell' of dense vapour surrounding the liquid droplet(s). This would give rise to spurious larger particle size values, and would also give rise to 'dense' spray type problems.

Fraunhofer diffraction has been proven as a measurement technique, and is commercially available as the Malvern Instruments particle sizer. This technique, principally in the Malvern guise, has been used in various measurement areas [10, 11, 12, 13, 14, 15, 16, 17], including relatively dense two-phase flows [18], and as a yardstick for other techniques.

7.3.2 Experimental System

The Fire Safety Section Malvern particle sizer operates as described above. It is an old style unit, designed for use as a front-line research tool, as opposed to the more modern Malvern particle sizers which are primarily intended for routine 'benchtop' analysis. It has recently been upgraded to operate with a modern personal computer. Data capture and initial inversion/processing are done by Malvern's own software programme. Subsequent data manipulation and processing of the data were undertaken using the Malvern software, and Jandel Scientific's SigmaPlot software.

The Malvern software has the capability to invert the energy data to droplet size distributions by use of a Rosin-Rammler, Log-Normal or Model Independent forms. For the purposes of this work the Model Independent form was chosen, as it makes no assumptions about the shape of the droplet size distribution. The droplet size data is therefore calculated directly from the energy data, thus removing the possibility of inversion errors as detailed in Section 7.3.1.

One drawback to this approach is that, for the Model Independent distribution, no commercial modified algorithm exists to reduce measurement error at high obscuration values. A purpose-written stand-alone algorithm was, however, obtained [19], although in practice this was found to be incompatible with the upgraded Malvern software data output so accurate comparison between the modified and unmodified data could not be made. Physical effects occurring in the jet also invalidated the algorithm's assumptions, and therefore its use introduced errors into the modified size distribution. This is explained in greater detail in Section 7.5.1.

Figure 7.2 - Malvern Sizer In Unmodified Configuration

Due to physical restrictions of the experimental chamber, it was necessary to remove the laser-head and receiving units from the alignment bed. The laser-head unit was mounted on a support stand and positioned on the top of the experimental chamber, so that the laser beam passed through the windows on the top and bottom faces of the chamber.

The receiving unit was similarly mounted on a vertically traversing support stand under the chamber. Again due to physical restrictions of the experimental chamber, and limitations of the effective 'focal length'/droplet size measurement range of the receiving optics, the FTL had to project through the bottom chamber window into the chamber itself. This did not interfere with the jet. The 'stand-alone' nature of the system did, however, mean that it had to be realigned at each new window position or after any prolonged period of inactivity. Realignment was also undertaken, if necessary, in-between experimental releases. In practice this did not prove to be a problem as very good alignment (equivalent to, or better than, that achievable on the bed) was always achieved and maintained.

Figure 7.3 - Malvern Operating in the Small Scale Release Facility

The unmodified Malvern can be seen in Figure 7.2, operating in a non-flashing kerosene spray and Figures 7.3 and 7.4 show the Malvern operating within the experimental chamber, in its modified format, on a two-phase flashing propane jet.

Figure 7.4 - Particle Sizing Beam Inside Two-Phase Flashing Jet

7.4 EXPERIMENTAL PROCEDURE

The vessel heater system was set to the required temperature and the system left to reach an equilibrium between heater element and propane liquid. In certain circumstances it was necessary to further manually adjust the heater setting to maintain the liquid propane temperature within the chosen temperature range.

During the heating period, the Malvern was positioned at the required windows for the measurements being undertaken, if necessary, and then manually aligned. Realignment and background measurements were also performed in-between positional changes, as required, to maintain the accuracy of the system.

When a suitable liquid temperature, within the acceptable range, had been attained the CyberDas data acquisition system was set in operation. The two remote pneumatic valves, one on the vessel and one between the header tank and the nozzle, were then opened simultaneously by use of the manual valve control panel. Once the two-phase jet had stabilised, the Malvern data acquisition system was set in operation, for 2000 scans. The duration of each release was normally dictated either by the Malvern data collection duration, or, in exceptional circumstances, the operator, the maximum being typically of the order of 20 seconds.

The various measurement positions were obtained by use of the nozzle traversing system, within a limited range for axial and lateral movement, and by the relocation of the laser-head and receiving unit for gross axial positional changes.

7.5 DROPLET SIZE DISTRIBUTION DATA ANALYSIS

The standard process for the generation of droplet size distribution data, from the measured light energy distribution, is performed computationally, using Malvern software. The generation of the percentage volume size distribution is as follows:

The software briefly displays the light energy data, and then calculates the percentage volume droplet size distribution, inverting the energy data using the chosen algorithm, which was the Model Independent one in this series of experiments.

The percentage volume droplet size distribution data is then displayed alphanumerically, and this information is printed, if desired. Finally, the percentage volume droplet size distribution is displayed graphically.

It is however possible, with saved light energy data, to 'break into' the calculation process and modify various parameters. This allows the light energy data values to be modified before inversion, the algorithm type to be changed, or modifications to be made to the results display (to number droplet size distribution, amongst others)

and graphical output. The following Section details how this capability was utilised to manipulate the data obtained, in order to generate useful droplet size distribution information.

Further information on the Malvern system, and software, can be found elsewhere [20].

7.5.1 Data Manipulation and Processing Techniques

After the initial series of measurements, the unusual shape of the size distributions suggested that the results were not accurate representations of the propane droplet size distribution. It was, however, evident that the results generated were highly repeatable for any position within the jet, and might still contain information related to the droplet size distribution.

After careful analysis, it was suggested that the data indicating large droplet sizes, starting at approximately 100μm and extending beyond the limit of the instrument range, was due to unscattered radiation (i.e. the source laser beam) being diffracted by the large density gradients likely to be present in the jet.

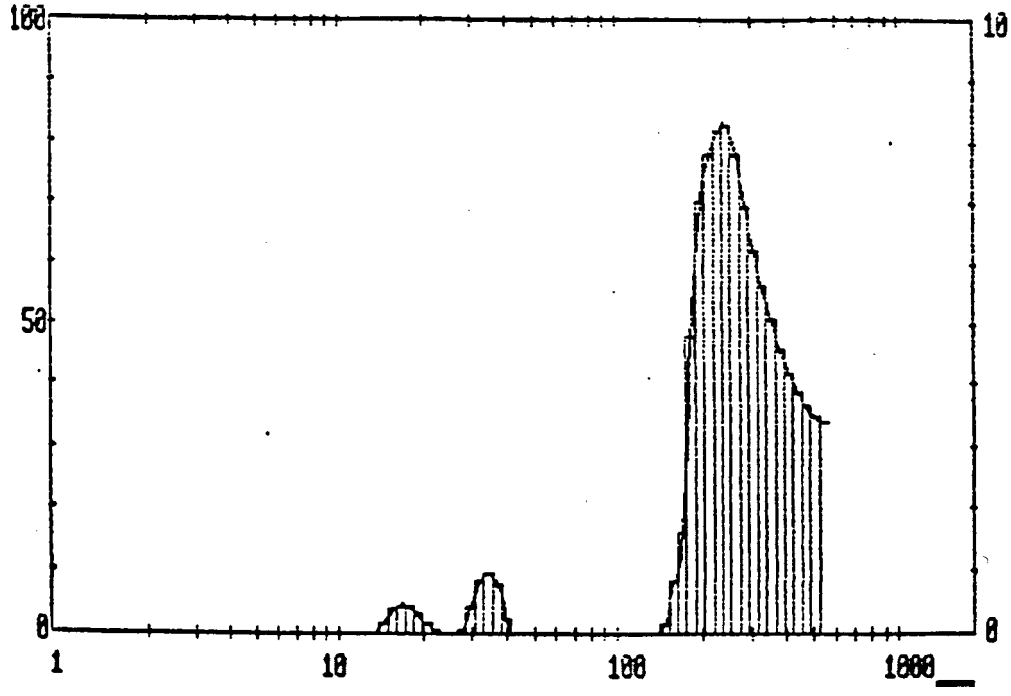

Figure 7.5 - Size Distribution Before Manipulation

This slight deviation from its normal path meant that, at the FTL, it appeared as though it was light that had been diffracted by large droplets and, therefore, it was focussed onto the appropriate detector rings, giving rise to a false distribution of very large droplets. Due to the volume size distribution presentational format of the Malvern software, the presence of a relatively small number of large droplets meant that the smaller 'real' droplet distributions were hardly visible. This is evident on Figure 7.5.

To better interpret the 'real' distribution, this 'false' data was removed, in the following manner:

The collected energy data was carefully analysed to assess the effect of the density gradient on its distribution, and to try to identify that part of it due to genuine droplet scattering. In all cases the energy distribution due to genuine droplet scattering overlapped that generated by the high density gradient. The energy data was modified to remove all the detector bands affected by the density gradient, and then an assumed energy profile was inserted for the region where overlap occurred. The assumed profile was that of a linear decrease in the light energy, the rate of decrease being determined by extrapolation of the non-overlapping region of the droplet light energy distribution. The editing of the light energy data was undertaken prior to the inversion process.

The modified energy data was then inverted into a droplet size distribution, using the Malvern software with the Model Independent algorithm. This process removed the false large droplet distribution peak, and made the 'true' droplet size distribution far more discernible. The process did, however, generate a 'ghost' peak in the distribution. The reason for this is not known, but is most likely to have been generated as a function the inversion process software. The modification and inversion process is shown in Appendix 7A.

Experimentation with the data removal and assumption process proved that the 'ghost' peak was a function of the above process, and that variations in the assumed

profile used for the energy data had a negligible effect on the 'real' distribution peaks, but a relatively large one on the 'ghost' peak. It was not, however, possible to remove the 'ghost' peak. This process is shown in Appendix 7B.

In some instances the 'ghost' peak overlapped with the 'real' distribution peaks, of which there appeared to be two. This peak rarely influenced the distribution significantly below 41.2μm, a size below which the majority of the percentage volume lay, at distances greater than ~530mm from the nozzle. For this reason it was decided to only analyse the data below 41.2μm. Analysis at a lower maximum size would have resulted in the loss of large amounts of valid data for distances greater than ~530mm.

Early analysis comprised examination of the data in three size bands, below 5.8μm, below 21.4μm, and below 41.2μm. From this analysis it was decided to only study two bands, 0-21.4μm and 21.4-41.2μm, as the majority of the valid droplet data lay within these bands, and the amount of valid data lost and 'ghost' peak data included was minimised over the entire range of experimental data.

As detailed earlier, the high obscuration values measured at virtually all measurement points would normally indicate the occurrence of multiple diffraction, thus implying that the droplet distribution as calculated above would overestimate the percentage volume of small size droplets present. It is probable, however, that the obscurations measured were artificially high due to the distortion of the unscattered beam by the high density gradient, so the degree of multiple scattering occurring in the jet was less than that suggested by the reported obscuration values.

A purpose-written Model Independent High Obscuration program [19] was utilised to try and remove this source of error, although it was found to be incompatible with the upgraded software data presentation, and so direct quantitative comparison of the high obscuration unmodified and modified data was not practical. Also, since the obscuration at some measurement points was not entirely due to multiple scattering, which is a central assumption of the multiple diffraction algorithm in the calculation

of the modified droplet distribution, errors will be introduced into the size distribution by its application. This, therefore, reduces the effectiveness of the algorithm. Some qualitative comparisons were carried out, and are presented in Figures 7.6 and 7.7. The conclusions from these comparisons are presented in Section 7.7.1.2

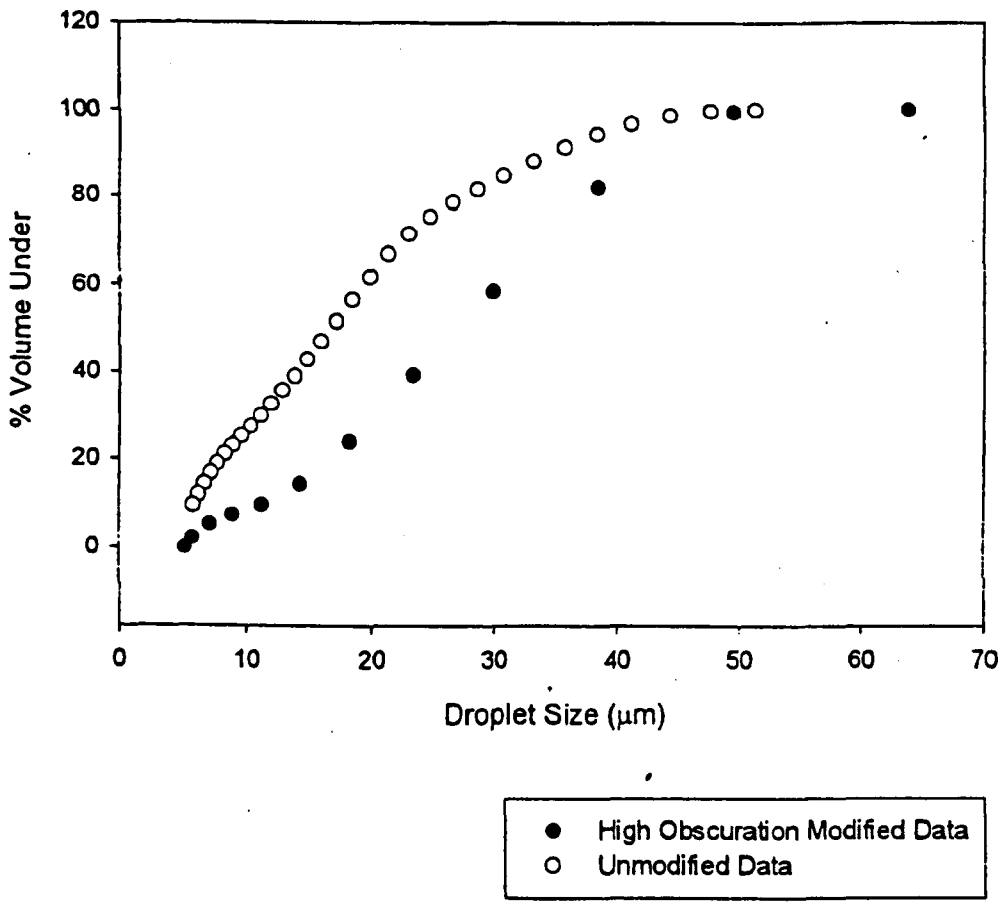

Figure 7.6 - Modified and Unmodified Data For an Obscuration Value of 0.99

It was not possible to estimate to what extent the dense vapour shell around the evaporating droplets affected the droplet size distributions obtained, and therefore no correction has been made for it. As a result, this process further adds to the unreliability of the absolute droplet size distributions obtained.

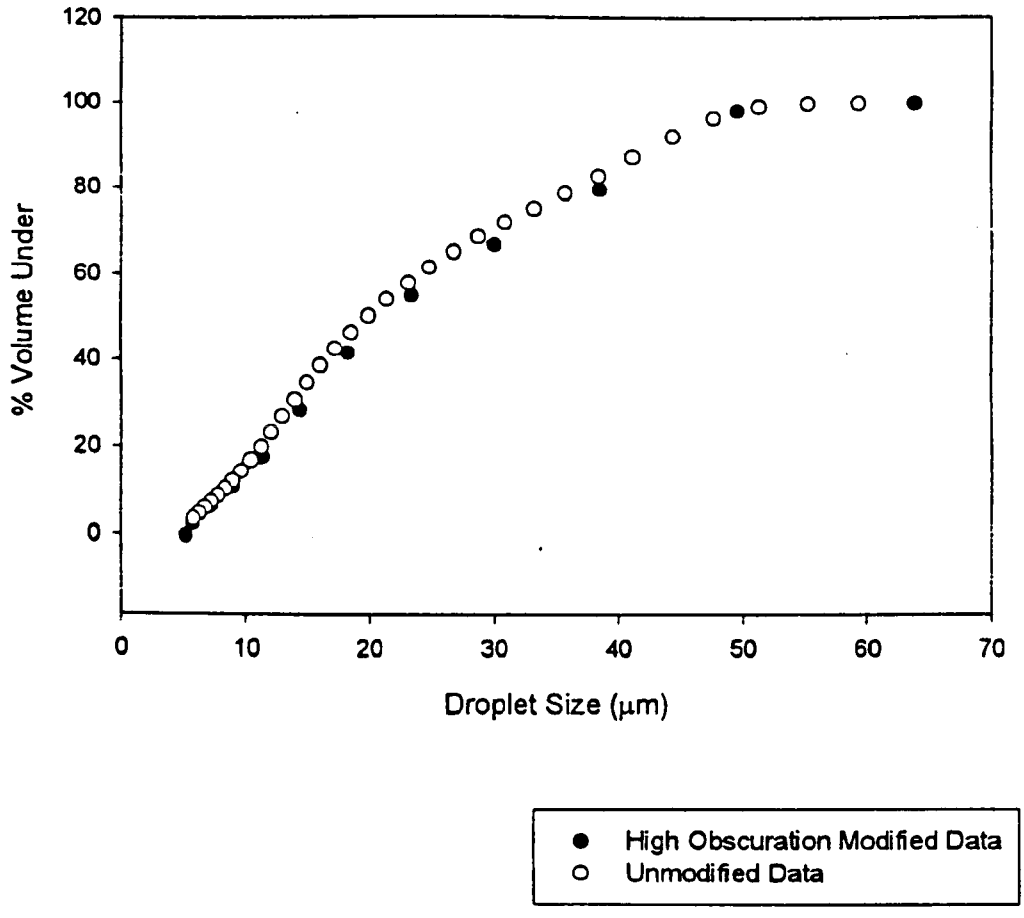

Figure 7.7 - Modified and Unmodified Data For an Obscuration of 0.5944

7.5.2 Conclusions

Due to the potential errors and uncertainties introduced by the light energy data manipulation, and the multiple diffraction and dense vapour shell distribution distortions, little emphasis should be placed on the absolute values obtained for droplet size at any one point. The droplet size data generated is, therefore, best expressed, and analysed, in terms of the general trends and overall size distribution behaviour.

Despite the uncertainty in the details of the droplet size distribution data, it is still felt that the trends reflect, as accurately as is possible, the general distribution changes along the centreline, and across the axis. The data obtained represents the best possible available with this measurement technique. Improvements could be made to the data in respect to the error introduced by not considering multiple diffraction,

although reliable obscuration measurements would first have to be obtained. The data would then have to be re-analysed by a suitable purpose-written high-obscuration program, or by a modification of the one obtained during the course of this work.

7.6 RESULTS

7.6.1 Droplet Size Distribution Data

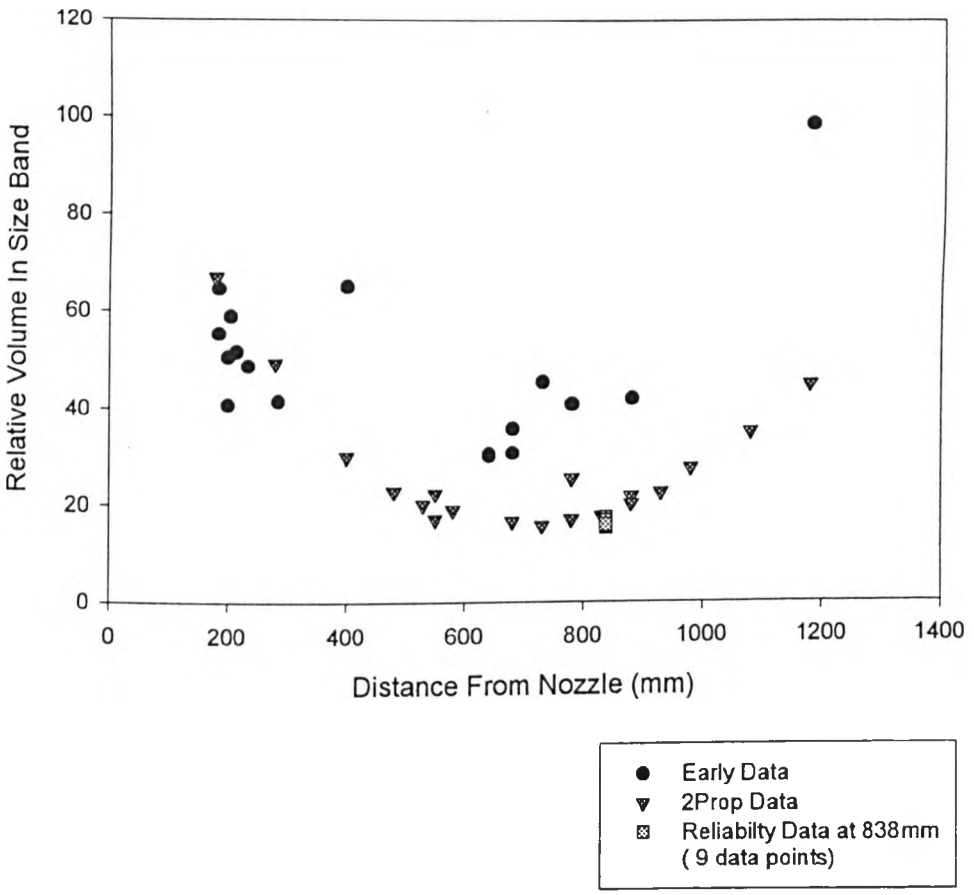

Figure 7.8 - Centreline Size Distribution 0 - 21.4μm

The centreline droplet size profiles are presented in Figures 7.8 and 7.9. The plots show the two chosen size bands, 0 - 21.4μm and 21.4 - 31.2μm, which account for the majority of the real size data obtained after the data manipulation process.

These two plots include a number of early data points, obtained as part of a series of preliminary measurements. These early data points were taken to assess the viability

of using the Malvern in such a harsh optical environment. The data was initially discarded as it did not appear to provide any useful information, but was later analysed when it proved possible to extract information from the more structured series of Malvern experiments. No mass release or temperature data exists for these measurements.

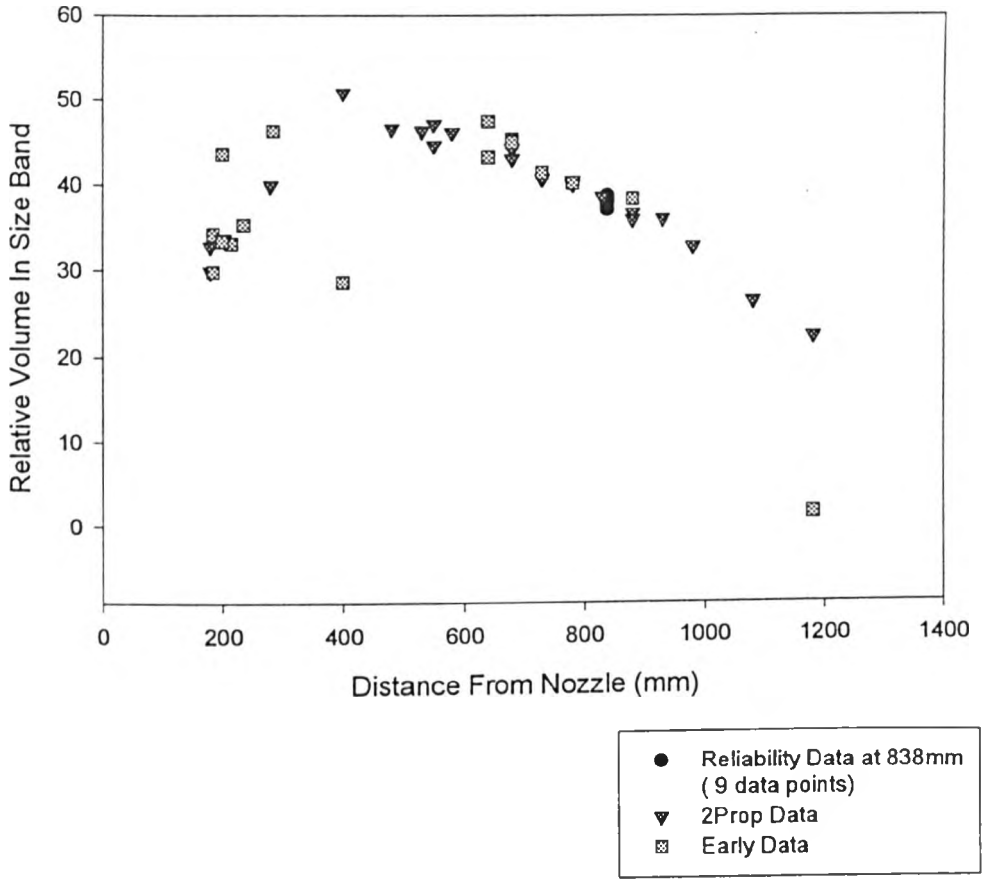

Figure 7.9 - Centreline Size Distribution 21.4 - 41.2μm

Both of the size bands chosen can be seen plotted together (without the early data points) in Figure 7.10. In each size distribution plot the relative size distribution is, effectively, the percentage of the total volume in each individual size band. The total volume is the sum of that in both bands, and that lying outside the two bands. The relative size distributions are therefore not exclusive, and a decrease in the distribution of one size band would automatically result in an increase in the other.

This is dealt with in greater detail in Section 7.7.1.

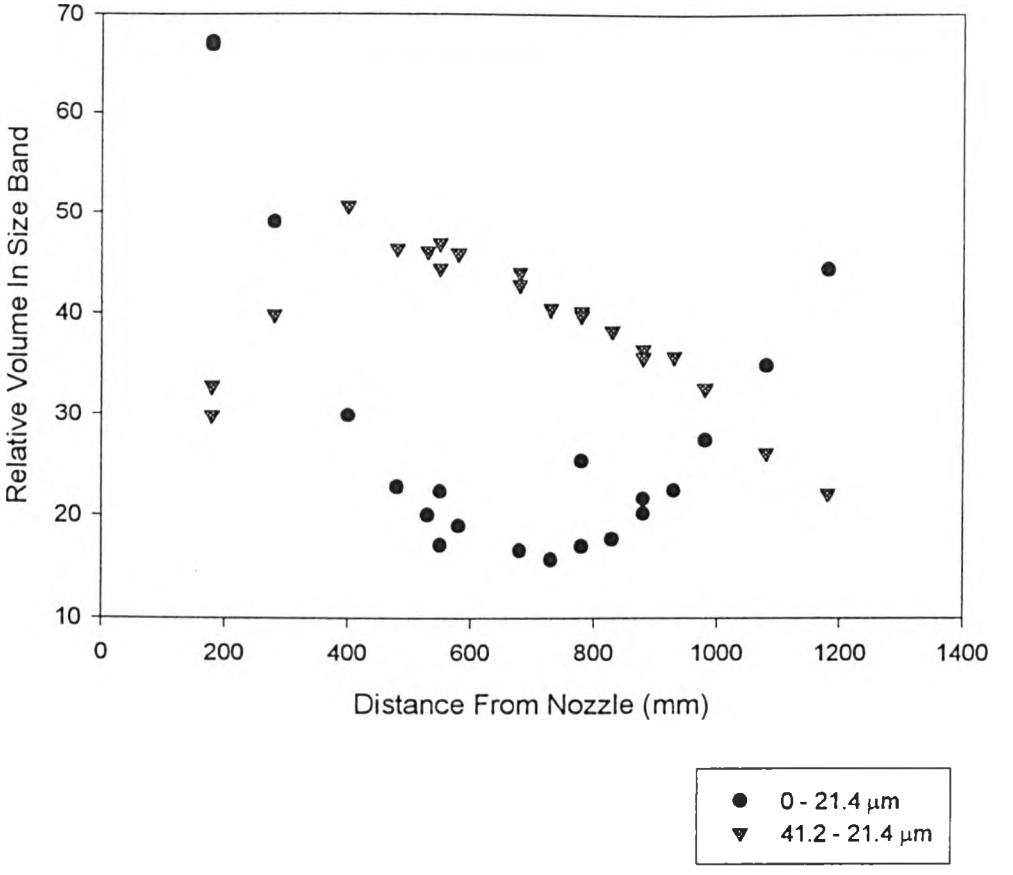

Figure 7.10 - Centreline Droplet Size Distribution Profile (2PROP Experimental Results Only)

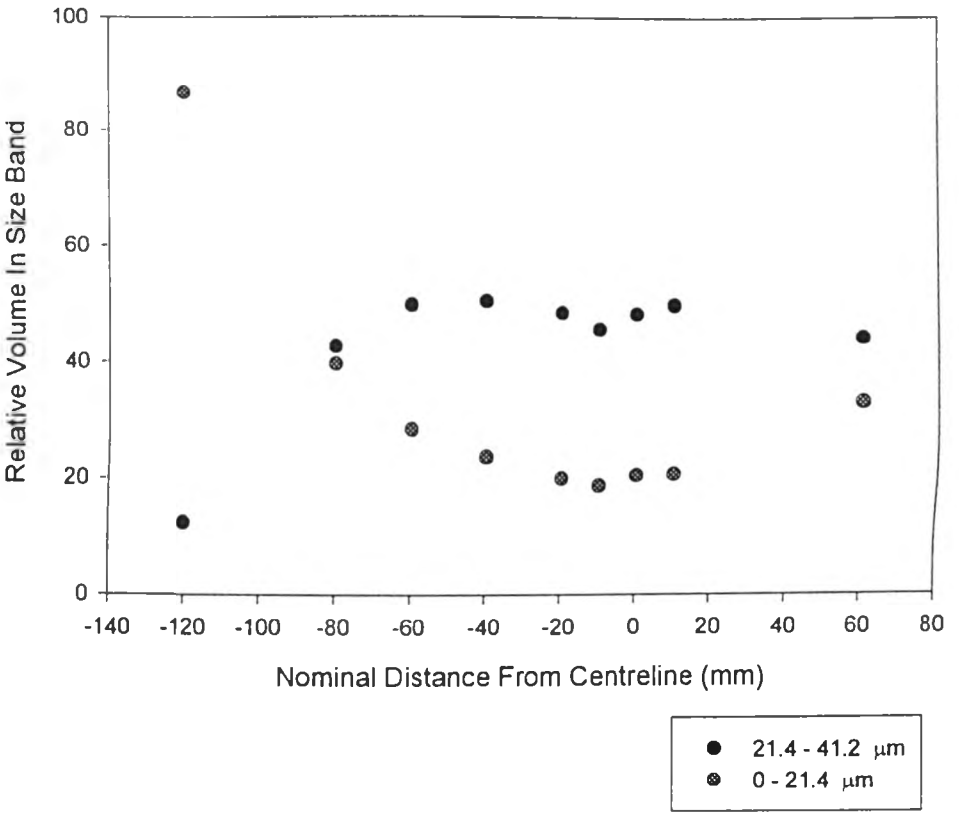

Figure 7.11 - Lateral Droplet Size Distribution at 500mm

Figures 7.11 to 7.13 present the droplet size distributions across the width of the jet at distances from the nozzle of 500mm, 688mm, and 1088mm.

A plot indicating the repeatability of the size distribution measurements is presented in Figure 7.14. These measurements were all taken at 838mm from the nozzle.

Data, in numerical form, for all of the above Figures can be found elsewhere [21].

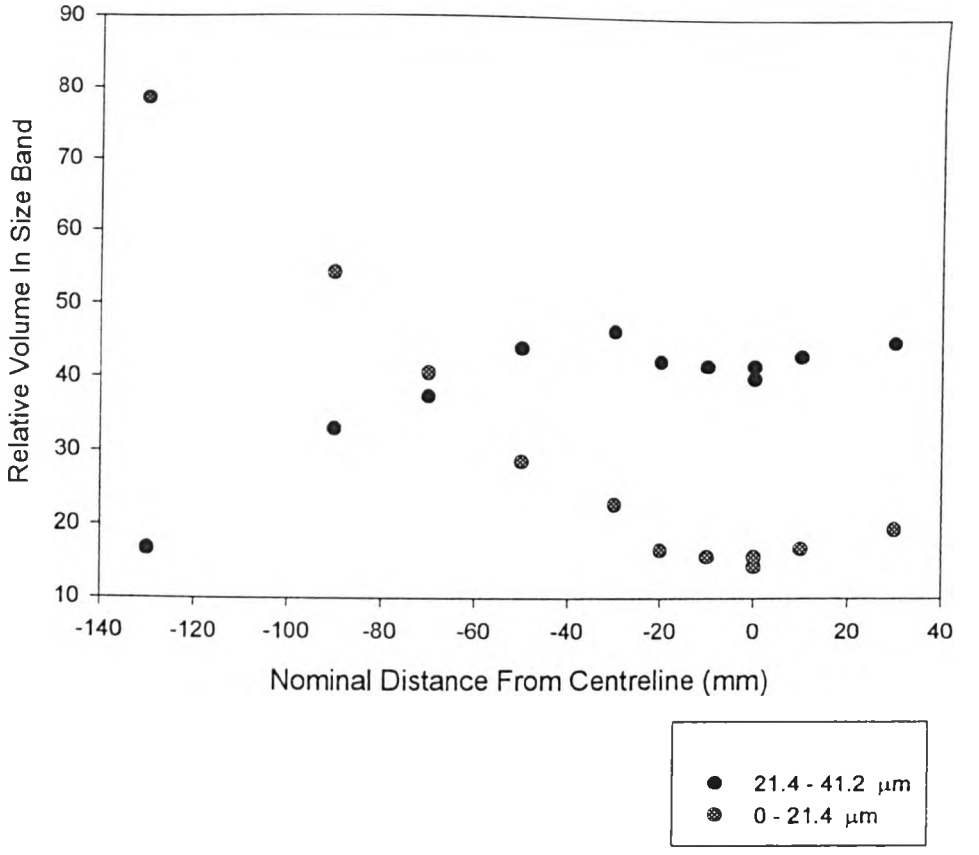

Figure 7.12 - Lateral Droplet Size distribution at 688mm

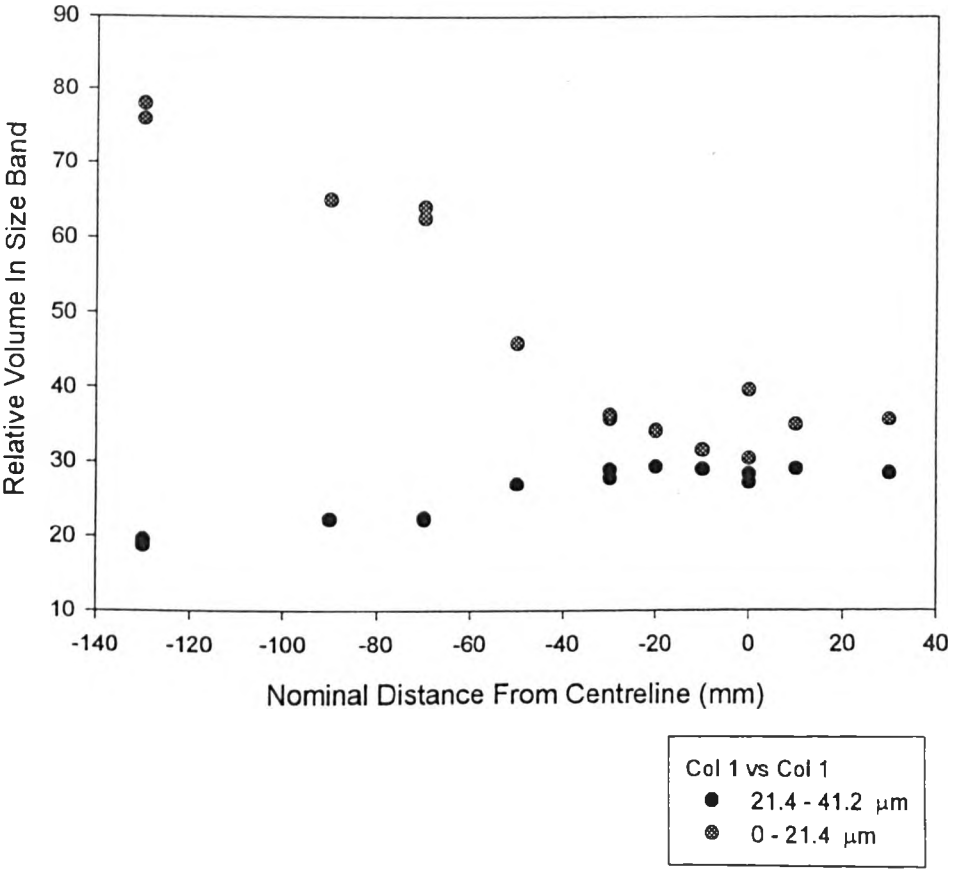

Figure 7.13 - Lateral Droplet Size Distribution at 1088mm

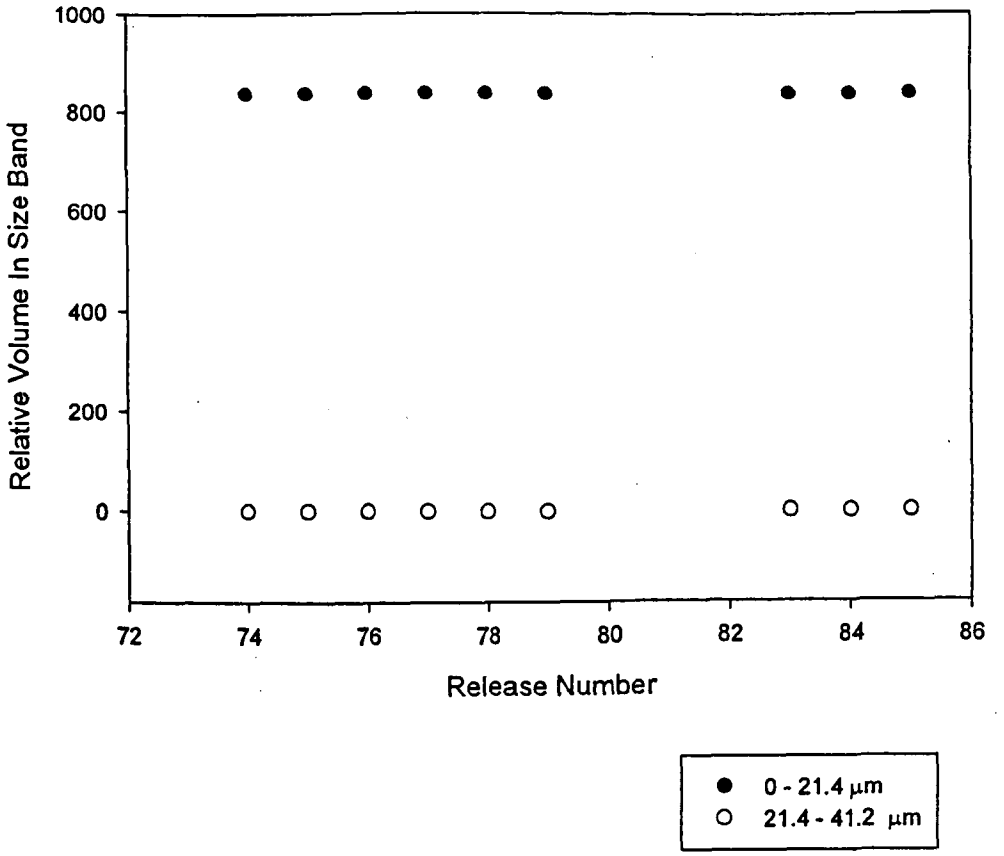

Figure 7.14 - Relative Volume In Size band Repeatability Plot (Centreline data at 838mm)

7.6.2 Obscuration Data

A three-dimensional plot of all the obscuration data is presented in Figure 7.15. Individual lateral obscuration profiles are presented, for distances from the nozzle of 500mm, 688mm, and 1088mm, in Figures 7.16 to 7.18.

Repeatability data for the obscuration measurements, taken at 838mm from the nozzle, is presented in graphical form in Figure 7.19. Numerical data for the obscuration plots can be found elsewhere [21].

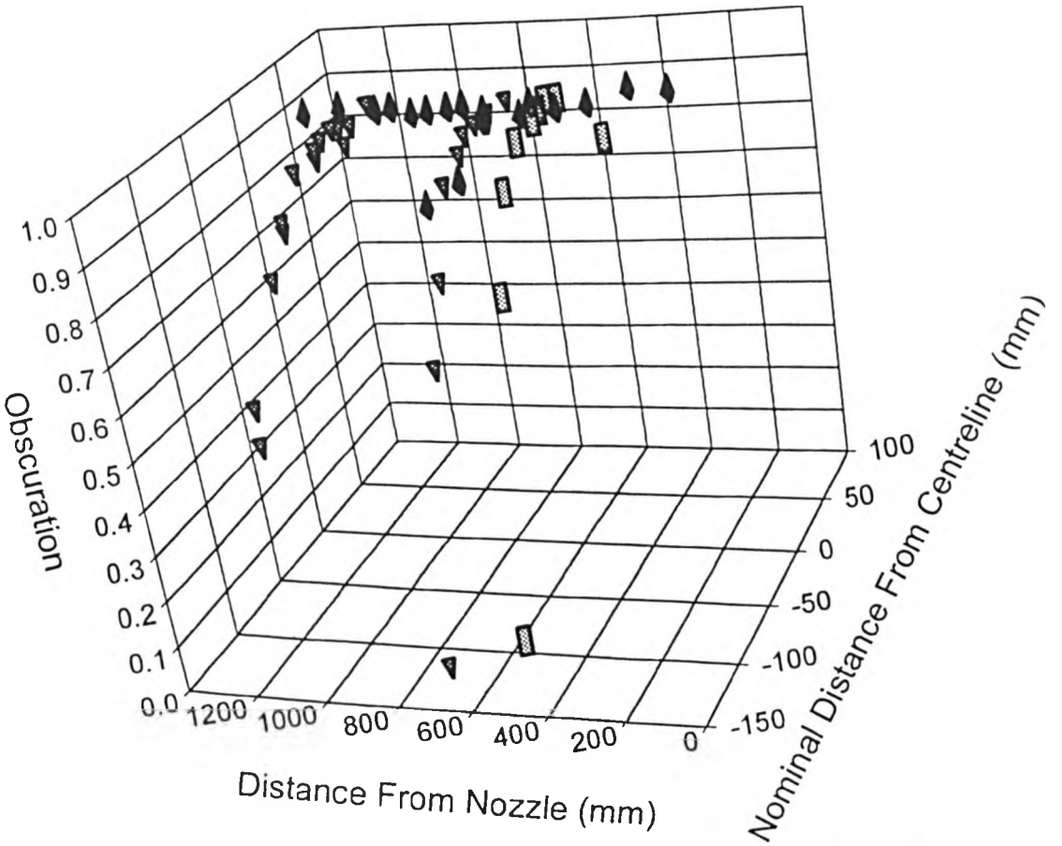

Figure 7.15 - 3D Plot of Obscuration On Centreline and at Lateral Positions of 1088mm, 688mm and 500mm

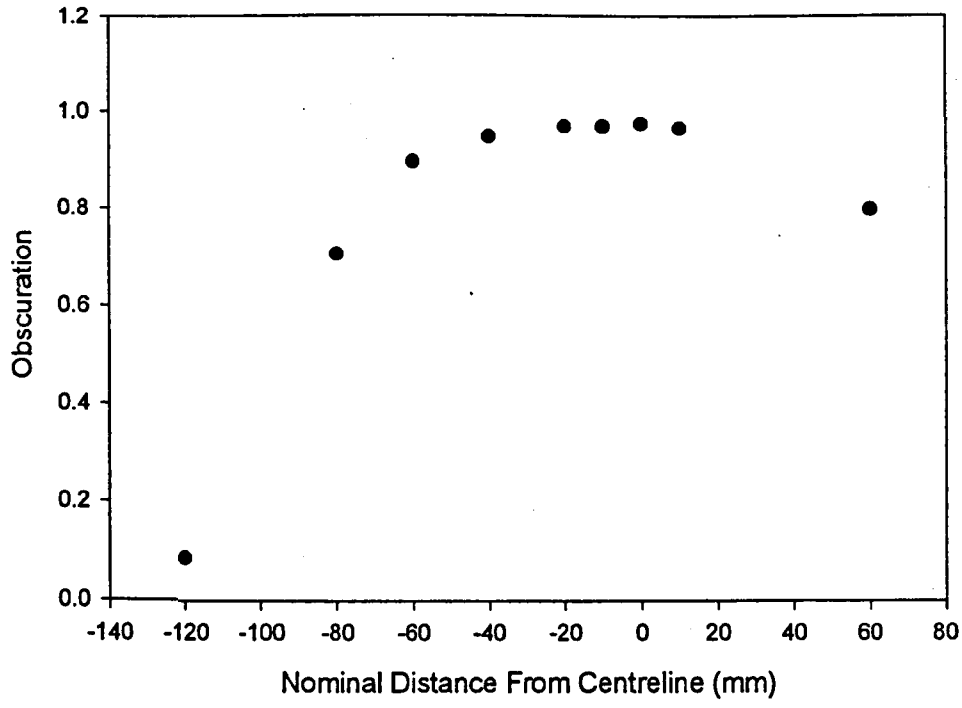

Figure 7.16 - Lateral Obscuration Profile at 500mm

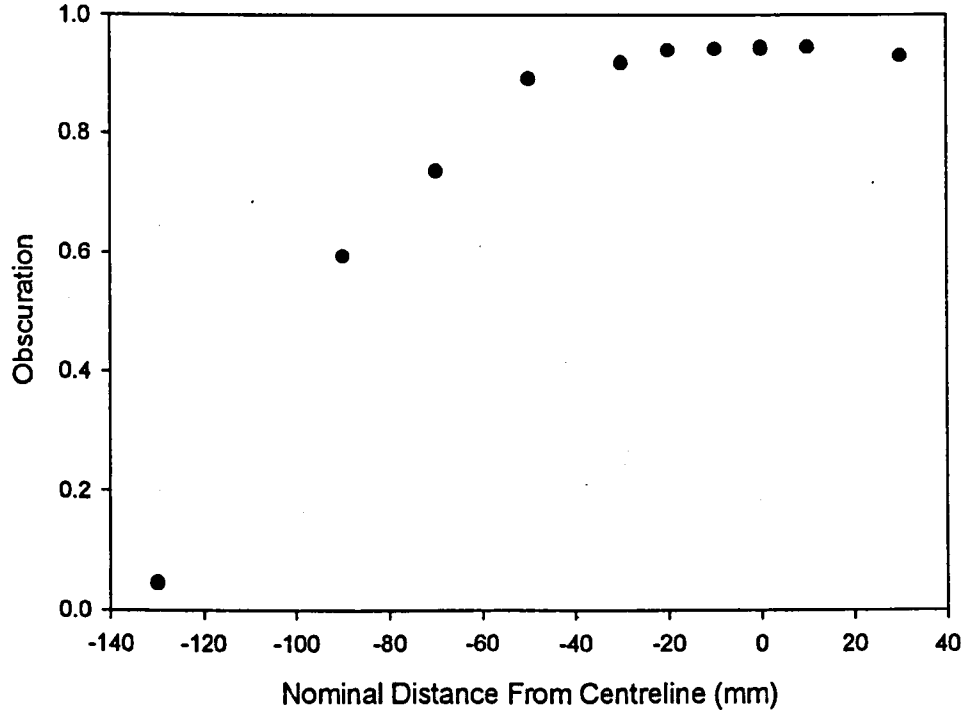

Figure 7.17 - Lateral Obscuration Profile at 688mm

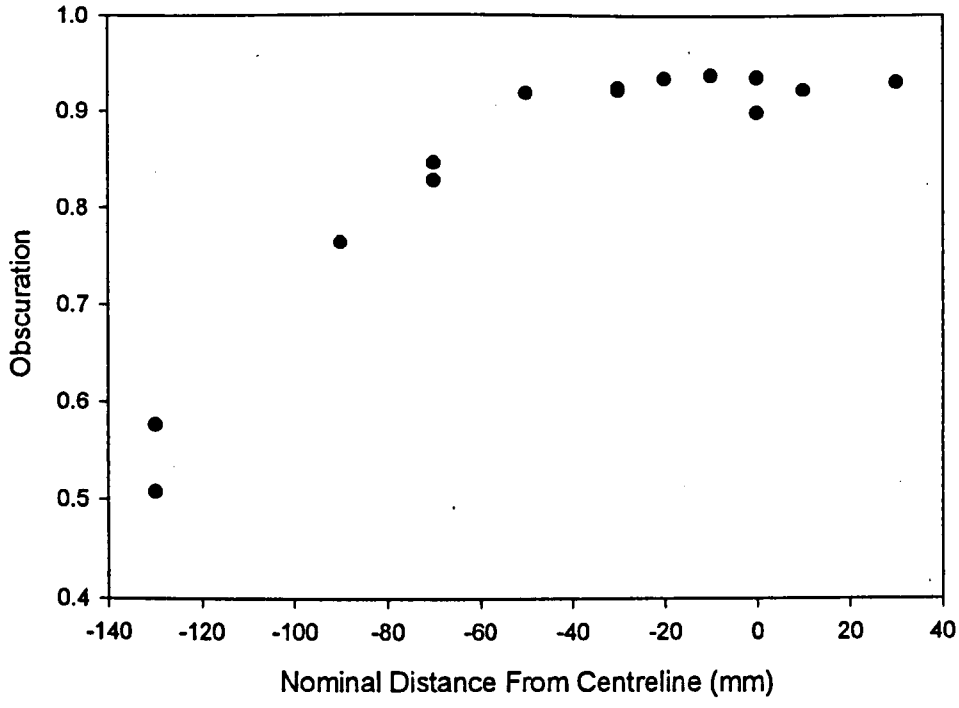

Figure 7.18 - Lateral Obscuration Profile at 1088mm

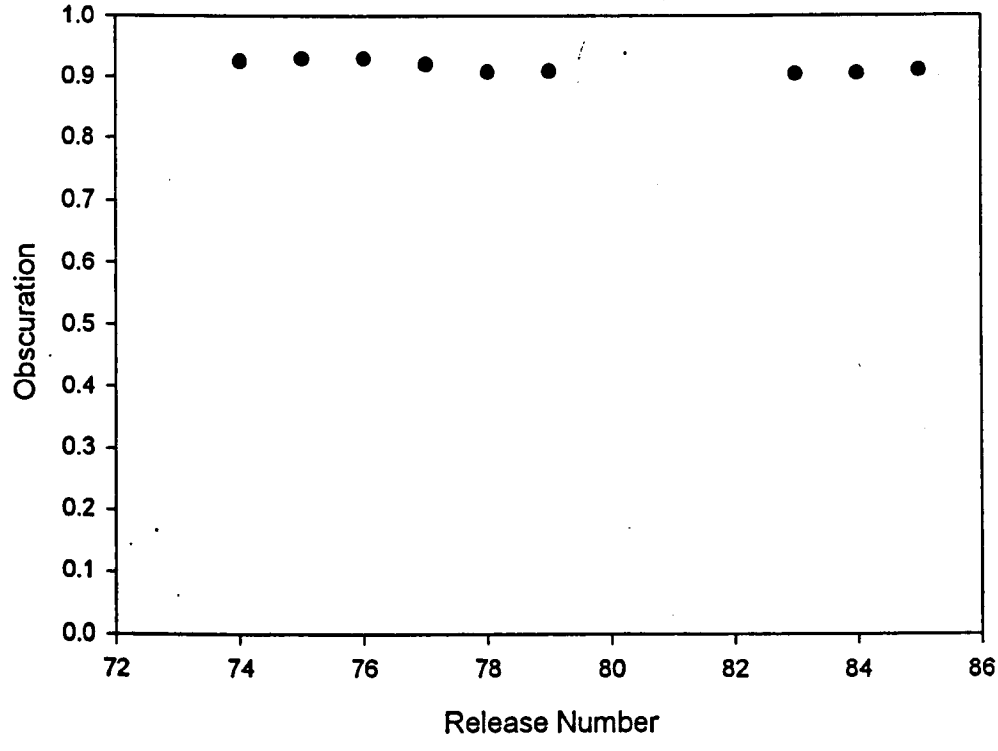

Figure 7.19 - Obscuration Repeatability Plot

(Centreline Data at 838mm)

7.6.3 Mass Release Rates

The average mass release rates for individual releases are presented graphically in Figure 7.20. More detailed tabulated data, if required by the reader, can be found elsewhere [21]. Certain mass release rates from each set of experiments are not included in the Figures, or in the average value calculations. Reasons for this are given in Section 7.7.3

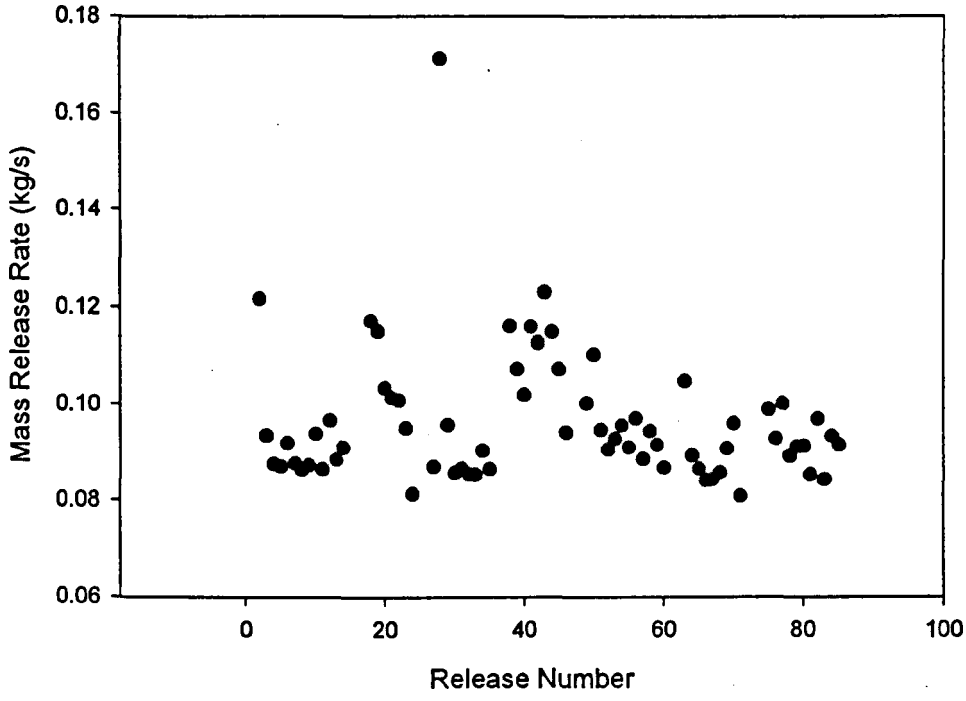

Figure 7.20 - Experimental Mass Release Rates (Invalid Data Points Removed)

The average mass release rates were obtained by the following formula:

$$(B_{av}-A_{av}) / t_r$$

where,

B_{av} is the average of all available mass data points before the pressure switch is activated

A_{av} is the average of at least 20 mass data points after the pressure switch is deactivated

t_r is the duration for which the pressure switch is activated (= jet release duration)

A comparison of the mass release rates obtained during these experiments and those obtained during the laser-based velocity experimental series (Chapter Six) is shown in Figure 7.21.

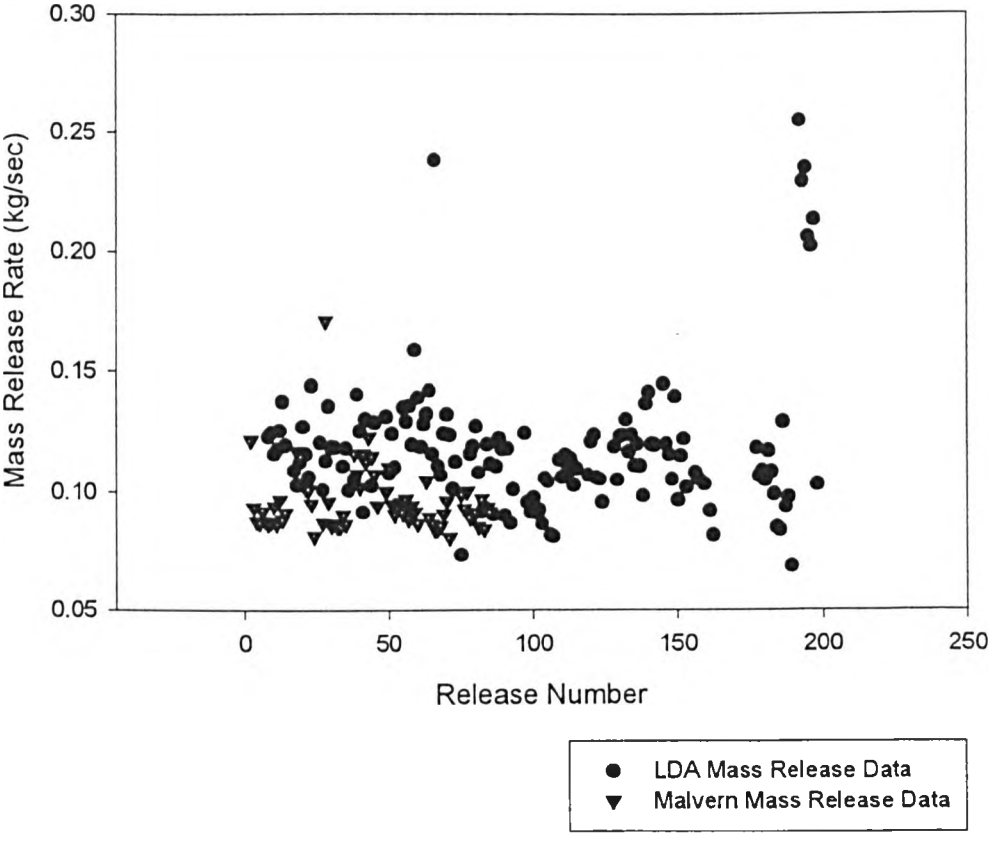

Figure 7.21 - Comparison of Malvern and LDA Experimental Mass Release Rates

7.6.4 Release Temperature Data

The average release temperature for each experiment is shown in Figure 7.22. It is the average of all temperature data points taken between the activation and deactivation of the pressure switch. It was determined in a similar manner to the average mass release rate.

The average release temperature of the experimental series was 16.1°C, with a standard deviation of 0.52°C.

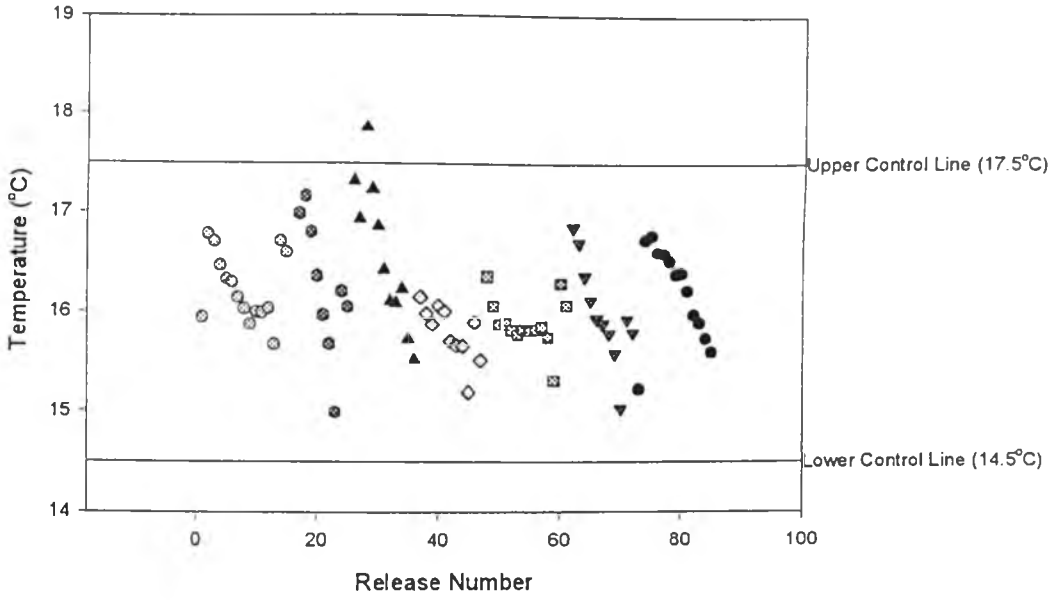

Figure 7.22 - Average Storage Vessel Temperatures For Individual Releases

7.7 DISCUSSION AND INTERPRETATION

7.7.1 Droplet Size Distribution Data

7.7.1.1 General Interpretation and Potential Errors

As detailed previously, the three main potential sources of error in the presented data are:

a) The occurrence of multiple diffraction (as indicated by the high obscuration). Although high obscuration occurs for the vast majority of measurements, it is probable that, for distances greater than 700mm from the nozzle, it is due to unscattered laser beam path distortion and not multiple diffraction by droplets. Data beyond 700mm, therefore, will have little or no multiple diffraction error.

b) The presence of the data manipulation generated 'ghost' peak - this primarily affects the 21.4-41.2μm band, at distances from the nozzle of less than 530mm.

c) The effect of the dense vapour shell surrounding the droplets. The effects of this are not known, but it has been assumed that they have been negated by either the data manipulation techniques, or by the multiple diffraction effect.

The presentation mode, percentage volume of total data, of the Malvern system increases the difficulty of accurately interpreting the data. The problem with this form of presentation is its ambiguity. For data presented in two size bands, as is the case here, a decrease in relative volume in one size band may be due to a real decrease in droplet number in that band, or may be a function of an increase in number of the other band. A relative increase in volume in one band will also generate a decrease in the other, e.g. when one band increases or decreases by a greater amount than the other, or one of them remains constant whilst the other increases or decreases. It should also be borne in mind that a small decrease in the droplet number of the large size band would generate a large relative volume increase in the smaller one and, inversely, a large decrease in the droplet number of the small size band would have a much smaller effect on the relative volume of the larger size band.

It is possible to generate a droplet number presentation, but this is directly derived from the percentage volume data and, therefore, is equally as misleading.

In the individual experimental plots, as demonstrated in Figure 7.5, it is evident that there are two genuine droplet size distribution peaks present. One of these lies at ~6μm, and the other at 10-20μm. This information is not readily apparent when the data is divided into only two size bands. It is possible that some of the measured droplets are due to water vapour condensing around the jet, and being entrained into it. It is not possible to discriminate between water and propane (or any other particulate matter) through this technique.

7.7.1.2 0-21.4μm Axial Plot

As can be seen in Figure 7.8, the relative volume in this size band decreases with increasing distance from the nozzle, until a minimum point is reached at ~700mm. This coincides with the minimum temperature distance obtained previously by use of conventional temperature measurement techniques (Chapter Five). The relative volume in the size band then increases. The shape of the curve is approximately parabolic, centred around 700mm. It is probable, however, that this band will be

overestimated at distances below 700mm from the nozzle, due to multiple diffraction artificially increasing the relative volume of small droplets.

As stated in Section 7.5.1 the data will thus contain an element of multiple diffraction error, decreasing with increasing distance from the nozzle, but not to the extent indicated by the obscuration values.

Although this invalidates the Model Independent multiple diffraction algorithm, an attempt to assess the multiple diffraction error using it was made. Due to the uncertainties outlined, only estimates of a worst case scenario could be obtained, and it is likely that the true distribution will lie somewhere between the unmodified and modified versions.

From Figure 7.6 it can be seen that, for an obscuration of 0.99, assuming that all obscuration is due to multiple diffraction (worst case), the correction algorithm predicts that the percentage volume under size was overestimated. The following guideline worst case values were estimated for the difference between the corrected and uncorrected distribution:

Percentage volume under 10μm was 20 % too high.
Percentage volume under 20-30μm was up to 30 % too high

In the case of the 0-21.4μm band (effectively the percentage volume under 21.4μm), assuming that the obscuration was entirely due to multiple diffraction, the size would have been overestimated by 20-30 on the 'relative volume under' axis. As this corresponds to a genuine obscuration of 0.99, this is obviously the maximum error.

The amount by which this band is overestimated decreases with decreasing obscuration, down to an obscuration value of approximately 0.59. At this point the multiple diffraction error is negligible, as shown in Figure 7.7.

7.7.1.3 21.4-41.2μm Axial Plot

This band increases to a maximum at around 400-500mm, the increase appearing to be near linear. From this distance, there is a near linear decrease to ~1000mm followed by a sharper decrease until the end of the axial measurement domain.
The band is affected, up to ~530mm, by the presence of the 'ghost' peak, resulting in an overestimation of the relative volume in the size band.

7.7.1.4 Possible Explanations

The rapid decrease in the 0-21.4μm band may be due to the large number of small droplets, initially generated in the flashing region (possibly by a shattering mechanism), evaporating through boiling to form vapour. This decrease would partly explain the increase in the relative volume in the 21.4-41.2μm size band.

Genuine larger droplets outside the 21.4-41.2μm band may also be adding to this increase in relative volume by boiling off material, thus bringing them into the band.
There is a noticeable change in the smaller droplet size band at 700mm, suggesting that this is possibly the point at which the majority of the propane droplets have been entirely converted to vapour. The few remaining droplets, which may be partly, or wholly, water, generated by condensation of water vapour in the co-flowing air, would then be responsible for the size distribution and velocity measurements (Chapter Six) seen beyond this point.

In thermodynamic terms, this position on the centreline may also be the point at which the latent heat losses exceed the enthalpy introduced into the jet by the entrainment of air, as suggested by the conventional temperature data presented in Chapter Five.

From 700mm the total relative volume in the two bands remains constant at ~60-65. This could imply that from this point onwards;
i) there is no addition to the 21.4-41.2μm size band from larger droplets outside this band, hence there are no longer any droplets larger than this band size remaining in the jet,

which could then lead to the assumption that;
ii) the remaining relative volume is in the false 'ghost' peak.

These assumptions would support the argument that the 'dry point' is reached at 700mm. That is to say, a droplet population minimum is reached at this point, and the remaining large relative volume of small droplets is most likely due to;
a) the absence of larger droplets (hence greatly increasing the small droplet relative volume)

coupled with;
b) a constant, or increasing, population of small water droplets formed through condensation.

A semi-quantitative understanding of the water droplet effect could have been obtained by measurement of relative humidity in the co-flowing air, but this was not considered until after the experimental work had concluded.

Due to the possible errors inherent in the data plots however, the shape of the axial profiles could be different from those presented for distances up to 530 or 700mm. The arguments above, therefore, must be regarded with some degree of caution.

7.7.1.5 Comparison With Published Droplet Size Distribution

The droplet size trends were compared with other reported data [18], which is shown in Figure 7.23. These measurements were taken on a two-phase flashing Freon 11 jet, released from various nozzles, using a Malvern particle sizer.

The release conditions corresponding most closely to those for the propane data are those at 6 bar pressure released through a 4 x 40mm i.d. nozzle. The Freon 11 superheat in these experiments was very similar to that of ambient temperature propane, (approximately 57 - 60°C). No information is available about how, or if, the raw Malvern data was manipulated to generate the presented data.

In Figure 7.23, the peak of weight distribution for the 4 x 40mm at 6 bar release is seen to increase in an approximately linear manner until ~700mm from release point. The peak of the weight distribution then remains constant until the end of measurement range, ~900mm. The propane droplet trends would, if plotted in such a manner, behave in a similar way. After ~900mm the propane peak weight size would decrease, and it is likely that this would have been the case for the Freon 11 measurements, had they been undertaken at greater distances from the release point.

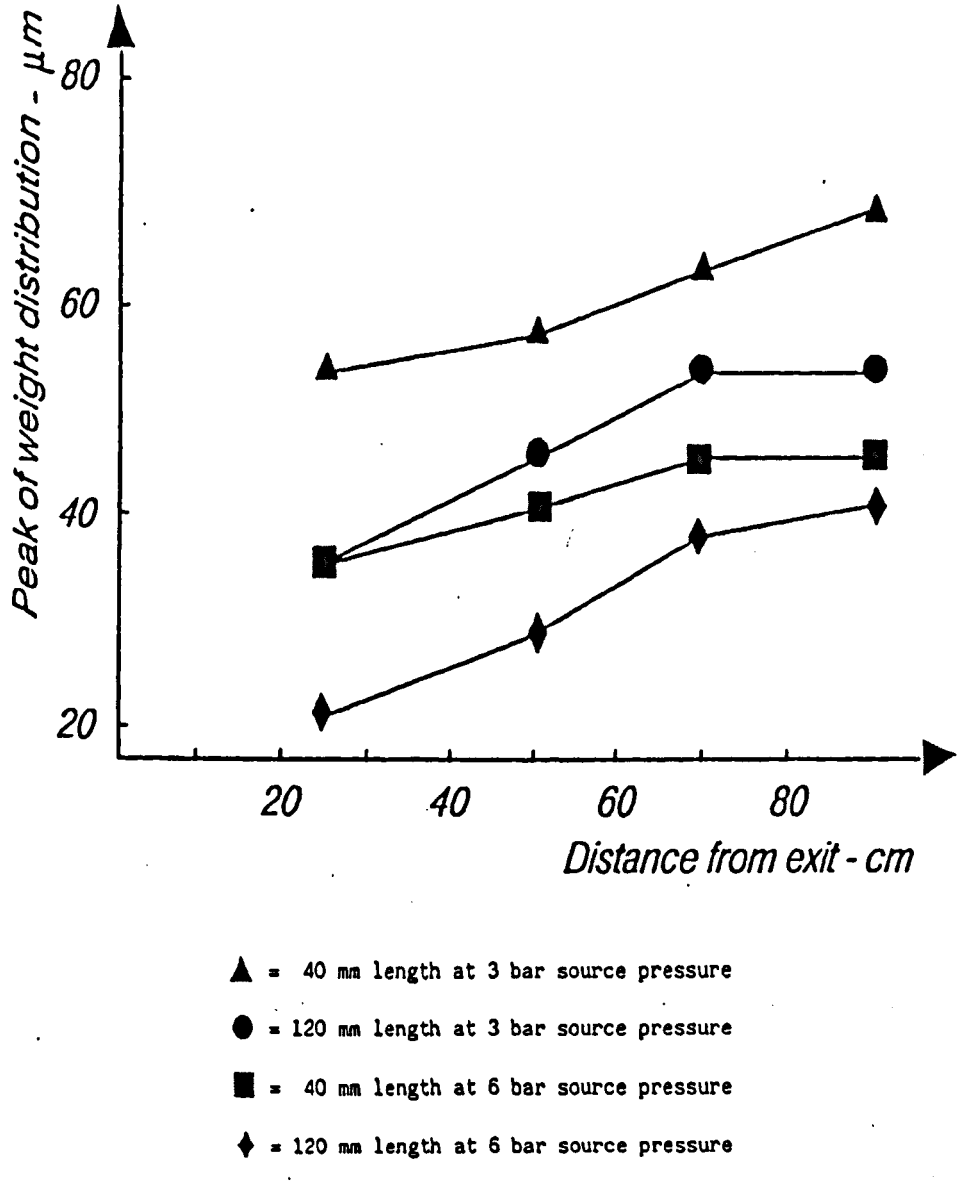

Figure 7.23 - Variation Of Peak Droplet Sizes In Weight Distribution For Freon 11 Jet Spray Field From 4mm i.d. Pipe [18]

The reasoning given for the Freon jet size trends [2] is similar to that presented for the propane in Section 7.7.1.4; a large number of small droplets is initially formed, which subsequently boil off thus increasing the droplet size at which the weight distribution peak occurs. After ~900mm, the large droplets have been lost to form smaller droplets, and the peak weight size will then shift back towards the smaller sizes. As with the propane data, it is possible that the absolute size values generated in the Freon experiments may not accurately reflect the distribution.

The single most important common feature of the two data sets is the change in droplet distribution behaviour at ~700mm, although, due to the limited measurement range in the Freon experiments, this change is not so noticeable.

7.7.2 Obscuration Data

The high centreline obscuration values found close to the nozzle are found to persist at all observed downstream distances. There is a slight decrease with distance from the nozzle, but the obscuration still remains at a high value - at all points on the centreline the reported obscuration is in excess of 0.9. That is to say, 90% of the light is not transmitted through the jet. This could indicate that multiple diffraction is taking place, and that droplet size distributions obtained at these values could be distorted accordingly.

However, due to the method used by the Malvern to calculate the obscuration, i.e. the energy reaching the 'unscattered' central detector is compared to the energy emitted by the laser unit, the obscuration recorded in these experiments may be artificially high. This occurs as a function of the distortion of the beam path, due to the high density gradient present in the beam. Light that has not been diffracted by droplets will suffer path distortion so that it is focussed on the large droplet size detector rings, rather than the central detector, and so will be counted as untransmitted light. This effect may account for the fact that, on the centreline, the obscuration remains at high values over the entire range of axial distances, the beam being affected by the high density gradient generated by the cold propane vapour.

The exact calculation used by the Malvern to determine the obscuration, O, is:

$$O = 1 - (S_0 / B_0)$$

where,

B_0 = intensity of light on the central detector during a background reading (no jet present)

S_0 = intensity of light on the central detector during sample measurement

The lateral obscuration plots show a high centreline obscuration, with a marked decrease in obscuration towards the edges of the jet, as would be expected. Even at the furthest measurement point from the centreline, the obscuration values are still relatively high, and there will be some degree of multiple diffraction taking place.

The shape of the three lateral profiles obtained are very similar, although all three were obtained in approximately the same region of the jet where similar physical processes were controlling its development.

The lateral obscuration values indicate, as would be expected, that the jet is wider at increasing distances from the nozzle.

7.7.3 Mass Release Rates

The mass release rates presented show relatively small standard deviations [21]. Certain values from each set of experiments have been omitted. This is due to two reasons:

i) In the majority of cases, the first release of each set of experiments gave an apparently high mass release rate. This was due to the fact that the first release started with an empty transfer line, and was terminated with a full one. Thus the mass of liquid propane lost from the vessel did not represent the mass of liquid released in the jet.

ii) In many cases, the final one, or occasionally two, mass release rate values were low. This was a physical effect, due to a reduction in the volume of propane

remaining in the vessel, and hence the reduced pressure/temperature of that liquid. This mainly affected the mass release rate due to the automated method of averaging employed.

Overall the repeatability of the mass release rate for a given set of stagnation conditions is good. Any differences are most likely due to variations in release quality, caused by differing heat transfer rates between the liquid and the transfer line/header tank.

From Figure 7.21, it can be seen that the repeatability of the mass release rates obtained from the facility, in two independent experimental programmes, is good. Differences between the two programmes is primarily attributable to the difference in the time between each release within an experimental series, and the energy transfer effects of this.

Effectively there was a greater delay between releases in the Malvern experiments thus giving the heater more chance to re-establish the liquid/vapour equilibrium at the required temperature. Coupled with the fact that the Malvern releases were of slightly shorter duration, less energy was lost by the liquid, and it had a greater chance to replace it, through the release mechanism than was the case in the LDA experiments.

7.7.4 Release Temperature Data

As seen in Figure 7.22, there is, typically, a steady decrease in the vessel temperature, within a series of releases, i.e. between vessel refills. The vessel temperature however stays within the intended range in most cases. The standard deviation for the data is small.

The decrease in temperature within a series of releases is due to the fact that the loss of energy (through latent heat of vapourisation to re-establish the equilibrium after mass loss) exceeded the capability of the heating system and the remaining smaller volume of liquid propane to input or redistribute energy. Towards the end of some experimental series the temperature is seen to rise. This is due to the fact that the

heater system had been adjusted to maintain the temperature within defined limits, and when the volume of liquid dropped to a low level the energy input was greater than that lost through mass release.

The temperature release data does not show the dramatic drop in temperature towards the end of an experimental series, as seen in the previous laser-based velocity measurements see Chapter Six). This is because the release duration for each release was lower for the droplet experiments, and so the energy losses due to mass loss were far less significant, especially towards the end of each series.

7.8 CONCLUSIONS

After detailed and careful data manipulation and analysis, centreline and lateral droplet size distribution profiles of a laboratory scale two-phase flashing propane jet have been generated. These are the first such profiles to be reported. Whilst the individual droplet size distributions are subject to significant potential errors, it is felt that the profiles generated provide useful information on the size distribution trends within the jet. No account has been taken of errors introduced by multiple diffraction, but these errors are smaller than suggested by the observed obscuration.

Overall, some useful droplet size information has been obtained using a technique which is not best suited to the extreme optical environment of a two-phase flashing jet. This work has also clearly demonstrated that the Malvern particle sizer cannot be used as a 'black box' in such environments.

A full discussion of the potential measurement errors has been presented, and ways of reducing them explored. The data obtained has been discussed and compared with that previously obtained for laboratory-scale Freon jets.

Further work could possibly improve the quantitative accuracy of the data, but this was not possible in the timescale of this project. Ideally the Malvern size data requires correlating against an alternative technique.

One such possibility worth investigating is the application of imaging techniques, coupled with the use of a high power pulsed laser illumination system, e.g. a copper vapour laser, in order to obtain absolute information on droplet sizes. Differential imaging of the propane and water droplets, most probably by a fluorescent marker, would also generate information on the effect of the water droplet population on the overall measured size distribution.

Due to the extreme optical environment, it cannot be predicted how successful such a technique would be, but it is the most likely candidate for obtaining such correlation information.

CHAPTER EIGHT

DEVELOPMENT OF A FLUORESCENCE -BASED TEMPERATURE MEASUREMENT TECHNIQUE

8.1 INTRODUCTION

The conventional temperature measurements undertaken in this project are understood to have produced the first temperature profiles for the early regions of a flashing two-phase propane jet. Due to the problems, and potential data errors, associated with intrusive measurement of the non-equilibrium two-phase flashing jet it was decided to attempt to undertake non-intrusive temperature measurement. This chapter details the development of a suitable technique for this purpose. The successful non-intrusive measurement of temperature would not only provide more accurate data for the predictive codes on propane, but would also allow the validity of other conventionally obtained two-phase jet temperature profiles to be assessed.

8.2 FLUORESCENCE TECHNIQUE

8.2.1 Fluorescence Theory

All laser-based techniques fundamentally revolve around the fact that molecules and particles 'scatter' light. In this context, the term scattering is used to imply that the light incident on a molecule, or particle, is re-emitted by it at the same, or a different, wavelength and may be spatially redistributed. The scattering processes can be divided into two distinct types, elastic and inelastic.

Fluorescence is an inelastic scattering process, which means that there is an exchange of energy between the molecule and the incident energy (light). The energy re-emission times for fluorescence range from 10^{-5} to 10^{-10} seconds.

Basically, the molecule is promoted to an excited electronic state by photon absorption. The molecule may then immediately revert to its initial energy state by emission of radiation of the same energy (wavelength) as that absorbed (termed resonance fluorescence). It is far more likely however that the molecule will lose energy, through collisions, intersystem crossing, etc before emitting radiation of a

lower energy value. In practice virtually all fluorescence processes involve energy loss prior to emission, as shown below.

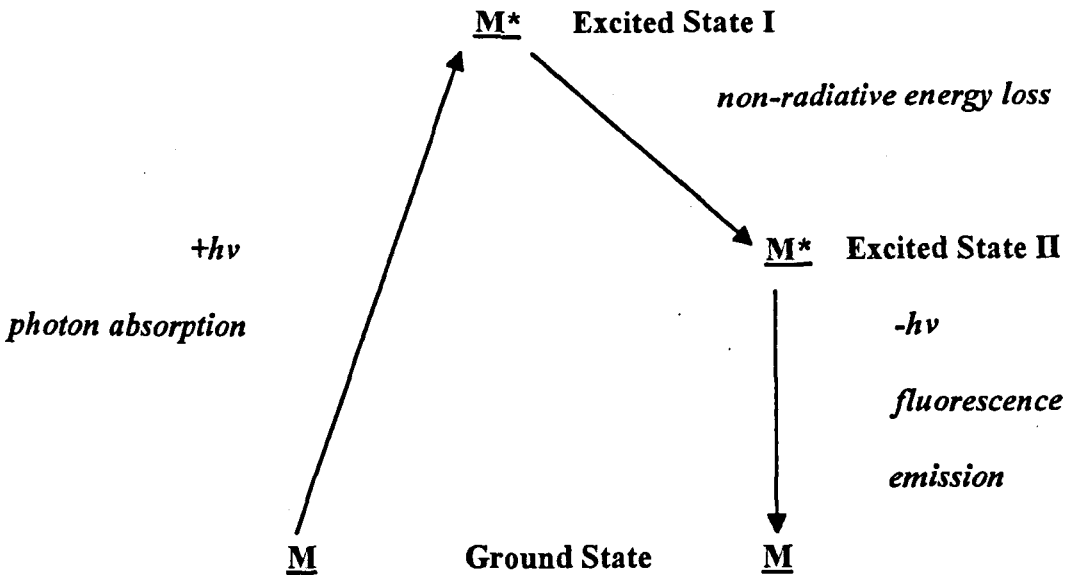

In some instances the excited state molecule forms a 'complex' structure with another molecule (intermolecular) or with itself (intramolecular) by electron transfer. Fluorescence from this 'complex' structure is termed exciplex (excited complex) fluorescence.

Fluorescence is a strong scattering process and is highly species specific, thus making it a sensitive tool for concentration and temperature measurements. A more detailed examination of fluorescence theory can be found in, inter alia, [1, 2, 3].

8.2.2 Application of Fluorescence

Fluorescence can be utilised to provide a wide range of both qualitative and quantitative information in many areas of interest, including two-phase flows and releases. It has been used, inter alia, to visualise flow patterns, measure pressure, velocity and temperature parameters. A study of such applications has been presented already and the reader is directed to Chapter Three for a more comprehensive review.

In direct relation to temperature determination, of two-phase entities, Melton first used the technique of fluorescence as a differentiating simultaneous visualisation technique [4] for the liquid and vapour phases of a diesel spray. Using laser sheets he then collected the independent liquid and vapour phase fluorescence in 'frozen flow' photographs, which were subsequently digitally analysed. From this work a dependency of the fluorescence spectrum on temperature was noted, and exciplex systems were used to obtain liquid temperature measurements [5] at relatively high temperatures. The technique was extended, by the choice of suitable fluorophores, to lower temperature, 0-100°C, boiling point materials [6] including butane. Accuracy of ±1°C in hydrocarbons up to 44°C was obtained [7].

The work of Melton was extended by Ewan to a system of more direct relevance to this work. LIFS was successfully applied to Freon 11 jets in order to obtain liquid temperature measurements [8, 9, 10], and measurements in the gas phase of such jets has also been developed [10, 11]. For a comprehensive review, by Melton, of the application of fluorescence to droplet and vapour phase temperature measurement the reader is directed to [12].

Briefly, the technique is based on the fact that the temperature of a compound effects the population of its various molecular energy levels. The variation of the energy level population in some fluorescing materials, termed fluorophores, affects the intensity and position of peaks in its fluorescence emission spectrum. If this phenomenon can be reliably calibrated then the intensities at given wavelengths can be used to determine the temperature. In order to remove any potential errors caused by shot-to-shot laser power variation it is possible to calibrate the temperature effect against the ratio of two measured fluorescence intensities at different wavelengths. This requires that the fluorophore generates a fluorescence spectrum that contains two independent peak wavelengths. This process also increases the accuracy of the calibration.

A potential disadvantage of the technique is that in many cases it is a 'mimic' technique, i.e. the temperature of interest, that of the host material, is effectively

inferred from the measured temperature of an added fluorophore. Care must therefore be taken to ensure that the fluorescing material accurately mimics the host. This includes ensuring that the fluorophore concentration levels are sufficiently low so as not to perturb the fluid in any way, whilst still generating a satisfactory fluorescence signal.

Other problems with fluorescence thermometry such as large droplets biasing the temperature obtained and reabsorption of generated fluorescence, are discussed in references [5, 13, 14, 12]. It should be noted that reabsorption is not a problem with exciplex fluorescence, as utilised in this work.

8.2.3 Fluorophore Identification

One of the major problems associated with this techniques, in relation to propane, is the fact that propane itself does not exhibit fluorescent properties. However, if it can be assumed that, when dissolved in a host material, a temperature-dependent fluorescent material achieves the same temperature as its host then its fluorescent signal can be used to measure the temperature of the host.

A material had, therefore, to be found that exhibited temperature-dependent fluorescence, was soluble in liquid propane , and would mimic the behaviour of its host, especially its temperature characteristics. A suitable fluorophore had to meet all of these criteria over the temperature range expected, approximately down to -70°C, the minimum temperature measured in the conventional study (see Chapter Five).

A literature survey revealed little information with regards to solubility and fluorescent properties of materials in liquid propane. Some information was available on materials in other, higher order, alkane solvents, but very few exhibited the temperature dependence required.

One series of papers [15, 16, 17], however, presented work on a chemically related group of compounds which exhibited fluorescence and was soluble in lower order alkanes. One of these compounds also presented the possibility of exhibiting the temperature dependence required.

The particular compound was:

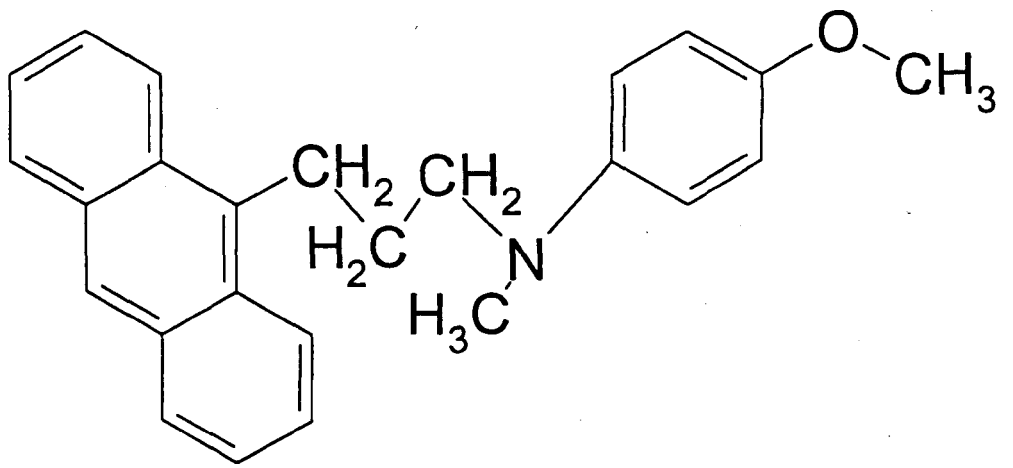

1 - (N-p-Anisyl-N-Methyl)-Amino-3-Anthryl-(9)-Propane
(referred to in this document as NpaNmaap for brevity)

8.2.4 Properties of NpaNmaap

NpaNmaap is a crystalline solid, at standard temperature and pressure, which was shown to exhibit intramolecular exciplex fluorescence emission in relatively low order alkane solvents, as part of an investigation into the influence of Donor groups on exciplex formation [15, 16, 17].

As detailed previously, in exciplex fluorescence there is electron transfer from one molecule, the donor, to another, the acceptor, thus forming an excited state 'complex'. In the case of NpaNmaap the electron is provided by one molecular

subgroup and donated to another on the same overall molecule. This process is therefore termed intramolecular exciplex formation.

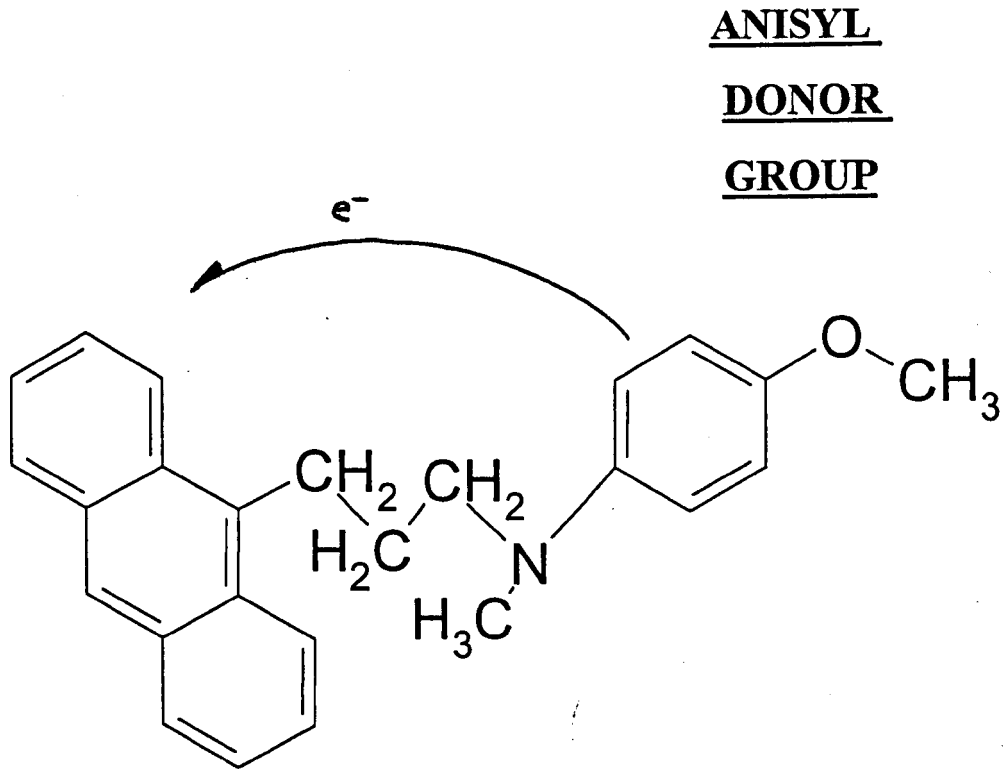

With this molecule excitation of either the acceptor or donor group leads to the formation of the same exciplex, thus allowing a broad range of excitation wavelengths to be used in order to generate the exciplex. The fact that there is no significant interaction between the acceptor and donor groups in the ground state results in relatively high population inversion and hence strong fluorescence signal. .

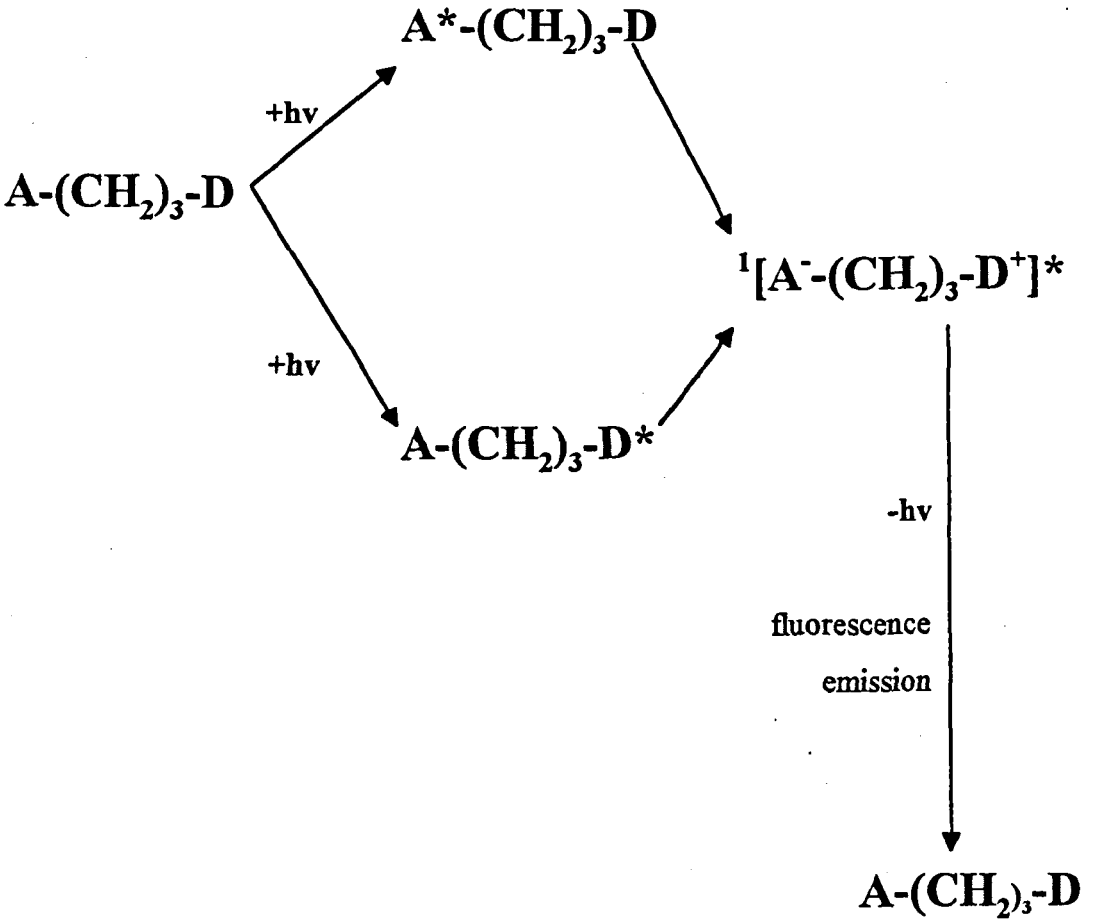

where:

A-$(CH_2)_3$-D is the ground state compound

* indicates excited state molecule or molecular sub-group

^{1}[—]* indicates excited state exciplex

In the work undertaken by Pragst et al, NpaNmaap was found to have a fluorescence spectrum that was temperature sensitive in solutions of hexane [17]. Its fluorescence spectrum contained two independent bands, a broad structureless band with a peak at ~540nm from the exciplex emission, and a structured band with a peak at around 420nm from the anthracene moiety. At higher temperatures the exciplex fluorescence dominated, but the intensity of the anthracene emission increased with decreasing temperature. An iso-emissive point (ie where the fluorescence intensity is independent of temperature) was also observed at approximately 481nm.

Thus NpaNmaap exhibited two high intensity peaks with direct (exciplex) and inverse (anthracene) proportionality to temperature, giving the possibility of high accuracy temperature determination. The fact that this phenomenon had been observed in hexane solutions, made it likely that NpaNmaap would be soluble, and would exhibit temperature-dependent fluorescence in other lower order non-polar alkanes such as propane and liquefied petroleum gas (LPG).

From the information obtained from the work of Pragst et al, additional standard literature, and other sources [18], it was decided that NpaNmaap presented the most viable option for use as a fluorophore in liquid propane over the range of temperatures desired. It should be noted however that NpaNmaap has very different physical properties to propane in terms of, for example, its molecular mass, and hence boiling point. This fact means that as the liquid propane boils off, say from a droplet, the concentration of the dissolved NpaNmaap will increase in the remaining liquid, it will not follow the propane into the vapour phase. Ultimately the point will be reached where there is no solvent (liquid propane) remaining and the NpaNmaap will recrystallise. If this occurs in a free jet then the NpaNmaap crystals will either be carried away by the flow stream, if sufficiently small aerodynamically, or will fall under gravity. For the purposes of this calibration work this factor is not a problem as only the liquid phase is of interest, and no loss of liquid propane will take place.

Efforts were then made to try and have small quantities of the substance synthesised, at a reasonable cost. Ultimately, synthesis of the material was undertaken by the Chemistry Department at the University of Sheffield. The synthesis was initially based on the route proposed by Pragst et al [15], but a more efficient route was developed [19], and small quantities were synthesised and supplied. This was the material utilised in this work.

8.3 PRELIMINARY WORK

8.3.1 Preliminary Work Experimental Layout

The system utilised for the preliminary work, which is shown schematically in Figure 8.1, basically comprised a double monochromator and focusing lens system, a photomultiplier tube (PMT), an excimer laser, a calibration cell, and a data acquisition system. These components and their function are described in detail in Section 8.3.2.

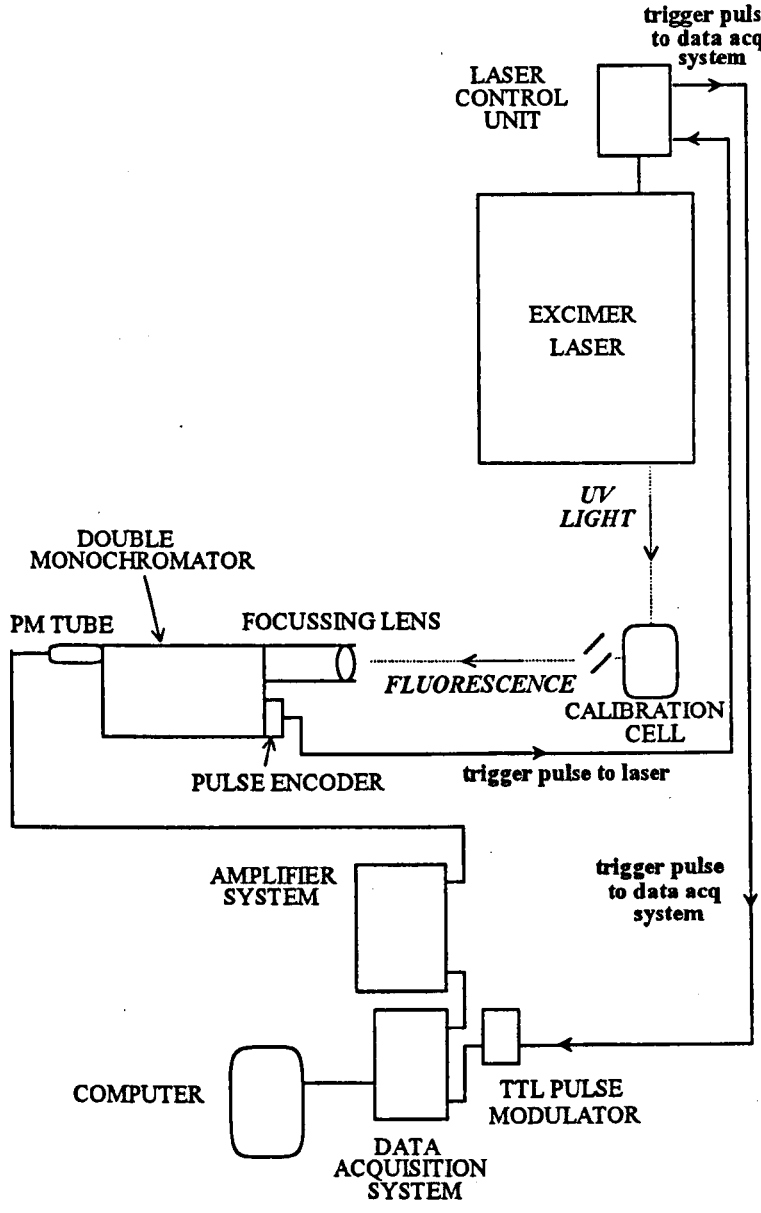

Figure 8.1 - Schematic Of Initial Experimental Layout

8.3.2 Experimental Equipment

8.3.2.1 Monochromator and Associated Components

Two single monochromators, both operating at the same wavelength and containing identical 1200 lines/mm holographic gratings with a blaze wavelength of 500nm, were combined to produce a double monochromator. The advantage of such a system is that it produces a greater spectral accuracy. Light, from the calibration chamber, was focussed onto the entry slit of the double monochromator system by the use of a suitable lens, mounted on a traverse system for ease of use.

A suitable PMT, for the wavelength range under consideration, was attached to the exit port of the double monochromator. This in turn was connected to the data acquisition system, via an amplifier system. The PMT was powered from a single dual-output stabilised voltage PMT power supply, at between -999 and -1000V.

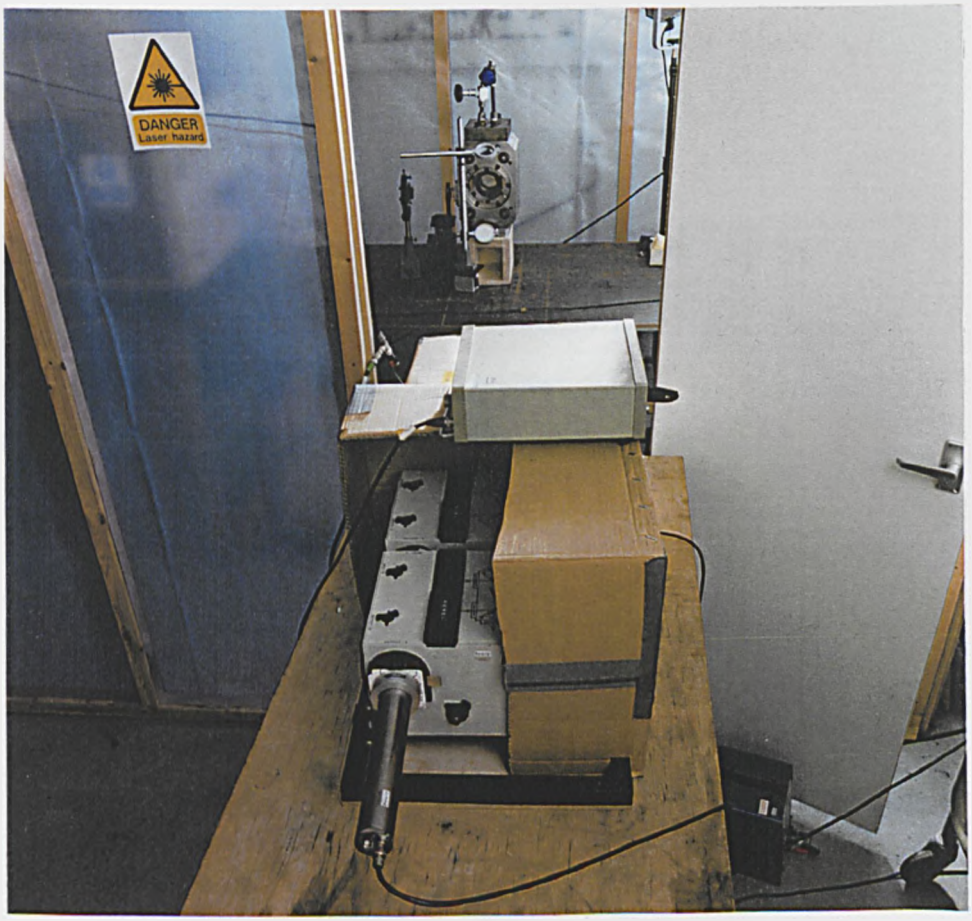

Figure 8.2 - Double Monochromator System

A purpose-built pulse encoder was attached to the wavelength indicator mechanism of the monochromator system, and was set up such that the laser was triggered to fire a single pulse at fixed wavelength intervals (<1nm) as the monochromator was manually traversed across the wavelength range of interest. The double monochromator system can be seen in Figure 8.2, along with the calibration chamber.

Figure 8.3 - Excimer Laser and Calibration Chamber

8.3.2.2 Excimer Laser

The laser employed for this work was a Xenon chloride excimer laser, manufactured by the Estonian Academy of Science, generating pulsed emission at 308nm. The laser could be manually or externally triggered to give variable pulse rates, or could be internally triggered at fixed rates of 10, 25 or 40Hz. In this case the laser was triggered by the pulse encoder attached to the monochromator system, as detailed above.

The laser unit produces an electronic output pulse at the start of each laser pulse. This was utilised to synchronise the data acquisition system with the laser. As the output pulses from the laser were very short and electrically noisy, they were first used to trigger a longer and more stable TTL pulse from a signal generator, and this 'clean' pulse was used to trigger the data acquisition.

A pulse counter was additionally paralleled into the laser output pulse system in order to indicate the number of laser shots fired. The Excimer laser and calibration chamber can be seen in Figure 8.3.

8.3.2.3 Calibration Chamber

The calibration chamber is shown schematically in Figure 8.4, and can be seen in its initial experimental layout in Figures 8.2 and 8.3. It is of stainless steel construction, with a UV quality input window and two UV quality output windows. The output windows are situated opposite each other and are above, and at 90°, to the axis line of the input window. Thus the fluorescence signal was collected at right angles to the line of excitation by the monochromator system. The chamber was fitted with a k-type thermocouple, situated close to the bottom face when the chamber was positioned in the experimental layout, to allow the liquid propane temperature to be determined. The temperature was read shortly before and immediately after any fluorescence measurement.

Extensive tests were undertaken prior to this work to ensure the suitability of this chamber both to contain propane under the range of temperatures and pressures required, and for its optical inactivity in terms of unwanted fluorescence generation.

For the range of experiments detailed in this report, the chamber contained liquid propane doped with a known concentration, 3.0×10^{-4}M, of NpaNmaap (see Appendix 8A for calculations). To obtain the temperature ranges required the chamber was cooled to around -50°C in a freezer unit and allowed to warm up by natural convection from the laboratory air.

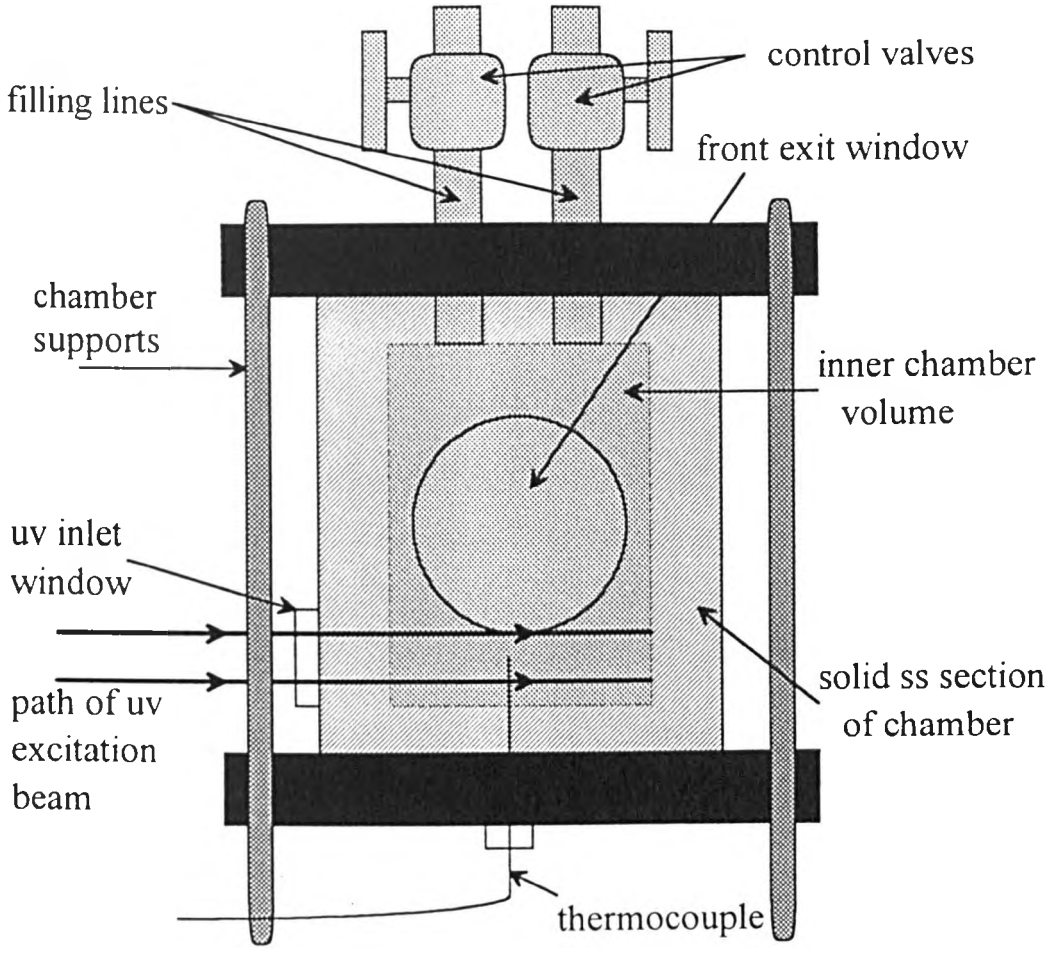

Figure 8.4 - Schematic Of Calibration Chamber

8.3.2.4 Data Acquisition System

The output from the PMT, following each laser pulse, was recorded by a Biodata Microlink data capture unit, running under Windmill's Streamer software on a standard personal computer. Subsequent data analysis and manipulation was undertaken using Jandel Scientific's Sigmaplot software.

8.3.3 Preliminary Work

After simple tests with the calibration chamber to confirm the solubility and fluorescence of the fluorophore in propane, the fluorescence emission spectrum and

preliminary temperature dependence was determined, using the system detailed in Section 8.3.1.

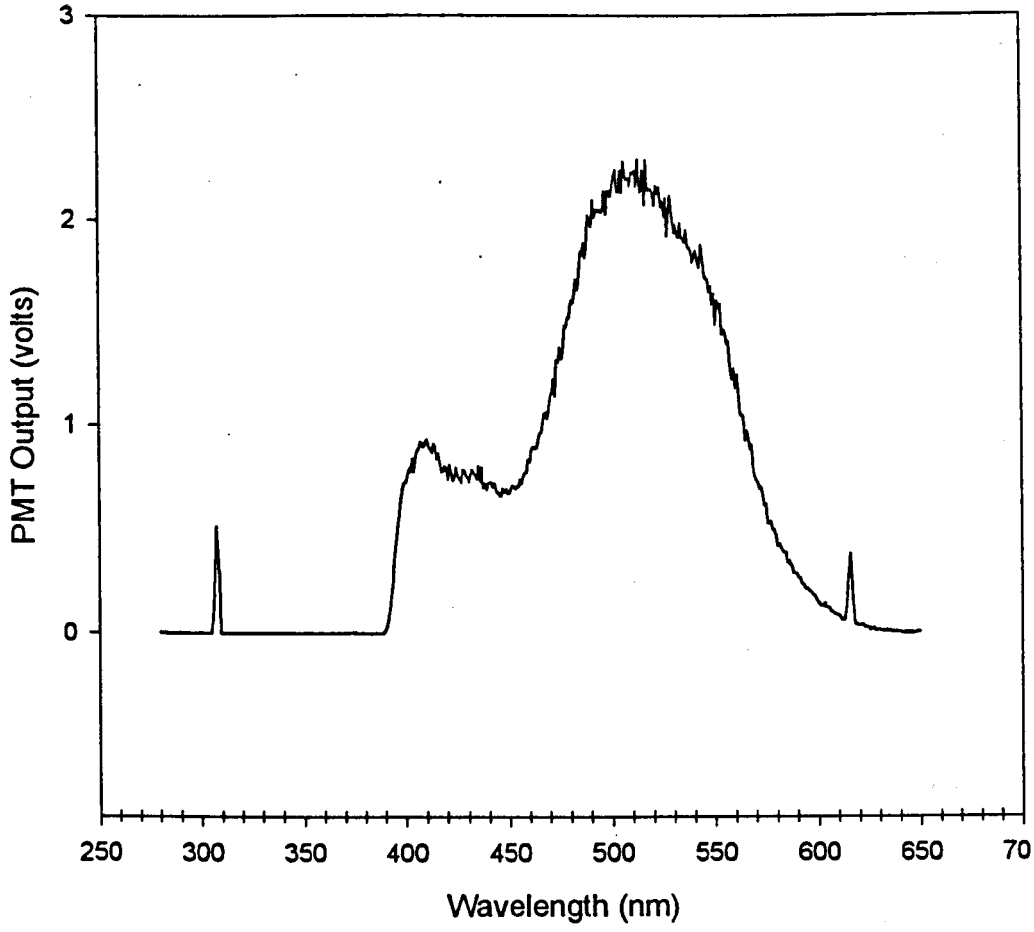

Figure 8.5 - Spectrum of NpaNmaap at -20°C

A spectrum of NpaNmaap, obtained from averaging of four independently obtained spectra, is shown in Figure 8.5. These spectra were obtained at a liquid propane temperature of -20°C. The two emission peaks expected from the literature can be clearly seen, as can the UV excitation peak at 308nm. The second harmonic of the excitation peak is also evident at 616nm.

The temperature dependence was studied by taking full spectra, in the manner described above, at a range of temperatures from -50°C to 10°C.. A temperature dependence was observed, but was not as clear as reported previously [19]. The system was improved by the addition of a nitrogen jet, applied to the measurement

(front exit) window, to ensure that ice formation did not occur. This resulted in improved quality spectra at lower temperatures.

The two main peaks were observed, but did not seem to be indirectly proportional to one another with respect to the temperature. The overall level of fluorescence measured across the spectrum was also seen to change with temperature.

The data acquisition system was modified by adding a signal amplifier and improving the wiring arrangement to give better signal quality. With this revised system, subject to normalisation of the spectra against the temperature-independent wavelength intensity value, the expected behaviour was observed, as shown in Figure 8.6.

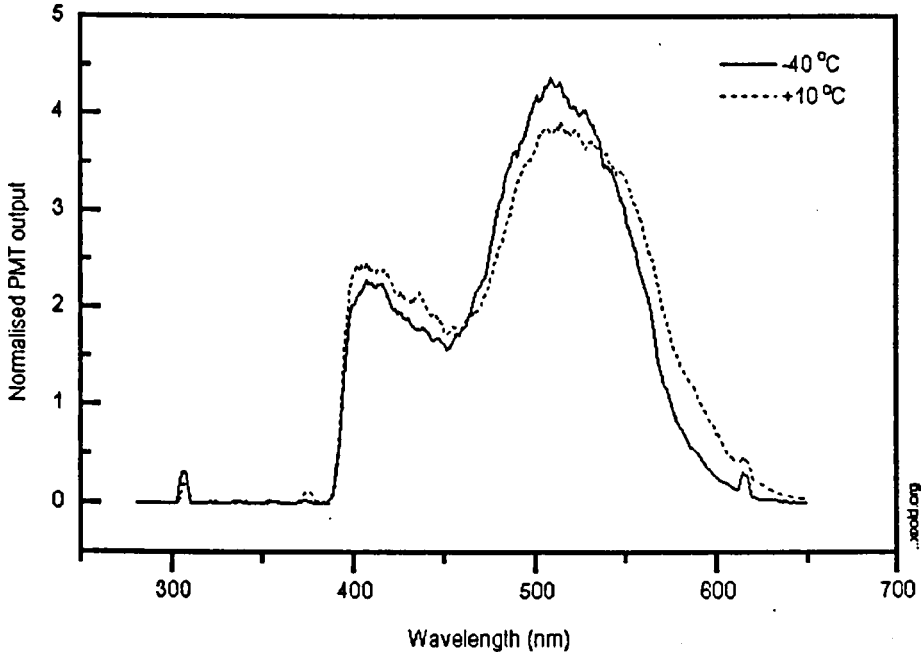

Figure 8.6 - Temperature Dependence Plot of NpaNmaap

The above plot demonstrates a definite temperature dependence in the fluorescence spectrum. It also suggests that accurate measurement of the temperature effect could be achieved by determination of the fluorescence intensity ratio of two wavelengths, one representative of each of the two peaks present in the spectrum.

Study of the spectra resulted in the choice of 410nm and 510nm as the representative wavelengths for the two peaks.

8.4 CALIBRATION DETERMINATION

8.4.1 Full Calibration Experimental Layout

In order to undertake the full calibration measurements, the double monochromator was dis-assembled into its two component single monochromators, each one fitted with an identical model PMT at its exit port.. This allowed the simultaneous measurement of intensity of the two chosen wavelengths, 410nm amd 510nm. The emitted fluorescence signal was split between the two monochromators, after focusing by the lens system, by the use of a 50:50 beam splitter, as shown schematically in Figure 8.7.

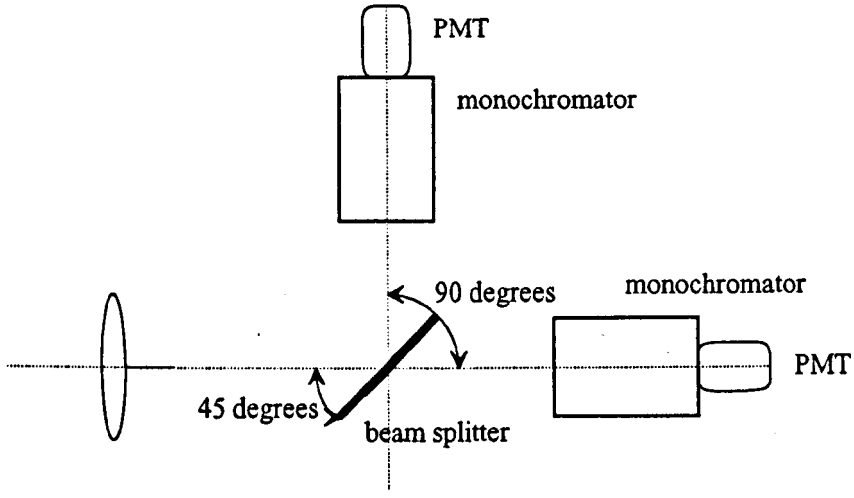

Figure 8.7 - Schematic of Dual Single Monochromator System and Beam Splitter

Care was taken to ensure that the fluorescence beam path lengths were equal for both monochromators, and that each split beam was therefore identically focussed onto the input slit of its respective monochromator.

For the full calibration experiments, where the monochromators were set at fixed wavelength values, the pulse encoder was removed from the system and the laser

was triggered by its internal system at a pulse rate of 10Hz, with a final few pulses being triggered manually by the operator so as to obtain a constant number of pulses.

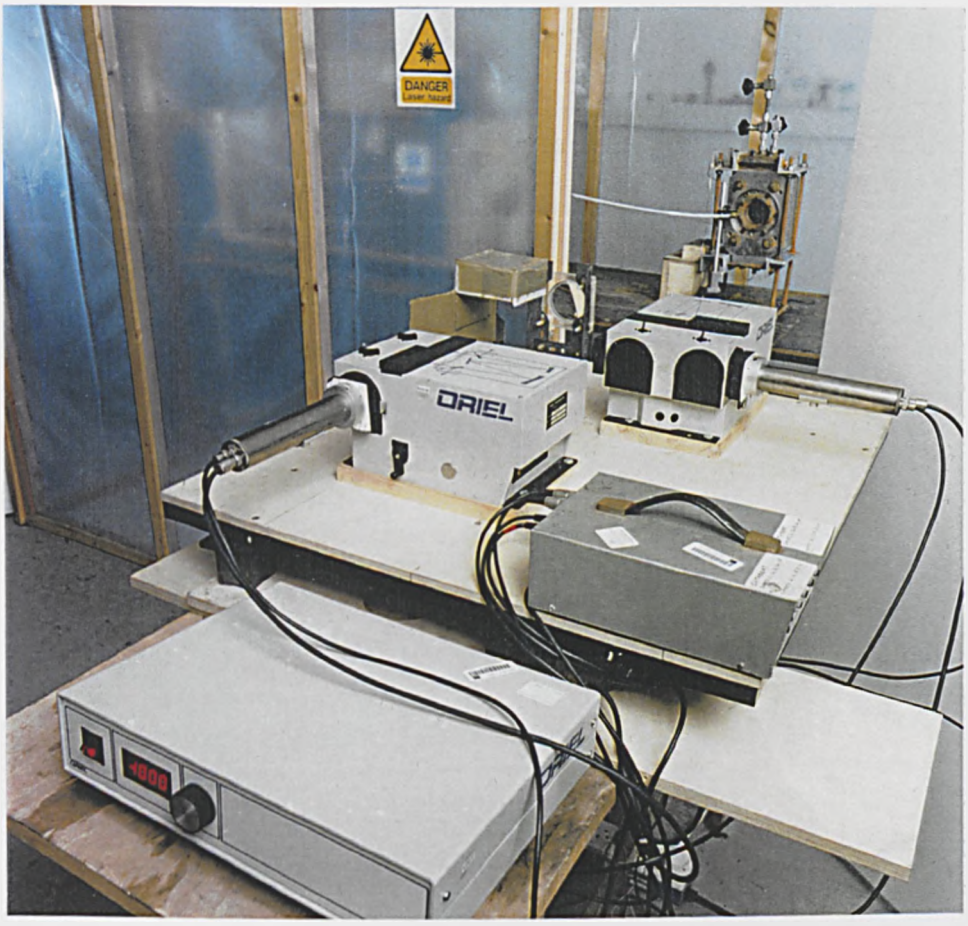

Figure 8.8 - Dual Single Monochromator System and Calibration Chamber

All experiments were undertaken in a totally dark environment, with the lens and monochromator system being enclosed to further reduce any effect of stray light. The experimental layout of the monochromator system can be seen, without enclosure, for the full calibration experiments in Figure 8.8. All other pieces of equipment used for the full calibration are the same as that used for the preliminary work and detailed in Section 8.3.2

8.4.2 Initial Full Calibration

A full calibration was then undertaken using the system outlined in Section 8.4.1. The number of laser pulses fired, and hence fluorescence intensity measurements

taken, at each temperature was 200 in order to provide a statistically viable average for use in the ratio calculation.

8.4.2.1 Calculation Of Fluorescence Intensity Ratio

As detailed previously, NpaNmaap possessed two fluorescence intensity emission peaks, one with direct and one with inverse proportionality to temperature. from the preliminary work, two wavelength values were chosen as representative of these two peaks; 410nm and 510nm. For the full calibration experiments, one monochromator was set to measure the intensity of the 510nm fluorescence emission, and the other 410nm emission.

The calibration plot was determined from the relationship between the ratio of these two wavelengths and temperature. This method of calibration has the advantages of removing the effects of any laser power variation from the equation, and increasing the accuracy of the temperature calibration process, as suggested in Section 8.2.2

The value of the fluorescence intensity ratio for the two wavelengths at any given temperature was calculated using the following equation:

$$\text{Ratio}=\frac{\text{PMT1}}{\text{PMT2}}$$

where PMT1 is the voltage output recorded at the data logger from PMT 1 (D0018, 410nm)

and PMT2 is the voltage output recorded at the data logger from PMT2 (D0017, 510nm)

8.4.3 Relative PMT Output Problems

It was noted in system trial runs that, with the monochromators set to the same wavelength, a significant change of ratio was obtained with small changes to the set up, particularly those resulting in a change in access for ambient light and fluorescence emission.

Using each PMT at each monochromator in turn, with both of the monochromators set to 410nm, gave the following output voltages:

Position / PMT	D00017	D00018
90°	1.64	2.4
180°	1.73	2.49

This shows a ratio of 1:1.45 for the PMT outputs, and a ratio of 1:1.045 (48.9%:51.5%) between the monochromators, for this single input. This deviation from a perfect 50:50 split of the incoming fluorescence beam would not, however, give rise to such a range of ratios at a single wavelength. These results appeared to indicate that the two PMTs were exhibiting different responses (i.e. voltage outputs) in relation to each other with respect to varying input light intensities. This effect would render the system inoperable, and so a number of tests were undertaken to try and find a solution to the problem.

8.4.4 PMT Intensity Sensitivity Tests

In order to investigate the effect of incident light intensity on the system a further sets of tests were carried out. In these tests the 180° (PMT1) position was occupied by D00018. The tests were carried out using the propane sample chamber at ~18.5°C.

A set of measurements were made using Neutral Density filters to introduce a constant change in incident light, assuming little variation in shot to shot power from the laser. Any power variation was reduced by taking 100 shots through each filter and using an average of these shots.

With both monochromators set to 410 nm, it was noted that the relationship between the two PMT outputs with changing intensity was not linear. A quadratic curve was fitted to the relationship, which has the following form:

$$PMT2 = 0.1482 \times PMT1^2 + 0.331 \times PMT1 - 0.037$$

A second test run was carried out using the same procedure, but with the monochromators both set to 510 nm.

Applying the same function to PMT1 gave a value which was ~0.7 of the equivalent PMT2 value across the range of ND filters. (i.e. the effect of intensity changes was eliminated by the process, but the relative values of the two PMT outputs were changed).

A third run was carried out with the 180° monochromator (PMT1/D00018) set to 410 nm and the 90° monochromator (PMT2/D00017) set to 510 nm.

The same function was applied to the PMT1 output, which gave a reasonably constant ratio of ~1.4 across the range of ND filters. This suggests that applying a correction in the form of a quadratic function to the PMT1 output should eliminate the effects of non-uniform response to incident light intensity, and leave any variation in PMT Ratio as a function of temperature alone.

In order to have the best possible correction to use for the calibration runs, a correlation was taken between the PMTs at the fixed wavelengths of 410 nm for PMT1(D00018) and 510 nm for PMT2 (D00017). These would then be the settings used throughout the calibration runs.

The quadratic best fitted to the data was

$$\textit{Corrected}\ \text{PMT1} = 0.1814 \times \text{PMT1}^2 + 0.4241 \times \text{PMT1} - 0.0687$$

This was applied to an initial calibration run giving the change to the ratio values as shown in Figure 8.9.

The inclusion of the correction to the PMT output makes a most significant difference to the results obtained. The fact that the corrected results show a reasonably good fit to a linear relationship between Ratio and Temperature across the measured range suggests that the change has improved the quality of the data.

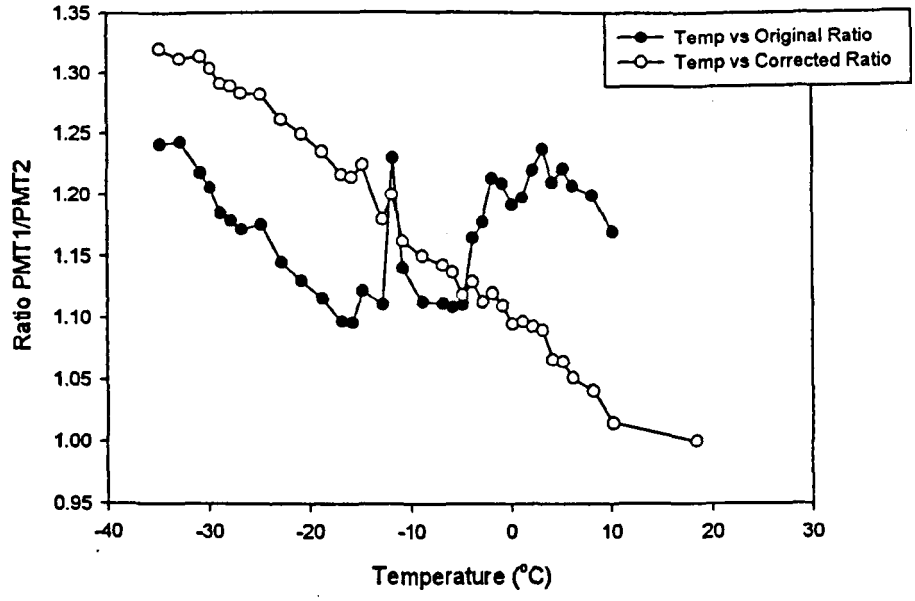

Figure 8.9 - Comparison Of Corrected and Uncorrected Ratio Data

8.4.5 Final Calibration

Having determined suitable normalisation parameters for the two PMTs, a final calibration was undertaken. This was undertaken with the dual single monochromator system as detailed previously. After application of the normalisation parameters, and suitable data manipulation, a relatively good plot was obtained. It was however noticed that, between ~-15°C and -5°C, a deviation from the approximately linear temperature/fluorescence intensity occurred, as can be seen in Figure 8.10.

Consideration of the problem suggested that this may be due to the formation and melting of ice occurring on the back window of the chamber. This process could result in an unequal transmittance/reflectance of the two measured wavelengths, giving rise to further variation in wavelength ratio, in addition to that generated by the temperature dependency of the fluorescence process..

To test this hypothesis, the oute surface of the back exit window was coated with a white non-fluorescing material. A plate was then attached over the window, the

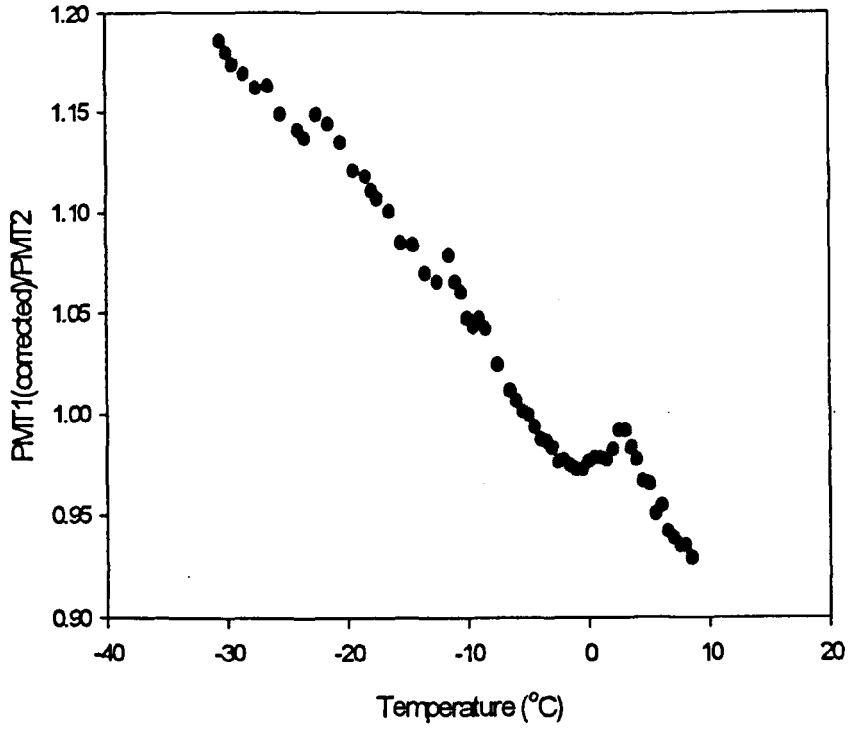

Figure 8.10 - Calibration Data Showing Anomalous Deviation

remaining volume being taken up with hygroscopic crystals to further reduce the likelihood of any ice formation. The calibration process was then repeated. In this final calibration determination, presented in Figure 8.11, the anomalous fluorescence/temperature dependence is not evident.

8.4.6 Conclusions

After application of the PMT normalisation parameters, a good temperature/fluorescence ratio relationship was obtained. Although not linear in its form, the calibration can be considered linear over a wide range of the temperatures studied. It should be noted however that the calibration will have to be extended down to ~80°C, the approximate minimum temperature determined by the conventional studies [1], in order to be usefully applied to a free jet situation. The pseudo-linear relationship is unlikely to be prevalent across this extended range, and a suitable mathematical fit to the relationship will need to be found.

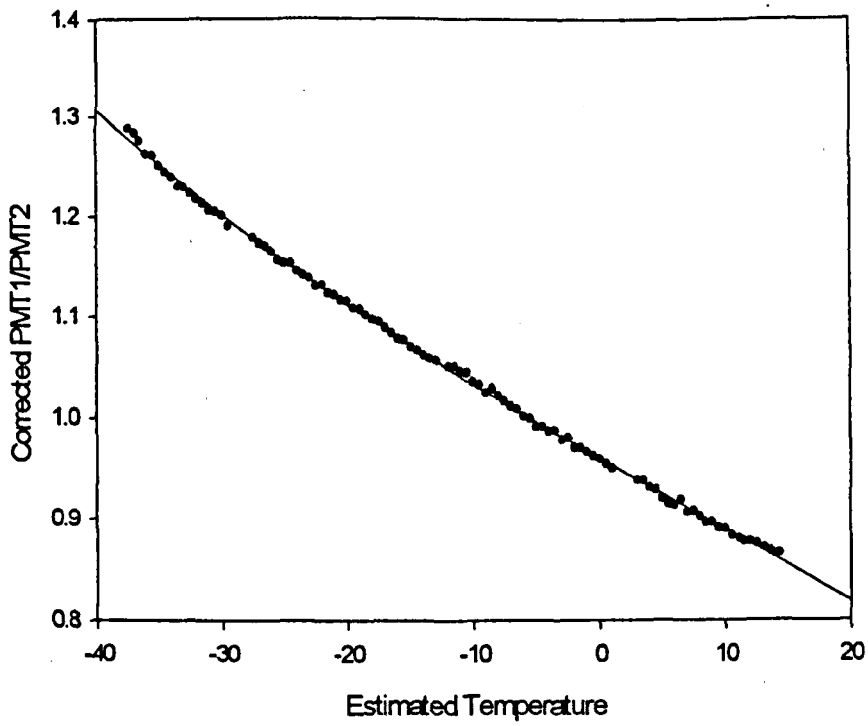

Figure 8.11 - Final Calibration Data

8.5 OVERALL CONCLUSIONS

In view of the amount of additional work that would have been required, it was deemed to be beyond the scope of the present project to carry out tests of the fluorescence system in the two-phase jet facility. Nevertheless, the material and system was found to be suitable for use in two-phase propane releases, and possibly other low boiling point (non-polar) alkanes of interest, e.g. butane, LPG, giving a potential accuracy of ±1°C.

The system should provide a way of making non-intrusive temperature measurements in the near-field regions of two-phase flashing propane releases. The next part of the work will involve the application of the technique to determine temperature profiles in a jet release, utilising the purpose built small-scale release facility.

Prior to the undertaking of any free jet measurements, consideration will have to be given to the consequences and safety implications of the release of NpaNmaap into the atmosphere and its possible deposition inside the small-scale jet release facility.

A number of potential experimental problems, such as the effects of droplet number density, droplet boiling, and possible fluorescence scattering and re-absorption, with respect to the fluorescence signals may also need to be addressed before the technique can be practically applied to a laboratory scale free jet.

CHAPTER NINE

RECOMMENDATIONS FOR FURTHER WORK

9.1 TEMPERATURE MEASUREMENT

The fluorescence-based temperature technique, after being calibrated down to the expected minimum jet temperatures, needs to be applied to measurements in a two-phase flashing jet. The data can then be compared to that obtained conventionally, and any systematic differences utilised to re-appraise conventional measurements taken in other media.

The technique could also be extended to allow vapour phase temperature and concentration measurements to be undertaken. To some extent this has already been attempted (outside the scope of this thesis) but only on Freon compounds.

9.2 DROPLET SIZE MEASUREMENT

Due to the largely qualitative nature of the data obtained, it is recommended that droplet size measurements should be attempted by an alternative means. The data thus generated can then be compared against that presented in this thesis to determine if a greater degree of accuraccy may be obtained. A suggested alternative technique would be Phase Doppler particle analysis (PDPA), or a more visual (photographic) method. It is felt unlikely, however, that a commercial PDPA system would fare any better in the dense near-field regions that the system employed.

The data obtained could be re-evaluated by the use of a more accurate light energy assumed profile in the manipulation stage. The improvement in the data, however, would probably not justify the level of effort required.

9.3 DROPLET VELOCITY MEASUREMENT

It is felt that the velocity profiles presented in this thesis present the best that may be obtained with the commercial system employed. It is likely that a forward scatter

instrument, due to higher levels of data signal strength, may be less affected by the dense jet and give greater information closer to, and in, the flashing region.

Correlation, to ensure quality, could be attempted with a PDPA system (allowing velocity and droplet size to be obtained simultaneously).

9.4 OTHER PARAMETERS OF INTEREST

For all the techniques mentioned it should be noted that this work, in the main, only reported on measurements taken with a single size nozzle (4mm i.d. x 40mm length). This work could be extended by repeating the measurements with differing size and configuration (ie slits) of releases.

It is important to undertake similar experiments with larger release nozzles in order to gain some understanding of the effects of scaling. This is essential so that the data, and models derived from them, can be accurately applied to real size events and releases. The author has touched on this problem in relation to velocity (Chapter Six), and some limited scaling measurements have been undertaken by others [1, 2] in conjunction with this work, but a systematic scaling programme would be more valuable.

A similar, but different, release material (ie butane) could also be studied to determine the relationship between measured physical parameters of the flashing jet and material properties.

The same measurements could also be undertaken with different storage temperatures to those studied here, to assess the affects of storage temperature on the physical characteristics of the jet. Some work has recently been done by the author, for a commercial customer, on releases of chilled propane/LPG and the degree of rainout produced. Laser-based measurements of droplet size distribution and velocity were obtained, by use of a PDPA unit, although the data is not available for publication due to the commercial nature of the customer and the project.

The study could be further extended to look at the parameters of interest to modelling not covered herein, such as vapour phase temperature and concentration, exit void fraction, degree of rain-out etc. The application of laser-sheet systems could be employed to obtain greater qualitative understanding of the jet structure (although the author has some doubts as to the effectiveness of this technique in the more dense near-field regions).

A further area of interest is the change in physical parameters of a two-phase jet when it is impinged upon a surface. This work is currently being undertaken by the author, for HSL, but is outside the scope of this thesis. It is hoped that this work will be published in the open literature at a later date.

CHAPTER TEN
OVERALL CONCLUSIONS

10.1 INTRODUCTION

It should be noted that this section contains only general conclusions from the body of work presented. Detailed conclusions from each technique are contained in the relevant chapter of this thesis.

10.2 OVERALL CONCLUSIONS

A laboratory facility has been designed and constructed which permitted the safe study of two-phase flashing propane jets. It has performed satisfactorily throughout the course of this work, and has also been utilised for other experimental releases (including those of other hazardous PLGs) outside the scope of this thesis. Minor modifications were made to the original facility design, such as the inclusion of the pressure switch, as a result of experience gained from its use.

A number of laser-based techniques have been successfully applied to the near-field regions of a two-phase flashing propane jet. Various approaches to data manipulation have been applied in order to generate useful data using these techniques in this optically harsh environment where successful measurements had not previously been obtained.

From this work, a body of quality data, utilising non-intrusive and conventional techniques, has been generated. This data has permitted current predictive mathematical codes to be evaluated and modified (by others) [1, 2], thus improving the state of knowledge in this area. Modelling work in two-phase flashing jets, including development of a new Computational Fluid Dynamics (CFD) code by HSL, is currently ongoing utilising the data generated by this project [3].

The work, and its data, has generated interest across the wider scientific community through the presentation and publication of various papers (see Publications

Chapter), and several requests for copies of the associated HSL reports have been received [e.g. 4, 5, 6,].

A technique has been developed to permit the non-intrusive temperature measurement of the liquid phase of liquid propane, and thus two-phase flashing propane jets. The technique may also be extended to other PLGs of interest within the safety field.

A correlation between pipe diameter and minimum temperature distance (MTD) has been shown for the HSL data, although further work would be required to confirm this, and to assess the effect of other parameters - such as material and storage pressure.

PUBLISHED WORK

The following papers have been generated by this work and have either appeared in journal form, or have been presented at conference and published in the associated proceedings.

Allen J T and Bettis R J, 'Development of a Fluorescence-Based Temperature Measurement Technique For Two-Phase Flashing Propane Jets', Ninth International Symposium On Applications Of Laser Technques To Fluid Mechanics, Lisbon, Portugal, 13th-16th July 1998, pp23.3(1)-23.3(8).

Allen J T, 'Laser-Based Measurements of Two-Phase Flashing Propane Jets, Part One: Velocity Profiles', J. Loss Prev., Vol. 11, No. 5, pp291-297, 1998.

Allen J T, 'Laser-Based Measurements of Two-Phase Flashing Propane Jets, Part Two: Droplet Size Distributions', J. Loss Prev., Vol. 11, No. 5, pp299-306, 1998.

Allen J T, 'Optical Measuremant and Data Manipulation of Droplet Size Distributions in Two-Phase Flashing Propane Jets', IMechE International Conference on Optical Methods and Data Processing in Heat and Fluid Flow, City University, London, 16th-17th April, 1998, pp97-112.

Allen J T and Bettis R J, 'Valid Data Abstraction From LDA Measurements in Two-Phase Flashing Propane Releases', Seventh International Conference on Laser Anemometry - Advances and Applications, University of Karlsruhe, Germany, Sept 8th-11th, 1997, pp509-516.

Allen J T, 'LDA Measurements in the Near-Field Regions of Flashing Two-Phase Propane Jets', UKALA Symposium on Laser Anemometry and the Validation of Computational Solutions, University of Loughborough, July 2nd-3rd, 1997.

In addition to the externally published papers, a series of more comprehensive reports have been produced on this, and closely related, work for the Health and Safety Laboratory. Details of these are presented below:

Bettis R J and Allen J T, 'Rainout From Jets Of Chilled Propane and LPG', FS/98/10, 1998.

Allen J T, 'Development of a Fluorescence-Based Temperature Measurement Technique For Two-Phase Flashing Propane Releases', FS/98/02, 1998.

Allen J T, 'Laser-Based Droplet Size Measurements In Two-Phase Flashing Propane Jets', IR/L/FR/96/6, 1996.

Allen J T, 'Laser-Based Velocity Measurements In Two-Phase Flashing Propane Jets', IR/L/FR/96/5, 1996.

Allen J T, 'Conventional Temperature Measurements In Small-Scale Two-Phase Flashing Propane Jet Releases', IR/L/FR/95/5, 1995.

Allen J T, 'The Design of a Laboratory Scale Two-Phase Jet release Facility', IR/L/FR/94/09, 1994.

Allen J T, 'The Application of Laser-based Measurement Techniques to Two-Phase Releases', IR/L/FR/93/10, 1993.

REFERENCES

Due to the varied nature of the different parts of this thesis it was deemed sensible to list the references in Chapter order. Whilst resulting in repetition of some references, this method allows readers who are interested in one aspect of the work to easily locate the references relevant to that area.

Chapter One

Background

[1] Ewan B C R, 'Study to assess the potential use of laser diagnostics at the Explosion and Flame Laboratory' Chementech Annual Report, Sept 1990. Contract report for RLSD, HSE.

[2] Ewan B C R, 'Development of spray diagnostics instrumentation' Chementech Annual Report, May 1991. Contract report for RLSD, HSE.

[3] Ewan B C R, 'Development of spray diagnostics instrumentation - gas phase studies' Chementech work outline plan, July 1990. Produced under contract to RLSD,

[4] Ewan B C R, 'Two-phase flashing jet properties' HSE Internal Report IR/L/FR/86/24, 1986.

[5] Ewan B C R, 'Spectroscopic concentration measurements in two-phase flows' HSE Internal Report IR/L/FR/87/10, 1987.

[6] 'Analysis of the LPG Incident in San Juan Ixhuatepec, Mexico City', TNO Report, 1985.

Chapter Two

Introduction

[1] Dr D Carter, CHID 7 (MHAU), HSE, Bootle. Private communication.

[2] Bettis R J, 'Two Phase Releases Following Rapid Vessel Failure', PhD Thesis, Polytechnic of the South Bank, London, 1987.

[3] T Fidell, Director General Designate, L P Gas Association. Private communication.

[4] Hervieu E and Veneau T, 'Experimental determination of the droplet size and velocity distributions at the exit of the bottom discharge pipe of a liquid propane storage tank during sudden blowdown', J. Loss Prev. in the Proc. Ind, 9(6), 413-425, 1996.

[5] Schumann S, Pasoi L M, Schmittberger H, and Walter H, 'An Experimental and Modelling Study of Two-Phase Flashing Jets', Final Report R-40.079-5E, Battelle Ingenieurtechnik GmbH, Germany, February, 1997.

[6] Kelsey A, 'CFD Modelling of Two-Phase Flashing Jets: Literature Review' HSL Report, FR/97/5, 1997.

[7] Vandroux-Koenig S, and Berthoud G, 'Modelling of a Two-Phase Momentum Jet Close to the Breach in the Containment Vessel of a Liquefied Gas', J. Loss Prev. Proc. Indust., Vol 10, pp17-29, 1997.

Chapter Three

Review Of Laser-Based Techniques

[1] Cates M R, Allison S W, Franks L A, Borella H M, Marshall B R, and Noel B W, 'Laser-induced fluorescence of Europium-doped Yttrium oxide for remote high-temperature thermometry', LIA, Vol. 49,51 and 52, ICALEO 1985.

[2] Lee M P, Paul H P, and Hanson R K, 'Quantitative imaging of temperature fields in air using planar laser-induced fluorescence of O_2' Opt Lett, Vol. 12, No. 2, 1987.

[3] Chang A Y, Battles B E, and Hanson R K, 'Simultaneous measurements of velocity, temperature, and pressure using rapid cw wavelength-modulation laser-induced fluorescence of OH' Opt Lett, Vol. 15, No. 12, 1990.

[4] Ariessohn P C and Vigeland K R, 'In-process demonstration of lime temperature measurement using laser induced fluorescence' LIA, Vol. 70, ICALEO 1989.

[5] Hess N J and Schiferl, 'Pressure and temperature dependence of laser-induced fluorescence of Sm:YAG to 100kbar and 700°C and an empirical model' J Appl Phys, 68 (5), 1990.

[6] Goss L P, Smith A A, and Post M E, 'Surface thermometry by laser-induced fluorescence' Rev Sci Instrum, 60 (12), 1989.

[7] Beshears D L, Capps G J, Cates M R, Simmons C M, and Schwenterly, 'Laser-induced fluorescence of phosphors for remote cryogenic thermometry' SPIE, Vol. 1370 Fibre Optic Smart Structures and Skins III, 1990.

[8] Kennedy I M, 'Pulsed laser measurements of particle and vapour concentrations in a turbulent jet' Experiments in Fluids, 7, 49-55, 1989.

[9] Biewer M C, Biehn C R, Platz M S, Després A, and Migirdicyan E, 'An exceptionally simple method of preparation of biradicals. 2. Low-temperature fluorescence spectra and ambient temperature laser-induced fluorescence spectra of 1,3-, 1,6-, 2,6-, and 2,7-Naphthoquinodimethane' J Am Chem Soc, Vol. 113, No. 2, 1991.

[10] Toda S, 'Laser beam techniques for measuring two-phase boundary motion in boiling' Proc Int Cent Heat Mass Transfer, Vol. 18, 3-26, 1985.

[11] Odnorozhenko V B, 'Some laser methods for the study of high temperature two-phase systems' Sverkhtverd I Tugoplav Materialy, 49-53, 1982.

[12] Abid K H, and Godfrey J G, 'Laser transmission technique for hold-up measurements in agitated tank' Solvent Extraction 1990 Proc Int Solvent Extraction Conf, Elsevier, 1992.

[13] Mayinger F, and Chávez A, 'Measurement of direct-contact condensation of pure saturated vapour on an injection spray by applying pulsed laser holography' Int J Heat Mass Transfer, Vol. 35, No. 3, 691-702, 1992.

[14] Namazian M, Kelly J, and Schefer R W, 'Concentration imaging in turbulent concentric-jet flows' AIAA Journal, Vol. 30, No. 2, 1992.

[15] Boiko V M, and Papyrin A N, 'The quick-acting laser visualisation of processes arising by interaction of shock and detonation waves and small particles' AIP Conf Proc, Vol. 208, 1990.

[16] Chávez A, and Mayinger F, 'Single- and double-pulsed holography for the characterisation of sprays of refrigerant R113 injected into its own saturated vapour' Experimental Heat Transfer, Fluid Mechanics, and Thermodynamics, 848-855, 1988.

[17] Kurita K, Okai T, Ueno K, Kawada N, and Kato M, 'Velocity and temperature distributions in an underexpanded supersonic jet by using a laser induced fluorescence' Anal Sci, Vol. 7, Supplement, 1991.

[18] Zuyev Y V, Kolesnikova L A, Lepeshinskiy I A, and Reshetnikov V A, 'Measuring the velocity of the dispersed phase in a two-phase flow by means of three-dimensional spectral analysis and pulsed 'laser-knife' methods' FLUID MECHANICS-Soviet Research, Vol. 20, No. 6, 1991.

[19] Miller N, and Mitchie R E, 'The development of a universal probe for measurement of local voidage in liquid-gas two-phase flow systems' ASME/AiChE Heat, Transfer Conf, Minneapolis, USA, 82-88, 1969.

[20] Hassan Y, and Blanchat T, 'Two-phase bubbly flow velocity measurements using pulsed laser velocimetry' HTD, Vol. 155, 173-178, 1990.

[21] Hassan Y, and Blanchat T, 'Flow velocity measurements using digital pulsed laser velocimetry' Opt Eng, Vol. 30, No. 8, 1991.

[22] Ereaut P R, and Shand A M, 'Quantitative Flow Measurement Using Laser Light Sheets' Report AERE-R 12968, UKAEA, Harwell, UK, 1987.

[23] Hu Z G, Tsai Y N, and Sheng D R, 'Measurement of droplet size distribution in a two-phase medium by optimised method of laser scattering' Int J Heat and Fluid Flow, Vol. 12, No. 1, 1991.

[24] Durst F, 'Optical techniques for fluid flow and heat transfer' Experimental Heat Transfer, Fluid Mechanics, and Thermodynamics, 32-49, Elsevier, 1988.

[25] Shorin V P, Zhuravlev O A, Logak L G, Medinskaya L N, and Fedosov A I, 'Holographic apparatus for study of two-phase flows' translated from Pribory i Tekhnika Éksperimenta, No. 5, 158-161, 1985.

[26] Hanzevack E L, McNeill S R, Bowers C B, and Ju C H, 'An inexpensive experimental system for study of two phase flow by laser image processing' Chem Eng Comm, Vol. 65, 161-167, 1988.

[27] Peters W D, Dutcher C R, and Venart J E S, 'Transient flow visualisation of gravity current using full-field laser-induced dye fluorescence' FED Vol. 128, Experimental and Numerical Flow Visualisation, ASME, 1991.

[28] Long M B, Lyons K, and Lam J K, 'Acquisition and representation of 2D and 3D data from turbulent flows and flames' Computer, IEEE, 1989.

[29] Prenel J P, and Porcar R, 'Performance analysis of an optical device for cylindrical flow visualisations' Opt and Las Tech, Vol. 24, No. 4, 1992.

[30] Melton L A, 'Spectrally separated fluorescence emissions for diesel fuel droplets and vapour' App Opt, Vol. 22, No. 14, 1983.

[31] Melton L A, and Verdieck J F, 'Vapor/Liquid visualisation in fuel sprays' Twentieth Symposium on Combustion, The Combustion Institute, 1283-1290, 1984.

[32] Melton L A, and Verdieck J F, 'Vapor/liquid visualisation for fuel sprays' Comb Sci and Tech, Vol. 42, 217-222, 1984.

[33] Murray A M, and Melton L A, 'Fluorescence methods for determination of temperature in fuel sprays' App Opt, Vol. 24, No. 17, 1985.

[34] Murray A M, and Melton L A, 'Exciplex visualisation systems for low boiling hydrocarbons'

[35] Guilbault G G, 'Practical Fluorescence - theory, methods, and techniques' Dekker, 1973.

[36] Ewan B C R, 'Development of spray diagnostics instrumentation' Chementech Annual Report, June 1989. Contract report for RLSD, HSE.

[37] Ewan B C R, 'Study to assess the potential use of laser diagnostics at the Explosion and Flame Laboratory' Chementech Annual Report, Sept 1990. Contract report for RLSD, HSE.

[38] Ewan B C R, 'Development of spray diagnostics instrumentation' Chementech Annual Report, May 1991. Contract report for RLSD, HSE.

[39] Ewan B C R, 'Development of spray diagnostics instrumentation - gas phase studies' Chementech work outline plan, July 1990. Produced under contract to RLSD, HSE.

[40] Bettis R J, Ewan B C R, Jagger S F, and Moodie K, 'Two-phase jet and cloud growth following a sudden release of liquefied gas' HSE Internal Report IR/L/FR/92/5, 1992.

[41] Moodie K, and Ewan B C R, 'Jets discharging to atmosphere', HSE Internal Report IR/L/FR/89/28, 1989.

[42] Ewan B C R, 'Two-phase flashing jet properties' HSE Internal Report IR/L/FR/86/24, 1986.

[43] Ewan B C R, 'Spectroscopic concentration measurements in two-phase flows' HSE Internal Report IR/L/FR/87/10, 1987.

[44] Ewart P, 'Degenerate four wave mixing techniques for combustion diagnostics' IOP Short Meeting No. 27 (Spectroscopy in combustion studies), 91-105, 1990.

[45] Danel F, Guilloud J C, Jacquet A, and Delhaye J M, 'High-speed multiple-spark cameras for gas-liquid two-phase flow studies' Measuring Techniques in Gas-Liquid Two-Phase Flows,IUTAM symposium proc Nancy/France, 67-89, Springer-Verlag, 1984.

[46] Hutchins J, Johnson G, and Marschall E, 'Flow visualisation in two-phase flow' Measuring Techniques in Gas-Liquid Two-Phase Flows, IUTAM symposium proc Nancy/France, 91-102, Springer-Verlag, 1984.

[47] Martin C J, and Walklate P, 'The measurement of liquid phase velocity profiles in vertical two-phase flow' Measuring Techniques in Gas-Liquid Two-Phase Flows, IUTAM symposium proc Nancy/France, 103-112, Springer-Verlag, 1984.

[48] Goosens H W J, and van Dongen M E H, 'A quantitative laser-interferometric measurement of gas density in a gas-particle mixture' Experiments in Fluids, 5, 189-192, 1987.

[49] Nakajima T, Utsunomiya M, and Ikeda Y, 'Simultaneous measurement of velocity and temperature of water using LDV and fluorescence technique' Applications of Laser Techniques to Fluid Mechanics, 34-53, Springer-Verlag, 1991.

[50] Muck K C, and Wallace J M, 'Simultaneous real-time line measurements of concentration and velocity in turbulent flows' Applications of Laser Techniques to Fluid Mechanics, 54-80, Springer-Verlag, 1991.

[51] Hinata S, 'A study on the measurement of the local void fraction by the optical fiber glass probe' Bulletin of JSME, Vol. 15, 1972.

[52] Beshears D L, Capps G J, Cates M R, Simmons C M, and Schwenterly, 'Laser-induced fluorescence of phosphors for remote cryogenic thermometry' Oak Ridge National Laboratory Report ORNL/ATD--44 DE91 001733, prepared for NASA, October 1990.

[53] Hofstraat J W, Schenkeveld A J, De Jonge C G-N, and Gooijer C, and Velthorst N H, 'Temperature effects on highly resolved laser induced fluorescence spectra of tetracene in solid solutions at cryogenic temperatures' J Mol Struct, 175, 85-90, 1988.

[54] Boiarski A A, Liu J S K and Collier R P, 'Three-dimensional characterisation of falling liquid film using laser induced fluorescence' Proc Symp on Polyphase Flow and Transport Tech, San Francisco, USA, Century Two Publ, 1980.

[55] Thornberg S M, and Maple J R, 'Laser-induced fluorescence spectrometry of methylnaphthalene derivatives prepared in low-temperature aromatic crystal' Anal Chem, 56, 1542-1544, 1984.

[56] Hamdullahpur F, Pegg M J, and MacKay G D M, ' A laser-fluorescence technique for turbulent two-phase flow measurements' Int J Multiphase Flow, Vol. 13, No. 3, 379-385,1987.

[57] Nakatami, Oshio, Kataoka, and Kishida, '... Optical fibre heterodyne interferometer ...' Laser Anemometry Advances and Applications, Vol. 1, pp 83, ASME, 1991.

[58] Himmelreich, and Riess, '... Laser-2-focus method ...' Laser Anemometry Advances and Applications, Vol. 2, pp 781, ASME, 1991.

[59] Andresen P, 'Laser fluorescence applications with tunable excimer lasers in flames, wind tunnels and internal combustion engines' IOP Short Meeting no. 27 Spectroscopy in Combustion Studies, 55-58, Institute of Physics, 1990.

[60] Chewter L, O'Connor D V, and Phillips D, 'Exciplex fluorescence in vapour phase mixtures of 1-cyanonaphthalene and triethylamine' Chem Phys Lett Vol. 84, No. 1, 1981.

[61] Hirayama S, Abbott G D, and Phillips D, 'Strongly fluorescent exciplexes in the vapour phase' Chem Phys Lett, Vol. 56, No. 3, 1978.

[62] Hirayama S, 'Temperature effects on the vapour phase exciplexes of cyano-substituted anthracenes' Int J Quantum Chem, Vol. 18, 1980.

[63] Chewter L A, O'Connor D V, and Phillips D, 'Temperature dependence of the cyanonaphthalene/triethylamine gas phase exciplex' J Chem Phys, Vol. 87, 1983.

[64] Gossage H E, and Melton L A, 'Fluorescence thermometers using intramolecular exciplexes' App Opt, Vol. 26, No. 11, 1987.

[65] Förster Th, 'Excimers' Angew Chem internat Edit, Vol. 8, No. 5, 1969.

[66] Hagan T, Pilloud D, and Suppan P, 'Thermochromic shifts of some molecular and exciplex fluorescence spectra' Chem Phys Lett, Vol. 139, No. 6, 1987.

[67] Pragst F, Hamann H-J, Teuchner K, Naether M, Becker W, and Daehne S, 'Steady state and laser spectroscopic investifations on the intramolecular exciplex formation of 1-(N-p-anisyl-N-methyl)_amino-3-anthryl-(9)-propane' Chem Phys Lett, Vol. 48, No. 1, 1977.

[68] Förster Th, and Kasper K Z, Phys Chem (N F), Vol. 1, 275, 1954.

[69] Förster Th, and Kasper K Z, Elektrochem, Vol. 59, 976, 1955.

[70] Birks J B, 'Excimer Fluorescence of Aromatic Compounds', Chapter Four, pp 181-272, 1970.

[71] Birks J B, and Munro I H, 'The Fluorescence Lifetimes of Aromatic Molecules', Chapter Seven, pp239-303, 1970.

[72] Bengtsson P-E, and Alden M, 'Optical investigationof laser-produced C_2 in premixed sooty ethylene flames' Comb and Flame, Vol. 80, No. 3/4, 1990.

[73] Newby K, Reichert W M, Andrade J D, and Benner R E, 'Remote spectroscopic sensing of chemical adsorption using a single multimode optical fiber' App Opt, Vol. 23, No. 11, 1984.

[74] Hanson R K, 'Combustion diagnostics: planar imaging techniques' Twenty-First Symposium (International) on Combustion, 1677-1691, The Combustion Institute, 1986.

[75] Anner O, Zuckermann H, and Haas Y, 'Fluorescence decay of jet-cooled acetone' J Phys Chem, Vol. 89, No. 8, 1985.

[76] Gross K P, McKenzie R L, and Logan P, 'Measurements of temperature, density, pressure, andtheir fluctuations in supersonic turbulence using laser-induced fluorescence' Experiments in Fluids, 5, 372-380, 1987.

[77] Eckbreth A C, Laser Diagnostics for Combustion Temperature and Species, Energy and Engineering Series Vol. 7, Abacus Press, 1988.

[78] Swithenbank J, Beer J M, Taylor D S, Abbot D, and McCreath G C, 'A laser diagnostic technique for the measurement of droplet particle size and distribution' Prog in Astro and Aero, Vol. 53, 421-447, 1977.

[79] Hamidi A A, and Swithenbank J, 'Treatment of multiple scattering of light in laser diffraction measurement techniques in dense sprays and particle fields' J Inst Energy, 101-105, 1986.

[80] Cao J, Brown D J, and Rennie A G, 'Laser diffraction particle sizing in dense suspensions and sprays with correction for multiple scattering' draft report Sheffield University, 1995.

[81] Dodge L G, 'Change of calibration of diffraction-based particle sizers in dense sprays' Opt Eng, Vol. 23, No. 5, 1984.

[82] Felton P G, Hamidi A A, and Aigal A K, 'Measurement of drop size distribution in dense sprays by laser diffraction' Proceedings of Third International Conference on Liquid Atomisation and Spray Systems (ILASS), Institute of Energy, London, 1985.

[83] Ewan B C R, 'The measurement of droplet sizes in water sprays' HSE Internal Report IR/L/FR/88/1, 1988.

[84] Yule A J, Ah Seng C, Felton P G, Ungut A, and Chigier N A, 'A laser tomographic investigation of liquid fuel sprays' Eighteenth Symposium (International) on Combustion, The Combustion Institute, 1981.

[85] Yamauchi T, and Ohyama Y, 'A study on the measurement of particle size distribution with laser diffraction systems' Bulletin of the JSME, Vol. 25, No. 210, 1982.

[86] Negus C, and Azzopardi B J, 'The Malvern particle size distribution analyser: its accuracy and limitations' AERE Harwell Report AERE-R 9075, 1978.

[87] Mitchell J P, Nichols A L, and van Santen A, 'The characterisation of water-droplet aerosols by Polytec optical particle analysers' Part Part Syst Charact, Vol. 6, 119-123, 1989.

[88] Mroczka J, 'integral transform technique in particle sizing' J Aerosol Sci, Vol. 20, No. 8, 1989.

[89] Gülder Ö L, 'Multiple scattering effects in dense spray sizing by laser diffraction' Aerosol Sci and Tech, Vol. 12, 570-577, 1990.

[90] Samirant M, Smeets G, Baras Ch, Royer H, and Oudin L R, 'Dynamic measurements in combustible and detonable aerosols' Propellants, Explosives, Pyrotechnics, Vol. 14, 47-56, 1989.

[91] Hu Z G, Tsai Y N, and Sheng D R, 'Measurement of droplet size distribution in a two-phase medium by optimised method of laser scattering' Int J Heat and Fluid Flow, Vol. 12, No. 1, 1991.

[92] Chigier N, 'Optical imaging of sprays' Prog Energy Combust Sci, Vol. 17, 211-262, 1991.

[93] Abrukov A S, Bykov V N, Krivchenko I V, and Lavrent'yev M Ye, 'Holography and light-scattering methods for studying transfer processes in two-phase flows' Heat Transfer - Soviet Research, Vol. 21, No. 4, 1989.

[94] Bryanston-Cross P J, Funes-Gallanzi M,Quan C, and Judge T R, 'Holographic particle image velocimetry (HPIV)' Opt and Laser Tech, Vol. 24, No. 5, 1992.

[95] Kurosaki Y, and Kashiwagi T, 'Visualisation of thermal behaviour of fluid by laser holographic interferometry' Experimental Heat Transfer, Fluid Mechanics, and Thermodynamics, 84-103, Elsevier, 1988.

[96] Reuss D L, and Adrian R J, 'Two-dimensional velocity measurements in a laminar flame using particle image velocimetry' Combust Sci and Tech, Vol. 67, 1989.

[97] Hind A K,and Christy J R E, 'Particle image velocimetry (PIV): obtaining instantaneous, multipoint velocity measurements throughtout a 2D plane in a time varying flow downstream of an artificial heart valve' Proc of I Chem E Research Event 1992, UMIST, Institute of Chemical Engineering, 1992.

[98] Danel F, and Delhaye J M, 'Sonde optique pour la mesure du taux de présence local en ecoulement diphasique' Mesure-Regulation-Automatisme, 99-101, 1971.

[99] Gibbons D B, Azzopardi B J, and Bott T R, 'Laser tomographic investigation of the entrained liquid in annular two-phase flow' International Conference on Physical Modelling of Multi-Phase Flow, Coventry, England, BHRA Fluid Engineering, 1983.

[100] Morris D, Tesyssedou A, Lapierre J, and Tapucu A, 'Optical fiber probe to measure local void fraction profiles' App Opt, Vol. 26, No. 21, 1987.

[101] Shu H-F, and Benton R D, 'Data acquisition and analysis on the two-color laser transmissometer system' Proc of South-East Conf '91 (USA), IEEE, Vol. 2, 810-814, 1991.

[102] Holländer W, Pohlmann G, and Morawietz G, 'A laser Doppler method for the determination of particle deposition velocities' J Aerosol Sci, Vol. 20, No. 3, 1989.

[103] Durst F, Melling A, and Whitelaw J H, Principles and Practice of Laser-Doppler Anemometry (2nd Edition), Academic Press Inc, London, 1981.

[104] Ju Y-H, 'The use of laser-holography techniques for studying two-phase steam-water critical flow' PhD Thesis dissertation, University of Washington (USA), 1977.

[105] Swithenbank J, 'Fundamentalstudy of three dimensional two phase flow in combustion systems' Sheffield University Final Contract Report 1 Oct 1983-30 Sept 1984, 1984. Report prepared for EOARD/LNB, London, UK, and European Office of Aerospace Research andDevelopment, London, UK.

[106] Hassan Y, and Blanchat T, 'Full-field bubbly flow velocity measurements by digital image pulsed laser velocimetry' Experiments in Fluids,Vol. 11, 1991.

[107] Hanzevack E L, Bowers C B, and Ju C-H, 'Study of two-phase flow by laser image processing' AIChE Journal, Vol. 33, No. 12, 1987.

[108] Chew T C, Britter R E, and Bray K N C, 'Laser tomography of turbulent premixed Bunsen flames' Comb and Flame, Vol. 75, 165-174, 1989.

[109] Meynart R, 'Instantaneous velocity field measurements in unsteady gas flow by speckle velocimetry' App Opt, Vol. 22, No. 4, 1983.

[110A] Ohba K, Kishimoto I, and Ogasawara M, 'Simultaneous measurement of local liquid velocity and void fractions in bubbly flows using a gas laser - Part 1 principle and measuring procedure' Tech Rep Osaka Univ, Vol. 26, No. 1328, 1976.

[110B] Ohba K, Kishimoto I, and Ogasawara M, 'Simultaneous measurement of local liquid velocity and void fraction in bubbly flows using a gas laser - Part II local properties of turbulent bubbly flow' Tech Rep Osaka Univ, Vol. 27, No. 1358, 1977.

[110C] Ohba K, Kishimoto I, and Ogasawara M, 'Simultaneous measurement of local liquid velocity and void fraction in bubbly flows using a gas laser - Part III accuracy of measurement' Tech Rep Osaka Univ, Vol. 27, No. 1383, 1977.

[111] Borrego C, and Olivari D, 'Simultaneous measurements of hot-wire anemometer and laser Doppler velocimeter in a turbulent flow' Proc Int Conf on Advances in Flow Measurement Techniques, Warwick, UK, BHRA Fluid Engineering, 1981.

[112] Dybbs A, and Ghorashi B (eds), Laser Anemometry: Advances and Applications, Vols 1 and 2, American Society of Mechanical Engineering (ASME), 1991.

[113] Zhu J Y, So R M C, and Otugen M V, 'Turbulent mass flux measurements using a laser/hot-wire technique' Int J Heat Mass Transfer, Vol. 31, No. 4, 1988.

[114] Yule A J, and Aval S M, 'A technique for velocity measurement in diesel sprays' Comb and Flame, Vol. 77, 385-394, 1989.

[115] Trolinger J D, Particle and flow field holography, Combustion Measurements, Chapter 3, Hemisphere Publishing Company, New York, 1990.

[116] Hanzevack E L, and Demetriou G D, 'Effect ofvelocity and pipeline configuration on dispersion in turbulent hydrocarbon-water flow using laser image processing' Int J Multiphase Flow, Vol. 15, No. 6, 1989.

[117] 'Optical methods of analysis of two=phase flows' Fluid Mechanics - Soviet Research, Vol. 18, No. 3, 1989.

[118] Hamdullahpur F, and MacKay G D M, 'Two-phase flow behaviour in the freeboard of a gas-fluidised bed' AIChE Journal, Vol. 32, No. 12, 1986.

[119] Whitelaw J H, 'Laser velocimetry: problems and opportunities' Proc ASME Winter Annual Meeting, Pheonix, USA, 1982, ASME 1982.

[120] Nouri J M, Whitelaw J H, and Yianneskis M, 'Particle motion and turbulence in dense two-phase flows' Int J Multiphase Flow, Vol. 13, No. 6, 1987.

[121] Lourenço L, and Riethmuller M L, 'Optical measurements applied to particulate two phase flows' Proc Int Symp Applications of Laser Doppler Anemometry to Fluid Mechanics, Lisbon, 1982.

[122] Verdeyen J T, Laser Electronics, Solid State Physical Electronics Series, Prentice-Hall, 1981.

[123] Atkins P W, Physical Chemistry, Oxford University Press, 1987.

[124] Hughes D, Notes on Protection against Laser Radiation in the Laboratory, HHSC Handbook No. 10, H and H Scientific Consultants Ltd, Leeds, 1992.

[125] Bayvel L P, and Jones A R, Electromagnetic Scattering and its Applications, Applied Science Publishers, 1981.

[126] Dreier T, and Rakestraw D J, Opt Lett, Vol. 15, 72, 1990.

[127] Durst F, and Völklein J, 'A laser Doppler anemometer for the measurement of wind velocities' Wind Engineering, Vol. 13, No. 2, 1989.

[128] Yeh Y, and Cummins H Z, 'Localised flow measurements with an He-Ne laser spectrometer' App Phys Lett, Vol. 4, 176-178, 1964.

[129] Lourenco L, and Krothapalli A, 'The role of photographic parameters in laser speckle or particle image displacement velocimetry' Experiments in Fluids, Vol. 5, 1987.

[130] Khalighi B, and Huebler M S, 'A transient water analog of a dual-intake valve engine for intake flow visualisation and full-field velocity measurements' SAE paper No. 880519, 1988.

[131] Lewis G S, Cantwell B J, Vandsburger U, and Bowman C T, 'An investigation of the structure of a laminar non-premixed flame in an unsteady vortical flow' Twenty-second Symposium (International) on Combustion, The Combustion Institute, 1988.

[132] Marko K A, Li P, Rimai L, Ma T, and Davies M, 'Flow-field imaging for quantitative cycle-resolved velocity measurements in a model engine' SAE paper No. 860002, 1986.

[133] Adamczyk A A, and Rimai L, 'Reconstruction of a 3-dimensional flow field from orthogonal views of seed track video images' Experiments in Fluids, Vol. 6, 1988.

[134] Galaup J P, and Delhaye J M, 'Utilisation des sondes optiques miniatures en ecoulement diphasique gaz-liquide' La Houille Blanche, No. 1, 17-29, 1976.

[135] Snowdon P, Skippon S M, Kaczmarek M, and Ewart P, 'NATO ASI on combusting flow diagnostics' Kluwer Publishers, 1990.

[136] Ewart P, and O'Leary S V, Opt Lett, Vol. 11, 279, 1986.

[137] Greenhalgn D A, 'Optical Combustion Diagnostics, Fundamental or Practical', p18 Joint Meeting of the British and German Sections, The British Section of the Combustion Institute, 1993.

[138] Stenberg J, and Hernberg R, 'Laser Photóacoustic Probe For In-Situ Gas Analysis In Fluidised Bed Reactors', p259 Joint Meeting of the British and German Sections, The British Section of the Combustion Institute, 1993.

[139] Hanlon T R, and Melton L A, 'Exciplex fluorescence Thermometry of Falling Hexadecane Droplets', J Heat Transfer, Vol 114, 450-457, may, 1992.

[140] Bernstein J S, Fein A, Choi J B, Cool T A, Sausa R C, Howard S L, Locke R J, and Miziolek A W, 'Laser-Based Flame Species Profile Measurements: A Comparison With Flame Model Predictions' Combustion and Flame, 92, 85-105, 1993.

[141] Erf R H and Ready J F (Eds), 'Laser Applications' Academic Press, New York, 1983.

[142] Radziemski L J, Solarz R W, and Paisner J A (Eds), 'Laser Spectroscopy and its Applications' Optical Engineering Series, Vol 11, Marcel Dekker, 1987.

[143] Zharov V P, and Letokhov V S, 'Laser Optoacoustic Spectroscopy' Springer-Verlag, Berlin, 1986.

[144] Adrian R J, Durao D F GT, Durst F, Meada M, and Whitelaw J H (Eds), 'Applications of Laser Techniques to Fluid Mechanics (5th International Symposium)' Springer-Verlag, 1991.

[145] Ruck B, Leder A, and Dopheide D (Eds), 'Laser Anemometry Advances and Applications (7th International Conference)', Karlsruhe, Germany, 1997.

[146] Proceedings of the Seventh International Symposium on Applications of Laser Techniques to Fluid Mechanics, Lisbon, Portugal, 1994.

[147] International Conference on Optical Methods and data Processing in Heat and fluid Flow, City University, London, 1998.

[148] Drain L E, 'The Laser Doppler Technique' John Wiley and sons Ltd, 1980.

[149] Guilbault G G, 'Practical Fluorescence' second edition, Marcel Dekker Inc, 1990.

[150] International Seminar on Optical Methods and Data Processing in Heat and Fluid Flow, City University, London, 1996.

[151] Proceedings of the Ninth International Symposium on Applications of Laser Techniques to Fluid Mechanics, Lisbon, Portugal, 1998.

[152] Symposium on Laser Anemometry and the Validation of Computational Solutions, University of Loughborough, July 2nd-3rd, 1997.

[153] Black D L, McQuay M Q, and Bonin M P, 'Laser-Based Techniques for Particle Size Measurement: A Review of Sizing Methods and their Industrial Applications' Prog. Energy Combust. Sci. Vol 22, pp267-306, 1996.

[154] Reitz R D, 'A Photographic Study of Flash-Boiling Atomization' Aerosol Science and Technology, Vol 12, pp561-569, 1990.

[155] Espey C, Dec J E, Litzinger T A, and Santavicca D A, 'Planar laser Rayleigh Scattering for Quantitative Vapor-Fuel Imaging in a Diesel Jet', Combustion and flame, Vol 109, 65-86, 1997.

[156] Westblom U et al, 'Laser-Induced Fluorescence diagnostics of a propane/Air Flame with a Manganese Fuel Additive', Combustion and flame, Vol 99, 261-268, 1994.

[157] Santangelo P J, and Sojka P E, 'Holograohic Particle Diagnostics', Prog. Energy Combust. Sci., Vol 19, pp587-603, 1993.

[158] Cheng T S et al, 'Raman Measurement of Mixing and Finite-Rate Chemistry in a Supersonic Hydrogen-Air Diffusion Flame', Combustion and flame Vol 99, 157-173, 1994.

[159] Bazile R, and Stepowski D, 'Measurements of vaporized and Liquid fuel Concentration Fields in a Burning Spreay jet of Acetone Using Planar Laser Induced Fluorescence', Experiments in Fluids, vol 20, pp1-9, 1995.

[160] Vandroux-Koenig S, and Berthoud G, 'Modelling of a two-phase Momentum Jet Close to the Breach, in the Containment Vessel of a Liquefied gas', J. Loss Prev. Process Ind. Vol 10 (1), pp 17-29, 1997.

[161] Laurendeau N M, 'Temperature Measurements by Light-Scattering Methods', Prog. Energy Combust Sci, Vol 14, pp147-170, 1988.

[162] Gabas N, Hiquily N, and Laguerite C, 'Response of Laser Diffraction Particle Sizer to Anisometric Particles', Part. part. Syst. Charact Vol 11, 121-126, 1994.

[163] Ikeda Y, Nishigaki M, Ippommatsu M, and Nakajima T, 'Optimum Seeding particles for Succesful Laser Doppler Velocimeter Measurements', Part. Part. Syst. Character. Vol 11, 127-132, 1994.

[164] Chen J C, Taniguchi M, Narato K, and Ito K, 'Laser Ignition of Pulverised Coals', Combustion and Flame, Vol 97, 107-117, 1994.

[165] Brandt A, and Merzkirch W, 'Particle Image velocimetry Applied to a Spray jet', Part. part. Syst. Charater. Vol. 11, 156-158, 1994.

[166] Tolles W M, Nibler J W, McDonald J R, and Harvey A B, 'A Review of the Theory and Application of Coherent Anti-Stokes Raman Spectroscopy (CARS)', Applied Spectroscopy, Vol 31, No 4, 253-271, 1977.

[167] Ozdemir I B and Whitelaw J H, 'Impingement of an Unsteady Two-Phase jet on Unheated Flat plates', Fluid Mech, Vol 252, pp499-523, 1993.

[168] Foss W et al, 'Studies of toxic Aerosols via Elastic and inelastic Light scattering', Aerosol Sci and Tech, Vol 18, 187-201, 1993.

[169] Hartfield R J, Hollo S D, and McDaniel J C, 'Planar Measurement Technique for Compressible flows Using laser-Induced Iodine Fluorescence', AIAA Journal, Vol 31, No 3, March 1993.

[170] Melton L A, ' Use of Fluorescence Methods for Measurement of Droplet and Vapor Temperatures', AIAA Progress Volume, Vol 1, Chapter 6, p143, 1996.

Chapter Four

Experimental Facility

[*] Health and Safety Laboratory Two-Phase Jet Release Facility Equipment Documentation File (EDF), 1993.

Part A: Specification, Design, Construction and Component Details (FR/11/002/93 Pt A).

Part B: Operating, Maintenance and Safety Procedures/Assessment Details (FR/11/002/93 Pt B).

[1] Allen J T, 'The Application of Laser-based Measurement Techniques To Two-Phase Releases' HSE Internal Report IR/L/FR/93/10, 1993.

[2] Greenhalgh D A, 'Optical Combustion Diagnostics, Fundamental or Practical' Joint Meeting of the British and German sections, The British Section of the Combustion Institute, p18, 1993.

[3] Ewan B C R, 'Development of spray diagnostics instrumentation' Chementech Annual Report, June 1989. Contract report for RLSD, HSE.

[4] Ewan B C R, 'Study to assess the potential use of laser diagnostics at the Explosion and Flame Laboratory' Chementech Annual Report, Sept 1990. Contract report for RLSD, HSE.

[5] Ewan B C R, 'Development of spray diagnostics instrumentation' Chementech Annual Report, May 1991. Contract report for RLSD, HSE.

[6] Ewan B C R, 'Development of spray diagnostics instrumentation - gas phase studies' Chementech work outline plan, July 1990. Produced under contract to RLSD, HSE.

[7] Bettis R J, Ewan B C R, Jagger S F, and Moodie K, 'Two-phase jet and cloud growth following a sudden release of liquefied gas' HSE Internal Report IR/L/FR/92/5, 1992.

[8] Moodie K, and Ewan B C R, 'Jets discharging to atmosphere', HSE Internal Report IR/L/FR/89/28, 1989.

[9] Ewan B C R, 'Two-phase flashing jet properties' HSE Internal Report IR/L/FR/86/24, 1986.

[10] Ewan B C R, 'Spectroscopic concentration measurements in two-phase flows' HSE Internal Report IR/L/FR/87/10, 1987.

[11] Murray A M, and Melton L A, 'Exciplex Visualisation Systems for Low Boiling Point Hydrocarbons', Internal paper, University of Texas at Dallas, 1985.

Chapter Five

Conventional Temperature Measurements

[1] Ewan, B C R 'Two-Phase Flashing Jet Properties' HSE Internal Report IR/L/FR/86/24

[2] Allen J T, 'Conventional Temperature Measurements In Small Scale Two-Phase Flashing Propane Jet Releases' HSL Section Report IR/L/FR/95/5, 1995.

[3] Jones, S J 'Propane Dispersion Calculations Using TRAUMA' AEA Technology Internal Report AEA/CS/16405307/z1, 1995.

[4] Tickle G A, Jones S J, Martin D, Ramsdale S A, and Webber D M, 'Development and validation of Integral Models of Two-Phase Jets', Final Report produced for The European Commission under Contract EV5V-CT94-0431, AEAT/1389, AEA Technology, 1997.

[5] Crespo A, Garcia J, and Hernandez J, 'An Experimental and Modelling Study of Two-Phase Flashing Jets', Final Report for CEC Contract EV5V-CT94-0431, Universidad Politecnica de Madrid, 1997.

[6] Bettis R J, Beckett H, Cooke G D, and Jagger S F, 'Measurements of Field-Scale Unignited propane Releases', HSL Report FS/98/01 & PS/98/01, 1998.

[7] Schumann S, Pasoi L M, Schmittberger H, and Walter H, 'An Experimental and Modelling Study of Two-Phase Flashing Jets', Final Report R-40.079-5E, Battelle Ingenieurtechnik GmbH, Germany, February, 1997.

Chapter Six

LDA Measurements

[1] Hervieu E and Veneau T, 'Experimental determination of the droplet size and velocity distributions at the exit of the bottom discharge pipe of a liquid propane storage tank during sudden blowdown', J. Loss Prev. in the Proc. Ind, 9(6), 413-425, 1996.

[2] Ewan B C R, 'Two-phase Flashing Jet Properties' HSE Internal Report IR/L/FR/86/24

[3] Yeh Y, and Cummins H Z, 'Localised flow measurements with an He-Ne laser spectrometer' App Phys Lett, Vol. 4, 176-178, 1964.

[4] Durst F, Melling A, and Whitelaw J H, 'Principles and Practice of Laser-Doppler Anemometry (2nd Edition)', Academic Press Inc, London, 1981.

[5] Durst F, 'Optical techniques for fluid flow and heat transfer' Experimental Heat Transfer, Fluid Mechanics, and Thermodynamics, 32-49, Elsevier, 1988.

[6] Drain L E, 'The Laser Doppler Technique' John Wiley and Sons Ltd, 1980.

[7] Durst F, and Volklein J, 'A laser Doppler anemometer for the measurement of wind velocities' Wind Engineering, Vol. 13, No. 2, 1989.

[8] T.S.I. Inc Laser Doppler Velocimeter Manuals (various), TSI Incorporated, 500 Cardigan Road, P.O. Box 64394, St Paul, MN 55164, USA.

[9] Allen J T, 'Laser-Based Velocity Measurements in Two-Phase Flashing Propane Jets', HSL Report, IR/L/FR/96/5, 1996.

[10] Dr G Tickle and Dr S Jones, private communication, AEA Technology, UK.

[11] Tickle G A, Jones S J, Martin D, Ramsdale S A, and Webber D M, 'Development and validation of Integral Models of Two-Phase Jets', Final Report produced for The European Commission under Contract EV5V-CT94-0431, AEAT/1389, AEA Technology, 1997.

[12] Crespo A, Garcia J, and Hernandez J, 'An Experimental and Modelling Study of Two-Phase Flashing Jets', Final Report for CEC Contract EV5V-CT94-0431, Universidad Politecnica de Madrid, Spain, 1997.

Chapter Seven

Droplet Size Measurements

[1] Hervieu E and Veneau T, 'Experimental determination of the droplet size and velocity distributions at the exit of the bottom discharge pipe of a liquid propane storage tank during sudden blowdown', J. Loss Prev. in the Proc. Ind, 9(6), 413-425, 1996.

[2] Swithenbank J, Beer J M, Taylor D S, Abbot D, and McCreath G C, 'A Laser Diagnostic Technique For The Measurement Of Droplet Particle Size and Distribution' Prog in Astro and Aero, Vol. 53, 421-447, 1977.

[3] Hamidi A A, and Swithenbank J, 'Treatment Of Multiple Scattering Of Light In Laser Diffraction Measurement Techniques In Dense Sprays and Particle Fields' J Inst Energy, 101-105, 1986.

[4] Cao J, Brown D J, and Rennie A G, 'Laser Diffraction Particle Sizing In Dense Suspensions And Sprays With Correction For Multiple Scattering' University of Sheffield Report, Dept. Process and Mechanical Engineering, 1993.

[5] Dodge L G, 'Change Of Calibration Of Diffraction-Based Particle Sizers In Dense Sprays' Opt Eng, Vol. 23, No. 5, 1984.

[6] Felton P G, Hamidi A A, and Aigal A K, 'Measurement Of Drop Size Distribution In Dense Sprays By Laser Diffraction' Proceedings of Third International Conference on Liquid Atomisation and Spray Systems (ILASS), Institute of Energy, London, 1985.

[7] Yamauchi T, and Ohyama Y, 'A Study On The Measurement Of Particle Size Distribution With Laser Diffraction Systems' Bulletin of the JSME, Vol. 25, No. 210, 1982.

[8] Negus C, and Azzopardi B J, 'The Malvern Particle Size Distribution Analyser: Its Accuracy And Limitations' AERE Harwell Report AERE-R 9075, 1978.

[9] Gulder O L, 'Multiple Scattering Effects In Dense Spray Sizing By Laser Diffraction' Aerosol Sci and Tech, Vol. 12, 570-577, 1990.

[10] Ewan B C R, 'The Measurement Of Droplet Sizes In Water Sprays' HSE Internal Report IR/L/FR/88/1, 1988.

[11] Yule A J, Ah Seng C, Felton P G, Ungut A, and Chigier N A, 'A Laser Tomographic Investigation Of Liquid Fuel Sprays' Eighteenth Symposium (International) On Combustion, The Combustion Institute, 1981.

[12] Mitchell J P, Nichols A L, and van Santen A, 'The Characterisation Of Water-Droplet Aerosols By Polytec Optical Particle Analysers' Part Syst Charact, Vol. 6, 119-123, 1989.

[13] Mroczka J, 'Integral Transform Technique In Particle Sizing' J Aerosol Sci, Vol. 20, No. 8, 1989.

[14] Samirant M, Smeets G, Baras Ch, Royer H, and Oudin L R, 'Dynamic Measurements In Combustible And Detonable Aerosols' Propellants, Explosives, Pyrotechnics, Vol. 14, 47-56, 1989.

[15] Abrukov A S, Bykov V N, Krivchenko I V, and Lavrent'yev M Ye, 'Holography And Light-Scattering Methods For Studying Transfer Processes In Two-Phase Flows' Heat Transfer - Soviet Research, Vol. 21, No. 4, 1989.

[16] Gibbons D B, Azzopardi B J, and Bott T R, 'Laser Tomographic Investigation Of The Entrained Liquid In Annular Two-Phase Flow' International Conference On Physical Modelling Of Multi-Phase Flow, Coventry, England, BHRA Fluid Engineering, 1983.

[17] Swithenbank J, 'Fundamental Study Of Three-Dimensional Two-Phase Flow In Combustion Systems' Sheffield University Final Contract Report 1 Oct 1983 - 30 Sept 1984, 1984. Report prepared for EOARD/LNB, London, UK, and European Office of Aerospace Research and Development, London, UK.

[18] Moodie K, and Ewan B C R 'Jets Discharging To Atmosphere' RLSD Internal Report IR/L/FR/89/28, 1989.

[19] Cao J, Model Independent multiple scatter algorithm provided under private agreement, by private communications, formerly University of Sheffield, Dept. of Process and Mechanical Engineering, and Malvern Instruments Ltd, Spring Lane South, Malvern, Worcs. WR 14 1AQ.

[20] Malvern System 2600 Instruction Manual, Issue 2.3, November 1993, Malvern Instruments Ltd., Spring Lane South, Malvern, Worcs. WR 14 1AQ.

[21] Allen J T, 'Laser-Based Droplet Size Measurements In Two-Phase Flashing Propane Jets', HSL Section Report IR/L/FR/96/6, 1996.

Chapter Eight

Development Of Fluorescence-Based Temperature Measurement Technique

[1] Allen J T, 'The Application Of Laser-Based Measurement Techniques To Two-Phase Releases', HSE Internal Report IR/L/FR/93/10, 1993.

[2] Guilbault G G, 'Practical Fluorescence - theory, methods, and techniques', Dekker, 1973.

[3] Guilbault G G, 'Practical Fluorescence', second edition, Marcel Dekker, 1990.

[4] Melton L A, and Verdieck J F, 'Vapour/Liquid Visualisation For Fuel Sprays', Comb Sci and Tech, Vol. 42, 217-222, 1984.

[5] Murray A M, and Melton L A, 'Fluorescence Methods For Determination of Temperature in Fuel Sprays' App Opt, Vol.. 24, No. 17, 1985.

[6] Murray A M and Melton L A, 'Exciplex Visualisation Systems for Low Boiling Hydrocarbons'. No additional reference data available.

[7] Gossage H E and Melton L A, 'Fluorescence Thermometers Using Intramolecular Exciplexes' App Opt, Vol. 26, No. 11, 1987.

[8] Ewan B C R, 'The Development of Spray Diagnostics Instrumentation', RLSD Section Report, IR/L/FR/89/26, 1989.

[9] Ewan B C R, 'The Development of Equipment for the Optical Investigation of Evaporating Sprays', RLSD Section Report, IR/L/FR/90/24, 1990.

[10] Bettis R J, Ewan BCR, Jagger S F, and Moodie K, 'Two-Phase Jet And Cloud Growth Following a Sudden Release Of Liquefied Gas', HSE Internal Report IR/L/FR/89/28, 1989.

[11] Ewan B C R, 'Development Of Spray Diagnostics Instrumentation - Gas Phase Studies', Chementech Work Outline Plan, July 1990. Produced under contract to RLSD, HSE.

[12] Melton L A, ' Use of Fluorescence Methods for Measurement of Droplet and Vapor Temperatures', AIAA Progress Volume, Vol 1, Chapter 6, p143, 1996.

[13] Melton L A, and Verdieck J F, 'Vapour/Liquid Visualisation For Fuel Sprays', Twentieth Symposium On Combustion, The Combustion Institute, 1283-1290, 1984.

[14] Hanlon T R, and Melton L A, 'Exciplex Fluorescence Thermometry of Fallong Hexadecane Droplets', J Heat Transfer, Vol. 114, 450-457, 1992.

[15] Hamann H-J, Pragst F, Jugelt W, 'Preparation and electrochemical properties of N,N-disubstituted 1-amino-3-(9-anthryl)-propane derivatives' J. prakt. Chem. 318, (8) pp369-380, 1976.

[16] Hamann H-J, Jugelt W, Pragst F, 'Intramolecular exciplex formation of some 1-(N-methyl-N-phenyl)-amino-3-(9-anthryl)-propane derivatives' Z. Chem. 14, (12) pp475-477, 1974.

[17] Pragst F, Hamann H-J, Teuchner K, Naether M, Becker W, and Daehne S, 'Steady State And Laser Spectroscopic Investigations On The Intramolecular Exciplex Formation Of 1-(N-p-Anisyl-N-Methyl)-Amino-3-Anthryl-(9)-Propane', Chem Phys Lett, Vol. 48(1), 36-40, 1977.

[18] Pragst F, University of Humboldt, Berlin, private communications, May-July 1995.

[19] Spivey A C, Bissell A J, and Stamman B,'A Practical Synthesis of N-p-Anisyl-N-methyl-amino-3-(9-anthryl)-propane: An Exciplex Fluorescence 'Thermometer", Synthetic Communications, Vol. 28 (4), 623-632, 1998.

Chapter Nine

Recommendations For Further Work

[1] Bettis R J, Beckett H, Cooke G D, and Jagger S F, 'Measurements of Field-Scale Unignited propane Releases', HSL Report FS/98/01 & PS/98/01, 1998.

[2] Schumann S, Pasoi L M, Schmittberger H, and Walter H, 'An Experimental and Modelling Study of Two-Phase Flashing Jets', Final Report R-40.079-5E, Battelle Ingenieurtechnik GmbH, Germany, February, 1997.

Chapter Ten

Overall Conclusions

[1] Tickle G A, Jones S J, Martin D, Ramsdale S A, and Webber D M, 'Development and validation of Integral Models of Two-Phase Jets', Final Report produced for The European Commission under Contract EV5V-CT94-0431, AEAT/1389, AEA Technology, 1997.

[2] Crespo A, Garcia J, and Hernandez J, 'An Experimental and Modelling Study of Two-Phase Flashing Jets', Final Report for CEC Contract EV5V-CT94-0431, Universidad Politecnica de Madrid, Spain, 1997.

[3] Kelsey A, 'CFD Modelling of Two-Phase Flashing Jets: Literature Review', HSL Report, FR/97/5, 1997.

[4] Bigot J P, Ecole des Mines Saint-Etienne, France, private communication, July 1998.

[5] Bricard P, Technische Universitat Hamburg-Harburg, Germany, private communication, September, 1997.

[6] Melton L A, University of Texas at Dallas, USA, private communication, June 1998.

APPENDICES

Note:

The appendices are presented in chapter order, their numerical title indicating the chapter to which they pertain.

APPENDIX 4A

FACILITY OPERATING PROCEDURE

This appendix contains the normal operating procedures for the facility, including those for filling of the vessel and other general duties.

The section also contains the procedures to be followed in the event and aftermath of an unsafe situation.

A4.1 Ownership, Approved Operators and Related Items

The Facility Owner is:

Mr J T Allen

The current list of Approved Operators is:

Mr J T Allen

Dr R J Bettis

Re-assignment of the facility ownership and additions to the Approved Operators list can only be made by Dr S F Jagger, Fire and Thermofluids Section Head, or his successors, subject to the criteria outlined below.

Prior to becoming an Approved Operator the person must have fulfilled the following criteria:

1) They must be deemed competent and safe to operate the facility and its associated equipment. It should be noted that academic qualifications alone are not sufficient proof of this competence.

2) They must have comprehensively read and understood the information and procedures laid out in the facility EDF and this report. There should be signed confirmation of this placed in the facility EDF.

3) They must be familiar with the actual operation of the facility. This is to be gained by working under the supervision of Mr J T Allen, Dr R J Bettis or any experienced Approved Operator.

Any change in the facility operation or related items, eg operational procedure, is to be made by, or in consultation with, the Facility Owner. This change extends to changes of:

i) use
ii) facility components
iii) experimental layout

and use of non-standard fluids

The Facility Owner should be an experienced Approved Operator, fully conversant with all aspects of the facility and its operation, and associated equipment.

A4.2 Operating Instructions

1. Check the status of the propane sensor safety systems (ie ensure that there has been no propane escape inside the storage facility otherwise there will be a big bang).

2. If storage facility is 'safe', visually check condition/status of the storage vessel and its components. Ensure that storage facility door is closed and locked upon exiting to prevent unauthorised access and to maintain designed safety conditions.

3. Check extract fan and chamber for safe operational condition (ie fan etc in good working order, no unauthorised objects inside experimental chamber).

4. Turn on extract system.

5. Check status of rest of safety system. (air flow through fan and experimental chamber above specified level).

6. Fill vessel if necessary. See 'Normal Filling Procedure'.

7. Turn on measurement devices eg thermocouples, pressure transducers, etc. Check header tank nozzle, change to different nozzle if required.

8. Start experiment: Turn on vessel heating system and set to desired temperature, set nitrogen pad pressure. Position header tank by use of traversing system.

9. When temperature reaches desired value, increase nitrogen pressure (if required).

10. Turn on laser and data acquisition systems.

11. Generate two-phase propane jet. See 'Jet Release'.

12. Allow jet to become stable.

13. Start laser data generation and acquisition systems.
Note: Depending on the laser technique employed, it may be desirable to perform action 13 before actions 11 and 12.

14. When sufficient data has been collected by the laser system, stop two-phase release. See 'Jet Release'.

15. If the header tank is to be moved, or access to the chamber is required, turn off any laser system. If it is possible to safely stop the laser beam, using system integrated stops, then this is permitted as an alternative to actually switching off the laser or laser system.

16. Repeat steps outlined above, as appropriate, to conduct further experiments.

17. For termination of experiment at end of experimental day, see 'Closing Down'.

Note: NEVER perform filling procedure without use of appropriate safety equipment (gloves to avoid cold burns, cotton outer clothing to avoid static discharge, eye protection, protective footwear, non-sparking tools for line disconnection)

A4.3 Operating Limits

The operating limits for this facility, as defined by the design criteria are:

Temperature: ambient to 45 degrees Celsius (propane liquid temperature in storage vessel)

Pressure: 15 barg (total pressure in storage vessel, including nitrogen padding)

Propane mass release rate : not to exceed 250 g/sec (extract system maximum to maintain <50% of LFL)

Air flow rate through experimental chamber: not less than 1.0 m/sec (to avoid propane vapour escape)

Air flow rate through extract fan system: not less than ~12 m^3/sec (to maintain <50% LFL of propane at all mass flow rates)

Air supply pressure to pump (maximum 8.6 barg (125psi), minimum 1.72 barg (25 psi))

Air supply pressure to release valves (min 80 psi, absolute max 120 psi)

Additional operational recommendations may be found in the current Operating Procedure, or in the EDF.

A4.4 Normal Filling Procedure

1. Determine number of strokes required from handpump to fill vessel to its maximum permitted volume. This is done by the use of a graph. Firstly, calculate the mass of propane required to fill the vessel by the use of the formula below:

mass of propane required = 23 - weight displayed on load cells (in laboratory)

Then determine number of handstrokes on pump required from the graph.

2. Ensure that vessel release valve (E) is closed, and both manual valves are closed.

3. Attach liquid delivery line to liquid take-off port on supply container and to input port of LPG handpump. Attach second liquid delivery line to output port of handpump and to storage vessel liquid intake port.

4. Attach vapour removal line to vapour take-off ports on both storage vessel and supply container.

5. Ensure that the connections are tight.

6. Open manual valves on vapour (B) and liquid (A) take-off ports. Open liquid (C) and vapour (D) take-off valves on supply container.

7. Verify that the number of handstrokes determined earlier is correct. Check the number calculated with a second person.

8. Pump the handpump the correct number of times required to fill the vessel to the desired level.

9. When the maximum permissible volume of propane has been transferred, close off the liquid and vapour lines at the supply vessel. Close the liquid supply line first. Close the vessel manual valves.

10. Disconnect supply lines from the vessel and the supply container. CAUTION: a small release of propane may result, and the potential exists for cold burns.

11. Check weight value on loadcell readouts in the laboratory. If there is a discrepancy between the value that should be showing on the readout (as determined by the maximum fill calculations) and the actual readout value DO NOT ATTEMPT TO PUMP ANY ADDITIONAL PROPANE INTO THE VESSEL. Try to ascertain the cause of the discrepancy.

If the readout is less, possible problems may be
a) faulty load cell or readout system
b) error in calculation of required fill
c) connection of vapour supply line to liquid intake on pump (thereby filling vessel with n number of handstrokes of vapour as opposed to the much denser liquid)
d) one handstroke may deliver a slightly less volume of propane than specified

If the readout is slightly greater than calculated, possible problem may be
a) faulty or incorrectly calibrated loadcell system, or readout
b) slightly worn pump system (thereby delivering a slightly larger volume per pump)

If the readout is considerably larger than the expected value:
a) release some propane through the usual experimental channel (via the extract system)
b) determine whether the fault is one of overfilling or loadcell failure
c) remedy problem

These brief lists of possible problems and remedies are intended as guides only. Always assume the worst possible scenario and ensure the safest response to any problem. In any potential case of overfill NEVER ACTIVATE THE VESSEL HEATING SYSTEM.

Note: Maximum vessel fill (by mass) is 22-23kg. See calculations, Appendix B8 and related Appendices.

A4.5 Supplementary Filling Procedure

If the handpump is not operational, the vessel may be filled by decanting liquid propane from a supply vessel. The procedure for filling by this method is given below. This method should only be utilised if operation of the facility is *essential* prior to the handpump being repaired and returned to service.

Prior to commencing filling procedure, disconnect electrical supply to all vessel components such as pressure transducer, load cells, etc.

Note: NEVER perform the filling operation without use of appropriate safety equipment (gloves, cotton outer clothing to avoid static discharges, eye protection, protective footwear, non-sparking tools for line disconnection).

1. Ensure vessel release valve is closed, and both manual vessel valves are closed.

2. Load filling container into filling inverter.

3. Attach liquid delivery line to filling container vapour offtake port and vessel liquid intake port.

4. Attach vapour removal line to vessel vapour offtake port and filling container liquid offtake port.

5. Ensure connections are tight

6. Invert filling container by use of filling inverter.

7. Ensure filling container mass loss system is operational. Determine maximum mass loss limit (to coincide with vessel maximum permissible total mass fill).

8. Open manual valves on vessel vapour offtake and liquid ports. Open filling container liquid and vapour offtake ports, and allow propane to decant into vessel.

9. When maximum permissible mass has been transferred, as determined previously, close off supply at filling vessel, closing vapour offtake line (the line actually carrying liquid to vessel) first. Close vessel manual valves.

10. Disconnect supply lines from vessel and filling vessel. CAUTION: small release of propane may result, and potential exists for cold burns.

11. Re-invert filling container and remove from inverter.
Maximum vessel fill (by mass) is 22-23 kg.

A4.6 Jet Release

The jet release system is designed such that the vessel and nozzle valves may be opened independently or simultaneously. The two valves may only be closed independently, except when operated by the automatic safety system.

The normal operating sequence of the valves is as follows:
to generate two-phase jet - depress 'both valves release' button.
to terminate jet - close vessel valve first by depressing appropriate button, and then close nozzle valve.

It may be permissible, in certain circumstances, to terminate the jet by use of the vessel valve alone. This would then require operation of only the 'open nozzle valve' button to regenerate the jet.

A4.7 Closing Down

ALWAYS LEAVE FAN RUNNING FOR A SUITABLE LENGTH OF TIME AT END OF EXPERIMENTAL DAY IN ORDER TO ENSURE THAT CHAMBER IS FREE FROM PROPANE. This time period will be a minimum of 5-10 minutes. ALWAYS OPEN AND CLOSE THE NOZZLE VALVE ONCE DURING THIS TIME TO ENSURE THAT THE TRANSFER LINE IS EMPTY.

Ensure that BOTH the nozzle and vessel release valves are closed.

Ensure that all electrical systems are switched off at the wall.

Close off nitrogen pad supply at bottle regulator. Close nitrogen pad supply line valve.

A4.8 Emergency Procedures

In emergencies: NEVER turn off extract system.

If small contained fire, fight with extinguishers located at exit doors

If propane release, open double emergency doors if safe to do so. Leave building as quickly as possible by safest route.

If possible turn off all laser systems. Turn off all electrically operated equipment with exception of extract fan and safety control panel.

If leak noticed in transfer line, immediately close vessel valve, thus preventing further propane from entering the line whilst still allowing propane in it to escape into the experimental chamber.

If large fire:

Fire: call fire brigade, warn other members of section, activate fire alarm, attempt to extinguish/contain fire if safe to do so

A4.9 General Operational Safety Points

A4.9.1 Experimental Chamber

Before entering the experimental chamber ensure that both the vessel and nozzle valves are closed AND that the transfer line between the two valves is empty of propane.

No entry to experimental chamber is permitted whilst the laser systems are on.

Ensure that the experimental chamber is free of propane before opening any of the side access panels. This can be accomplished by leaving sufficient time between the last propane release and the opening of the access panels for the extract system (which should be constantly working) to have swept out several chamber volumes. This time period is a minimum of 5-10 minutes.

A4.9.2 Vessel

Ensure that the vessel is completely empty, and has been purged with nitrogen before removing any intrusive objects, eg pressure transducers, thermocouples etc. Purging details given in Maintenance Schedule section.

Ensure that only NITROGEN is used to pad and purge the vessel and transfer line. Air, or any other gas, is NOT to be used under any circumstances.

A4.9.3 Laser Systems

Before introducing any new, unauthorised, laser beam into the chamber make sure that the beam energy is insufficient to ignite the propane. Also ensure that the beam path is known, by use of the 2mW HeNe laser or the new system on low power, and is, or has been made, safe for the operator (ie path of reflections known and suitable stops incorporated into experiment if necessary).

Always turn off laser systems before repositioning header tank so as to avoid accidental intrusion of traversing system into laser beam path. Never attempt to position header tank whilst releasing propane.

A4.10 Unsafe Situations and Safe State Recovery

The main hazard associated with this experimental facility is that of propane, and its ignition.

There are three main unsafe situations involving the unsafe release of propane. These are:

1) loss of containment by the storage vessel
2) loss of containment by the transfer system
3) failure of the extract system

A4.10.1 Loss Of Containment By The Storage Vessel

Loss of containment by the storage vessel can occur in a number of ways. Catastrophic failure would result in the release of up to ~50 litres of liquid propane (NB 50 litres is the capacity of the vessel, but maximum fill will always be less than this). The vessel has been constructed to sustain pressures in excess of the maximum working pressure, 15 Barg, and is also equipped with a bursting-disk type pressure relief valve. Operation, or failure, of the burst disk would also be a method by which propane could be released into the storage facility.

One of the most likely causes of excessive pressure in this system would be failure of the heating system. This problem is overcome by the type of system employed - the temperature of the heating system is continuously monitored, and any increase above that desired results in a system shut-down.

Should there be a propane release from the vessel, it is contained within a one-hour fire-rated storage facility whose internal volume (taking into account the volume of the contents) is able to accommodate 50 litres of liquid propane, assuming that it is all vapourised (worst possible case, largest volume). The facility is completely sealed except for eight flame arrestor vents. In the event of a release the intention is to allow the propane vapour to diffuse out through these vents. Any ignition source outside the storage facility will be unable to ignite the bulk of the vapour inside it. At

worst, the vapour which has escaped will burn back to the flame arresting elements and effectively flare off the vapour inside.

Any escape of propane will be detected by the propane detection system. This system is set to alarm at a low value of 20% LEL (~0.44% v/v propane in air) and also indicate (and continue to alarm) a higher value of 40% LEL (~0.88% v/v). The system indicates propane detection by visual signals inside the laboratory (one light for each of the two stages per detector), and a visual and audible signal outside the storage facility, as well as continuously displaying the actual % LEL being measured at the two detection points. The system is latching, and has to be manually re-set after the hazard has been removed.

A safe situation inside the storage facility can be easily determined by reference to the continuously displayed concentration measurements. Due however to the sump contained within the storage facility, and despite the positioning of the propane detector within this sump, it is recommended that prior to entering after a safe concentration has been displayed, the drain tap and doors are opened and left to vent for a further 10 minutes. An additional personal flammable gas monitor should also be taken into the storage facility, and normal safety precautions for entering a potentially flammable environment should be adhered to until it has been demonstrated that the hazard no longer exists.

When a major leak or other release from the storage vessel is indicated, as much propane as is possible, or practical, should be safely released from the vessel to atmosphere via the normal experimental route. That is to say it should be released into the experimental chamber and passed to atmosphere via the extraction system, which will ensure that it is released at concentrations not exceeding 50% LEL.

A4.10.2 Loss Of Containment By The Transfer System

For the purposes of this document, the transfer system is those parts of the transfer line which are not either located inside the storage facility or inside the experimental chamber. This is essentially the part of the solid transfer pipeline which goes from

the storage facility to the laboratory (external) wall, and the solid/flexible pipeline combination which goes from the laboratory (internal) wall to the header tank (positioned inside the experimental chamber).

This transfer line has been made such that it is capable of containing pressures far in excess of the maximum working pressure (15 Barg). The likelihood of a pipeline failure is very low. No specific safety precautions have been taken to counter any catastrophic failure of this line. A catastrophic failure of either part of the transfer line would not pose any threat unless there was an experimental release being undertaken on the basis that this is the only time at which the line would contain any propane. Under such circumstances, the operator would be quickly aware that there was a problem and would manually close down the system by the use of the emergency shutdown button.

It is estimated that the maximum mass of propane released by such an event would be a few kg (~2kg) dependent upon the position of the failure relative to the vessel release valve. Procedure for dealing with a release between the storage facility and the laboratory (external) wall would be similar to that for a storage facility release. Likewise, the procedure for a laboratory release would be similar to that for an extract fan failure release.

A4.10.3 Failure Of The Extract System

In the event of total failure of the extract system, or a drop in the extraction flowrate below its specified minimum, one or both of the two flowswitches should activate. Activation of either, or both, of the flowswitches results in automatic closure of the nozzle and vessel release valves. The presence of a propane detector at the entrance of the experimental chamber ensures that even if both switches fail, then the system would undergo automatic shutdown as soon as 20% LEL was measured at this point.

Should propane vapour 'back-up' against the extract flowrate (eg by impinging on an experimental obstacle in future use) then the propane detector would again detect this and force the system into automatic shutdown.
All shutdowns, either through flowswitch or propane detector initiation, are latching and need direct action to re-start the system. Also, neither type of initiation results in the shutdown of the extract system (except where that initiation was caused by extract fan failure) so that maximum propane extraction capability is maintained.

In the event of a propane release into the laboratory, the procedure is as follows:
a) If the release is not due to an extract fan failure, leave fan running.
b) Turn off all electrical equipment, if safe to do so.
c) Leave laboratory, by double safety doors if safe to do so.
d) If possible, ensure that double safety doors are open (to aid dispersion of propane cloud).
e) Inform other section personnel, and appropriate site personnel eg gatehouse, senior management, and estates.

Then, move section personnel to safe location, as determined by size and type of release. Due to the location of the official emergency collection point, opposite the jet rig facility, the collection point for jet rig emergencies should be around the emergency water supply (known as 'the pond'). Authority to be assumed by most senior section member present, acting on information of release given by section member responsible for facility at time of release.

Ensure that an adequate area around the release point, dependent on size of release, is isolated from potential ignition sources. This includes closing the road access barrier located on the hill descending into Fire Section. Any member of section staff sent to close this barrier should proceed via the safest route, such as down the side of the storage bays, and not through the quickest, eg main car park.

Employ remote or personal flammable gas monitors to ensure that safe environment exists prior to entry. Especial care should be taken if risk of ignition still present.

Also, special attention must be paid to any area where dense propane may have accumulated and not been dispersed. One such area is the 'pit' inside the laboratory. Remote sensing (eg oxygen depletion monitor on a probe) of such areas must be undertaken, with forced dispersion of any flammable material if necessary, eg by blowing air or nitrogen into them to generate turbulence and thus force out the flammable material.

If any release results in a fire the following action should be taken:

If the fire is small or contained, fight fire with fire extinguishers (located at both exits to the laboratory and in close proximity to the extract fan and storage facility) if safe to do so.

If ignition of propane diluting out from release in storage facility occurs, extinguish flames with extinguishers, if safe to do so.

If ignition of release inside storage facility occurs, do not attempt to enter the storage facility. Do not attempt to vent propane through extract system (ignition might be transferred to laboratory).

Inform section and site personnel, and send for emergency services. Move section personnel to safe location, as determined by size and location of fire.

Attempt to contain fire if safe to do so. Not to be undertaken if there is any risk of subsequent explosion.
Remove any explosive or otherwise unstable material (eg flammable liquids, combustible foams, etc) from vicinity of fire, or any area fire may realistically reach, if safe to do so.

Do not return to scene of fire until declared safe by senior fire fighter.

A4.10.4 Filling Procedure

It is also possible that a propane leak may be generated during the filling procedure. This leak may occur from either the storage vessel, or more likely from the supply vessel and associated supply line.

If a leak occurs from the storage vessel, as opposed to a leak from a supply line connection to the vessel, during filling the following procedure should be adopted:

If possible, and safe to do so, turn off all supply of propane to the vessel and close all filling valves.

Leave storage facility, closing doors.

Allow propane to dilute out from storage facility and proceed as for 'loss of containment by storage vessel', as detailed above.

If the leak is from any connector or fitting in the supply line, close off the supply to the vessel. Attempt to tighten the connection, and then re-test the connection with a low volume flow. If the leak is still present replace the connection/fitting.

If the leak is from the supply line itself, close off the supply, and replace the line.

If the leak is from the supply vessel, close off the supply, if safe to do so, and leave the storage facility closing the doors. Follow procedure for 'loss of containment by storage vessel'.

A4.10.5 Power Supply

Failure of the power supply to any part of the facility, including detectors, flowswitches, main panels and extract fan, will result in a fail-safe condition. That is to say that all release valves will be in the closed position, and will not be manually operable. Visual and audible power failure warnings (from the propane detection system powered by battery back-up) will also be in operation.

APPENDIX 4B

FACILITY MAINTENANCE PROCEDURE

This Appendix details the maintenance procedure for the facility at the time of writing (August 1994). The facility EDF should be consulted for any supplementary procedures in the light of new legislation/recommendations. The primary source for this schedule is the LPGITA Code Of Practice Number 1 (Installation and maintenance of bulk LPG storage at consumer's premises), Part 3 (Periodic inspection and testing), 1991.

B4.1 Maintenance Schedule

B4.1.1 General

All equipment not specified in this maintenance schedule shall be checked and maintained in accordance with the manufacturers' instructions, especial attention being paid to items not normally called upon to function, such as safety devices.

B4.1.2 Storage Vessel

The propane storage vessel system shall be externally examined at not more than one year intervals, and immediate attention given to any problems which may be encountered. Due to the construction of the system, the annual inspection will not include examination of the vessel itself. This is not a problem as the vessel is of stainless steel construction, and any corrosion problems are highly unlikely.

Every five years the vessel should be subjected to a hydrostatic test to test its integrity.

It is envisaged that both the immediate attention and the hydrostatic test would require evacuation of the vessel contents, details of which are given below:

Emptying Vessel: The vessel shall be emptied of its contents by evacuation through the normal experimental procedure, or if this is not possible, by evacuation to atmosphere by disconnection of the transfer line and operation of the vessel release valve. This secondary method of evacuation should be performed in a controlled

manner either at a suitable remote location, or within the confines of the fire-proof safety storage facility if it is not possible to transport the vessel due to its condition.

Note: If the pre-experiment visual checks are conducted to a suitable standard it is deemed highly unlikely that a situation will arise where a discharge through the transfer line will be not possible.

Prior to being emptied, the vessel must be completely isolated from any liquid or gaseous source of propane supply by physical disconnection. It should be noted however that in normal operation the propane supply vessel should not be attached to the vessel under any circumstances. All valves permitting release from the vessel should be verified as being closed, and should only be operable by the person in charge of the emptying procedure.

Having been evacuated, the vessel should then be purged to ensure that any vapour left in the vessel is removed, thus making certain that the contents is incapable of forming an explosive mixture on dilution with air. The preferred method of purging with this facility is by the application of nitrogen.

The remaining propane vapour may be removed by dilution (nitrogen allowed to flow through the vessel and carry out vapour with it) or by pressurisation (nitrogen used to pressurise the closed system and then released as per an experiment).

B4.1.3 Vessel and System Components

All safety devices, such as pressure relief valves and bursting disks, should be examined at least annually, in addition to the pre-experiment visual checks. The pressure relief valves should be tested for correct operation against a calibrated gauge at periods not exceeding five years. Valves which fail this test should be replaced. This includes relief valves on components such as the LPG handpump, and any additional valves which may be utilised at a later date.

As previously detailed it has been decided that the current vessel bursting disk system should be visually inspected on an annual basis, and replaced after 18-24 months service.

Any signs of leaking or other fault recognised during the visual inspection should be dealt with immediately either by specialist repair or replacement.

Shut-off valves should be tested for ease of operation regularly, not less than once a year. Lubrication of the valves, in accordance with manufacturers' instructions and using material suitable for propane bearing systems, should be carried out at this time. Filling valves should be maintained in the same manner as shut-off valves.

Valves, or systems incorporating valves, which form part of the safety shut-down system should be tested regularly, not less than twice per annum.

All other equipment not specifically covered should be subjected to a yearly check as a minimum.

The propane release system should be leak tested annually. The leak test must be done to a pressure of at least 6 barg (for propane), but not more than 90% of the vessel design pressure.

The leak test may be accomplished either by the use of a hydrostatic test (water and nitrogen - not air) or the use of Freon 22 (a propane simulant).

If any process of inspection or maintenance requires flanged or screw connections to be broken then these, and their components, must be inspected for cleanliness, integrity, etc and reassembled with new propane resistant sealant. Care must be taken to ensure that any damaged parts, such as gaskets, are replaced. All parts of a reassembled system should be leak tested to an appropriate pressure.

Pumps should be lubricated and maintained in accordance with the manufacturers' instructions. Particular attention should be paid to seals.

Regulators should be checked regularly with particular attention being paid to valve seats, seals and diaphragms.

Any hose connections should be checked regularly, ideally before each filling operation. If any signs of wear, distortion are seen then they must be replaced immediately.

B4.1.4 Electrical

The integrity of any zoned electrical equipment, and its supply, should be checked not less than once a year.

The resistance to earth of the system, including any housing into which the propane may be discharged, should be checked at least annually. The measured resistance should be below 10^6 ohms, if this value is not achieved then steps must be taken to rectify this.

B4.1.5 Fire Fighting

All fire extinguishers should be checked, tested and maintained at regular intervals according to the manufacturers' instructions.

The immediate surroundings of the storage area should be kept free of vegetation, or other flammable material.

The existence, location and legibility of warning notices should be checked regularly, and any visual warning systems tested likewise.

APPENDIX 4C

PRINCIPAL TECHNICAL COMPONENTS LIST

Below is presented a brief list of the technical components of the facility, and relevant information. The numbers in the brackets indicate appendices in the facility EDF (Equipment Documentation File) where further information may be found.

Load Cells (A1)
TEDEA-HUNTLEIGH
model: 104H COATED
capacity: 100 kg
total error: <0.015% rated load

Pump (A1, A5, A6)
HASKEL
model: MDSTV-5
serial No: P2269/07

Heating Tape (A1, A3):
COOPERHEAT
PSL54 110 V self-limiting

Heating Control (A2):
EUROTHERM
model: 91

Pressure Transducers (A20)
DRUCK
model: PTX 561-I
serial Nos: 526357, 526370
max pressure: 20 barg

Pressure Transducer Readouts (A20, A21)

DRUCK

model: DPI 262

serial Nos: 1110/92-11, 1111/92-11

max readout: 19.999 barg

Pneumatic Valve Actuators (A9, A10, A11)

NORBRO

model: 15-RKB-40R on vessel

model: 05-RDB-40R on nozzle

Pneumatic Valve (A7, A8)

WORCESTER

model: 12AF4466 TM.SET.SET on vessel

model: 05 F4466 TZ.SEN.SEN on nozzle

Quick Release Mechanisms

SWAGELOK

'full flow' quick connect QF series

LPG Safety Store (A22, A23, A24)

SAFETY UNLIMITED

model: SS8 (one hour fire rated)

LPG Handpump

ZWIKKY ENGINEERING LTD.

model: 60 mm x 65 mm, Mk 3 (drwng 70056).

delivery rate = 11.35 litres/min at a pumping rate of 70 double handstrokes/min

APPENDIX 4D

STORAGE VESSEL AND TRANSFER LINE DESIGN SPECIFICATIONS

This is a copy of the original initial design specification issued to tendering contractors late 1992

It should be noted that in the final design certain aspects detailed in this specification sheet were modified, the most obvious of which being the move from a vertical experimental chamber to a horizontal one. This was due to available height restrictions, and safety considerations. Such modifications however had no direct bearing on the vessel/transfer line design.

One modification to the design of this system was the inclusion of a second fail-safe remote valve, situated between the header tank and the nozzle system, and a secondary quick release coupling between the transfer line and the header tank. Both of these were installed after delivery and installation of the vessel system by the Facility Owner, Mr J T Allen.

PROPANE RELEASE SYSTEM

A system is required to produce a propane jet from a variety of storage conditions. The jet will discharge vertically into a controlled volume, which will stand approximately two metres high and be 1 metre square. The system will consist of a main storage vessel sited adjacent to the controlled volume, a transfer line into the volume, a small header tank, and the discharge nozzle.

Main Vessel

This vessel stores the propane prior to its' release, and will be used to produce the release conditions for each experimental run.

This should contain up to 50 litres (23 kg) of propane at temperatures up to 45°C and pressures up to 1500 kPa.

A system to heat the propane uniformly to the required temperature and hold it at that temperature will be required.

The temperature will be between ambient, say 15°C, and 45°C, held to a repeatable accuracy of +/- 1°C. The required temperature should be obtained with a full vessel at the worst case (ie. heating from 15 to 45°C) in less than 30 minutes.

note: previous work we have undertaken shows that a system with a circulating pump and an external heater can be employed, though care is required to avoid cavitation in the pump and boiling in the heater.

Connections to allow filling of the vessel should be included. These will allow connection to both the liquid and vapour take-offs from a standard 47 kg commercial propane cylinder. Valves should be provided to seal these filling and vent lines when not in use; these may be manually operated.

A connection should be provided to the transfer line , taking liquid from at, or close to the bottom of the vessel. This should be provide with a remotely operable valve which will seal the vessel from the rest of the system. This valve should have an operating time of less than 1 second, and should fail closed. It should be a ball valve or similar, giving a straight flow path when open and should have a minimum I.D. of 25 mm.

Two instrument connections are required. If possible these should accept 1/8" BSP and 1/4" BSP male, parallel taper fittings. The instruments themselves will be supplied and fitted by HSE.

It is required that the mass of propane in the vessel is measured immediately before and after each test, or possibly during the course of each test, which will last between 10 and 30 seconds. The weight measurement should be accurate to +/- 2.5g. It is envisaged that this will be achieved by using a load cell system supporting

the entire vessel. HSE will provide the necessary excitation, bridge and readout units for standard load cells.

The complete main vessel/heater/weighing system should be mounted on a wheeled frame, allowing it to be regularly moved to a safe area, away from the experiment, for filling. The wheels must be of a suitable size, and with sufficient ground clearance to allow the vessel to pass over the 20 mm high doorframe. Once in position a braking or similar system should be available to lock the vessel in place.

Transfer Line

The pipe carrying propane from the vessel to the jet header tank must be at least 25 mm I.D. It must be readily separated from the sealed main vessel, allowing the latter to be moved without requiring access to the jet header tank inside the controlled volume.

Jet Header Tank

The header tank is required in order to make measurements of temperature and pressure close to the discharge point, and also to allow some disengagement of any vapour that may have been formed in the transfer line.

The header tank should be an upright cylinder, with a volume of 0.75 litres.

It should be fitted with similar instrument connections to those on the main vessel, and with a connection to the transfer line made on the upper face.

The nozzle attachment should fit on the opposite (lower) face, directing the nozzles vertically downwards.

Nozzles

Four nozzles should be provided, which should be readily interchangeable. These should be of sizes:

4 mm I.D. x 40 mm long

4 mm I.D. x 80 mm long

6 mm I.D. x 60 mm long

6 mm I.D. x 120 mm long

The nozzle must be the narrowest part of the discharge system once the control valve on the vessel is fully open.

Movement

The nozzle must be able to move up to 300 mm in both the vertical and horizontal planes independently. It is envisaged that this will also involve the movement of at least the header tank. The traversing system will be supplied by HSE, but the pressure system design must incorporate mounting points for this.

Flameproofing

The main vessel and heating system should be regarded as a Zone 1 flameproof area, and the header tank as being in a Zone 0 area. The HSE supplied instrumentation will meet the requirements for use in these areas.

Materials and Design Standards

All vessels and pipework should be fabricated in stainless steel. Design and manufacture should comply with BS5500, to the class deemed appropriate for the size and proposed use of the system.

APPENDIX 5A

MEASUREMENT THERMOCOUPLE CALIBRATION PLOTS

This appendix contains the calibration plots for the five k-type thermocouples used on the measurement array. Each plot also includes the regression line of best fit for the data. The equations for these lines, which were used to correct the measured data, are presented in Section 5.2.1. Calibration was undertaken by the use of an electronic reference, itself calibrated to NAMAS standards.

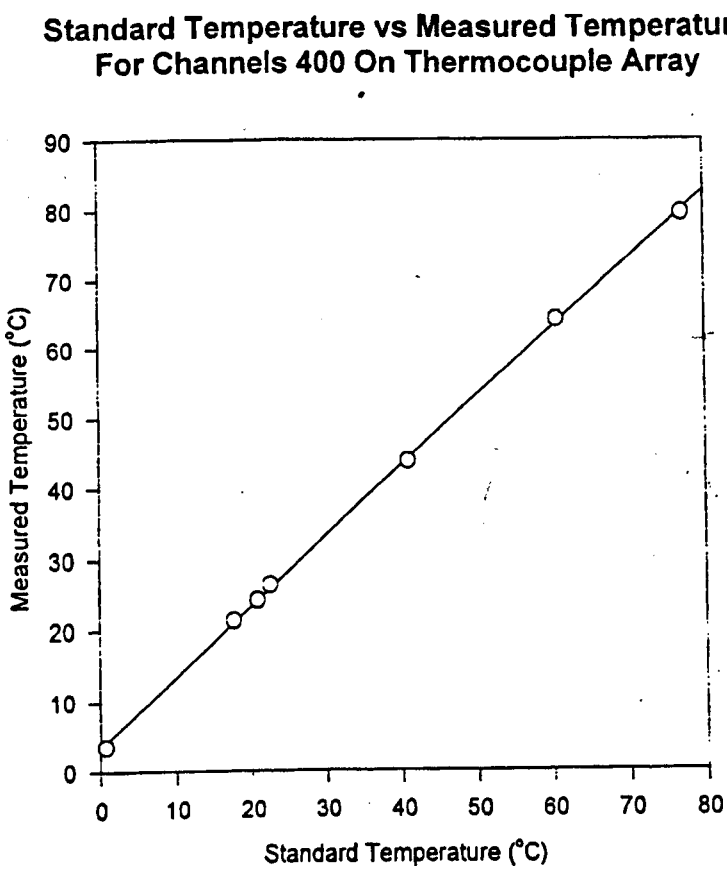

Standard Temperature vs Measured Temperature For Channels 401 On Thermocouple Array

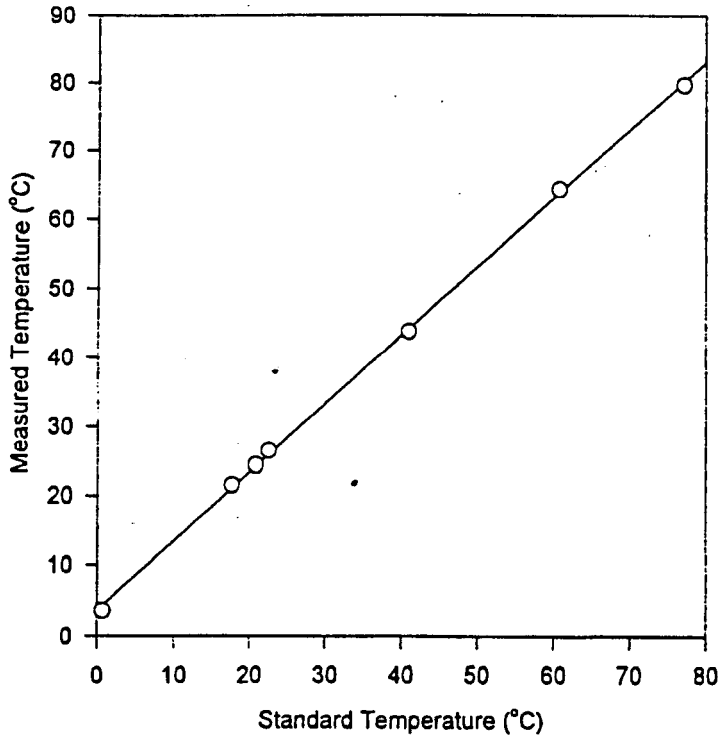

Standard Temperature vs Measured Temperature For Channels 402 On Thermocouple Array

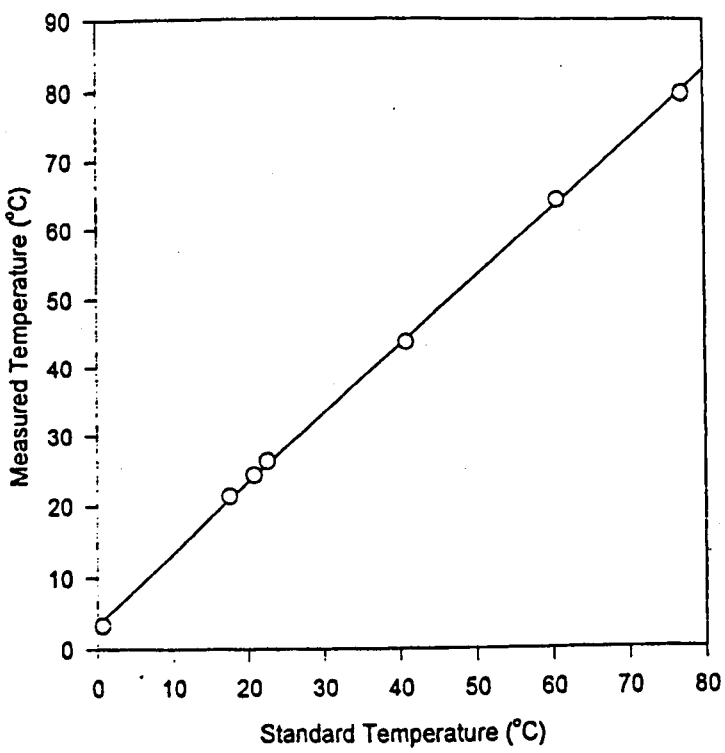

Standard Temperature vs Measured Temperature For Channels 403 On Thermocouple Array

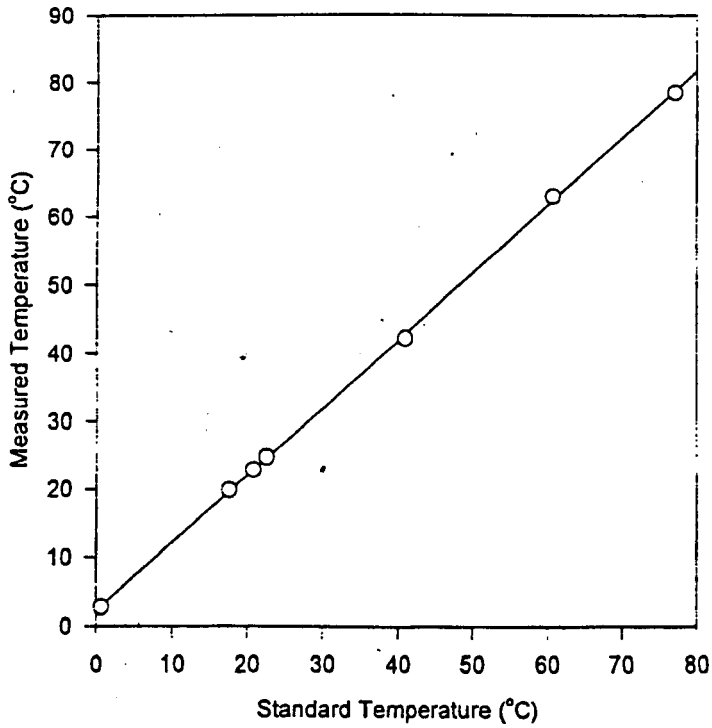

Standard Temperature vs Measured Temperature For Channels 404 On Thermocouple Array

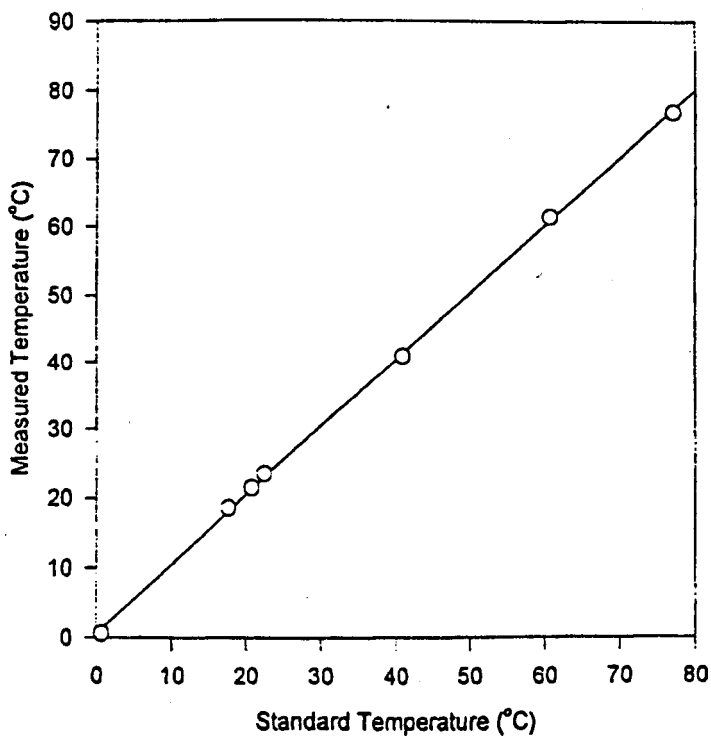

APPENDIX 7A

MODIFICATION AND INVERSION PROCESS

Initial Light Energy Distribution

Light energy distribution as measured by Malvern particle sizer.

MALVERN Series 2600 SB.00 Master Mode 16 Apr 1996 10:31 pm

Source Zprop Record no. 10 1024
Ring Data Focus 300

0	0.97	16	220.60
1	573.63	17	245.91
2	590.76	18	257.00
3	586.59	19	261.19
4	477.71	20	257.06
5	351.51	21	244.47
6	221.56	22	230.02
7	167.64	23	214.92
8	125.60	24	198.45
9	113.72	25	184.34
10	109.60	26	171.12
11	110.52	27	158.31
12	133.30	28	147.69
13	157.10	29	138.93
14	100.62	30	131.49
15	205.93		

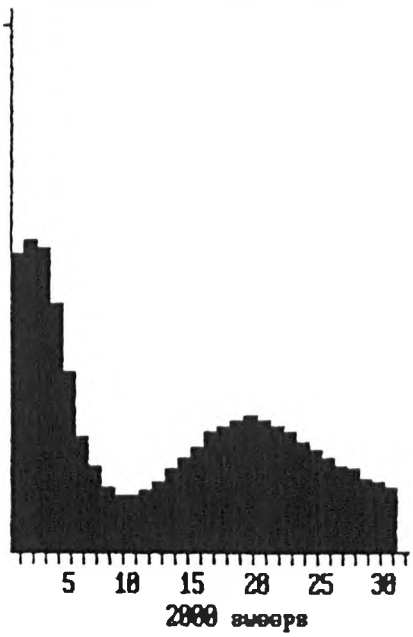

1710 pla 150240M / 0/ 0/0.00/1.00/
Customer : Health & Safety Laboratory, Buxton Fin 300
Instrument: 2600 Serial no 1710 00000002747

Modified Light Energy Distribution

Light energy distribution due to beam path distortion removed. Assumed linear light energy profile substituted in overlap region.

MALVERN Series 2600 SB.0D Master Mode 07 Aug 1996 6:29 am

Source Input 512

Ring	Data	Focus	300
0	0.97	16	220.60
1	0.00	17	245.91
2	0.00	18	257.00
3	0.00	19	261.19
4	0.00	20	257.06
5	0.00	21	244.47
6	0.00	22	230.02
7	10.00	23	214.92
8	43.00	24	198.45
9	68.00	25	184.34
10	93.00	26	171.12
11	118.52	27	158.31
12	133.30	28	147.69
13	157.10	29	138.93
14	180.62	30	131.49
15	285.93		

1710 pla 15024CM / 0/ 0/0.00/1.00/

Customer : Health & Safety Laboratory, Buxton Fin 300

Instrument: 2600 Serial no 1710 0000002747

Calculated Droplet Size Distribution

Assumed light energy distribution inverted to give droplet size distribution, using Model Independent algorithm. Droplet size distribution then plotted as histogram.

MALVERN Series 2600 SB.0D Master Mode 17 Apr 1996 1:42 am

High Size	Under %	High Size	Under %	High Size	Under %	High Size	Under %	High Size	Under %	High Size	Under %	Span
564	100	254	100	114	100	51.3	76.6	23.1	22.4	10.4	4.1	1.44
524	100	236	100	106	100	47.7	72.5	21.4	19.0	9.64	3.4	D[4,3] 37.0µm
488	100	219	100	98.6	100	44.4	68.7	19.9	16.4	8.97	2.9	
454	100	204	100	91.7	100	41.2	64.9	18.5	14.2	8.34	2.5	D[3,2] 26.1µm
422	100	190	100	85.3	100	38.4	60.3	17.2	12.4	7.76	2.1	
392	100	176	100	79.3	99.1	35.7	55.0	16.0	10.8	7.21	1.8	
365	100	164	100	73.8	97.1	33.2	49.2	14.9	9.4	6.71	1.5	D[v,0.9] 63.6µm
339	100	153	100	68.6	94.0	30.8	43.1	13.9	8.1	6.24	1.2	
315	100	142	100	63.8	90.1	28.7	37.1	12.9	6.9	5.80	0.9	
293	100	132	100	59.3	85.6	26.7	31.5	12.0	5.8			D[v,0.1] 15.4µm
273	100	123	100	55.2	81.0	24.8	26.6	11.2	4.9			

Source = Data:Input	Beam length = 100.0 mm	Model Indp	D[v,0.5] 33.5µm
	Log. Diff. = 5.186		
Focal length = 300 mm	Obscuration = 0.9687	Volume Conc. = 0.0301%	
Presentation = pia	Volume distribution	Sp.S.A 0.2298 m^2/cc.	Shape OFF

1718 pia 15024CM / 0/ 0/0.00/1.00/
Customer : Health & Safety Laboratory, Buxton Fin 300
Instrument: 2600 Serial no 1718 000002764

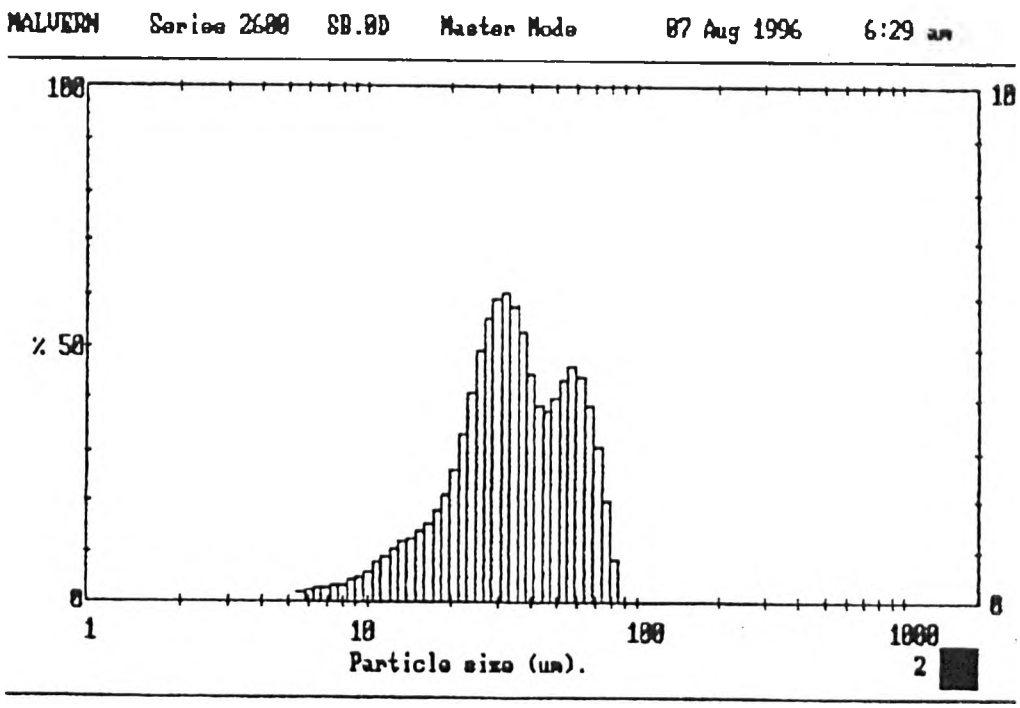

APPENDIX 7B

SENSITIVITY OF INVERSION PROCESS TO LIGHT ENERGY DATA MANIPULATION

In this Appendix, the light energy distribution data is presented, along with the calculated droplet size distribution, in both numerical and graphical forms. Comments on the inversion process are presented at the end.

Raw Light Energy Data - No Manipulation

Ring Data Focus 300

0	0.97	16	286.86
1	564.40	17	223.72
2	586.94	18	235.90
3	541.40	19	239.95
4	438.82	20	237.17
5	381.68	21	226.22
6	199.90	22	213.41
7	139.19	23	199.93
8	100.30	24	185.20
9	95.71	25	172.73
10	94.60	26	161.16
11	102.83	27	149.97
12	117.32	28	140.87
13	139.10	29	133.56
14	161.35	30	127.45
15	184.90		

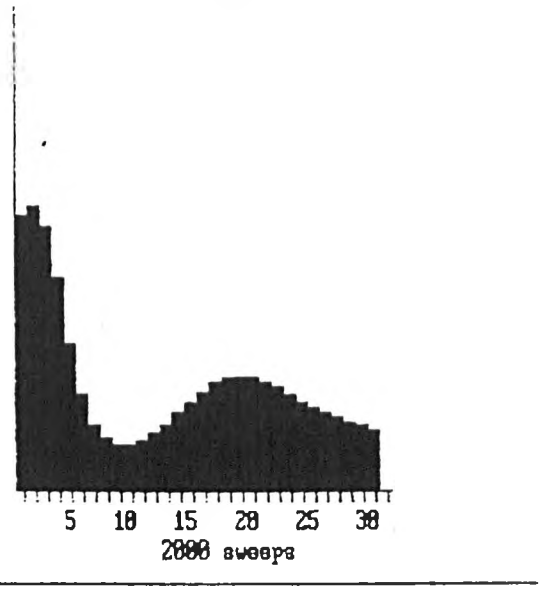

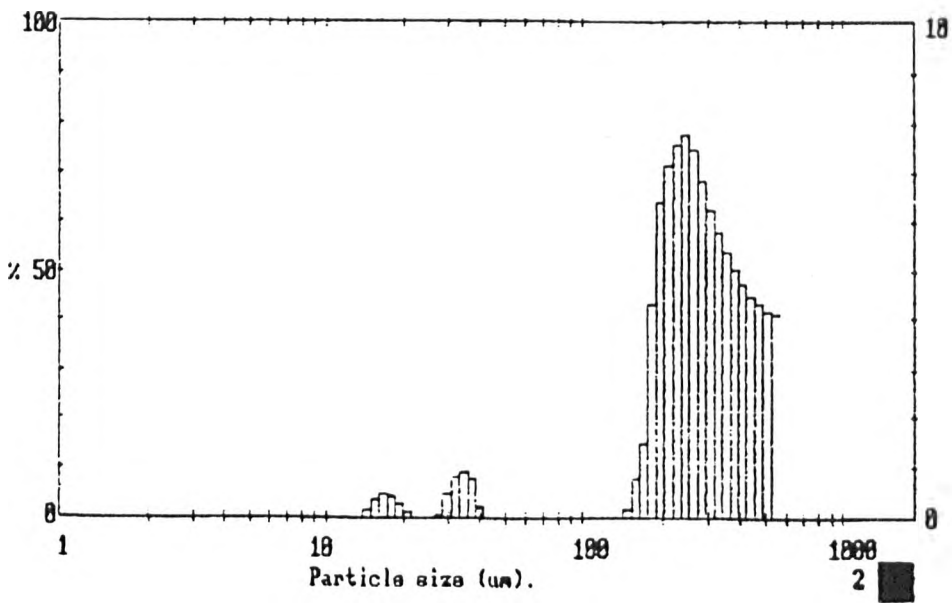

Linear Assumption A

The light energy in the overlap region is assumed to decrease in a linear manner. The rate of the decrease is determined, approximately, by the rate of decrease of the real light energy distribution at the start of the overlap region. This is the method employed to generate the droplet size distributions presented in this report, partly for reasons of expediency.

Source 2prop Record no. 17 1024
Ring Data Focus 300

0	0.97	16	206.86
1	564.40	17	223.72
2	506.94	18	235.90
3	541.40	19	239.95
4	438.02	20	237.17
5	381.60	21	226.22
6	199.90	22	213.41
7	139.19	23	199.93
8	100.30	24	185.20
9	95.71	25	172.73
10	94.60	26	161.16
11	102.83	27	149.97
12	117.32	28	140.87
13	139.10	29	133.56
14	161.35	30	127.45
15	184.90		

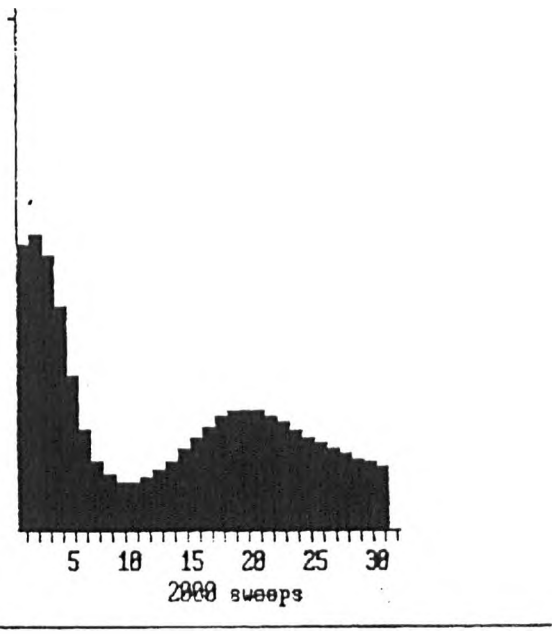

Source Input 256
Ring Data Focus 300

0	0.97	16	206.86
1	0.00	17	223.72
2	0.00	18	235.90
3	0.00	19	239.95
4	0.00	20	237.17
5	0.00	21	226.22
6	0.00	22	213.41
7	7.00	23	199.93
8	29.00	24	185.20
9	51.00	25	172.73
10	73.00	26	161.16
11	95.00	27	149.97
12	117.32	28	140.87
13	139.10	29	133.56
14	161.35	30	127.45
15	184.90		

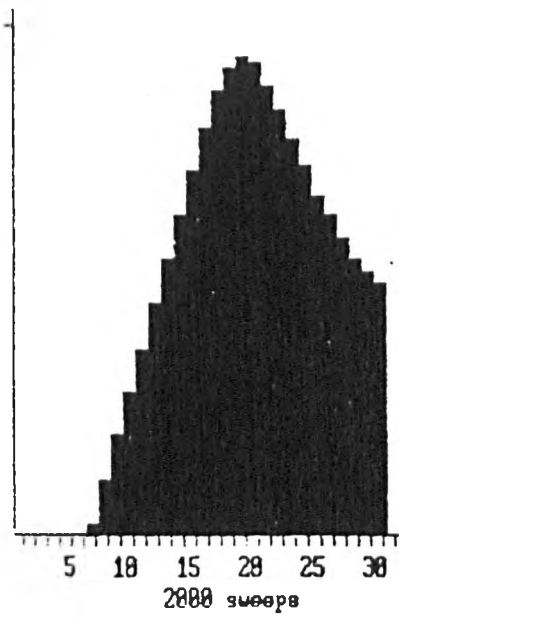

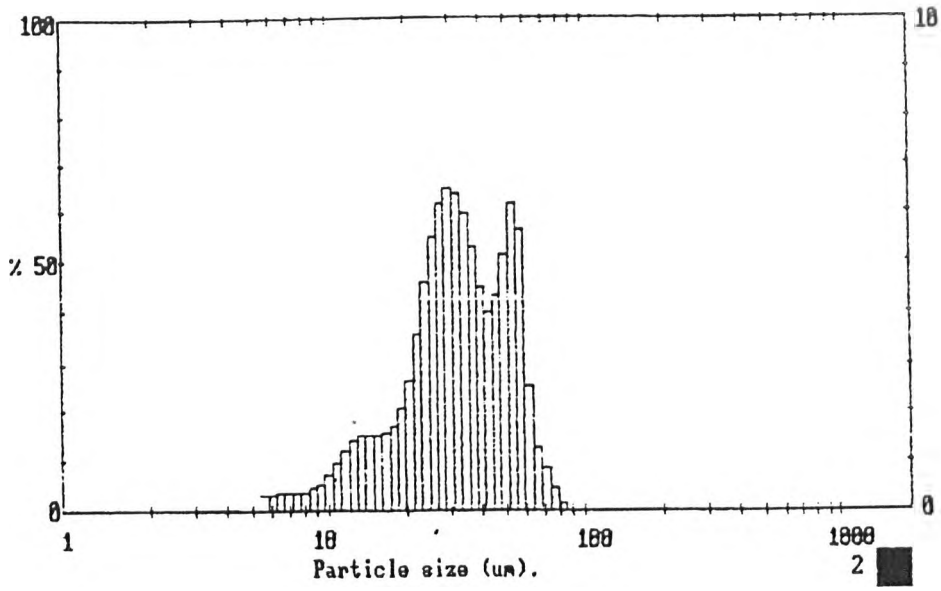
100
% 50
0
1
10
100
1000
Particle size (um).
10
0
2

Linear Assumption B

The start of the overlap region is assumed to be at a slightly different position in the light energy distribution. A different linear rate of decrease is, therefore, determined from this new region.

Source Input 256

Ring	Data	Focus	300
0	0.97	16	286.86
1	0.00	17	223.72
2	0.00	18	235.90
3	0.00	19	239.95
4	0.00	20	237.17
5	12.00	21	226.22
6	27.00	22	213.41
7	42.00	23	199.93
8	57.00	24	185.20
9	72.00	25	172.73
10	87.00	26	161.16
11	102.83	27	149.97
12	117.32	28	140.87
13	139.10	29	133.56
14	161.35	30	127.45
15	184.90		

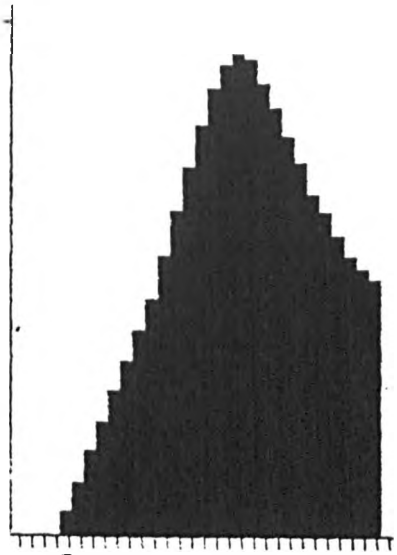

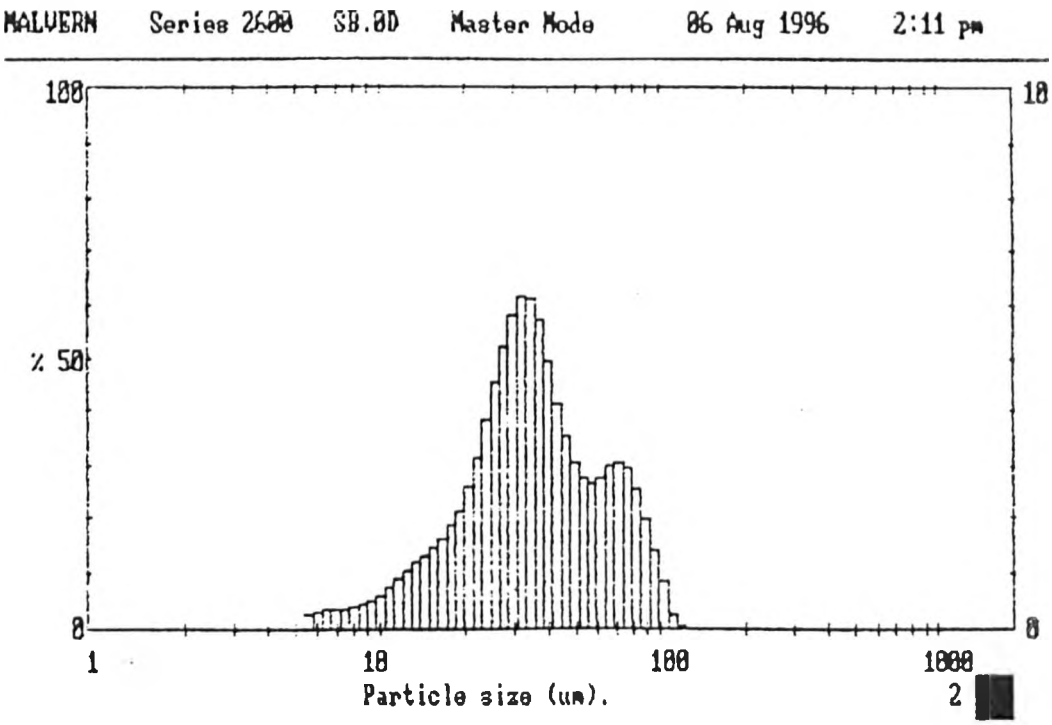

Non-Linear Assumption A

The light energy is assumed to have a non-linear rate of decrease in the overlap region. In this assumption (A) the rate decreases.

Source Input 256
Ring Data Focus 300

0	0.97	16	206.86
1	0.00	17	223.72
2	0.00	18	235.90
3	6.00	19	239.95
4	12.00	20	237.17
5	18.00	21	226.22
6	27.00	22	213.41
7	37.00	23	199.93
8	49.00	24	185.20
9	63.00	25	172.73
10	79.00	26	161.16
11	97.00	27	149.97
12	117.32	28	140.87
13	139.10	29	133.56
14	161.35	30	127.45
15	184.90		

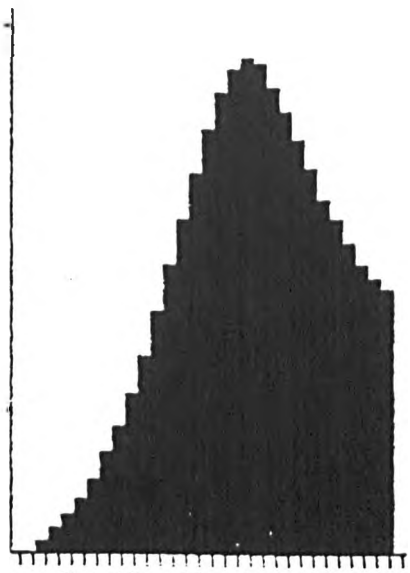

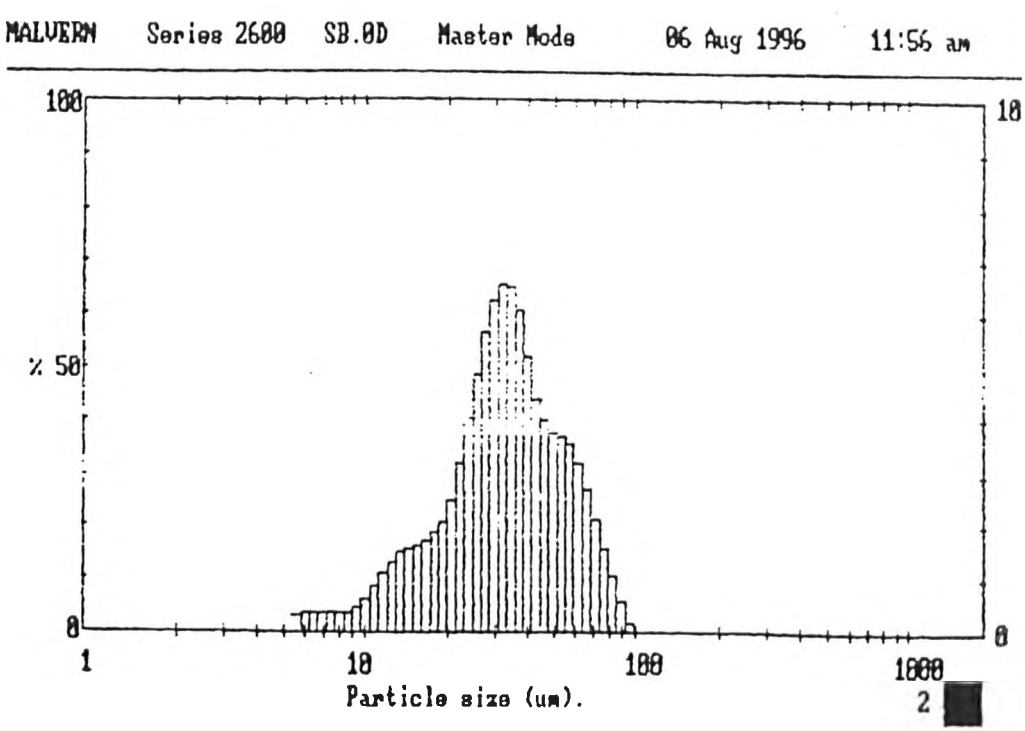

Non-Linear Assumption B

The light energy is assumed to have a non-linear rate of decrease in the overlap region. In this assumption (B) the rate increases.

Source Input 256

Ring Data Focus 300

0	0.97	16	206.86
1	0.00	17	223.72
2	0.00	18	235.90
3	0.00	19	239.95
4	0.00	20	237.17
5	0.00	21	226.22
6	0.00	22	213.41
7	0.00	23	199.93
8	5.00	24	185.20
9	36.00	25	172.73
10	65.00	26	161.16
11	92.00	27	149.97
12	117.32	28	140.87
13	139.10	29	133.56
14	161.35	30	127.45
15	184.90		

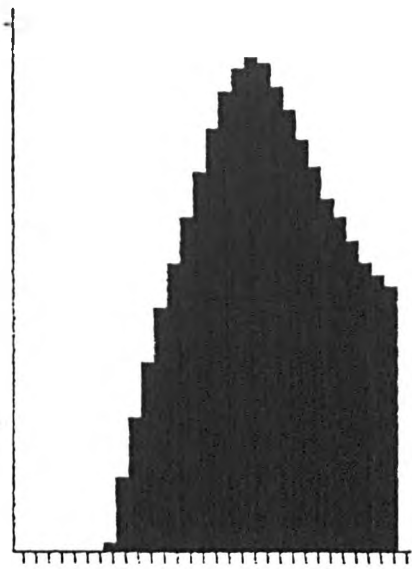

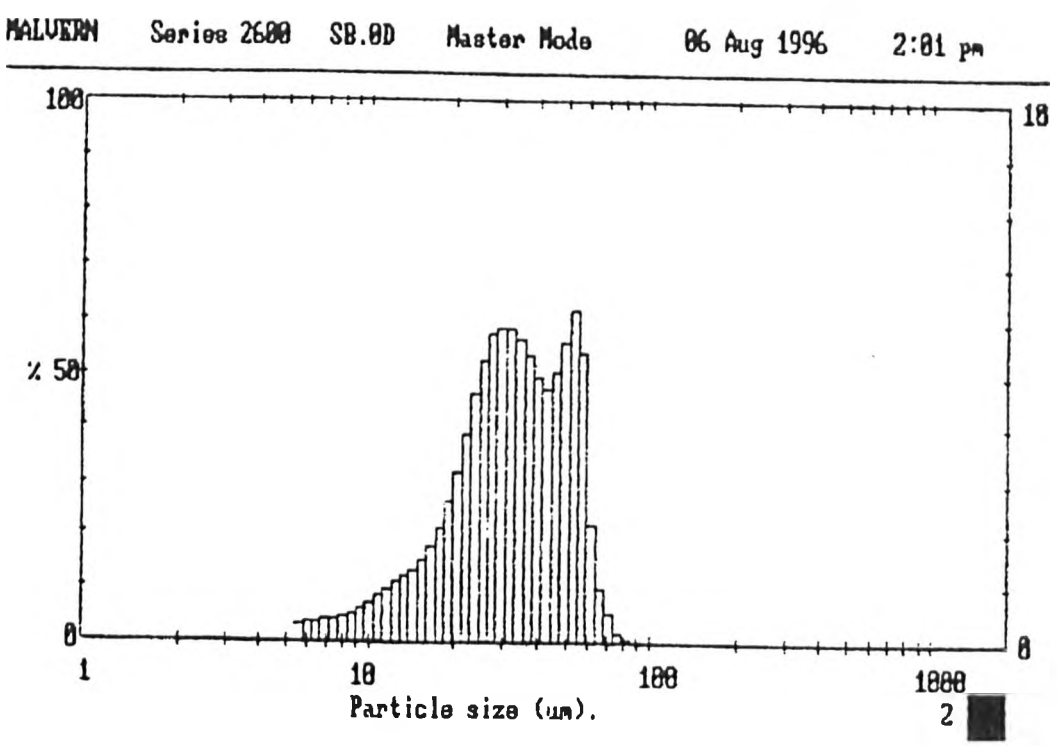

Sharp Termination Assumption A

The light energy distribution has been immediately reduced to zero at the assumed start of the overlap region. This is not a realistic situation, but demonstrates the distribution generated by the real data, and the effect of sharp terminations.

Source Input

Ring	Data	Focus	300
0	0.97	16	286.86
1	0.00	17	223.72
2	0.00	18	235.90
3	0.00	19	239.95
4	0.00	20	237.17
5	0.00	21	226.22
6	0.00	22	213.41
7	0.00	23	199.93
8	0.00	24	185.20
9	0.00	25	172.73
10	0.00	26	161.16
11	0.00	27	149.97
12	117.32	28	140.87
13	139.10	29	133.56
14	161.35	30	127.45
15	184.90		

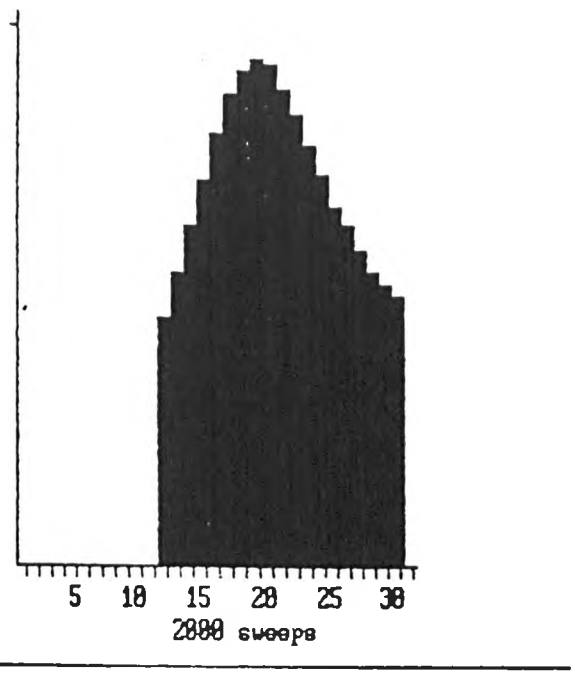

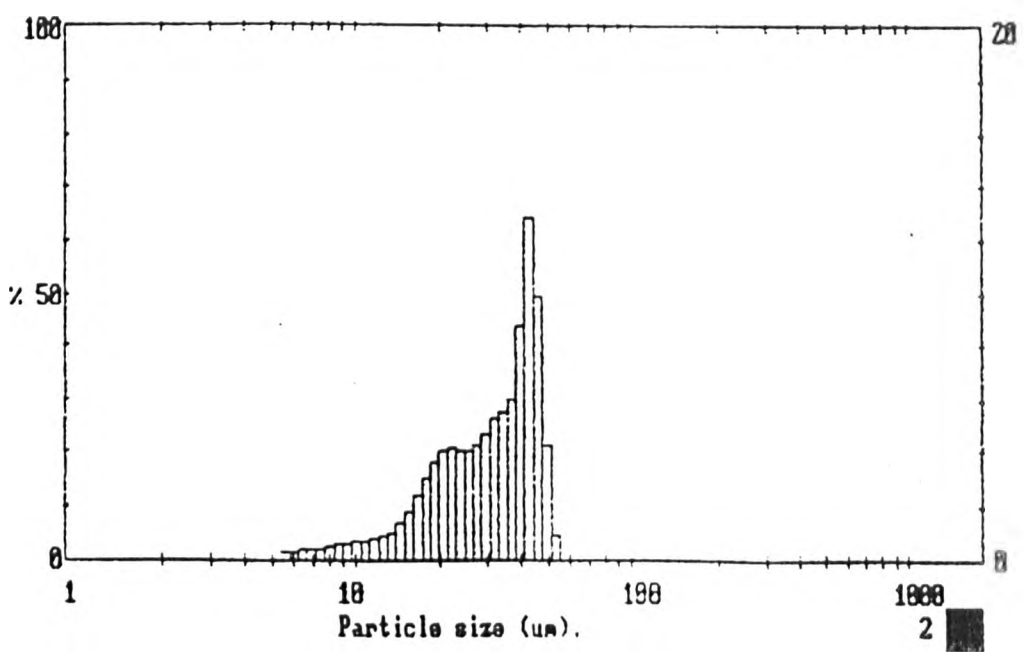

Sharp Termination Assumption B

The light energy distribution is, again, immediately reduced to zero. In this instance a section of the overlap region is not removed, in order to see how it effects the calculated droplet size distribution.

Source Input 256

Ring	Data	Focus	300
0	0.97	16	286.86
1	0.00	17	223.72
2	0.00	18	235.90
3	0.00	19	239.95
4	0.00	20	237.17
5	0.00	21	226.22
6	199.90	22	213.41
7	139.19	23	199.93
8	100.30	24	185.20
9	95.71	25	172.73
10	94.60	26	161.16
11	102.83	27	149.97
12	117.32	28	140.87
13	139.10	29	133.56
14	161.35	30	127.45
15	184.90		

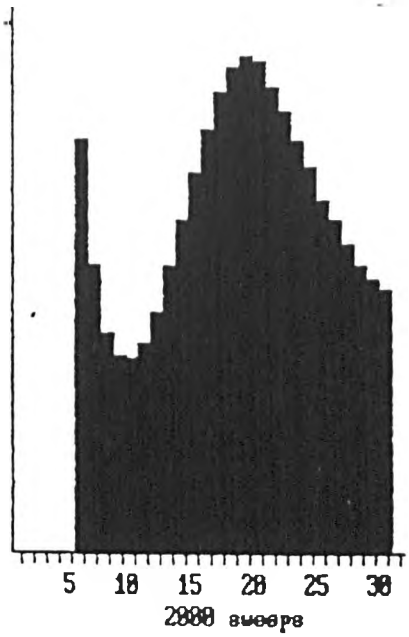

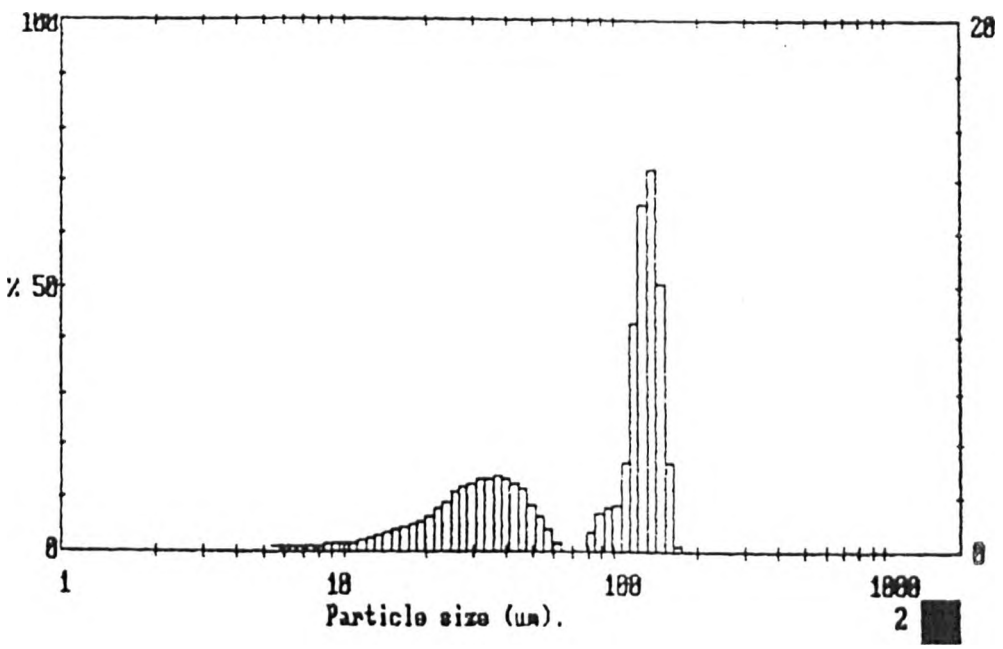

Comments On Sensitivity Tests

It appears that the most accurate assumption is that the light energy spectrum decay occurs at a decreasing rate. The difference between this and the linear assumption is, in many cases, marginal. The linear assumption was chosen primarily for convenience, and its rate of decay was, in each case, chosen subjectively. Re-manipulation using the decreasing rate assumption would, to some extent, probably improve the absolute accuracy of the data.

The 'ghost' peak appears to be related to how abruptly the light energy profile is terminated, i.e. how the inversion process deals with the last non-zero value detector block. This effect does not occur if the termination occurs on the first, or last, detector block. Further work would be required to prove the validity of this statement.

Overall, the droplet size distribution is, within sensible limits, relatively insensitive to the manipulation/inversion process, whilst the form of the 'ghost' peak, and its position, seem to depend on the manipulation/inversion process. The linear spectral decay assumption, although not the most accurate, is considered to be perfectly adequate, especially considering time constraints, and the droplet size distributions generated from it more than satisfactory.

APPENDIX 8A

SAFETY CASE FOR FLUOROPHORE TRANSFER PROCEDURE

Transfer Procedure

The Transfer procedure will involve three main processes:

1) Weighing out of an appropriate mass of NpaNmaap. This will involve transferring the substance from its container into a weighing boat (and possible replacement of small quantities into the container).

2) Transfer of the weighed mass into the fluorescence chamber.

3) Sealing of the calibration chamber.

Hazards

The main hazard from this operation is the chemical compound being transferred, 1-(N-p-Anisyl-N-Methyl)-Amino-3-Anthryl-(9)-Propane. An exact determination of the hazards posed by it is not possible as it is a relatively unknown compound, only having been synthesised once previously [A, B]. The information which is available does not detail any of its hazardous properties.

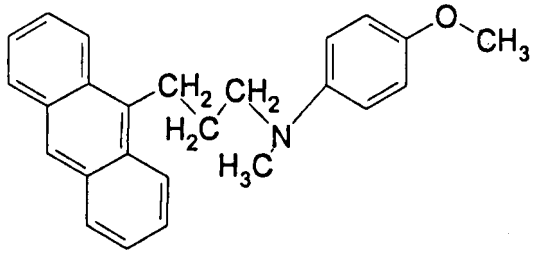

1 - (N-p-Anisyl-N-Methyl)-Amino-3-Anthryl-(9)-Propane

In order to ascertain the nature of any hazards, the chemical name, formula and structure were passed on to relevant HSL and HSE Departments. Both parties ran the structure through the in-house DEREK program, which flags up known hazardous groupings within the overall chemical structure. The assessments from Martin Payne, HSL, and Penny Barker, HSE, are presented in Appendix 8B.

In both instances there was reported a potential for carcinogenicity and mutageneity, but of unknown likelihood. Skin sensitisation and lipophillic behaviour were thought

to be definite hazards. Due to the unknown nature of the compound, no definite information could be provided, although opinion from these two sources was that it was likely to be of relatively low carcinogenic and mutagenic hazard. In the absence of comprehensive information however, it must be assumed that the hazards are the most extreme plausible.

Justification For Use Of NpaNmaap and Mitigation of Associated Risks

In the light of the unknown toxicology of the compound, its use must be justified. In this case there are very strict experimental conditions and physical property requirements that must be met by any compound. In brief these are:

1) an ability to dissolve in liquid propane

2) the compound must exhibit a temperature dependent fluorescence spectrum in a desirable temperature range

3) Within the requirements of 2), the compound must also
   a) be excited by incident radiation at 308nm
   b) exhibit differential wavelength/temperature behaviour (i.e. different wavelengths of the emitted fluorescence must behave inversely with temperature).

4) the compound must be a solid of an appropriate molecular weight for the range of temperatures and pressures required, in order to be compatible with the behaviour of the propane host.

NpaNmaap was the only compound found, during a 2-3 year search, which has the potential to fulfil these requirements.

The use of the compound is favoured, in hazard and risk terms, by the fact that the preliminary information (DEREK) suggests that it is of possibly low carcinogenicity and mutageneity. Further to this, the compound is in a crystalline form and there is,

therefore, a lower risk of airborne contamination and inhalation. The compound's relatively high melting point of 122°C, and its low vapour pressure also combine to reduce the risk of toxic exposure.

The risk from the hazards detailed, or assumed, above is low by virtue of the mechanical, administrative, and personal protective safety measures being employed. The use of small quantities of the compound further reduce the risk of exposure during the transfer processes. Details of the calculated concentration and mass transfer quantities is given below:

Fluorophore Concentration Calculations

MRR of NpaNMaap = 355

$C_{25}H_{25}NO$ = (25x12) + (25x1) +16 +14

Volume of chamber = 50mm x 50mm x 250mm = 625, 000mm^3

= 625cm^3

= 0.625 litres

1.0M solution in chamber = 0.625 x 335 = 221.875g

Assuming 1.5 x10^{-4}M solution,

mass required = 0.03328125g

~ 0.033g

Assuming 3.0 x 10^{-4}M solution,

mass required = 0.0665625g

~0.067g

Safe Operational Procedure

The transfer and weighing operation must be undertaken in a safe area, such that any spillage can be confined and easily dealt with in a safe manner. In this instance the designated safe area is the local exhaust ventilation (LEV) unit in the Combustion Laboratory, Building 96 (HSL Laboratory, Buxton). The LEV unit provides an area in which the material can be safely manipulated, whilst remaining effectively separated from the main laboratory. In the event of a spillage, the LEV unit can

quickly and easily be closed to contain the spillage with no interaction between its contents and the remainder of the laboratory.
The LEV unit will not be in operation during the course of the transfer and weighing operations, due to its adverse effect on the weighing process and the possible generation of airborne particulate matter. It is merely used to provide a safe area during the transfer process.

The transfer procedures will be performed on a tray, lined with suitable paper material. In the event of any spillage, the lining (and the tray if necessary) will be placed inside a suitable disposal bag and disposed of by a specialist contractor, via the Safety Office. All operations, including bagging up of spillage materials, will be undertaken inside the LEV unit. The operations inside the LEV unit should be performed with a minimum practicable opening in the front access window in order to reduce the risk of loss of material into the laboratory area, and that of exposure of personnel to the compound.

During the weighing process, the floor and pan of the balance will also be lined with paper to allow easy disposal of any spillage. All disposal bags must be labelled with the name of the compound and assumed hazards. care should be taken to avoid transferring any material on the operator's gloves onto the weighing balance. If necessary, new gloves should be put on prior to operation of the balance.

During the transfer of the material into the calibration chamber, the exposed areas of the chamber should be covered with a paper lining, and the process should take place over the lined tray.

Once the compound has been transferred into the calibration chamber, the chamber will be sealed. This process will take place inside the LEV unit. The calibration unit is designed for the storage of liquid propane, and is therefore capable of containing high pressure volatile materials. Escape of the compound from the sealed chamber is not possible.

The chamber will then be removed from the LEV unit to allow a small quantity of liquid propane to be added, and the compound will be dissolved into it. Further liquid propane will be added until the chamber contains the desired volume of solution. It may be necessary to cool the liquid propane inside the chamber prior to the second addition. Both fills of solvent will take place into the sealed chamber, with no likelihood of escape of the compound, or any solution containing.

The material is stored in a glass vial, which is itself contained within a metal canister. The glass vial should only be removed from the metal canister inside the LEV unit. This limits the area of spillage, should accidental breakage of the vial occur, to the lined tray.

It is advised that 'deactivation' of the material can be achieved by the application of 2M aqueous HCl [C], although this is unlikely to be required given the measures to contain spillages set out previously. It should be noted that absolute deactivation (i.e. disassembly of the chemical structure) is unlikely to be achieved with any acceptable chemical reagent.

All weighing and transfer operations must be performed by an Authorised Operator, as detailed and listed in Appendix A, and the appropriate PPE must be worn. For the material in question the appropriate PPE is deemed to be safety spectacles, disposable laboratory overcoat, and safety gloves. After the procedure any item of PPE which has come into contact with the material must be disposed of as detailed above. Gloves and laboratory overcoats should be disposed of after each operation, the process taking place, as far as is reasonably practicable, inside the LEV unit.

After bagging up of the paper lining, the LEV unit should be operated to remove any airborne material generated during the process.

During the transfer and weighing operations a suitable warning sign must be employed at the entrance to the Combustion Laboratory, detailing the operation and

its potential hazards. As the process will be of short duration it is advisable to restrict access to the room whilst these processes are being undertaken.

All transfer and weighing processes should be recorded in the Carcinogen Hazard Book, detailing the date, quantity, operator, and any unforeseen circumstances that arose (e.g. spillage). The CHB will be kept in the locked Laser Dye/Carcinogen Storage Facility in the Laser Laboratory (HSL, Buxton).

The procedures detailed above should be read, and undertaken, in conjunction with those presented in the General Safety Procedures section of the Section Safety Manual.

References

[A] Hamann H-J, Jugelt W, Pragst F, 'Intramolecular exciplex formation of some 1-(N-methyl-N-phenyl)-amino-3-(9-anthryl)-propane derivatives' Z. Chem. 14, (12) pp475-477, 1974.

[B] Hamann H-J, Pragst F, Jugelt W, 'Preparation and electrochemical properties of N,N-disubstituted 1-amino-3-(9-anthryl)-propane derivatives' J. prakt. Chem. 318, (8) pp369-380, 1976.

[C] Dr A Spivey, Chemistry Department, University of Sheffield, private communication.

Authorised Operators

An authorised operator should have suitable experience, or undergone suitable training, as deemed by the Head of Fire Safety Section, Dr S F Jagger. The following are deemed as Authorised operators:

Mr J T Allen, Fire Safety Section

APPENDIX 8B

TOXICOLOGY ASSESSMENTS

Author: Penny Barker at HSE-HD-BOOTLE2
Date: 09/12/96 16:48
Priority: Normal
TO: John Allen at HSL-BUXTON
Subject: Chemical structure - alerts
---------- Message Contents ----------

John,

You sent a copy of the structure of compound
1-(N-p-Anisyl-N-Methyl)-Amino-3-Anthryl-(9)- Propane to me for evaluation of possible structural alerts for toxicity.

I and my colleagues in HD D3 have looked at this structure and it has been put through the DEREK computerised SAR system. The conclusions are that the 3-ring structure and the benzene ring with - N- grouping give rise to possible concern for potential carcinogenicity by analogy with other compounds. However, metabolism could be an important factor in any carcinogenic potential and we do not have relevant information on this. Also, there are structures in the molecule which could influence activity by producing steric hindrance. The benzene ring with -O-CH3 group produced an alert for skin sensitisation but given the cautious approach to handling required as a result of the lack of toxicity data on this compound, I expect that it will not come into contact with the skin.

Penny Barker
HD D3.

Toxicological Assessment of 1-(N-p-Anisyl-N-Methyl)-Amino-3-Anthryl-(9)-Propane

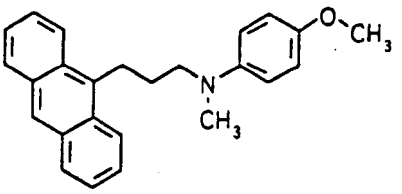

DEREK Assessment

The following rule were fired when the structure was scanned by the DEREK programme:

Rule	Hazard	Why (Toxcphore)?	Rule Reliability/Applicability (MPP)
42	Irritancy	Amine (any)	Poor - not applicable
108	Carcinogenicity	Aromatic amine	Moderate -Applicability to alkylanilines is questionable.
113	Carcinogenicity	Fused polynuclear aromatic	Low specificity - more specific rules were not fired
332	Mutagenicity (bacterial)	Aromatic amine	Moderate- Applicability to alkylanilines questionable
439	Skin sensitisation	Phenol precursor (methoxybenzene)	Moderate-high. Influence of substituent unclear.

Although DEREK predicts potential for the substance to be carcinogenic, an in vitro mutagen and a skin sensitiser, the reference screen information provided gives few examples of structurally similar active compounds. The presence of alkyl substituents on the amine group is expected to reduces the potential carcinogenic activity via hydroxylamines and the anthacene structure is not one well-known to be associated with high activity.

In my view the substance is unlikely to be a potent carcinogen. There is some potential for skin sensitisation and from the lipophilicity, skin absorption. I recommend therefore that skin contact with the substance or its solutions should be avoided.

Martin P Payne
6th December 1996